Reliability of a dike influenced by a building

Development of a probabilistic method for slope stability of a dike containing a building inside the soil profile

Y.R. Jongerius

TU Delft & Royal Haskoning DHV

TU Delft Delft University of Technology

Royal HaskoningDHV
Enhancing Society Together

Challenge the future

Technical University Delft

MSc. Thesis

Reliability of a dike influenced by a building

Development of a probabilistic method for slope stability of a dike containing a building inside the soil profile

Author:
Y.R. Jongerius

Supervisors:
Prof. Dr. Ir. S.N. Jonkman
Dr. Ir. J.G. de Gijt
Ing. M.Z. Voorendt
Dr. Ir. K.C. Terwel
Ir. J.J. Kool
Ir. A. Bäcker

A thesis submitted in fulfillment of the requirements for the degree of Master of Science

in the

Hydraulic Structures & Flood Risk
department of Hydraulic Engineering

30 March 2016

Royal HaskoningDHV
Enhancing Society Together

TU Delft
Delft University of Technology

Photo cover image:
Location: Waalbandijk, Beneden Leeuwen, The Netherlands
Doris Jongerius, 2016, ©
http://www.dorisjongerius.com

Preface

This thesis report is the final result of the graduation project to complete my master degree in Hydraulic Engineering at Delft University of Technology. It contains a research performed in cooperation with the company Royal Haskoning DHV. They offered me the opportunity to study this topic by means of a graduation internship at their Infrastructure department in Amsterdam. For this opportunity I would like to thank my committee members Job Kool and Anne Bäcker, furthermore I would like to thank them for their extensive feedback and the interesting conversations we had on this topic. More over I would like to thank all other colleagues from Royal Haskoning DHV that have helped me by sharing their knowledge on this subject with me.

I would also like to express gratitude to my committee members from the university, Bas Jonkman, Mark Voorendt, Jarit de Gijt and Karel Terwel, for their constructive feedback and guidance throughout this project. Their varying fields of expertise have made it possible to perform research on this multidisciplinary subject. For this research I spoke with numerous professionals from the field, and therefore I would like to express sincere gratitude to these professionals from Deltares, Concretio, Hoogheemraadschap Rijnland, Waterschap Rivierenland and Waternet, for sharing their knowledge and experience of the daily practice with me.

Special thanks to my friend Leslie Nooteboom, for drawing a visualization of the case study, and my sister Doris Jongerius for the photo shoot of the cover of this thesis. The dike on the cover, used to be under responsibility of my grandfather, in his role as 'Heemraad' within the waterboard 'Polder district Maas & Waal'. Finally I would like to thank my parents, Eugene and Marianne, for their full and loving support during my study period.

Yoeri Jongerius
Utrecht, March 2016

This page intentionally left blank.

TU DELFT

Extensive Summary

Faculty of Civil Engineering and Geosciences
Hydraulic Engineering

Master of Science

Reliability of a dike influenced by a building

Development of a probabilistic method for slope stability of a dike containing a building inside the soil profile

by Y.R. Jongerius

Introduction

Dikes are the major part of the 17,500 kilometers of primary and regional water defenses in The Netherlands. Along some Dutch dikes buildings have been built in the past. However, it is unclear how these buildings affect the reliability of a dike. Therefore, this research will attempt to answer the following research question: *What is the influence of a non-water retaining building on the reliability of a dike, and how can this be determined and included into the assessment of water defenses?*

During the third assessment round (2006-2011) of Dutch water defenses, the non water retaining objects (NWO's), like buildings,also had to be assessed. The statutory assessment tool for this round was the VTV (2006). An advanced assessment, as described in VTV (2006), appears never to have been fully performed. Partly because of this, the assessment of many buildings has not been completed. The developed method could be seen as a first step towards an advanced assessment.

In 2017 a new assessment round of the primary water defenses will start. Currently new assessment tools (WBI2017) are being developed for this round. These tools are based on a 'probability-of-flooding-approach' instead of a probability of exceedance approach. This allows for the inclusion of specific properties of dikes , such as buildings, into the safety assessment. This could be done as long as the total probability of flooding, which is determined for each dike, is satisfied. Because the new tools are based on probabilities of flooding, the developed method will be probabilistic.

Influence of buildings on dikes

A dike might fail due to various failure mechanisms. The presence of a building within the influence zone, could affect the resistance against the different failure mechanisms and thereby influence the reliability of the dike. Additionally, the possible collapse of a building might also affect the reliability of a dike. Within this research the known effects of a building on the most relevant failure modes are identified. These effects are identified for three

building properties:

1. Horizontal location relative to the dike (foreland, outer slope, crest, inner slope, hinterland)

2. Foundation method (shallow, pile)

3. Vertical location relative to the dike (in the soil profile, on the soil profile).

This has been done for both a scenario in which the building remains intact as well as for a scenario in which the building collapses. The results are shown in tables 4.1 and 4.2. It is remarkable that a building can have both positive and negative effects, while within the assessment tools only negative effects are mentioned. The inner slope stability appears to be affected by several different effects which is why this research focuses on this particular mechanism.

By means of a simple analysis, a distinction can be made based on two causes of building collapse: an independent building collapse to a high water event (for example due to an earthquake) and a dependent building collapse to a high water event (for example by an increase of the freatic level). For independent collapse, the probability of flooding is barely increased, because it is unlikely that simultaneously a high water event occurs. However, in the case of dependent collapse, a high water event occurs simultaneously, since this is the cause of the building collapse . In section 4.2.1, this is exemplified by means of a numerical example.

By sliding plane calculations (see section 5.2 and tabels 5.3 & 5.4), it is concluded that buildings low in the inner slope may beneficially affect the stability. However when these buildings collapse, the stability may be significantly affected. Therefore, in this research, a probabilistic method is developed to determine the stability of the combined system of dike and building.

Probabilistic method

The soil profile of the combined system of dike and building can be described by two appearances (see figure 8), depending on whether or not the building collapses. For both soil profiles conditional probabilities of instability can, given that the building remains intact or collapses, be calculated ($P_{(instab|intact)}$ & $P_{(instab|collapse)}$).

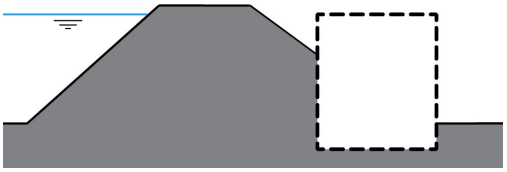

(A) Building intact, probability of instability : $P_{(instab|intact)}$

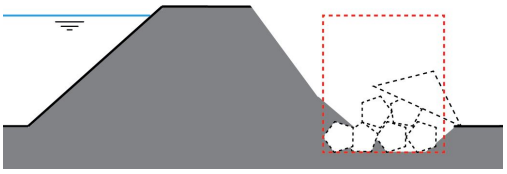

(B) Building collapses, probability of instability:: $P_{(instab|collapse)}$

FIGURE 1: Twee verschijningsvormen van dijk met gebouw in het grondprofiel

For both soil profiles the probability of instability will increase with a rising water level (h_w). However, for the profile with a collapsed building, the probability of instability will already be higher for lower water levels. This is illustrated in the fragility curves in figure 9, which describes the performance of the two soil profiles as a function of the water level. The probability of collapse of the building ($P_{collapse}$) will, through an increase of the forces on the building, also increase with rising water level. When a fragility curve of the combined system is imagined, this would move for a rising water level from the curve of $F_{(instab|intact)}$ towards the curve of $F_{(instab|collapse)}$, as is done for the curve F_{instab} in figure 9.

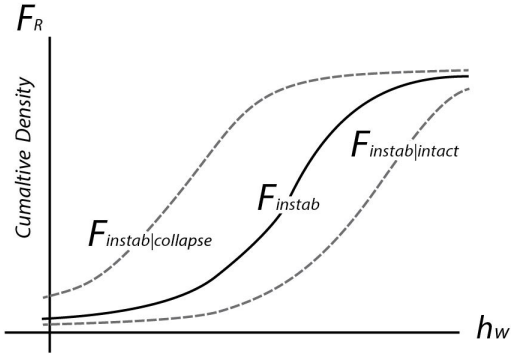

FIGURE 2: Fragility curves for dike with building

To determine P_{instab} of the combined system, this probabilistic method is developed and contains three steps.

- **Structural model**
  The objective of this model is to determine the performance of the building during a high water event. This will be expressed in the probability of collapse ($P_{collapse}$) and the probability the building remains intact (P_{intact}).
- **Geotechnical model**
  In the next model, the performance of the two soil profiles will, given that the building collapses or remains intact, be determined. This will be expressed in the conditional probabilities of instability: $P_{(instab|collapse)}$ & $P_{(instab|intact)}$
- **Integration of both models**
  Lastly, the results of the two models have to be integrated towards a probability of instability of the combined system (P_{instab}). With the aid of the "law of total probability" the following equation is derived:

$$P_{instab} = P_{(instab|intact)} \cdot P_{intact} + P_{(instab|collapse)} \cdot P_{collapse}$$

In figure 6.4 a flow chart of the developed probabilistic method is depicted.

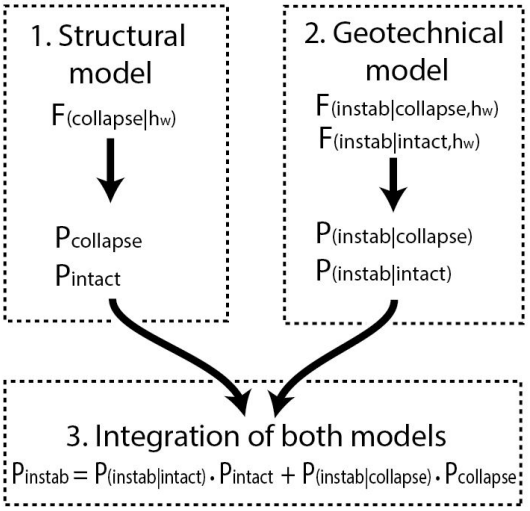

FIGURE 3: Flow chart of the developed probabilistic method

Case study

To test the developed probabilistic method, it is applied to a case study. The case study contains a dike profile for which a building with a masonry soil retaining wall is located inside the inner slope. To get an impression see figure 4.

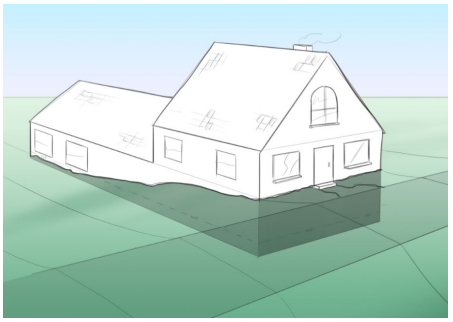

FIGURE 4: Impression of the combined system of dike and building

Structural model Just like the dike, the building can collapse through different failure mechnisms. To describe the performance of the building during a high water event, one failure mechanism of the building is examined in detail. This mechanism is out of plane bending of the soil retaining wall. This is done to

perform the first step of the method and additionally to get a sense of the parameters and their influence. For the probabilistic calculations the wall is schematized as a beam supported by two supports, see figure 5. The collapse is then modeled linear elastically as a wall loaded by a horizontal forcing and a normal force. The probabilistic calculations are then performed by a compiled calculation scheme with a FORM and a Monte Carlo method with the software package Prob2B (Courage and Steenbergen, 2007).

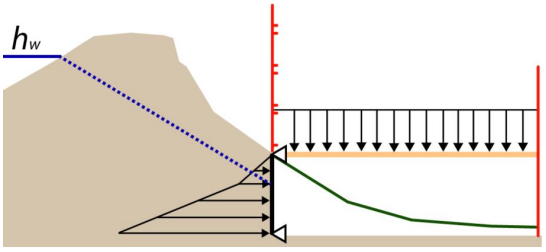

FIGURE 5: Schematisation structural model

Geotechnical model For the geotechnical model, the probabilistic calculations are performed with the reliability module of the Deltares software package D-Geo-Stability (Deltares, 2014). Probabilistic soil stability calculations are performed for a soil profile without a building, with an intact building and an assumed profile given that the building collapses (residual profile), see figure 6. For these profiles the conditional probability of instability is calculated.

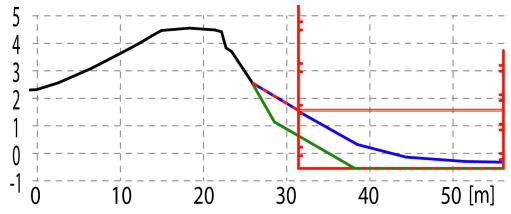

FIGURE 6: Soil profiles of the case-study (red = building intact, green = building collapses, blue = without building)

Integration of both models Subsequently, the results of the structural & geotechnical model are combined into a probability of instability of the combined system (P_{instab}). In subsection 6.1.2 the effects of this step are illustrated by means of a numerical example. This example shows that the developed method can potentially determine a positive or a negative influence of a building on the stability.

Results

An important assumption that was made is that all uncertainties induced by models or schematizations are not included in the case study. These were excluded because more information is needed to implement these uncertainties, especially within the structural model. A consequence of this is that the results of the case study can not yet be used for a risk assessment in practice.

Structural model The probabilistic calculations of the structural model show that $P_{collapse}$ is most severely affected by the wall thickness, the water level (h_w) and the flexural tensile strength (f_{x1}). This can also be seen from the calculation results of figure 14, in which a certain wall thickness is assumed and Monte Carlo samples for f_{x1} & h_w are presented. In this figure a Z function line can be drawn, which divides the domain of collapse and non-collapse. It is relevant to conclude that the flexural tensile strength has a large influence as it is known that the tensile strength of masonry can reduce significantly when cracking occurs.

Geotechnical model The results of the geotechnical model show that the profile without a building and the one with an intact

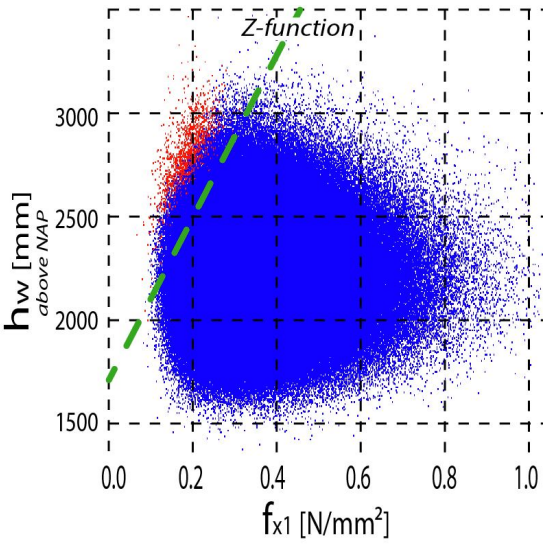

FIGURE 7: Graphical presentation of probabilistic calculations of $P_{collapse}$ (Red samples represent building collapse)

building are equally stable. This means that the building from the case-study has no positive effect on the stability. The stability of the residual profile does appear to be significantly reduced.

Integration of both models When the probabilistic method is applied within the boundaries of the case study it is determined that this building, when collapse is included, has a negative influence on the dike stability.

Conclusion

The most important conclusion from this research are the following:

- **No advanced assessment**
  Despite of the possibility for an advanced assessment of dike buildings exist since 2006, it seems that this step has never been fully performed. Because of the buildup of the assessment this is one of the reasons that the assessment has not been completed for a large amount of NWO's.
- **Dependent collapse**
  The dependent collapse of a building to a high water has a larger influence on the reliability of a dike, compared with an independent cause of building collapse. For buildings inside the soil profile of a dike the collapse can significantly reduce the stability.
- **Buildings do not satisfy**
  It is remarkable that masonry buildings that are located inside the soil profile of a dike do not satisfy the current guidelines for buildings. This is because the flexural tensile strength should not be taken into account.
- **Developed method**
  In this research a probabilistic method is developed that can be seen as a start of an advanced assessment for the stability of dikes with buildings inside the soil profile, for which building collapse might affect the stability.
- **Application in practice**
  When model- and schematization uncertainties would be implemented into the models belonging to this method, in practice it could be used for risk assessment. That would make it possible to accommodate the effects imposed by the presence of a building at the failure space that is reserved for 'remaining mechanisms' within the new assessment tools (WBI2017)

Recomendations

The recommendations for further research that follow from this research are as follows:

- **Structural**
  In regards tothe structural aspects of this research, it is recommended to perform more research to the model- and schematization uncertainties. This is still needed to put

this probabilistic method into practice. Furthermore it is suggested to further research other mechanisms of building collapse during a high water event.

- **Loading**
  It is recommended to do more research on the exact loads of soil and freatic water on the building. Currently these loads are determined separately, while in reality this is a combined system, and will therefore also influence the loads. Other aspects that might influence the size and distribution of the loads and displacements, which are not yet implemented, are: Undrained soil behavior and arching within the soil and the building, but also in between different elements of the building. It is advisable to conduct further research into these effects.
- **Geotechnical**
  Little is still known about the impact of the possible collapse of a building on the soil profile of a dike. Therefore, more research needs to be done on this so called residual profile, which appears after building collapse. Additionally further detailed research needs to be performed on the effects of buildings on other failure mechanisms of dikes, such as piping and failure by overtopping and overflow.
- **Extension in longitudinal direction**
  The probabilistic method is now developed and applied on 2D profiles. Some effects of the implication of the third dimension are described, but it is still unclear how this can be processed in the probabilistic method. Furthermore, this extension could be done for a dike with multiple buildings in or on the profile.

TU DELFT

Samenvatting

Faculteit Civiele Techniek en Geotechniek
Waterbouwkunde

Master of Science

Betrouwbaarheid van een dijk beïnvloed door bebouwing

Ontwikkeling van een probabilistische methode voor de stabiliteit van een dijk met een gebouw in het grondprofiel

door Y.R. Jongerius

Introductie

Dijken vormen het grootste gedeelte van de 17.500 kilometer aan primaire en regionale keringen in Nederland. Op veel plekken in Nederland zijn in het verleden gebouwen op en langs de dijken gebouwd. Echter is het onduidelijk hoe dit de betrouwbaarheid van de dijk beïnvloed. Daarom wordt in dit onderzoek getracht de volgende onderzoeksvraag te beantwoorden: *Wat is de invloed van een niet-waterkerend gebouw op de betrouwbaarheid van een dijk, en hoe kan dit bepaald worden en inbegrepen worden in de toetsing?*

In de derde toetsronde (2006-2011) van Nederlandse waterkeringen dienden ook de niet waterkerende objecten (NWO), zoals gebouwen, beoordeeld te worden. Het wettelijk vastgestelde toetsinstrumentarium voor deze beoordeling was het VTV (2006). Een geavanceerde toetsing, zoals beschreven in VTV (2006), blijkt nog nooit volledig te zijn uitgevoerd. Mede daarom is de toetsing van veel gebouwen niet volbracht. De ontwikkelde methode zou gezien kunnen worden als een eerste stap naar deze geavanceerd toetsing.

In 2017 zal een nieuwe beoordelingsronde van de primaire waterkeringen starten. Hiervoor wordt op dit moment een nieuw beoordelingsinstrumentarium (WBI2017) ontwikkeld. Dit instrumentarium wordt gebaseerd op overstromingskansen in plaats van op overschrijdingskansen. Dat betekent dat er ruimte komt om specifieke eigenschappen van dijken, zoals bebouwing, onder te brengen in de toetsing. Dit kan zolang er wordt voldaan aan de totale overstromingskans die voor de dijk is vastgesteld. Omdat de nieuwe normering toetst op overstromingskansen, is er voor gekozen om een probabilistische methode te ontwikkelen.

Invloed van bebouwing op dijken

Een dijk kan via verschillende faalmechanismen bezwijken. De aanwezigheid van een gebouw binnen de invloedszone kan de werking van deze faalmechanismen beïnvloeden en daardoor de betrouwbaarheid van de dijk aantasten. Het eventueel bezwijken van een gebouw kan ook doorwerken in een aangepaste betrouwbaarheid van de dijk. In dit onderzoek zijn de bekende effecten van een gebouw op de meest relevant faalmechanismen geïnventariseerd. Dit is gedaan aan de hand van drie gebouweigenschappen:
1. Horizontale locatie t.o.v. de dijk (voorland, buitentalud, kruin, binnentalud, achterland)

2. Funderingswijze (op staal, paalfundering)
3. Verticale locatie t.o.v. de dijk (in het grondprofiel, op het grondprofiel).
Dit is gedaan voor een scenario dat het gebouw intact blijft zowel als voor een scenario dat het gebouw bezwijkt. De resultaten hiervan zijn in tabelvorm weergegeven in tabel 4.1 en 4.2. Opvallend is dat een gebouw zowel positieve als negatieve effecten kan hebben, terwijl in het instrumentarium alleen getoetst wordt op negatieve effecten. De binnenwaartse stabiliteit blijkt op meerdere manieren beïnvloed te worden, daarom ligt de focus van dit onderzoek op dit mechanisme.

Door middel van een simpele analyse kan onderscheid worden gemaakt tussen twee soorten bezwijken van het gebouw. 1. Onafhankelijk bezwijken van het gebouw aan een hoogwater (bijvoorbeeld door een aardbeving). 2. Afhankelijk bezwijken van het gebouw aan een hoogwater (bijvoorbeeld door een verhoogde freatische lijn). Bij onafhankelijk bezwijken wordt de kans op overstromen nauwelijks vergroot, omdat de kans klein is dat er tegelijkertijd hoogwater staat. Echter bij afhankelijk bezwijken, staat er tegelijkertijd hoogwater, omdat dit de oorzaak is van het bezwijken. In sectie 4.2.1 is dit geillustreerd aan de hand van een getallenvoorbeeld.

Door middel van van glijvlakberekeningen (zie sectie 5.2 en tabellen 5.3 & 5.4) wordt geconstateerd dat bebouwing laag in het binnentalud de stabiliteit ten goede kan komen als het gebouw intact blijft. Echter wanneer het gebouw bezwijkt kan de stabiliteit lager uitvallen dan voor een vergelijkbaar profiel zonder gebouw. Daarom wordt in dit onderzoek een probabilistische methode ontwikkeld om de stabiliteit van een gecombineerd systeem bestaande uit een dijk en een gebouw te bepalen.

Probabilistische methode

Het grondprofiel van het gecombineerde systeem van dijk en gebouw kenmerkt zich door twee verschijningsvormen (zie figuur 8), afhankelijk van het al dan niet bezwijken van het gebouw. Voor beide grondprofielen kunnen conditionele kansen op instabiliteit berekend worden ($P_{(instab|intact)}$ & $P_{(instab|collapse)}$).

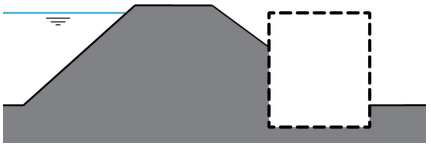

(A) Gebouw intact, met kans op instabiliteit: $P_{(instab|intact)}$

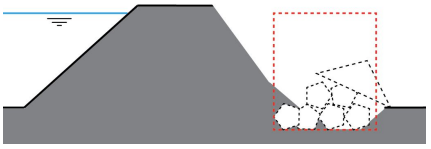

(B) Gebouw bezwijkt, met kans op instabiliteit: $P_{(instab|collapse)}$

FIGUUR 8: Twee verschijningsvormen van dijk met gebouw in het grondprofiel

Voor beide grondprofielen zal de kans op instabiliteit toenemen bij een stijgende waterstand (h_w), echter voor het profiel met een bezweken gebouw zal voor lagere waterstanden de kans op instabiliteit al groter zijn. Dit is inzichtelijk gemaakt in de fragiliteitscurven in figuur 9, die de prestaties van de beide profielen beschrijven als functie van de waterstand. De kans op bezwijken van het gebouw ($P_{collapse}$) zal, door een toename van de krachten op het gebouw, ook stijgen naarmate de waterstand toeneemt. Wanneer een fragiliteitscurve van het gecombineerde systeem voorgesteld wordt, zou deze zich voor een toenemende waterstand verplaatsen van de curve van $F_{(instab|intact)}$ richting de curve van $F_{(instab|collapse)}$. Zoals is gedaan voor de curve F_{instab} in figuur 9.

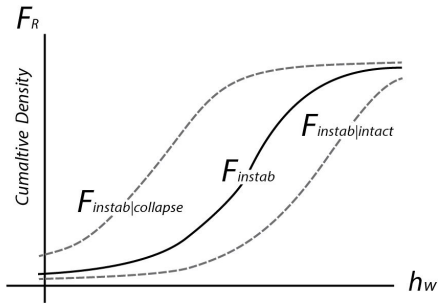

FIGUUR 9: Fragiliteits curve voor dijk met gebouw

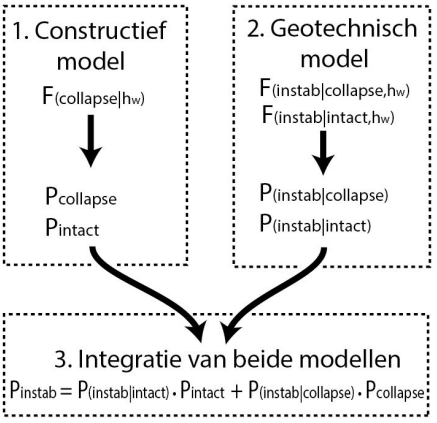

FIGUUR 10: Stroomdiagram probabilistische methode

Om de P_{instab} van het gecombineerde systeem te bepalen is deze probabilistische methode ontwikkeld en deze bestaat uit drie stappen.

- **Constructief model**
  Het doel van dit model is om de prestatie van het gebouw te bepalen tijdens hoogwater. Dit wordt uitgedrukt in de kans op bezwijken ($P_{collapse}$) en de kans dat het gebouw intact blijft (P_{intact}).
- **Geotechnisch model**
  Voor de tweede stap dienen de prestaties van de grondprofielen, gegeven dat het gebouw bezwijkt dan wel intact blijft, bepaald te worden. Dit wordt uitgedrukt in de conditionele kansen op instabiliteit: $P_{(instab|collapse)}$ & $P_{(instab|intact)}$
- **Integratie van beide modellen**
  Ten slotte dienen de resultaten van de beide modellen geïntegreerd te worden naar een kans op instabiliteit van het gecombineerde systeem (P_{instab}). Met behulp van de "law of total probability" wordt de volgende formule afgeleid:

$$P_{instab} = P_{(instab|intact)} \cdot P_{intact} + P_{(instab|collapse)} \cdot P_{collapse}$$

In figuur 6.4 is een stroomdiagram van de ontwikkelde methode weer gegeven.

Case study

Om de ontwikkelde probabilistische methode te testen, wordt deze toegepast op een case-study. De case-study behelst een dijkprofiel waarbij een gebouw met een metselwerk grondkerende muur in het binnentalud staat. Zie voor een impressie figuur 11.

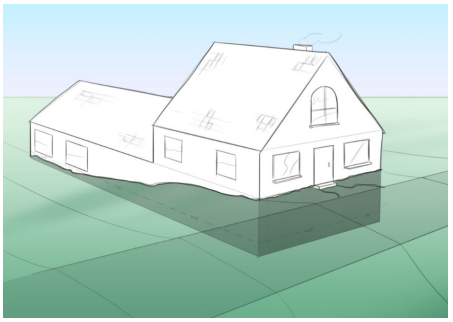

FIGUUR 11: Impressie van het gecombineerde systeem van dijk en gebouw

Constructief model Net als de dijk kan het gebouw via verschillende faalmechanisme bezwijken. Om de prestatie van het gebouw gedurende hoogwater te beschrijven, wordt één faalmechanisme van het gebouw verder uitgelicht, ten invulling van het constructief model en daarnaast om een gevoel te krijgen van de factoren en hun invloed. Het mechanisme dat uitgelicht wordt is: uit het vlak buiging

van de grondkerende muur. Voor de probabilistische berekeningen binnen het constructief model wordt de muur geschematiseerd als een ligger op twee steunpunten, zie figuur 12. Het bezwijken wordt vervolgens lineair elastisch gemodelleerd als een horizontaal belaste wand met een normaalkracht. De probabilistische berekeningen worden vervolgens uitgevoerd door middel van een opgesteld berekenings schema met een FORM en een Monte Carlo methode met behulp van het TNO software pakket Prob2B (Courage and Steenbergen, 2007).

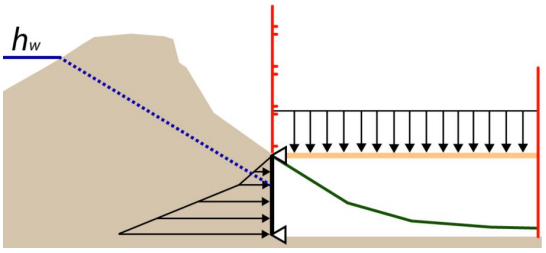

FIGUUR 12: Schematisering constructief model

Geotechnisch model Voor het geotechnische model wordt gebruik gemaakt van de betrouwbaarheidsmodule van het Deltares software pakket D-Geo-Stability (Deltares, 2014). Hierin worden berekeningen uitgevoerd voor een grondprofiel zonder gebouw, een grondprofiel met een intact gebouw en een aangenomen grondprofiel voor een bezweken gebouw (het restprofiel). De verschillende grondprofielen zijn afgebeeld in figuur 13. Voor deze profielen worden de conditionele kansen op instabiliteit berekend.

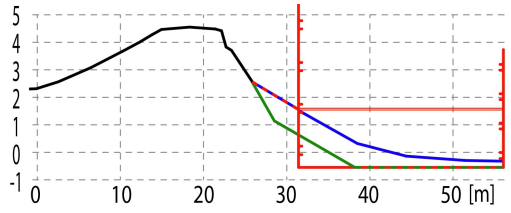

FIGUUR 13: Profielen uit de case-study (rood = gebouw intact, groen = gebouw bezweken, blauw = zonder gebouw)

Integratie van beide modellen Vervolgens worden de resultaten van het constructief en geotechnisch model gecombineerd tot een kans op instabiliteit van het gecombineerde systeem (P_{instab}). In subsectie 6.1.2 is aan de hand van een getallenvoorbeeld de werking van deze stap geïllustreerd. Hieruit blijkt dat de ontwikkelde methode in potentie een positieve dan wel een negatieve invloed van een gebouw op de stabiliteit kan vaststellen.

Resultaten

Een belangrijke aanname die gedaan is voor deze case-study is dat alle onzekerheden geïnduceerd door modellen en of schematiseringen buiten beschouwing gelaten zijn. Dit is gedaan omdat er nog meer informatie nodig is om deze model en schematiseringsonzekerheden te implementeren, voornamelijk binnen het constructief model. Een gevolg hiervan is dat de resultaten van de case study (nog) niet gebruikt kunnen worden voor een risico afweging in praktijk.

Constructief model Uit de probabilistische berekeningen binnen het constructief model blijkt dat $P_{collapse}$ het sterkst wordt beïnvloed door de muurdikte, de waterstand (h_w) en de buigtreksterkte van het metselwerk (f_{x1}). Dit is ook te zien aan de hand van de berekeningsresultaten in figuur 14, waar een muurdikte is aangenomen en Monte Carlo waardes van f_{x1} en h_w zijn weergegeven. Hierin kan een Z functie lijn getekend worden, die het domein van bezwijken en niet-bezwijken scheidt. Dat de buigtreksterkte zo gewichtig is blijkt een relevante conclusie aangezien bekend is van metselwerk dat

de treksterkte aanzienlijk kan reduceren wanneer scheurvorming optreedt.

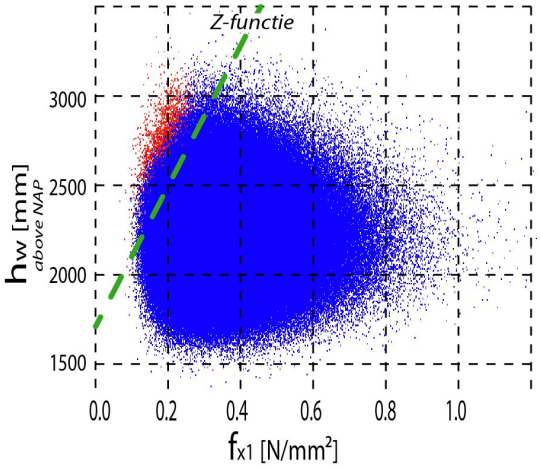

FIGUUR 14: Graphische weergave probabilistische berekeningen $P_{collapse}$ (rood representeert bezwijken)

Geotechnisch model Uit de uitkomsten van het geotechnische model blijkt dat de stabiliteit van het profiel zonder gebouw en met een intact gebouw praktisch even groot zijn. Dit betekent dat het gebouw in de case-study geen positief effect heeft op de stabiliteit. De stabiliteit van het restprofiel blijkt wel significant lager te zijn.

Integratie van beide modellen Wanneer de probabilistische methode wordt toegepast binnen het kader van de case-study kan worden vastgesteld dat het gebouw, wanneer bezwijken hiervan wordt inbegrepen, een negatieve invloed heeft op de stabiliteit.

Conclusies

De belangrijkste conclusies van dit onderzoek zijn hieronder weer gegeven.

- **Geen geavanceerde toetsing**
  Ondanks dat er al sinds 2006 een geavanceerde toetsing bestaat voor bebouwing nabij dijken, lijkt het erop dat deze stap nog nooit compleet is uitgevoerd. Dit is, binnen de afgelopen toetsronde, een van de oorzaken dat voor veel NWO's de toetsing niet is gecompleteerd.
- **Afhankelijk bezwijken**
  Het afhankelijk bezwijken van bebouwing aan een hoogwater heeft een grotere invloed op de betrouwbaarheid van een dijk, in vergelijking met een onfhankelijke oorzaak. Voor bebouwing in het grondprofiel van de dijk kan het bezwijken de stabiliteit aanzienlijk reduceren.
- **Gebouwen voldoen niet**
  Het is opvallend dat metselwerk gebouwen die zich bevinden in het grondprofiel van een dijk niet zullen voldoen aan de huidige normen voor gebouwen. Dit komt omdat de buigtreksterkte van het metselwerk niet in rekening gebracht mag worden.
- **Ontwikkelde methode**
  In dit onderzoek is een probabilistische methode ontwikkeld die als aanzet gezien kan worden voor het uitvoeren van een geavanceerde toetsing voor de stabiliteit van dijken met bebouwing in het grondprofiel, waarbij het bezwijken van de bebouwing de stabiliteit zou kunnen beïnvloeden.
- **Toepassing in praktijk**
  Wanneer de model- en schematiseringsonzekerheden geïmplementeerd zouden worden in de modellen behorende bij de methode, kan deze gebruikt worden voor een risicoafweging in praktijk. Tevens zou het resultaat van de methode dan gebruikt kunnen worden om de invloed van dit soort bebouwing in de nieuwe toetsing (WBI2017) onder te brengen binnen de faalkansruimte die gereserveerd is voor de 'overige faalmechanismen'.

Aanbevelingen

De belangrijkste aanbevelingen voor verder onderzoek die voortvloeien uit deze scriptie zijn hieronder per onderwerp weergegeven.

- **Constructief**
  Op constructief vlak is het aan te bevelen om meer onderzoek te doen naar de model- en schematiseringsonzekerheden van de bebouwing. Dit ontbreekt op dit moment nog om de methode in praktijk te gaan gebruiken. Daarnaast is het ook aan te bevelen om ook andere faalmechanismen van het bezwijken van de bebouwing, gedurende hoogwater, te onderzoeken.
- **Belastingen**
  Het is aan te bevelen beter onderzoek te doen naar de exacte belastingen van grond en freatisch water op het gebouw. Nu worden die belastingen afzonderlijk bepaald, terwijl dit in realiteit een samengesteld systeem is, dit zal ook invloed hebben op de belastingen. Andere aspecten die de grootte en de spreiding van de belastingen en vervormingen kunnen beïnvloeden en nog niet geïmplementeerd zijn, zijn de volgende: Ongedraineerd grondgedrag, boogwerking binnen de grond maar ook binnen het gebouw, stijfheidsverschillen tussen gebouw en de dijk, maar ook tussen verschillende elementen van het gebouw. Het is raadzaam om verder onderzoek te doen naar de effecten hiervan.
- **Geotechnisch**
  Over de invloed van het bezwijken van bebouwing op het grondprofiel van een dijk is nog weinig bekend. Daarom zou er meer onderzoek gedaan kunnen worden naar het restprofiel, dat ontstaat na het bezwijken van een gebouw. Daarnaast zou vergelijkbaar onderzoek gedaan kunnen worden met de focus op andere faalmechanismen zoals piping, en falen door overslag en overtopping.
- **Uitbreiding in langsrichting**
  De methode is nu ontwikkeld en toegepast op 2D profielen. Enkele effecten van het implementeren van de 3e dimensie zijn beschreven, maar het is nog onduidelijk hoe dit in de methode verwerkt kan worden. Daarnaast kan hierbij ook gedacht worden aan het uitbreiden van deze methode om toepasbaar te maken op een dijksectie met meerdere huizen in de langsrichting van de dijk.

Contents

This page intentionally left blank.

Part I

Introduction

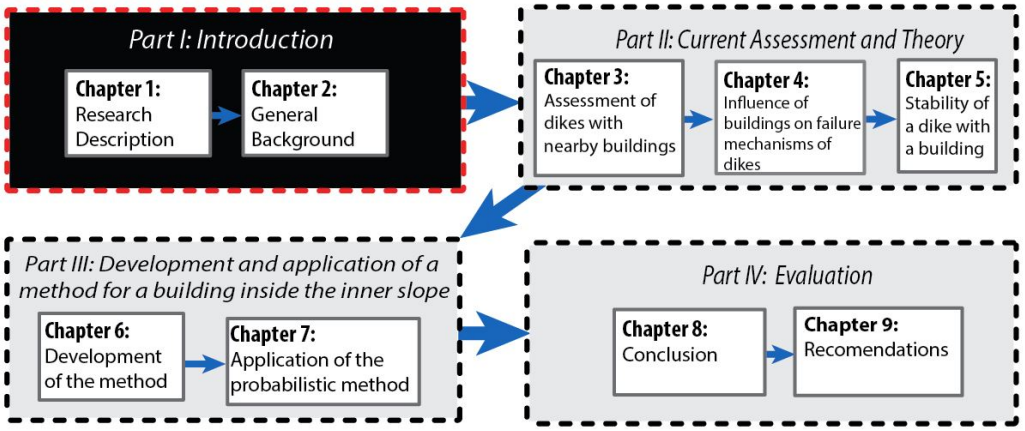

This page intentionally left blank.

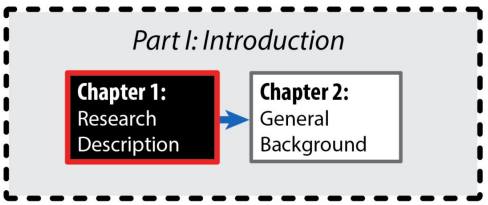

Chapter 1

Research Description

In The Netherlands almost 17.500 kilometers of water defenses are present, from which 3.800 kilometer are primary water defenses. These primary defenses prevent the flooding of area's that are prone to floods from the major rivers and the North Sea. Especially the low-lying parts of the Netherlands are highly populated which gives a lot of pressure on the spatial development of these areas. In addition, in the past, populated areas have often grown nearby strategic locations such as rivers, seas and estuaries. This has often resulted in multifunctional use of water defenses. A variety of other functions and objects can therefore be found nearby water defenses. For instance housing, roads, fences, stairs, livestock, ducts and cables.

An common example of multifunctional use of a water defense is the presence of buildings near or in dikes. In the past a lot of buildings have been built near or on the dikes. Buildings also have become part of the dike system due to reinforcements of these dikes. Nowadays operators of water defenses try to avoid new buildings near dikes, because it could influence the safety of the dike and it could interfere with future maintenance, and inspection of the dikes. However during dike reinforcements, operators still have to deal with these buildings near dikes. Sometimes buildings have to be demolished or special structures (like: sheetpiles or slurry walls) are needed to guarantee the safety of the water defense. Nowadays demolishing houses is not that socially accepted anymore, while special structures are rather expensive. Recently the call for research to a safe and multifunctional way of using water defenses is getting stronger (2e Deltacommissie, 2008a). However there are still a lot of impediments that interfere with this necessity.

An example of multifunctional use of water defenses that occurs for a long time are buildings near dikes. These buildings are classified as non water retaining objects (NWO) in the dutch safety standards. Just like pipelines, roads, trees and other objects near water defenses that are also classified as NWO's. These objects have in common that

they do not fulfill a water retaining function but because they are in the influence zone of the water defense they could influence their behavior.

1.1 Problem Description

During the assessment of water defenses it is often difficult for the operators to deal with a building near or on the dike. In the past assessments this has often resulted in dike stretches which could not be judged. When reinforcements needed to be executed, buildings often interfered with these reinforcements. This could lead to demolishing of the buildings or the implementation of expensive structural measures to assure the safety of the defense. In the assessment of defenses with nearby buildings there is only looked into possible negative effects that they have on the defense. And by ignoring the possible benefits or including negative effects that are not realistic, water defenses are on the locations of buildings designed in a (too) conservative way.

The safety of a flood defense system depends on the parts in this system. Parts can be for instance dike stretches, which can fail in different ways, or other words: due to different failure mechanisms. This can be illustrated by means of a fault tree, which is a schematization of events that could lead to one unwanted "top event". When a closer look at the fault tree of a dike ring is taken , it can for instance be drawn as in figure 1.1, where some of the failure mechanisms have been included. The failure probability, for the top event "failure dike ring", is (for example) determined to be $P_f = \frac{1}{10{,}000}$ per year and when a distribution over failure mechanisms is assumed, this results in demanding failure probabilities for the different mechanisms.

When a dike ring is considered that contains a building, failure could occur at the location of the building or somewhere else on the dike. A fault tree of this situation, illustrates this see figure 1.2. The demand probabilities from the part without a building could be kept the same. But the part with the building is more difficult because the failure probabilities of this part could change because of the presence of the building and are therefore more difficult to determine.

The building could have a negative effect on the safety, i.e. increase the failure probability. And there are also positive effects a building can have on the failure probability and therefore cause a reduction of failure probability. Sometimes these changes in failure probability are referred to as additional or reduced failure probability (see text box).

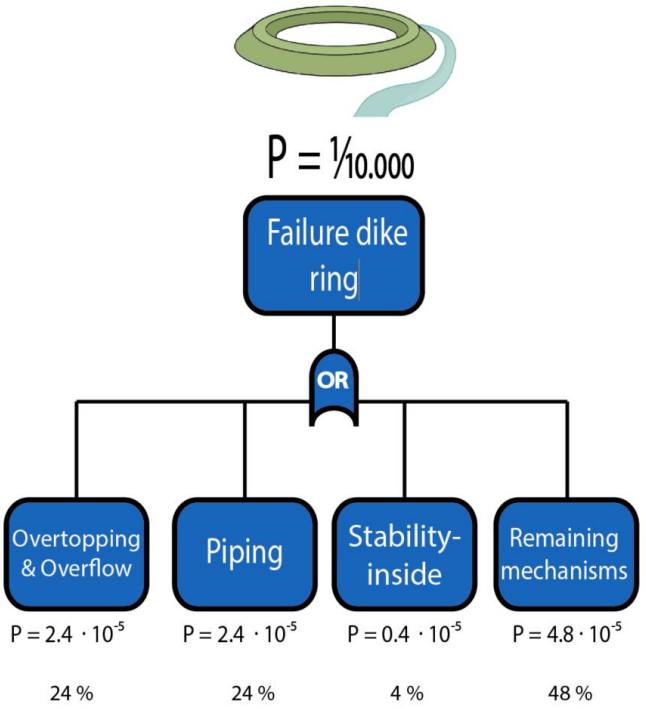

FIGURE 1.1: Fault tree of a dike section (This figure is only for illustration of the problem and do not fully represent the Dutch safety assessment approach)

Terminology: Additional failure probabilities

In this report when an additional failure probability is mentioned, the increase of failure probability induced by the presence of a structure near the water defense compared to a situation where only a dike is present, is meant. The opposite: a reduced failure probability means a decrease of failure probability induced by the presence of a structure near the water defense.

In 2017 new safety standards regarding flood defenses will come into force (see subsection 2.3.1 page 19), in which more advanced probabilistic methods for assessment are available. When the influence of a building on the safety of a dike can be determined in a more precise way, this might make it possible to include these effects in the assessment. Perhaps, on a cross section level, when the effects of a building can be determined in a more precise way, the beneficial effects of a building could be used to compensate for the negative influence of the same building.

The possible failure or collapse (see text box) of a building itself also influences the effects that a building has on a dike. How to treat the possibility of collapse of the building is challenging during an assessment. A safe way to cope with this could be to assume that the building is absent. But possibly this leads to a (too) conservative approach that results in the implementation of unnecessary structural measures.

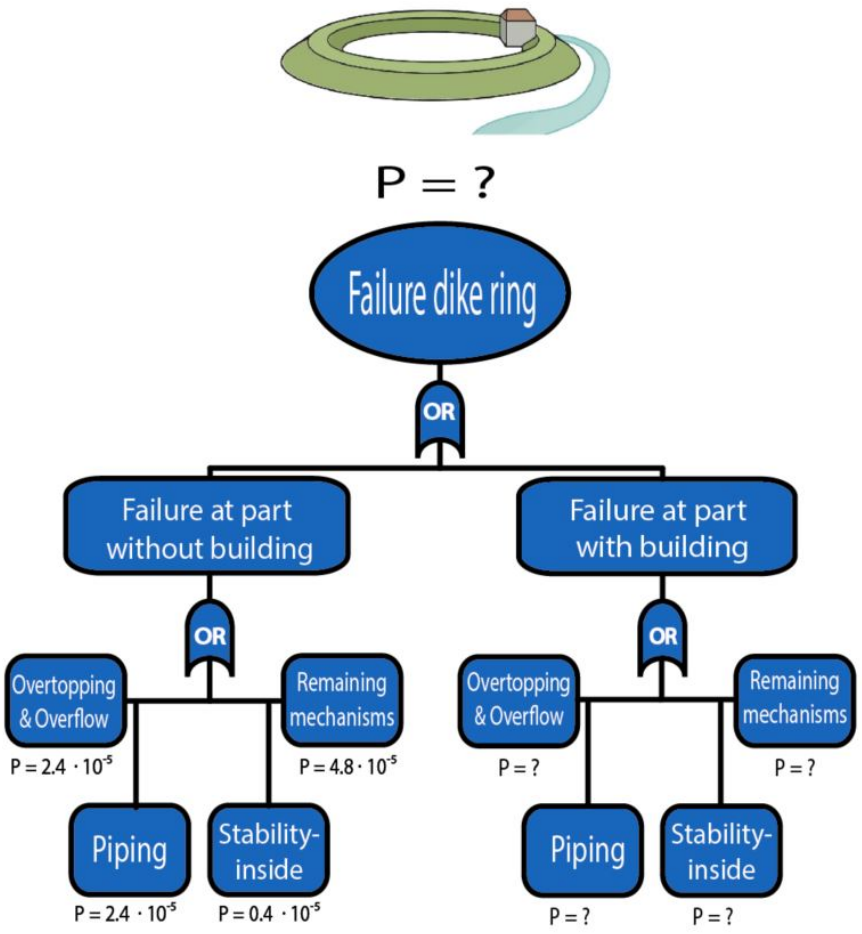

FIGURE 1.2: Fault tree of a dike section with a building (This figure is only for illustration of the problem and do not fully represent the Dutch safety assessment approach)

Terminology: Dike failure and building collapse

To distinguish the difference between failure of a dike or a building, the failure of a building is always referred to as collapse. So the term collapse is used for structural failure of the building and failure itself only for dikes. Within the field of structural safety collapse is often mentioned as one sub category of structural failure, and is defined as: "The (sudden) breakdown of a structure due to insufficient strength or stability". (Terwel, 2014) This definition is also adopted in this thesis; so for instance collapse does not refer to the occurrence of cracks or settlements.

The flood risk of a certain dike ring area depends on the safety of the dike ring. The dike ring itself can be seen as a collection of different dike cross sections. The overall safety of a dike ring is most influenced by the cross section that is relatively the weakest i.e. the dike ring is as safe as the weakest cross section. Therefore in an idealized situation a dike ring would be totally homogeneous. In reality this is never the case and therefore when dike reinforcements are executed it is economically beneficial to start with the

weakest parts. Since the safety of a cross section can be influenced by a building the weakest sections could be the ones that contain a building. In that case it is economically beneficial to reinforce this section. However when a building is part of a relatively safe (overdimensioned) cross section the influence of structural measures for this section, on the overall safety of the ring is negligible and therefore not economically efficient. When the influence of a building can be determined in a more precise way, it can become more clear whether dike cross sections with a building are a relatively weak or strong part.

Another problem of the assessment of NWO's is the huge amount of work that is needed for this assessment. This is caused due to the structure of the assessment and that is arranged by object. Because of the large amount of NWO's this results in a lot of work for the operators. For example there are an estimated amount of 44.000 buildings and 314.000 trees classified as NWO's near Dutch river dikes[1].

1.2 Research objective

The objective of this thesis is described in this section. First a categorization for buildings near dikes will be proposed, later the approach of the research is clarified and then the corresponding research questions are elaborated.

1.2.1 Categorization of buildings near dikes

In this part of the study the focus lies on all kind of buildings near water defenses. Therefore a categorization, that is used in the remainder of this thesis, is proposed. To distinguish the different effects and to clarify the possibilities of buildings on dikes this categorization is proposed and shown in figure 1.3. This categorization is based upon five possible locations of the building (foreland, outer slope, crest, inner slope or the hinterland), two foundation methods (shallow foundation or a pile foundation) and two positions of the building regarding the water retaining profile of the dike (on (soil) profile or in (soil) profile). Off course also other combinations of intervening locations are possible, but in this categorization the most important properties that are relevant are exemplified. This categorization will be the starting point for the research performed in this thesis.

[1]Based on an extrapolation of 34 % of the Dutch river dikes

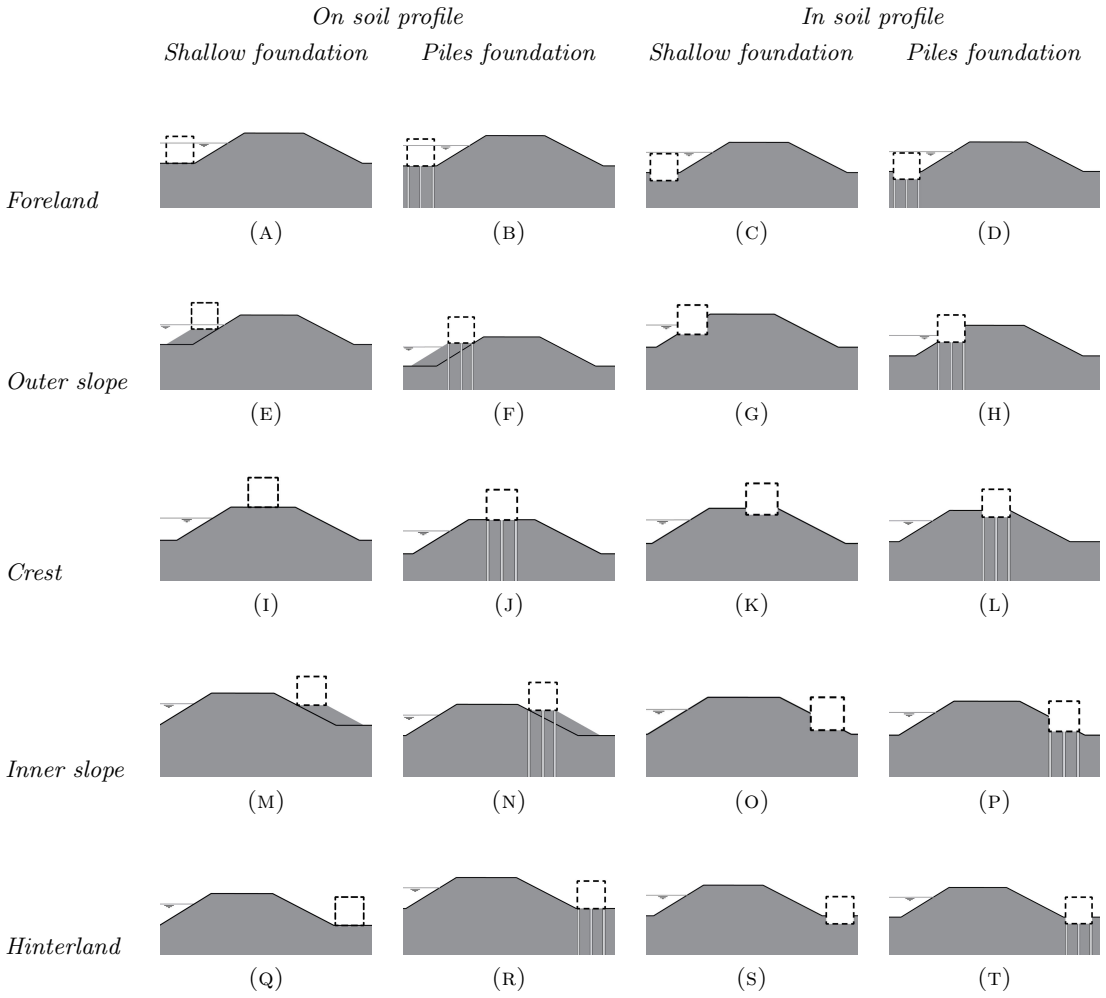

FIGURE 1.3: Categorization of buildings near dikes, (Location, Foundation method, In or On Profile)

Terminology: Configuration

The here introduced categorization of building properties with respect to the dike profile is further on referred to as the configuration. Thus a configuration of figure 1.3 A, is a situation where the building is on the foreland, located *on* the soil profile and with a shallow foundation.

1.2.2 Approach

First the current assessment of water defenses and nearby buildings is analyzed. This is done by a literature study and some interviews with professionals from the field. This is followed by a theoretical description, supported by illustrations, of the possible influence of buildings on the safety (and failure mechanisms) of a dike. This is all done for some relevant failure mechanisms (according to (VTV, 2006)) and all possible configurations shown in figure 1.3. In the next chapter further research, with some

theory and corresponding basic calculations, is performed for the influence of a building on the stability, and these results are also used to select a configuration to further delve into
This next part is only focused on a selected configuration for one failure mechanism. At the beginning a probabilistic method is developed for the selected configuration. Besides some theory and calculations are presented that focus on the interaction between the building and the dike for this configuration. Thereafter this new developed theory is applied to a case study, where it is checked whether this probabilistic method can be used to determine the influence of the building on the stability of the dike.
In the final part recommendations and conclusions of this research are presented.

1.2.3 Main research question

The above described objective is elaborated in the following main research question.

What is the influence of a non-water retaining building on the reliability of a dike, and how can this be determined and included into the assessment of water defenses?

1.2.4 Research questions

In order to perform this research the following sub-questions will be elaborated.

1. *How is the assessment of water defenses, with buildings nearby, at the moment performed?*
2. *How can building characteristics have influence on the failure mechanisms of a dike?*
3. *What configurations and failure mechanism are most interesting to focus this study on, and why?*
4. *How can the influence of a building for the selected configuration be determined, and which information should be available to perform this method?*
5. *Can this probabilistic method be applied to a case study to determine the influence of a building?*

1.3 Structure of the report

In the introduction part I the research is described (chapter 1) and this is followed by some general background (chapter 2) on flood defences and flood risk (regulation).

In the next part, 'Current Assessment and Theory' (part: II), the assessment (chapter 3) and effects (chapter 2.3.2) for all configurations are discussed. In chapter 5 the focus is shifted to the mechanism inner slope stability, where some basic calculations are performed. In this part the first three research questions are answered and the selection of configuration and mechanism, for further research, is made.

In the third part, 'Development and application of a method for a building inside the inner slope', (III) a probabilistic method is developed (chapter 5) for the selected configuration. Furthermore relevant theories and calculations, necessary for this method are collected. This is followed by chapter 7, where the developed method is applied to a case study. In this part the fourth and fifth research question is treated.

In the fourth part, 'Evaluation' (IV) there is space for conclusions (chapter 9) and recommendations (chapter IV).

In the last part (V) annexes are included.

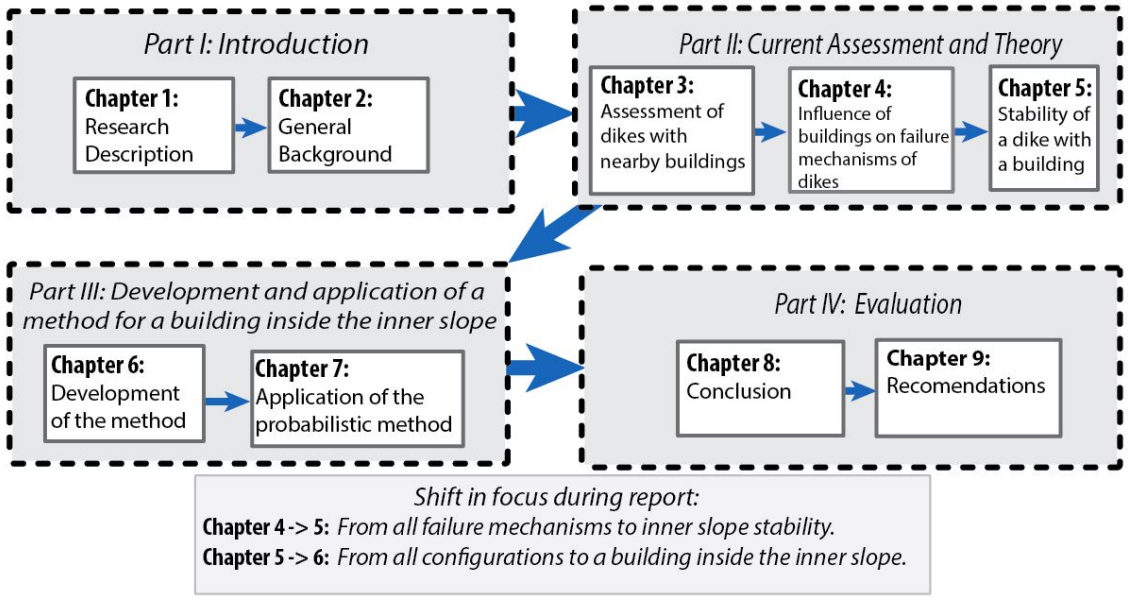

FIGURE 1.4: Visualization of structure of the report

1.4 Scope of the study

In order to define the boundaries of this study the following scope is proposed. The study focuses on buildings in or on river dikes. The priority hereby lies on buildings that are not designed for a water retaining function and are therefore part of the overall group of NWO's. Their influence on river dikes is investigated. Most of the times these are rather old buildings and are not designed to be close to a water defense. At present

newly build houses near defenses have to satisfy extra loading demands. The research focuses on the assessment of these old buildings. The dealing of buildings near dikes during a dike reinforcement is not treated in this thesis. In appendix A.1 on page 141 a short enumeration of possible measures for dike reinforcement around buildings is presented.

This page intentionally left blank.

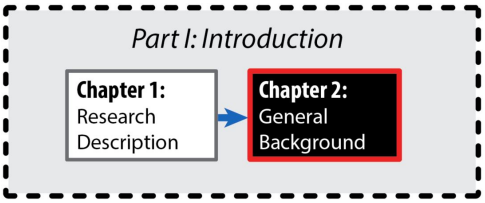

Chapter 2

General background

In this chapter general background concerning the topics of this study are given. First the topic of flood defences is introduced with a focus on dikes. Secondly relevant failure mechanisms for dikes are introduced. And finally some recent developments of flood risk regulation in The Netherlands is treated.

2.1 Flood defences

In this section background on different flood defences is presented, with a focus on dikes.

2.1.1 Types of flood defences

The main function of a flood defense is to prevent flooding of the embanked area. These area's are often embanked because they are lying beneath the occurring water levels. In general flood defenses can be divided in four different categories, see figure 2.1.

Naturally occurring defenses This category includes all parts of a flood defense system that could have originated by nature, for instance dunes or higher grounds. At coasts dunes can arise due to sand movement by water and wind, but the dunes can also be strengthened by nourishments. The water retaining principle of dunes is based upon the large amount of sand that is present in a dune. During a high water event a lot of sand can disappear because of erosion, but enough sand should stay in place to prevent flooding of the hinterland.

Soil structures This category mainly consists of dikes and dams. Dikes and dams are both artificial soil structures that have to be somewhat resistant to erosion. Dikes retain water on one side, while dams retain water on both sides.

Retaining structure In this category are all kind of structures that retain water on one side and soil on the other and are part of the flood defense system. Examples of this are quay walls, sheet piles or cofferdams. The advantage of these structures is often that they have a smaller profile, opposite thereto is that these structures are generally more expensive. Sometimes these structures are primarily used for berthing of ships.

Hydraulic structures In this category are all hydraulic structures that are part of a flood defense system. These structures have a primary function of transport through the flood defense. The transport for instance can be water, ships and cars. Examples are storm surge barriers, locks, pumping stations and coupures.

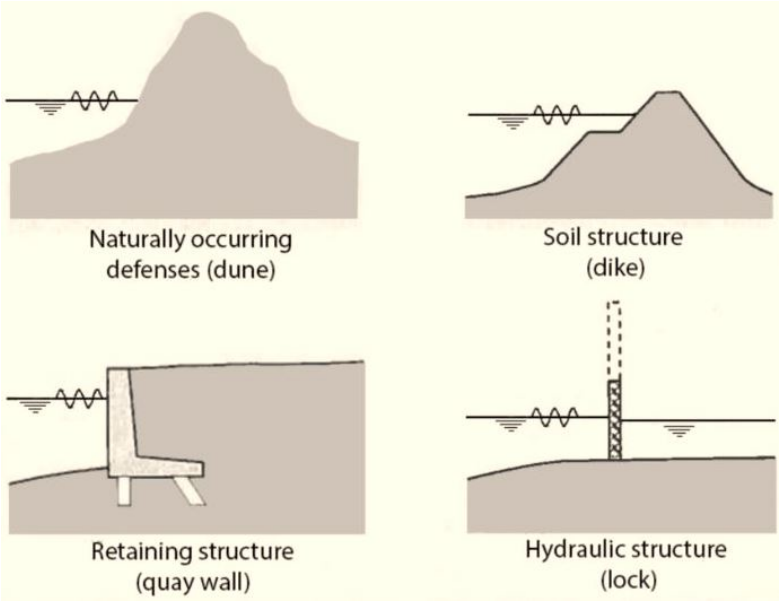

FIGURE 2.1: Types of flood defenses (TAW, 1998)

The flood prone area's in The Netherlands are embanked in so called dike ring area's by the *primary water defenses*. Other flood defenses that retain water from canals, smaller waterways or lakes are called *secondary water defenses* or *regional water defenses*. Within the primary flood defenses the Dutch safety standards also makes a distinguishing, see figure 2.2 and the explanation below:

Type A flood defenses are directly retaining water during high water events, examples can be dunes, dikes or quay walls.

Type B defenses connect different dike ring area's and do have to retain water during high water events, examples can be storm surge barriers, dams or locks.

Type C defenses are not directly retaining water during high water events, but may have to retain water when other defenses fail. An example is a land dike that divides two dike ring area's with different safety norms.

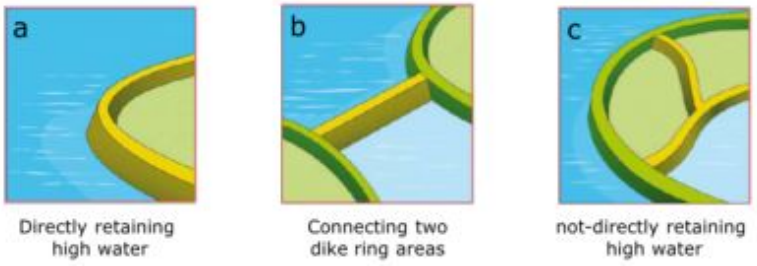

FIGURE 2.2: Division of category A,B & C flood defenses (I-V&W, 2011)

2.1.2 Dikes

Dikes form the largest part of the almost 3800 kilometers of primary water defenses in The Netherlands (Pleijster and van der Veeken, 2015). These dikes often have already a very long history in protecting low-land area's from flooding. Partly because of this they appear in numerous forms (see for typical dimensions figure 2.3). Also geotechnical boundary conditions affect the design and important properties such as subsoil conditions of the dike. An important distinction for dikes in the Netherlands is the material that is used for the soil body. In the Netherlands dikes appear that are completely constructed with low permeability materials like clay and peat but also dikes with a sand core appear (figure: 2.3). An important difference of this is the development of the freatic line inside the soil body.

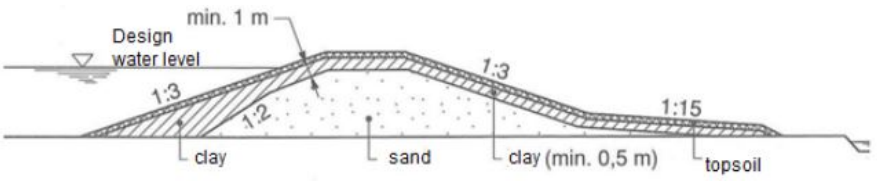

FIGURE 2.3: Example of design of dike in The Netherlands (van Leusen and Velden, 1998)

The terminology of different parts of the dike is shown in figure 2.4. The total profile of a dike is called the core zone, around it a larger protection zone is established to protect the safety of the water defense. The protection zone has a typically width of 20 meters on both sides of the dike (Jonkman and Schweckendiek, 2015). The core zone and the protection zone together are the so-called influence zone of the dike (see figure 2.4). For

construction activities in this zone nowadays a permit of the waterboard is needed. This permit will only be given if the safety of the water defense is not affected.

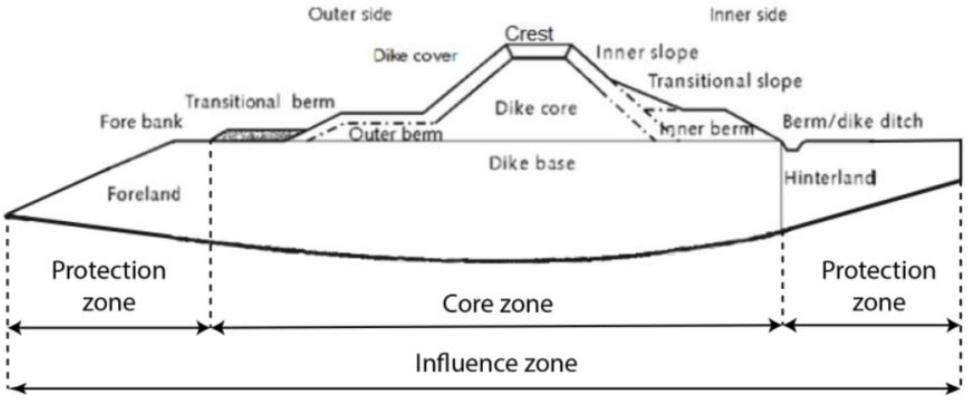

FIGURE 2.4: Terminology of parts of a dike (TAW, 2001)

Unless this regulation multifunctional use of dikes occur and the following functions can be distinguished.

Infrastructure Dikes often have roads on the crest. And also other infrastructure elements like pipelines and ducts are sometimes present, these elements can have an influence on the safety.

Living or working function Over history a lot of houses have been build in the presences of dikes. This can also result in safety issues for the dike.

Agricultural use Often dikes have an agricultural function. For dikes with a grass cover grazing livestock can help with the maintenance of the cover.

Landscape values The dikes can have a large beneficial effect for the perception of the landscape. Trees can for instance be present on dikes, but these could have a negative impact on the safety however.

Other function Other functions are also possible, like parking garages or windmills. The influence on the safety of the water defense is sometimes unknown and this can result in a reluctant approach by operators.

2.1.3 Failure mechanisms of dikes

The failure of a flood defense can occur in different ways. These are often called failure mechanisms or failure modes. The most important ones for dikes are given in figure 2.5. In the literature it is stated that some of these mechanisms are influenced by buildings.

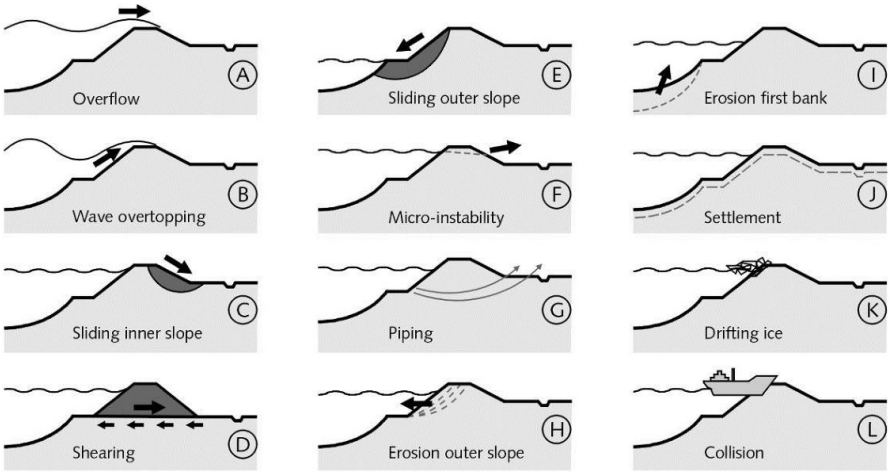

FIGURE 2.5: Overview of most important failure mechanisms for dikes (Jonkman and Schweckendiek, 2015)

These mechanisms are briefly introduced below. In (VTV, 2006) the mechanisms that have to be included in the safety assessment are also considered as assessment tracks. The corresponding assessment tracks and their abbreviations will also be introduced.

Overflow and overtopping Overflow occurs when the water level is higher than the crest of the dike. In contrast to overflow, with overtopping the water level remains under the crest but the waves cause a water flow over the dike. The combination of overflow and overtopping can result in a discharge over the inner slope of the dike. When this discharge causes erosion of the inner slope failure of the dike is assumed. In the safety assessment this mechanism is related to the height of the dike and so the corresponding assessment track is referred to as height (HT). Mechanisms A & B in figure 2.5.

Micro stability When seepage causes a high freatic line in the dike this can result in a pressure against the inner cover of the dike. When this cover is pushed off and the core of the dike is made of granular material this seepage can erode also the core and can eventually result in failure. The assessment track is abbreviated as (STMI). Mechanism F in figure 2.5.

Macro Stability Stability problems of large parts of the soil body are classified under macro stability. The most known failure mechanisms here are rotational instability of the inner or the outer slope, but also horizontal and vertical instabilities belong here. In the safety assessment these are called respectively stability inner slope (mechanism C in figure 2.5) (STBI) and stability outer slope (mechanism E in figure 2.5) (STBU).

Piping When due to a large hydraulic gradient over the dike sand particles from under the dike erode and are brought to the hinterland by seepage, pipes under the dike

can arise. When this is causing instability of the dike the corresponding failure mechanism is known as piping. The assessment track in the regulations speaks about instability due to piping and heave (STPH). Mechanism G in figure 2.5.

Erosion outer slope Erosion of the cover layer of the outer slope can initiate the failure of a dike. This cover layer of river dikes consists often of a clay layer with a grass cover. The corresponding assessment track is called stability revetment (STBK). Mechanism H in figure 2.5.

2.2 Buildings around dikes

In the influence zones of Dutch dikes there might be buildings present. Often this buildings are houses but this could also be for instance buildings related to water management (for instance pumping stations). Water management authorities try to prevent housing near dikes because it causes problems for maintenance, inspection and management of the defense (VTV, 2006). Additionally a building could also endanger the safety of the dike. Unfortunately for the water boards they have to deal with the buildings because they are already present around a lot of dikes.

In the Dutch standards objects that do not fulfill a water retaining function but could have influence on the water defense are called non-water retaining objects(abbreviated as NWO's). Four different categories are distinguished (VTV, 2006):

- Buildings.
- Vegetation.
- Pipelines.
- Other non water retaining objects.

When these objects are in the influence zone of a water defense they are classified as NWO's. The assessment of NWO's in dikes and also around dunes (Boers and Steetzel, 2012) is often complicated and not very clear. In chapter 3 a more detailed description is given on this assessment.

2.3 Flood risk regulation

In this section background on flood risk regulation in The Netherlands is presented. In the second subsection also a research project on flood risk in The Netherlands is described since it is based on the principles of the new safety standards.

2.3.1 Recent developments of flood protection

In 2007 the Dutch government appointed a new delta committee. The task of this committee was to advice on how to keep The Netherlands protected against floods concerning the consequences of climate change. One of the recommendations of this delta committee was to update the safety standards in a more advanced way. The advice of the committee was adopted by the government and this resulted in the enforcement of a new Delta-law in 2012. In this Delta Act the needed developments and funds for the coming decades are fixed by law. Since 2008 the recommendations of the delta committee are further elaborated and this resulted in new research projects and the start of the new safety standards. (2e Deltacommissie, 2008b)

Since 1996 the act of the water defense prescribes an assessment of the primary water defenses once every five years, later this frequency was reduced to once every six years. The results of this assessment have to be reported to the responsible ministry of the Dutch state. After the third assessment(2006 - 2011) the frequency of assessment has been adjusted to once every 12 years. This was partly done because the new regulations for the fourth assessment were not ready yet (EurECO, 2014). In order to reduce the amount of 'not judged' sections of water defenses, the third assessment round was extended. The result of the extended third assessment is shown in table 2.1 and in figure 2.6. (I-V&W, 2011) (I-L&T, 2013)

Table 2.1: Results extended third assessment round

Judgement	**Length of dikes [km]**	**Number of structures**
Sufficient	2408	868
Insufficient	1302	799
No judgement	39	110
Total	3749	1777

The dike stretches that have been assessed insufficient, are included in the dutch flood protection program (Hoogwaterbeschermingsprogramma abbreviated as HWBP). Within this program the rejected dikes are reinforced based on financial agreements between the water boards and the national government. Reinforcements are financed for 50 % by the national government, for 40 % by all the waterboards together and the last 10 % by the waterboard that operates this specific dike. (Rijkswaterstaat, 2014)

Currently there is a shift in the approach of designing and assessing flood defenses. In the past this was done according to standards which were based on the probability of exceedance of the water level. From 2017 flood defenses have to be assessed and designed in accordance with the probability of flooding of the hinterland . In order to calculate

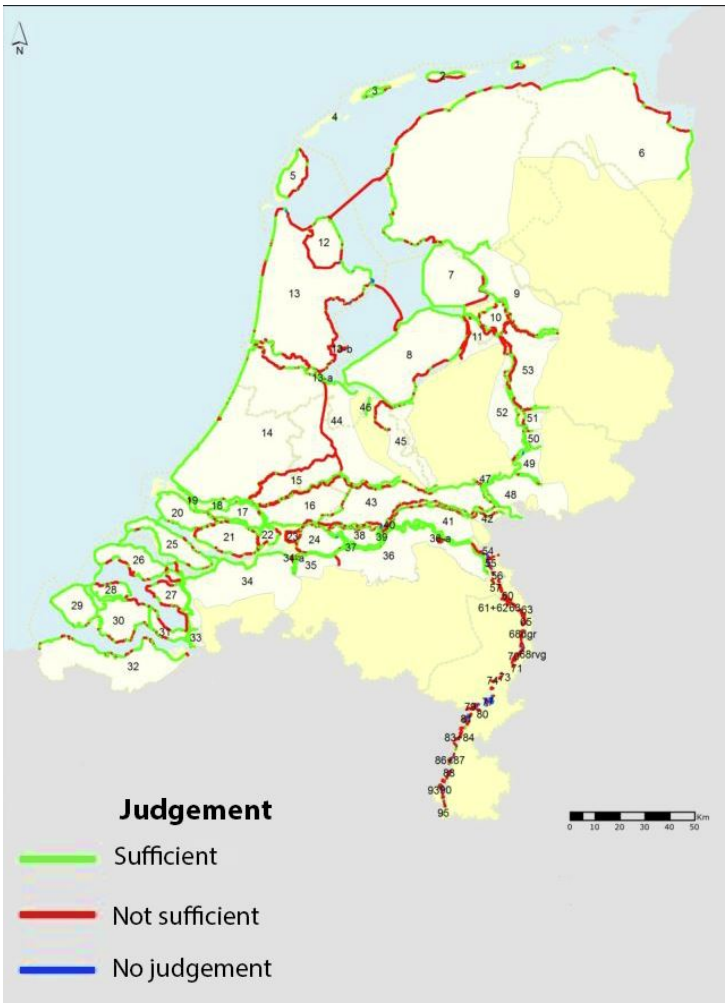

FIGURE 2.6: Map with results of the extended third safety assessment (I-L&T, 2013)

this, many more parameters of the water defense have to be known. This new approach also has been used in the research project VNK 2, and therefore this is elaborated in the subsection below.

2.3.2 Flood Risk in the Netherlands

The project 'Veiligheid Nederland in Kaart 2'(VNK 2, in english: Flood Risk in the Netherland) was a research project to determine the flood risks in the Netherlands. The project was initiated by the Ministry of Infrastructure and the Environment in 2006 and was finished in 2014. The knowledge and findings that were revealed during the project are being used in the development of the new Statutory Assessment Tools(WBI, see section 2.3.3). Therefore the approach of VNK2 is discussed.

To determine the flood risk, VNK2 determines the probability of a flood and the consequences of a flood, multiplying both gives the flood risk.

$$Risk = Probability \cdot Consequences \tag{2.1}$$

The probability of a flood is determined by calculating the failure probability of the different homogeneous dike stretches of the dike ring. For all possible locations of failure the consequences (economic damage and casualties) are determined. The result is the flood risk of one dike ring. The risk is calculated by three different methods; Economic risk, local individual risk and societal risk. The economic risk is a yearly expectation of the economic damage caused by floods expressed in $euro's$. The local individual risk (LIR) is the probability that a person on a certain location dies due to a flood. Finally there is looked into the societal risk, this is the probability of a flood with a certain amount of fatalities. The risk is expressed in a relationship between number of fatalities of a certain flood and the probability of this flood.

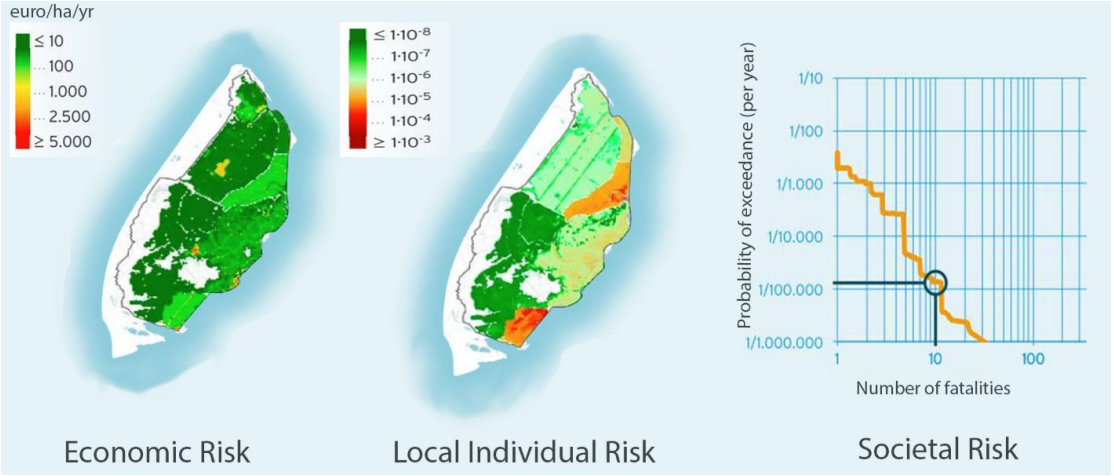

FIGURE 2.7: Risks calculated in VNK2 (VNK2, 2014)

The result of the VNK2 project shows that the coastal area is relatively safe, because the probability of failure of the dunes is rather low. The risks in the river area's on the other hand are larger(see figure 2.8). Also inside dike rings the risks vary a lot. This is caused by difference in elevation, population density and the differences in failure probabilities of different dike stretches. Therefor the new standards will have a safety level per dike stretch instead of a safety level per dike ring. During dike reinforcement programs it is then possible to invest more focused and efficient. The failure mechanism piping in the riverine area appears to be more important then was thought. This finding is taken into account in the development of the new Statutory Assessment Tools for 2017, see subsection 2.3.3 (WBI2017: Wettelijk Toets Instrumentarium 2017).

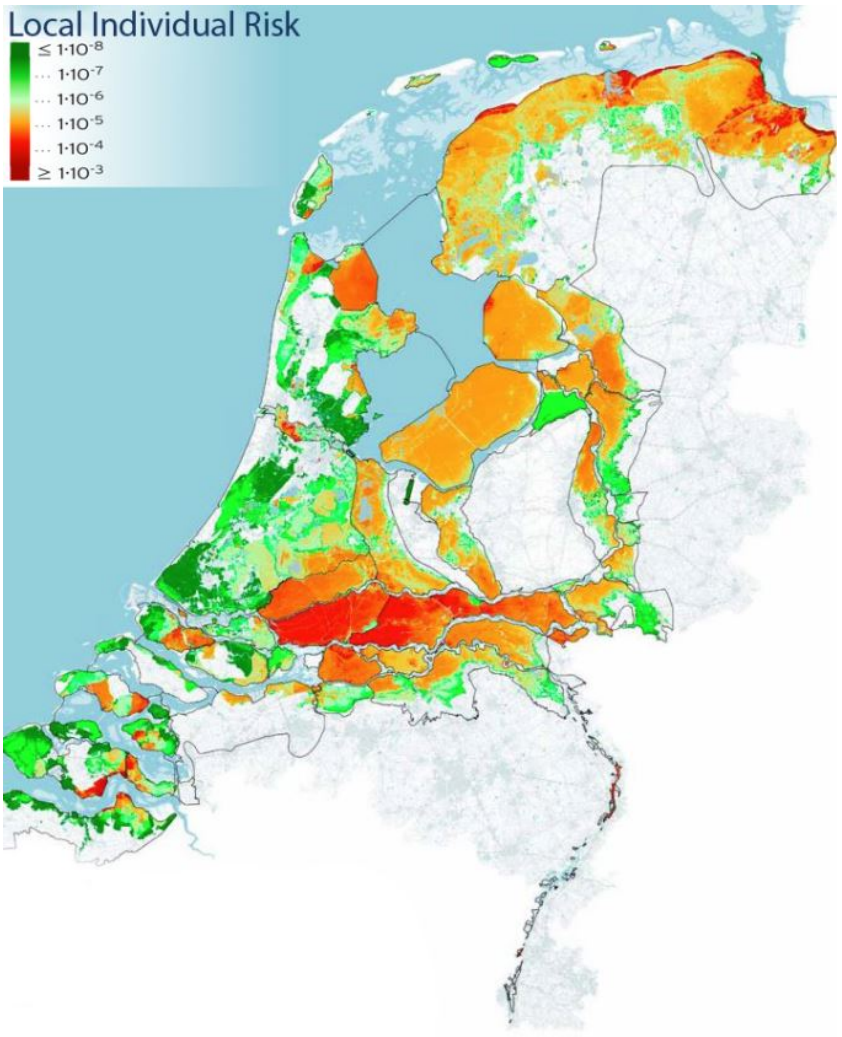

FIGURE 2.8: Local individual risk The Netherlands (VNK2, 2014)

In the VNK project the probability of exceedance approach (explained in subsection 3.1.1 on page 31) is not used anymore. Instead there is looked at the chance a flood occurs. This probability of flooding equals the chance that a load occurs which is larger than the strength of the water defense, somewhere in the dike ring. To compute this probability all loading and strength parameters need a probability distribution that properly quantifies the uncertainty. This approach is called the probability of flooding approach. (VNK2, 2011b) The benefit of this approach is that a certain safety level can be achieved in a more efficient way and could be cheaper. (VNK2, 2011a)

2.3.3 Statutory assessment tools 2017

The fourth assessment round of the Dutch primary water defenses will start in 2017 and the results will be reported in 2023. For this fourth assessment round the new Statutory Assessment Tools 2017 (WBI-2017) have to be used. Some new principles

of the WBI-2017 are already published or communicated. Some of these principles are already introduced in section 2.3.2 about the VNK project. Other (new) principles of WBI-2017 are discussed in this section. These principles are already published so that they can be used during current dike reinforcement programs, in order to prevent that these dikes will be rejected in 2023.

As mentioned before the new standards are based on the probability of flooding approach. There are three different probabilities that are used for the primary water defenses.

Maximum allowable probability This probability is defined as the chance that the damage of a flood expressed in costs is as large as the costs of reinforcement of the dike. This probability is rejection limit.

Mid Probability The mid probability lies in between the maximum allowable probability and the optimal design probability and is related to the mean damage in between two dike reinforcements. This value is used as signal value and is also suggested as the new safety standard value. see figure 2.10.

Optimal design probability This probability is based on economic considerations what the optimal reinforcement ratio of a certain dike is.

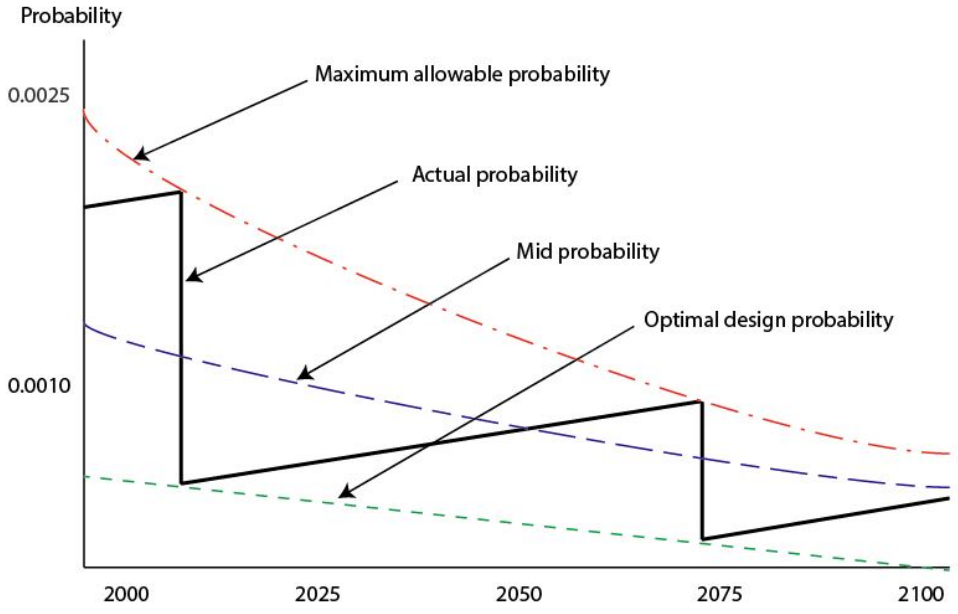

FIGURE 2.9: Example development of the different probabilities that are described in WBI2017

These probabilities behave during the life cycle of a water defense for instance as follows: When the maximum allowable probability of flooding is reached, a reinforcement design

is made based on the optimal design probability. Due to the reinforcement the probability of flooding suddenly decreases. During the life cycle of the defense this probability gradually increases again due to climate change and land subsidence. On the other hand the mid and maximum allowable probabilities decrease due to an assumed increase of consequences of a flood because of economic growth. When the mid probability equals the actual probability new reinforcement plans have to be made, these will be executed when the actual probability equals the maximum allowable probability. The development of these probabilities and the actual probability of flooding are exemplified in figure 2.9. So, for the assessment of water defenses the actual probability will be compared with the maximum allowable probability. The relation between the signal value(mid probability) and maximum allowable probability is a factor three. So the maximum allowable probability can be obtained by dividing the signal value by three. (KPR, 2015)

The signal values(mid-probabilities) for the different dike stretches which will be used from 2017 are not yet officially established. But in (Staf deltacommissaris, 2014) a proposal is made (see figure 2.10). If these demanding probabilities of flooding are compared with the old probabilities, which where homogenous per dike ring, large differences can be seen especially in the riverine area.

FIGURE 2.10: Proposal values for new standard (Staf deltacommissaris, 2014)

In order to determine the required failure probability per failure mechanism WBI2017 uses a fixed division of failure mechanisms. This division divides the total failure probability over the different failure mechanisms. In this way the division determines the design of the water defense. For instance if a relatively large amount of failure probability is reserved for the height of a dike, the needed failure probability for this mechanism is relatively low, compared to other mechanisms. This will result in a relatively low but wide dike. The other way around if a small amount of probability is reserved for height, the needed failure probability for the mechanisms related to height becomes relatively high. This leads to a higher but smaller dike.

The division of failure probabilities of WBI2017 can be seen in table 2.2 (Jongejan, 2013). This division is made with so called 'failure space', which is the part of the total available failure probability that is reserved for a certain mechanism. This division is made under the assumption that the different mechanisms are independent. This division is made in such a way that dikes in The Netherlands will be designed in a economic efficient way. An economic division is a division where the dominant mechanisms have a large failure space and less relevant mechanisms have a smaller failure space. Besides that also policy considerations can be taken into account in the division of failure mechanisms.

TABLE 2.2: Proposed division of failure space (Jongejan, 2013)

Type of water defense	**Failure mechanism**	**Dune**	**Dike**
Dike	Overflow & Overtopping	0 %	24 %
	Heave & Piping	0 %	24 %
	Macro stability inside	0 %	4 %
	Failure due to revetment or erosion	0 %	10 %
Structure	Non closure	0 %	4 %
	Piping	0 %	2 %
	Structural failure	0 %	2 %
Dune		70 %	0 %
Remaining mechanisms		30 %	30 %
Total		100 %	100 %

In the table 2.2 it can be seen that there is also an item, remaining mechanisms, which has a failure space of 30 %. This space is intended for other failure mechanisms like micro-stability and erosion of the first bank. But also failure due to earthquakes or terrorism belong in this group. And for the assessment of buildings near dikes this is an important group because failure due to the presence of a NWO is also included in this category. This group of remaining mechanisms is also referred to as indirect failure mechanisms. In the current elaboration of WBI-2017 no extensive assessment tools are developed for this group of remaining mechanisms. This also implies that operators can

use this 30 % for specific dike properties that might not be common for all dikes. For instance the additional risk imposed by buildings on or near a dike.

So, with help of the division of mechanisms the step is made from a failure probability for a water defense to a failure probability per mechanism. This is an important step because for the design and assessment of water defenses the failure probabilities can only be calculated separately. The last step is to achieve a failure probability per mechanism for a certain cross section in the dike stretch. This step is related to the so called 'length effect'.

The length effect has to do with uncertainty. Because in practice data is only available at a limited amount of locations, it is not exactly known what the conditions are between these points. The longer the stretch, the greater the possibility that there are somewhere relatively weak conditions on this stretch. The length effect can also have an influence on the loading conditions of a water defense. For example for a long stretch of a dike with different orientations the probability that somewhere the wave run up exceeds a certain value increases. To account for this effect WBI2017 adjusts the failure probabilities for a profile. The longer the stretch, the stricter the demanding failure probability in a cross-section is, to meet the demanding failure probability on a section level.

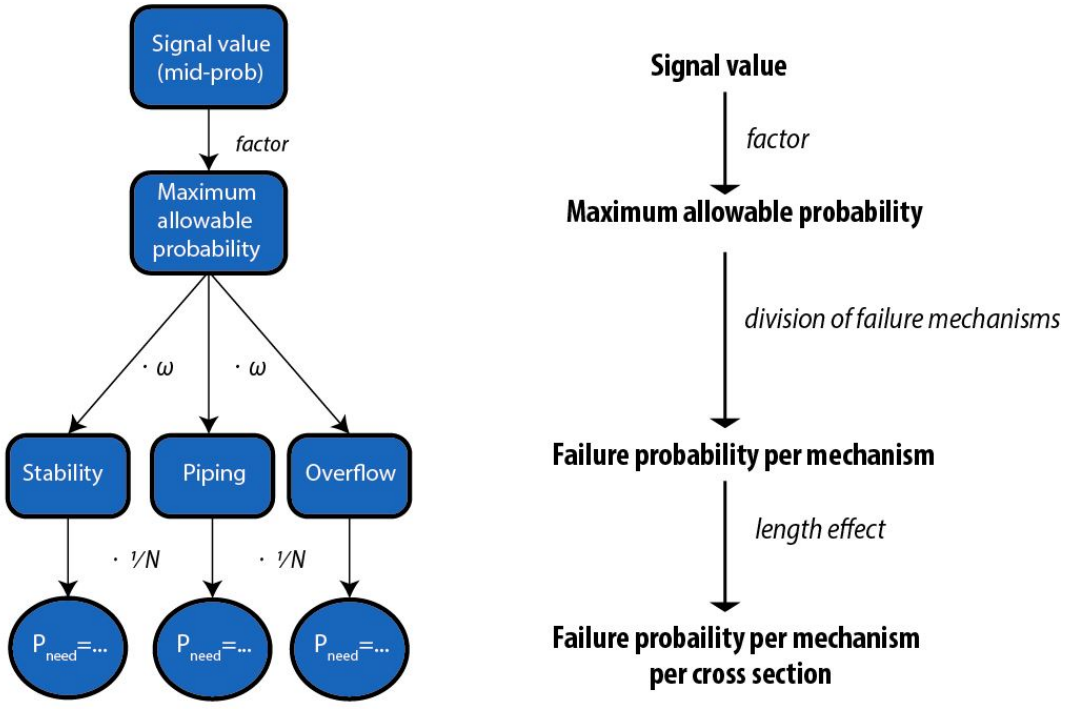

FIGURE 2.11: Overview calculation method of failure probability

The formula's to transform a standard value to a failure probability per mechanism on profile level are (Rijkswaterstaat et al., 2014):

$$P_{dem,fm} = \frac{P_{norm} \cdot \omega}{N} \tag{2.2}$$

$$N = 1 + \frac{a \cdot L_{section}}{b} \tag{2.3}$$

in which:

	$P_{dem,fm}$	=	The demanded failure probability for a mechanism in a profile $[yr^{-}1]$
	P_{norm}	=	Maximum allowable probability according the norm $[yr^{-}1]$
	ω	=	failure space factor $[-]$
	N	=	Length effect factor $[-]$
	a	=	factor related to the sensitivity of the length to the failure mechanism $[-]$
	b	=	factor related to length of independent equivalent sections $[m]$
	$L_{section}$	=	Length of a dike section $[m]$

In figure 2.11 an overview is given of the methodology on how to transform a signal value to a failure probability value which can be used for assessment.

This page intentionally left blank.

Part II

Current Assessment and Theory

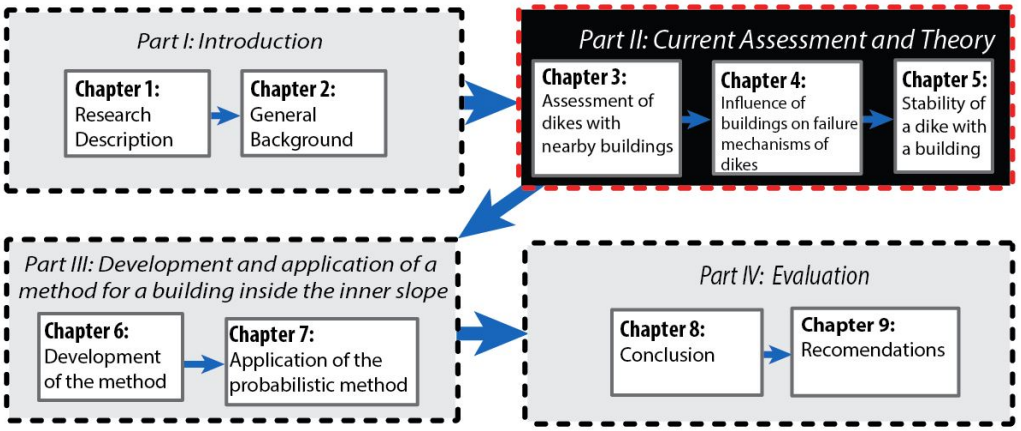

This page intentionally left blank.

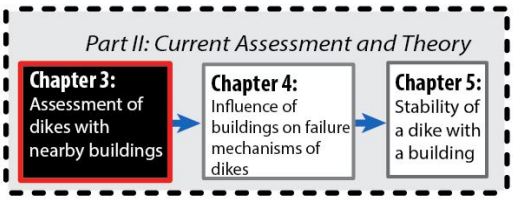

Chapter 3

Assessment of dikes with nearby buildings

In this chapter the first research question is answered; *How is the assessment of water defenses, with buildings nearby, at the moment performed?* First the statutory regulation (VTV-2006) and other publications regarding the assessment of NWO's are over-viewed. Afterwards the assessment of buildings in practice is discussed. Finally, the subquestion is answered compactly in the conclusion section.

3.1 Current safety assessment of dikes with nearby buildings

In this section documentation concerning safety assessment of dikes that are influenced by the presence of buildings, is treated.

3.1.1 Statutory regulation

The "Voorschrift Toetsen op Veiligheid 2006"(abbreviation: VTV2006, in English: Regulation for the Safety Assesment 2006) is the legal provision which had to be used for the third assessment (2006-2011) of the Dutch primary flood defenses. The VTV2006 is part of the Statutory Assessment Tools 2006 (WTI2006) which are currently valid (Helpdesk Water, 2015). The VTV safety standard is based on design water levels. Each dike ring has been standardized with a standard-frequency of for instance $\frac{1}{1250}$ *per year*, this means that the height of this dike ring should be designed to safely retain a water level which is exceeded on average once every 1250 years. It was assumed that if only

a small amount of overtopping or overflow would occur during this design water level, the safety against the other failure mechanisms was guaranteed because of the use of (partial) safety factors relating to the remainder mechanisms. This approach is called the probability of exceedance approach.

One of the failure mechanisms mentioned in (VTV, 2006) is:"The occurrence of one of the mentioned failure mechanisms (see section: 2.1.3) as a result of the presence of a non water retaining object". In the VTV2006 a section is dedicated to the assessment of non water retaining objects. For this assessment the scheme of figure 3.1 is used. The assessment consists of a total of six steps which are elaborated below.(VTV, 2006)

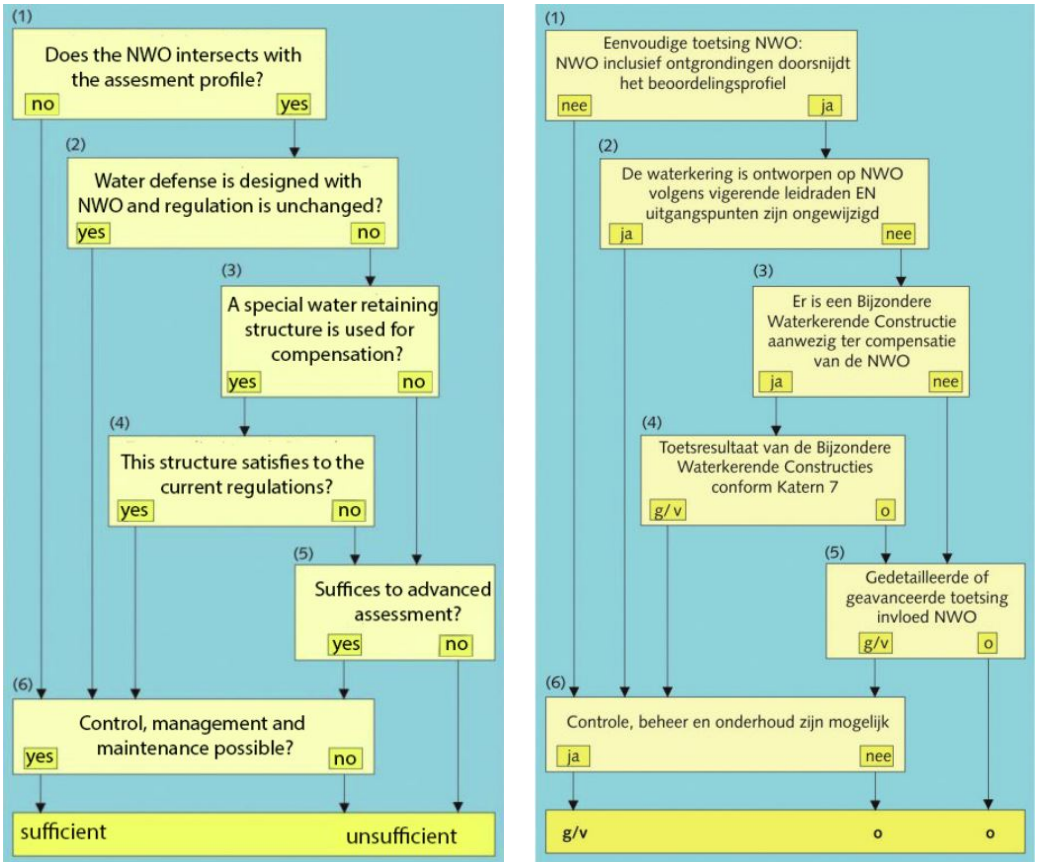

(A) Translated in English (B) Original Dutch scheme

FIGURE 3.1: Assessment scheme non water retaining objects (VTV, 2006)

1. The first step is to determine whether the object intersects with the assessment profile of the water defense. The possible earth removal zone, that could occur after collapse of the building, should also not intersect with the assessment profile. Some foundation elements are allowed in this profile, provided that they are water tight. The assessment profile of the dike is the part of the profile which is minimally needed to retain the water level that is prescribed in the safety standard. It can be constructed by combining critical lines that are needed for the different failure

mechanisms. The envelope of these lines is the assessment profile (see figure 3.2). Furthermore it is mentioned that if a building is placed on the crest or the slopes and it can not be excluded that a negative force is imposed due to the building, the assessment has to be continued with step 2.

2. If the building intersects the profile the assessment continues with step two. Here the question is whether the building is designed in accordance with the current guidelines for buildings or structures near water defenses. Referred is to the Guidance for Hydraulic Structures (TAW, 2003), Guide for Constructive Design (TAW, 1994) and the Technical Report Water-retaining Soil-structures (TAW, 2001).

3. If this is not the case in step three, the object has to be checked, whether there are structural measures that are capable of compensating for the presence of the building in the assessment profile. If this is not the case the assessment proceed with step five.

4. If there are structural measures to compensate these should be assessed and approved according to the relevant guidelines. Referred is to chapter seven of (VTV, 2006), or Guidance for Hydraulic Structures (TAW, 2003) and CUR Publication 166 for Sheetpile-structures (CUR 166, 2008).

5. If no compensating measures are taken the additional failure probability of the building has to be determined in an advanced assessment. Which probability is acceptable is not clear.

6. The last step for approval always is to asses whether monitoring, management and maintenance of the water defense is possible despite of the presence of the object.

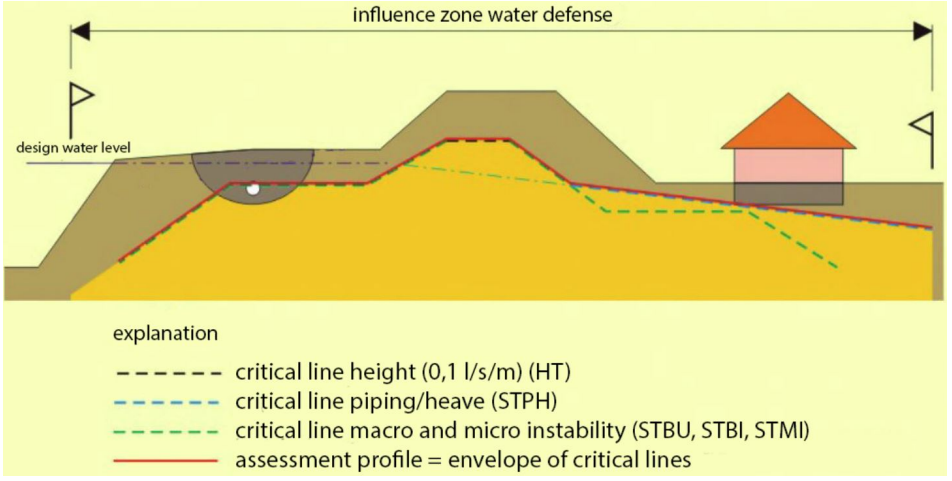

FIGURE 3.2: Example of assessment profile (VTV, 2006)

Regarding collapse of a building the following is mentioned in the VTV2006: In the assessment the possible absence of the building has to be taken into account, including

the possible soil failure due to building collapse. This soil profile after collapse is referred to as the residual profile. When it is possible to exclude building failure caused by a poor state of maintenance or calamities the building collapse scenario can be dropped. From this it can be concluded that there are no clear guidelines when it is possible to drop the scenario of an absent building and a residual profile. The determination of this residual profile is also not further described therefore it might be difficult to assess whether an residual profile intersects with the assessment profile.

3.1.2 Additional documentation for assessment

In the years after publication of VTV-2006 it appeared that water defenses operators had some difficulties with the assessment of NWO's. Therefore some additional reports have been published in order to assists operators with this assessment. The publications from (Hoffmans and Knoeff, 2012) & (Beijersbergen and Spaargaren, 2009) will be treated in this section. For pipelines an advanced (probabilistic) assessment has been applied. This method is described in (Sanders and Wiggers, 2015) and is also treated.

According to (Beijersbergen and Spaargaren, 2009) some problems with the assessment of NWO's after the publication of the (VTV, 2006) were:

- The collection of properties of the large amount of NWO's.
- In the urbanized area's the large amount of buildings and pipelines cause problems.
- The construction of the assessment profile is experienced as (to) difficult.
- The lack of detailed assessment methods.

Because the third assessment round was focused, among others, on NWO's and because of the mentioned problems it was feared that a lot of NWO's could not be assessed. I.e. get the verdict 'no judgment'. To prevent this they made a publication with basic rules to get to an operators judgment. This operators judgment, which should be well substantiated, could then be used to approve NWO's, which could not been approved based on (VTV, 2006).

Therefore for buildings that are located in the assessment profile of the water defense figures 3.3 should give operators the knowledge which assessment tracks are influenced by the building. In that way some extra calculations within the specific assessment track can be made to approve or disapprove the building. Or at least to be able to assure that the effects of the building seem acceptable. Also some basic rules for the assessment tracks are given to make sure that only for the complicated cases these extra research and calculations steps are necessary. Some of these basic rules are given below:

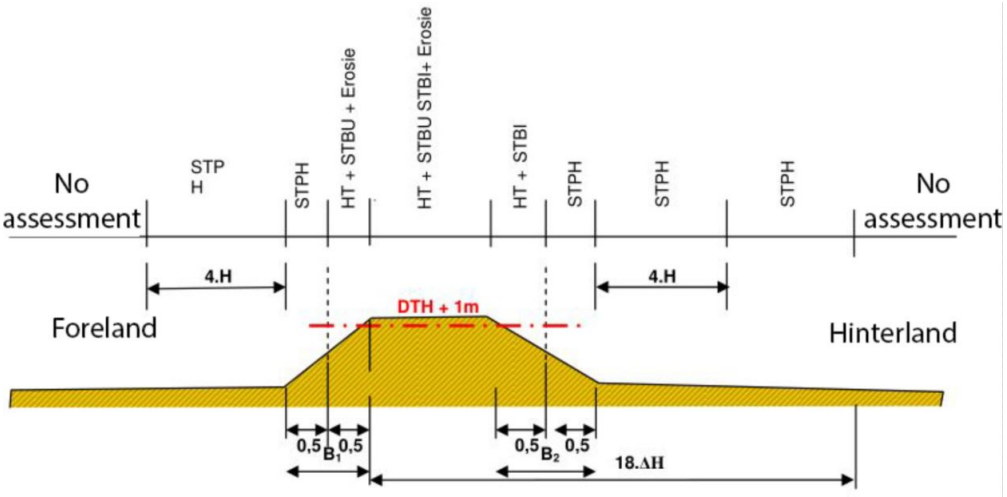

(A) Dike cross section with assessment tracks for different locations

Effect location building within influence zone water defense						
Location	Failure mechanisms - assessment tracks					
	Erosion	STBU	STPH	HT	STBI	STMI
Foreland	0/- 5)	0	0 4)			
Outer slope	0/-	0/-				
Outer crest		-		afh DTH 2+3)		
Inner crest				afh DTH 2+3)	-	
Inner slope				afh DTH 2)	0/-	
Hinterland			-		0	

+	Positive effect
0/+	Neutral/positive effect
0	neutral effect
0/-	Neutral/negative effect
-	Negative effect
	n.v.t.

(B) Table with assessment tracks and locations

FIGURE 3.3: Tool to assess which failure mechanisms are affected by a certain building (the used abbreviations are introduced in subsection 2.1.3 (page 16) and also included in the abbreviations list) (Beijersbergen and Spaargaren, 2009)

- For buildings in the hinterland and foreland within the assessment track of piping: If it has a shallow foundation and under the foundation there is a minimum covering clay layer of 1 m present the building can be approved.
- For buildings on the slope or the crest within the assessment track of stability(inner or outer): When the building has a pile foundation the building can be approved, because no force is introduced that could negatively impact the stability.
- For buildings on top of the outer slope within the assessment track erosion (STBK): If the core material of the dike is clay the building can be approved (the rest profile can probably withstand further erosion).

Within the research program SBW, strength and loads water defenses, (Sterkte & Belastingen Waterkeringen) new research was performed to be used for the new statutory assessment and design tools. Also research concerning NWO's was performed and this was published in (Hoffmans and Knoeff, 2012). In general, concerning NWO's, Hoffmans and Knoeff state that the additional failure probability has to be compared with a yet to be determined requirement. This might be used in an advanced assessment (see step

five in figure 3.1. Hoffmans and Knoeff mention that this could be done according to different classes like is mentioned in table 3.1.

TABLE 3.1: Suggested acceptable additional failure probabilities for NWO's (Hoffmans and Knoeff, 2012)

Additional failure probability	**Assesment**
>1 % of standard	Insufficient
0.1-1 % of standard	Doubtful
<0.1 % of standard	Sufficient

Furthermore it is mentioned that in an advanced assessment it is also possible to include the strength of the building. Where the strength of the soil retaining parts of the building, like walls and floors/foundation elements, are included in the assessment. It seems that this assessment that includes the strength of the building has not yet been performed in The Netherlands.

The step five from figure 3.1, the so called advanced assessment, has not been described in detail by the above mentioned sources. A method for advanced assessment of pipelines is described in (Sanders and Wiggers, 2015). Sanders and Wiggers developed their method for dikes in the south of The Netherlands along the river Meuse. A lot of pipelines were present in the primary water defenses, so these could not be approved with the help of the assessment profile (step one from figure 3.1). Relocating the pipelines or the dikes would severely impact on social and economic aspects. The result of the used advanced approach resulted in the approval of most pipelines, which resulted in a large cost saving because less pipelines had to be replaced. The method uses a semi-probabilistic approach, where the expected likelihood of dike failure due to pipeline rupture ($P_{f(_{HW \bigcap Rupture})}$) is compared with the allowable probability of failure for dike failure due to pipeline rupture (P_{all-P_f}):

$$P_{f(_{HW \bigcap Rupture})} \leq P_{all-P_f} \tag{3.1}$$

The allowable probability of failure is derived from a fault tree analysis and an assumed distribution over the subsequent failure modes. The allowable probability of failure for the failure mechanism 'dike failure due to pipeline rupture' is set to 1.5 % (ω) of the top event 'flood of the hinterland' (P_{flood}), which is standardized for these dikes with: $P_{flood} = \frac{1}{250}$ per year. This results in:

$$P_{all-P_f} = \omega \cdot P_{flood} = 1.5\% \cdot \frac{1}{250} = \frac{1}{16,667} \tag{3.2}$$

The probability of failure of a dike due to pipeline rupture is calculated with the following formula:

$$P_{f(HW \cap Rupture)} = P_{HW>res-prof} \cdot P_{rupture} \cdot P_{repair} \cdot P_{f|rupture,HW} \tag{3.3}$$

in which:

	ω	=	failure space factor $[-]$
	P_{all-P_f}	=	allowable probability of failure for dike failure due to pipeline rupture $[yr^{-1}]$
	$P_{f(HW \cap Rupture)}$	=	probability of dike failure due to pipeline rupture $[yr^{-1}]$
	P_{flood}	=	probability of flood of the hinterland $[yr^{-1}]$
	$P_{HW>res-prof}$	=	the probability of exceedance that the water level exceeds the dike after pipeline rupture $[yr^{-1}]$
	$P_{rupture}$	=	the probability of rupture of a pipeline $[yr^{-1}]$
	P_{repair}	=	the probability that the period of high flood level overlaps with the period that is needed for repair of the dike after a rupture
	$P_{f\|rupture,HW}$	=	the conditional probability of failure of the dike given two simultaneous events: rupture and highwater event $[yr^{-1}]$

To calculate the maximum flood level that can be retained after rupture, first the residual profile has to be determined. The residual profile is set up by implementing the disturbance of the ground near the rupture. This is done in a robust conservative way, so that the residual profile is resistant against all possible failure modes.

In the application of this semi-probabilistic method, the probability of exceedance of the water level is adopted according to a level that is higher than the residual profile. Thus a probability is calculated that a water level exceeds the dike after rupture, for this situation $P_{f|rupture,HW}$ can be set to one. This is because the water level is now higher than the dike, and therefore the water is flowing over the dike while the cover of the inner slope is not present anymore due to the rupture, this justifies the assumption that the dike will certainly fail in this situation.

This method assumes that a pipeline rupture is independent from a high water event. This might be questionable when for instance due to a high water event large deformations in a dike occur. These deformations might influence the probability of rupture of the pipeline.

3.1.3 Regional defenses

Recently the government has decided that also regional water defenses have to satisfy a standard in 2020. Therefore in 2015 a new update of the assessment tools has been

published by STOWA. This update replaces the previous assessment tools. In this new version the non water retaining objects on regional defenses will be assessed for the first time. The water boards are responsible for assessing their regional water defenses and to report their findings to the Dutch provinces. The regional defenses are subdivided into five different classes based on the possible economic damage of a breach. The five different safety classes have to retain water levels with probability of occurrence of $\frac{1}{10}$ *per year* to $\frac{1}{1000}$ *per year*. For the assessment of buildings referred is to the approach described in (VTV, 2006) and (Beijersbergen and Spaargaren, 2009). An easy assessment, based on the intersection of the building with the minimal required assessment profile of the water defense, is preferred. (STOWA, 2015)

3.2 Assessment in practice

This section is based on interviews with people from the field. Professionals from waterboards, engineering firms and research institutes have been interviewed. In appendix D on page 189 a list of the people who have been interviewed for input of this section has been added.

Since the introduction of the present statutory assessment tools in 2006 the NWO's on water defenses have to be assessed. Despite of the provided information, water defenses operators had difficulties with the assessment, as was mentioned before in section 3.1. It appears that from the assessment steps that are provided in figure 3.1 only step one was conducted frequently, steps two till four only occasionally, and it seems that step five has never probabilistically been performed for buildings. This means that, according to (VTV, 2006), no buildings have been disapproved because this can only be done after completion of all the steps. This means that there is a large group of NWO's that have not been fully assessed. In this group there might be buildings that have been approved on basis of an operators judgment. Also there are (at least one) waterboards that further investigate the buildings that are on their dikes, which were not approved, to identify certain unsafe dike sections.

In (Larsen, 2004) some kind of advanced assessment for buildings in the outer slope of a dike in the Krimpenerwaard is performed. In this assessment is, among others, the strength of the soil retaining parts of the building, under hydraulic pressure and forces induced by wave attack, assessed in a deterministic way.

The result of the assessment according to (VTV, 2006) is also referred to as the technical judgment. As mentioned before, due to the difficulties with the technical judgment for NWO's, also an operational judgment was developed (Beijersbergen and Spaargaren,

2009). With this development it became possible to approve NWO's that were assessed insufficient or 'not assessed'. To do this, it was required to properly substantiate such a decision, based on the operational judgment. How to exactly deal with these two judgments to get to a general one is not entirely clear.

Another method for approval of buildings during assessment or during dike reinforcement programs is to construct a special structure, like a sheet pile. In this way the assessment profile of the water defenses reduces so that the building does not intersect with the profile anymore. Waterboards use this as an easy option to allow and approve buildings around dikes. This option is also attractive for them because it separates the function of a water defense from other functions, which is convenient for them since it simplifies the operational management of the water defense in the future. When reinforcements are part of the HWBP program the additional costs for a waterboard are low because their own contribution, within the financial agreements of the HWBP, are only 10 %. This could be an incentive for a waterboard to prefer a rather expensive solution, for a dike with nearby buildings, such as sheet piles or slurry walls. It could therefore be wondered whether this financial agreements cause unnecessarily high costs for society.

The aim of the extended third assessment round was to reduce the amount of water defenses that were assessed to have; 'no judgment'. That is why it was decided to approve dike sections that itself were approved but NWO's near or on them were not approved. When the results of the third assessment round for NWO's of the largest Dutch waterboard are observed this can also be recognized. See table 3.2. When this data is extrapolated to all dutch river dikes ($+-$ 1600 km), with the same proportions

Table 3.2: Assessment data for NWO's of the Dutch waterboard Rivierenland (Waterschap Rivierenland)

Rivieren -land (252 km river dikes):	**Total:**	**Not assessed**	**Appr-oved:**	**Disapp-roved:**	**Further investigat-ion needed:**	**Amount within assess-ment profile:**
Buildings	15300	5751	9081	0	468	5 %
Trees	108860	47315	54893	0	6652	11 %
Pipelines	292	0	207	8	77	29 %

Table 3.3: Extrapolation of the data of table 3.2 to all Dutch river dikes

Extrapolation dutch river dikes	**Total**	**Within assessment profile**
Buildings	44000	2200
Trees	314000	34000
Pipelines	850	250

of NWO's that intersect the assessment profile, the bottom part of table 3.2 is retrieved. Observing these two tables illustrates the huge amount of NWO's near Dutch river dikes.

3.3 Conclusion

In this section conclusions from this chapter are drawn which gives a compact answer to the subquestion that was treated in this chapter is: "*How is the assessment of water defenses, with buildings nearby, at the moment performed?*"

Buildings near dikes belong to the the group of NWO's according the Dutch safety guidelines. These have to be assessed according a flow diagram containing six steps. When the first step, no intersection of the NWO including disturbance zone with the assessment profile, is not successfully completed, the remaining chart has to be completed to approve the NWO. Since it is not very clear how these remaining steps should be proceeded many NWO's have gotten the verdict: 'no judgment'. Besides, because there are a lot of unique NWO's, the completion of six steps results in a huge amount of work for the operators of the water defenses.

When a building got the verdict 'no judgment' there are some rules of thumb available to come to an operators judgment. Also additional calculations can be made to check the NWO's that did not pas the flow diagram, to assure the safety of the dike at these locations. These current problems with the assessment of buildings could result in expensive structural measures at building locations, which may be unnecessary.

It is also not very clear when the possibility of collapse of the building can be let out of the assessment. When this possible collapse always has to be assumed, this might locally result in over-dimensioning which is economically not efficient. When possible collapse would be included in the assessment this could result in more efficient dike designs.

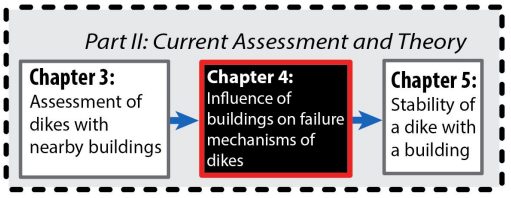

Chapter 4

Influence of buildings on failure mechanisms of dikes

In this chapter an answer to the following research question is given: "*How can building characteristics have influence on the failure mechanisms of a dike?*". The effects of a building on the failure mechanisms are described and explained. First this is done for the situation that the building remains intact and subsequently for the scenario of building collapse. This chapter inventories the effects based on a literature study, while in the end an overview of these effects is presented, on which a selection of a failure mechanism is based that is further elaborated in the next chapter.

4.1 Effects of buildings on failure mechanisms

The presence of buildings around dikes could influence the failure mechanisms. In the following subsections a collection of possible effects on failure mechanisms is collected. Effects of the following failure modes are included: 1. Failure due to overtopping/overflow. 2. Failure due to erosion or failure of revetment. 3. Piping. 4. Macro stability. 5. Micro stability. This is done by use of the following references: (van Mechelen, 2013), (Hoffmans and Knoeff, 2012), (Boers and Steetzel, 2012) , (VTV, 2006) and (TAW, 2001).

4.1.1 Dike failure due to overtopping and or overflow

When water overtop or overflow a dike, the dike is not yet considered to be failed. It could be regarded as functional failure since the dike is not retaining all the water

anymore, but the dike itself is still intact. However when large volumes of water are flowing over the inner slope of the dike the cover of the slope can be damaged, and result in erosion. Eventually this could lead to breaching of the dike, which is regarded as structural failure. During recent flood events in for example France, Thailand and New Orleans a lot of breaches occurred at so called transitions due to overtopping and overflow. An possible example of these transitions are buildings on and in the dikes (Pijpers, 2013).

To prevent structural failure due to overtopping Dutch dikes have a critical overtopping discharge that depends on the properties of the inner slope. If the discharge remains under this critical limit, no erosion of the top layer should occur and therefore the dike should remain intact. The occurring loads on the top layer near buildings can be enlarged by increased discharge due flow concentration and increased turbulence. Also the resistance of the top layer against erosion can be influenced because a building can impose material transitions of the top layer. Therefore, buildings can reduce the allowable overtopping discharge of inner slopes. This influence of buildings is especially important for buildings on the inner slopes. Also buildings located on the crest or the hinterland, provided that they are close to the inner slope, could decrease the allowable overtopping discharge, because they can influence the flow of water on the inner slope. This threat could potentially be compensated with local soil improvements or revetments.

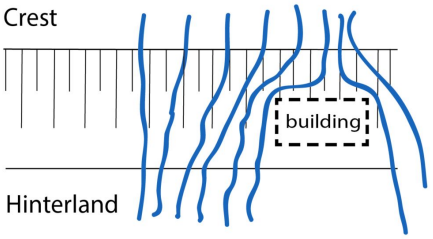

FIGURE 4.1: Increased overtopping discharge due to presence of a building

4.1.2 Erosion or failure revetment

The outer slope of a dike is usually covered with grass. The function of this grass is to prevent erosion due to water that is retained by the dike. When this cover fails and erosion of the dike starts this can proceed in failure of the dike. When buildings are located on the outer slope or close to the outer slope on the foreland these transitions are extra vulnerable for erosion due to increased water flow and or turbulence. Especially for dikes with a sand core, which are not erosion resistant, the consequences could be severe. This risk could also potentially be avoided with local soil improvements or revetments.

4.1.3 Piping

The failure mechanism piping can occur if there is a large hydraulic head difference over a dike with a permeable sublayer. When the low permeable cover layer (aquitard) is lifted by the water pressures under the dike (uplift) and water can seep out of so called wells and this results in the erosion of sand particles from the sub layer of the dike (heave). When this erosion continues pipes can be formed under the dike (piping) and this can endanger the stability of the dike. Nowadays the piping process is modeled and assessed as an independent parallel system of three physical sub mechanisms; uplift, heave and piping. When all sub mechanisms occur the major piping mechanism occurs.

For the assessment of the failure mechanism piping, the seepage length (L_{seep}) is an important aspect, because it directly influences the hydraulic gradient over the soil structure ($L_{seep}/\Delta H$), which is the driving force of the piping process. This seepage length is the distance between the entry point and the potential exit point. The location of these points depend on the local subsoil conditions. The influence of buildings on the piping mechanism is mainly based on the possibility that a building could induce a new location for an entry or exit point which results in a shorter seepage length. This results in a larger hydraulic gradient over the dike and eventually in an enlarged probability for

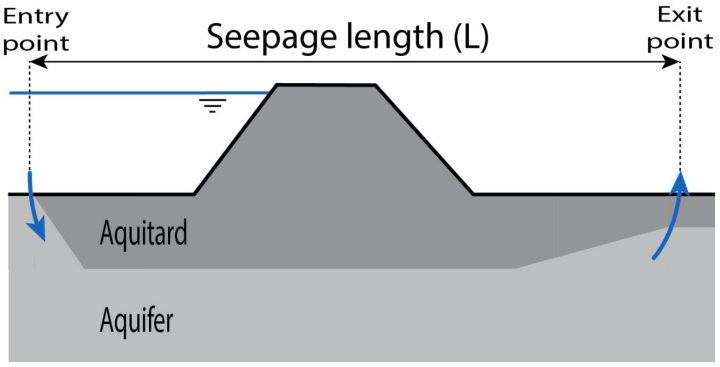

(A) Piping visualization without buildings

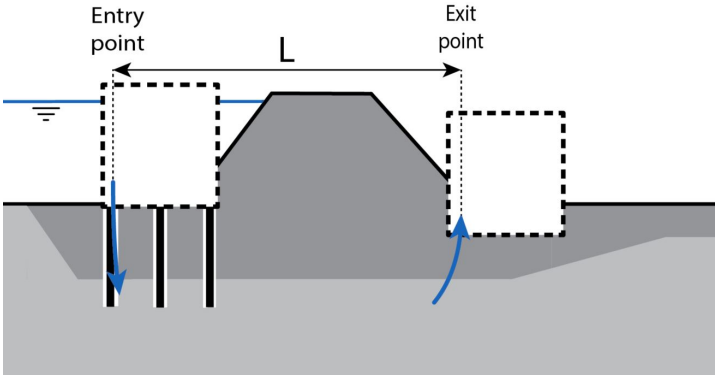

(B) Piping visualization with buildings

FIGURE 4.2: Piping mechanism influenced by buildings

piping on this specific location. See figure 4.2. This effect of a shortened seepage length can be induced by buildings with a pile foundation or buildings that are located in the soil profile.

Besides the negative influence of buildings due to the shortening of the seepage length the piping mechanism can be influenced in another way. Namely when buildings are located in the soil profile at the hinterland, the aquitard is locally thinner at the building location. This could result in an increased probability of uplift and thereby influence the failure mechanism piping.

Not all kind of pile foundations allow the seepage of water through the aquitard, soil displacing piles should not interfere with the water-tight function of the aquitard. A possible hazard of a pile foundation is that these buildings do not subside while the dike itself does. This could result in hollow spaces around the foundation piles. This could induce the beginning of entry or exit points. Buildings with a shallow foundation could also potentially beneficially affect the piping mechanism because their weight, which is borne by the subsoil, can reduce the probability of uplift locally. Buildings that are located in the foreland, the hinterland or low in the slopes could affect the piping behavior of a dike.

4.1.4 Macro stability

Slope stability problems can occur for the inner and the outer slope. For the inner slope this mechanism is most likely to occur during high water events. If the water level rises, water starts to infiltrate in the dike body which results in higher pore pressures. By this the effective stresses decrease and so does the shear strength. If the driving forces become larger than the resisting forces this will lead to slope failure along a sliding plane. Stability problems of the outer slope are most likely to occur after the peak of a high water event, if the water level drops quickly, the pore pressure inside the soil body can not follow the pore pressure drop outside of the dike and therefore the outer slope can slide towards the foreland.

The selfweight of a building can introduce an extra force on the soil body. This force has a negative effect on the stability, if the resultant force of the selfweight is on the active side of the sliding plane and thereby increasing the driving moment. When the resultant forces of the selfweight is on the passive side and thereby increasing the resisting moment this effect becomes positive. See figure 4.3. The introduction of forces due to selfweight only occurs for buildings with a shallow foundation. In addition, a building could also introduce extra external loads on the water defense, for example a wind load transferred by the building to the dike could also influence the stability of the dike.

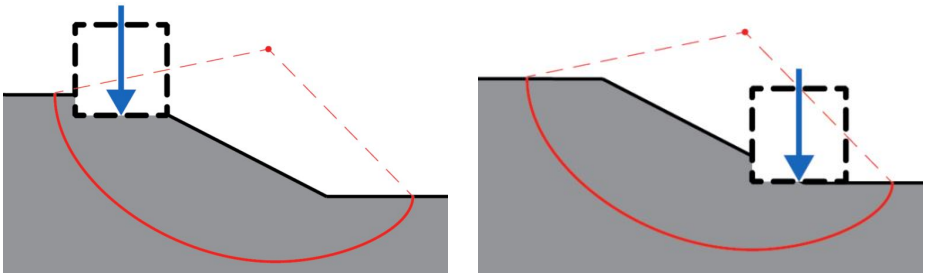

(A) Negative force on active side

(B) Positive force on passive side

FIGURE 4.3: Building introducing force affecting slope stability

If a building has a pile foundation the self weight of the building is transferred to a lower lying subsoil layer, and therefore no additional loads for stability problems are introduced. But if piles of the foundation of a building cross the normative slip circle the horizontal pressure against the piles can yield some additional resistance. This will result in shear forces in the piles. The magnitude of this (positive) effect is not entirely clear because the width of a slip plane is often much larger than a foundation. It thus depends largely on the amount of piles and the strength and stiffness properties of these piles. The effect has the most influence when the piles are in the slope, because all possible slip planes go through the slope (see figure 4.4 A). For instance when piles are in the hinterland they only cause a movement of the normative slip plane, so that it does not intersect with the foundation piles anymore (see figure 4.4 B). The effect in that case is marginal.

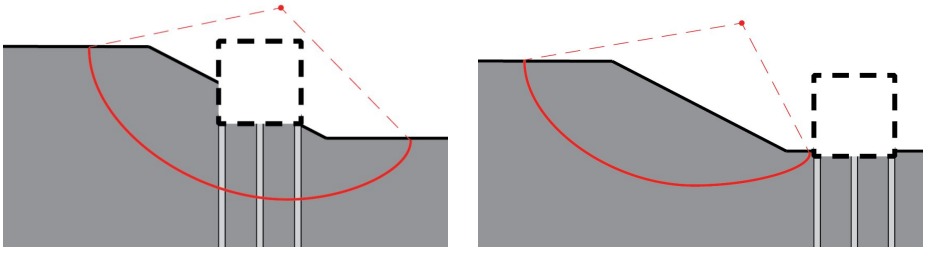

(A) Piles providing additional resistance

(B) Piles providing marginal additional resistance since normative sliding plane moves

FIGURE 4.4: Effects of a building with a pile foundation

When a building is in the profile of the dike this can influence the water level in the dike. This could occur due possible leakage of water along the foundation of the building. With the increased water level, the pore pressures in the dike increase, the effective stresses decreases and the shear stress decreases. For the inner slope stability buildings in the outer slope or the crest can influence the water level in the dike. See figures 4.5.

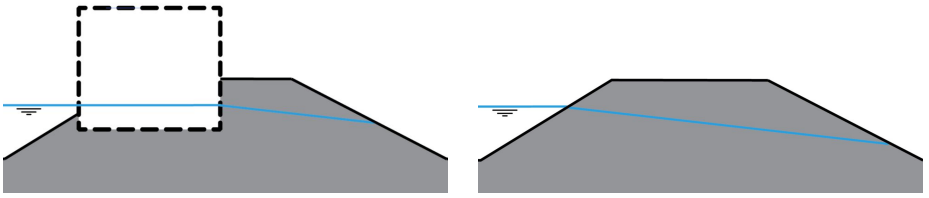

(A) Ground water level in dike with water leakage along building

(B) Groundwaterlevel without leaking building

FIGURE 4.5: Building in outer slope influencing freatic line in dike

A building can also beneficially influence the macro stability due to a structural element, for instance a wall or floor/foundation element, that is located in the soil profile. This is because these structural elements intersect with potential slip planes. The influence of this thus does depend on the strength of the specific element. Just as with piles, the effect is the greatest for elements located at the slope. For structural elements that intersect at the passive side, as well as for longer elements, the positive influence is the largest. This effect only applies to buildings in the soil profile and that are located in (close to) the slope.

4.1.5 Micro stability

The failure mechanism micro instability is in particular relevant for dikes with a core made out of granular material like sand. When the freatic surface inside the core is high these water pressures can push off the cover of the inner slope. As mentioned in the previous subsection for a building in the outer slope some leakage under the building can occur which can result in a higher freatic line. This results in an increase in pore water pressure in the core, and can therefore increase the water pressure against the cover layer. This effect applies to dikes with a sand core and a water tight cover layer of clay.

4.2 Effects of building collapse on failure mechanisms

When a building is present on or near a dike this can influence the behavior of the dike. But when the building collapses this influence might also change. Therefore in this section relevant aspects of building collapse on the failure mechanisms of a dike are treated.

4.2.1 General

In subsection 3.1.1 it was mentioned that within the current assessment tools, the possible absence of a building including disturbance zone has to be taken into account. Furthermore in the previous chapter it was concluded that further specification of the 'building collapse' scenario might be beneficial. In this subsection a specification of the building collapse scenario is analyzed by means of an example. This proposed specification is based on the dependency between building collapse and a high water event. This example is based on the analogy that was used in the advanced assessment of pipelines near dikes (Sanders and Wiggers, 2015) (section: 3.1.2 page 34).

Example

When a situation as in figure 4.7 A is imagined (configuration: inside the soil profile, located at the inner slope), it is conceivable that collapse of the building will influence the stability of the dike. For dike failure due to collapse of this building a fault tree like in figure 4.6 can be made.

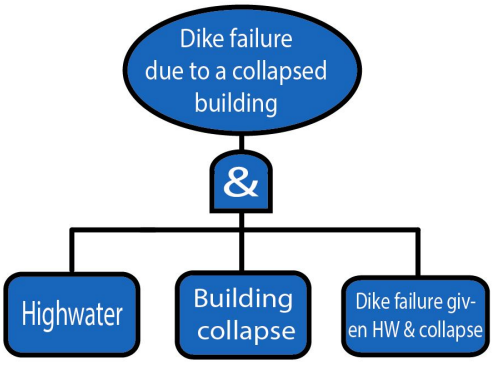

FIGURE 4.6: Fault tree for dike failure due to collapse of a building

The fault tree is a parallel system, so when all events occur the top event 'dike failure due to a collapsed building' occurs. The highwater event, P_{HW}, here is the probability that a water level is exceeded that is higher than the crest of the dike after collapse of the building. So the assumption is made here that collapse of the building results in a new profile of the dike that is more narrow and lower (see figure 4.7 B). The probability of building collapse is given as; $P_{collapse}$. The third component of the fault tree is the conditional probability that the dike will fail given building collapse and a high water; $P_{f|collapse,HW}$. In this example this conditional probability is set to 1, just as is done in (Sanders and Wiggers, 2015) (section: 3.1.2 page 34). This means that it is assumed that the dike will definitely fail when a water level occurs that is higher then the residual profile while building collapse occurs simultaneously.

When these two events are independent the combined failure probability also depends on the probability that the two events occur at (somewhat) the same time. So in this

case the probability that within a year the highwater event and the period that the dike is damaged due to the building collapse overlap $P_{overlap}$.

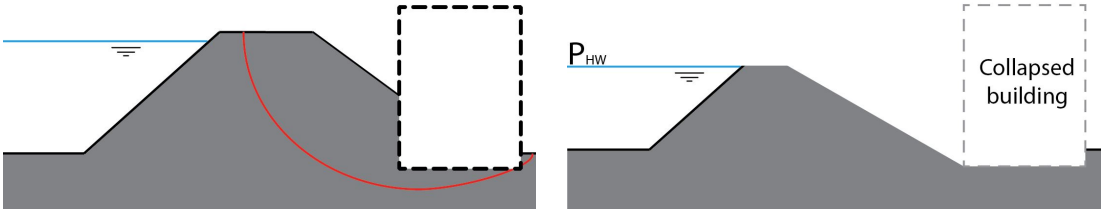

(A) Example configuration without collapse

(B) Example configuration after collapse

FIGURE 4.7: Example configuration

When the dependencies between collapse and a high water are considered, a division can be made for two kinds of building collapse.

Independent A collapse of the building which cause is independent of a high water event. For example collapse due to a gas explosion, earthquake or a construction defect.

Dependent A collapse of the building which is caused by a dependent mechanism of a high water event. Examples are collapse due to high water pressures or large soil deformations near a wall or overtopping/overflow that results in collapse of the building.

To illustrate the differences of these two scenario's a calculation example will be performed with the following values:

$$P_{HW>res-prof} = \frac{1}{500} \tag{4.1}$$

$$P_{collapse} = \frac{1}{1000} \tag{4.2}$$

$$P_{overlap} = \frac{1}{10} \tag{4.3}$$

$$P_{f|collapse,HW} = 1 \tag{4.4}$$

in which:

$P_{HW>res-prof}$	=	the probability of exceedance of a water level that can be retained by the dike after building collapse. $[yr^{-1}]$
$P_{collapse}$	=	the probability of building collapse. [1] $[yr^{-1}]$
$P_{overlap}$	=	the probability that the period of high water level overlaps with the period that the dike is affected by building collapse.

[1] The probabilities of collapse are assumed the same for the dependent and independent calculation. In practice these could differ from each other but since this is a illustrative calculation and for simplicity now they are assumed equal.

$P_{f|collapse,HW}$ = the conditional probability of failure of the dike given two simultaneous events: collapse and a highwater event

$P_{f(HW \bigcap Collapse)}$ = the failure probability of the dike due to a collapsed building. $[yr^{-1}]$

When the two events are assumed to be fully independent the top event becomes:

$$P_{f(HW \bigcap Collapse)} = P_{HW>res-prof} \cdot P_{collapse} \cdot P_{overlap} = \frac{1}{5,000,000} \tag{4.5}$$

When the two events are assumed to be fully dependent the failure probability becomes: [2]

$$P_{f(HW \bigcap Collapse)} = min\{P_{HW>res-prof}, P_{collapse}\} = \frac{1}{1000} \tag{4.6}$$

When the results of these example calculations are compared the huge differences can be seen, and the very low probability outcome of the independent scenario (equation (4.5)) can be seen. Therefore it is concluded that the occurrence of dependent causes for building collapse are most relevant to delve further into. In the remainder of this research the focus will be on these dependent causes of building collapse. For the assessment tools of NWO's it might therefore also be beneficial to specify the scenario of building collapse according to this dependency between collapse and a high water.

Unless the possibilities with this specification between dependency and collapse, it remains very important to realize for which situations this specification can be applied. This is because the analogy that is derived in this example does not always have to be valid. For instance when a dike is closer to the sea or the ocean, a highwater event can be caused by a storm, due to the progression of storm surge levels from the ocean upstream the river. And this same storm could induce a collapse of the building by a wind loading. This results in different configurations that are influenced by building collapse due to an event that is dependent to a high water.

Because of the arguments given here above the possible negative effects of building collapse, that will be described in the subsections below, are only included when the collapse of a building could be dependent to a high water event.

[2] The overlap failure probability drops out because the two events are assumed to be fully dependent, which implies that they overlap by definition.

4.2.2 Dike failure due to overtopping and or overflow

It is assumed that the inner slope will fail earlier than a building on or near the slope due to the overtopping flow. According to (Rijkswaterstaat et al., 2015) the limit of the allowable overtopping discharge for well maintained grass covers becomes 10 $l/s/m$ from 2017. Thus it is assumed that a building will not collapse for overtopping discharges smaller than 10 $l/s/m$. For higher discharges the dike is assumed to already have failed due to overtopping and or overflow. Therefore buildings that are located *on* the profile of a dike and located at the inner slope or the hinterland the building collapse scenario is dropped for the assessment track height (failure due overtopping or overflow) because dependent collapse could only occur when large overtopping discharges take place, and in that case the slope itself has already failed.

Non water retaining buildings that are 'in the profile' could collapse due to a dependent cause and therefore have to be assessed for overtopping and overflow. Collapsing buildings on the crest, the inner slope or the hinterland will leave an interruption of the grass cover of the dike. This grass cover should prevent the start of erosion of the inner slope during overtopping. When this cover is not fully intact anymore erosion could start and could eventually lead to a breach. So the collapse of a building could change the inner slope from a closed sod to an open sod. For an open sod the allowable overtopping discharge has to be reduced to 0.1 $l/s/m$ if the clay layer beneath is less thick than 0.4 m and the slope is steeper than 1 : 4 (Rijkswaterstaat et al., 2015). In any other case the value of 10 $l/s/m$ can be maintained.

4.2.3 Erosion or failure revetment

For buildings that are located on the outer slope, building collapse due to highwater conditions can not be excluded, since it may be caused by dependent mechanism. Because an occurring high water could lead to collapse of a building on this location. When a building on the outer slope collapses a part of the slope becomes unprotected and becomes vulnerable for erosion. Especially for dikes with a sand core, which are not erosion resistant, the consequences can be large.

4.2.4 Piping

For buildings that can have an influence on the piping process not a lot changes when collapse of the building is regarded (i.e. the same configurations that influence piping for buildings that do not collapse are relevant for buildings that do collapse). But building

collapse, for instance due to uplift, can enlarge the negative influence on the piping process. Since after collapse the occurrence of exit or entry points may by eased.

4.2.5 Macro stability

An important consideration regarding building collapse for the stability is that the weight of a building does not disappear after collapse. If a building on a shallow foundation collapses the weight of the remaining rubble will still be transferred to the soil mass below. For buildings that have failed on the outer slope or foreland due to a high water event it could be that the remaining rubble is moved due to flowing water around the rubble heap. Therefore it should be taken into account, that positive effects of the selfweight of buildings on the water-side of a dike could change, when building collapse can not be excluded due to a high water event (dependent causes of building collapse).

For buildings that are located in the dike profile, and thus have a soil retaining wall, collapse caused by a dependent cause of a high water event is conceivable. When a dike is retaining water on one side, the freatic level inside the soil body may rise which could impose forces against the soil retaining wall. When the wall fails the building itself will collapse and the soil behind the wall will not be retained anymore. This will result in soil movement towards the location of the former building. This movement will change the shape of the dike, such a 'changed' shape of the dike profile is called a residual profile. The residual profile can have steeper slopes which are more sensitive for instability.

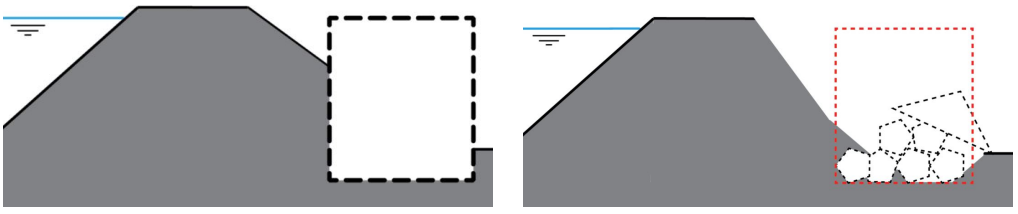

(A) No collapse (B) After collapse

FIGURE 4.8: Building collapse influencing macro stability

4.2.6 Micro stability

When a building is located in the inner slope, the crest, or the hinterland and when it collapses, this can result in steep slopes in the soil profile. When these steep slopes are below the freatic level in the dike the occurrence of micro instability problems can increase. This is caused by the increased probability of seepage through the steeper slope.

4.3 Overview of effects

In this section some overview of the described effects are given. The effects are arranged for the relevant configurations and failure mechanisms, first for scenario that the building does not collapse and after wards for a scenario of building collapse. This overview is given in a table format in which all configurations and assessment tracks (failure modes) are included. When in these tables a cell is empty it means that according to the analysis performed in this chapter, no effect is expected for the mechanism that belongs to this assessment track. These tables could be used for a first impression on the expected effects of a building on the failure mechanisms of a dike, however in specific situations there could be other or different effects, therefore always the specific situation should be analyzed.

4.3.1 Building does not collapse

In table 4.1 an overview of the effects is given for the scenario that the building does not collapse. The effects and possible calculation checks that match the numbers are clarified below.

TABLE 4.1: Overview of effects of a building on the failure mechanisms of a dike(In red: negative effects, in green: positive effects, black: effect can be positive or negative depends on exact location)

Location	**In/On Profile**	**Foundation**	**Assessment track**					
			STBK	**STBU**	**STPH**	**HT**	**STBI**	**STMI**
Foreland	On	Shallow	(8)	(1)	(5)			
		Piles	(8)	(2)	(4)			
	In	Shallow	(8)	(1) & (3)	(4) & (5)			
		Piles	(8)	(2) & (3)	(4)			
Outer Slope	On	Shallow	(8)	(1)	(5)			
		Piles	(8)	(2)	(4)			
	In	Shallow	(8)	(1) & (3)	(4) & (5)		(7)	(7)
		Piles	(8)	(2) & (3)	(4)		(7)	(7)
Crest	On	Shallow		(1)		(6)	(1)	
		Piles		(2)		(6)	(2)	
	In	Shallow		(1) & (3)		(6)	(1) & (3)	
		Piles		(2) & (3)		(6)	(2) & (3)	
Inner Slope	On	Shallow			(5)	(6)	(1)	
		Piles			(4)	(6)	(2)	
	In	Shallow			(4) & (5)	(6)	(1) & (3)	
		Piles			(4)	(6)	(2) & (3)	
Hinterland	On	Shallow			(5)	(6)	(1)	
		Piles			(4)	(6)	(2)	
	In	Shallow			(4) & (5)	(6)	(1) & (3)	
		Piles			(4)	(6)	(2) & (3)	

① Introduction of selfweight of the building, depending on the location the effect is positive or negative. Stability calculation can be performed with the selfweight as a surcharge load. See section 4.1.4 on page 44.

② Piles on providing a some additional resistance against slope failure. 3D slope stability calculation can be performed, with piles, if effect needs to be implemented. This effect is at its greatest when the piles cross the slopes, otherwise the effect is negligible. See section 4.1.4 on page 45.

③ Structural element providing some additional resistance against slope failure. Calculation with structural element can be performed, if effect needs to be known. This effect is at its greatest when the element is in the slope, otherwise the effect is negligible. See section 4.1.4 on page 46.

④ A building could induce a new exit or entry point for piping, which can reduce the seepage length. A calculation could be made with a shortened seepage length. See section 4.1.3 on page 44.

⑤ A building on a shallow foundation could locally have a beneficial effect for uplift due to it's weight. See section 4.1.3 on page 44.

⑥ Possible locally earlier start of erosion of sod. Calculation with a reduced overtopping discharge could be performed. See section 4.1.1 on page 42.

⑦ Possible higher freatic line in dike due to leakage under building. This can decrease the macro and micro stability of the inner slope. A Stability calculation can be performed with a higher freatic level. See section 4.1.4 on page 45.

⑧ At transitions possibly earlier start of erosion of the cover which could result in erosion of the dike core. See section 4.1.2 on page 42.

4.3.2 Building collapses

In table 4.2 an overview of the effects is given for the scenario that the building collapses. The effects and possible calculation checks that match the numbers are clarified below.

① Collapse can lead to soil failure which can change the profile; residual profile. Besides the beneficial effect of the structural element on the stability drops out. A stability calculation with this residual profile can be performed. See section 4.2.5 on page 51.

② Due to collapse the sod can become classified as open. A possible calculation with a reduced allowable overtopping can be performed. See section 4.2.2 on page 50.

TABLE 4.2: Overview of effects of a collapsed building on the failure mechanisms of a dike (In red: negative effects, in green: positive effects, black: effect can be positive or negative depends on exact location)

Location	**In/On Profile**	**Foundation**	**Assessment track**					
			STBK	**STBU**	**STPH**	**HT**	**STBI**	**STMI**
Foreland	On	Shallow		(7)				
		Piles			(6)			
	In	Shallow		(1) & (7)	(6)			
		Piles		(1)	(6)			
Outer Slope	On	Shallow	(4)	(7)				
		Piles	(4)		(6)			
	In	Shallow	(4)	(1) & (7)	(6)		(3)	
		Piles	(4)	(1)	(6)		(3)	
Crest	On	Shallow						
		Piles						
	In	Shallow		(1)		(2)	(1)	(5)
		Piles		(1)		(2)	(1)	(5)
Inner Slope	On	Shallow						
		Piles			(6)			
	In	Shallow			(6)	(2)	(1)	(5)
		Piles			(6)	(2)	(1)	(5)
Hinterland	On	Shallow						
		Piles			(6)			
	In	Shallow			(6)	(2)	(1)	(5)
		Piles			(6)	(2)	(1)	(5)

(3) Possible higher freatic line in dike due to extra infiltration due collapsed building, this can reduce the stability. Stability calculation can be performed with a higher freatic level. See section 4.2.5 on page 51.

(4) Due a collapsed building erosion of the dike material could occur which could proceed in failure. See section 4.2.3 on page 50.

(5) When collapse leads to soil failure this can result in steeper soil profiles that are more vulnerable for micro instability. See section 4.2.6 on page 51

(6) Building collapse could ease the negative influence of buildings for piping. See section 4.2.4 on page 51.

(7) Due to flowing water conditions the bearing of the weight of the building to the subsoil might change. See section 4.2.5 on page 51.

4.4 Conclusion

In this section conclusions from this chapter are drawn which gives a compact answer to the subquestion treated in this chapter: "*How can building characteristics have influence on the failure mechanisms of a dike?*"

In this chapter various effects of buildings on the failure mechanisms of a dike are described. These have been compactly charted in tables 4.1 & 4.2. In figure 3.3 *B* (page: 35) a somewhat similar table has been shown adopted from (Beijersbergen and Spaargaren, 2009). Some entries of these tables correspond but there are also differences. The tables made as part of this thesis namely also includes positive effects, the scenario of building collapse and more important properties of the building are included in the configurations. Furthermore some additional conclusions regarding the research of this thesis can be drawn:

Through a number of different effects, a building can influence the stability of a dike. Some of these are positive and some are negative and it also depends whether the building remains intact or that it does collapse. Since a lot of different effects can be expected for this mechanism, the focus of the next chapter is put on the (slope)stability of a dike with a building. In this chapter also calculations are performed to investigate the amount of influence these effects have on the stability.

Another conclusion from this chapter is that scenario of building collapse that could be dependent to a high water event has the largest influence on the safety of a dike. By including this specification into the safety assessment, this may result in multiple benefits. In table 4.2, where an overview of effects of building collapse are collected, this specification has been included, and it can be seen that for mutiple configurations the scenario of building collapse can be left out now.

This page intentionally left blank.

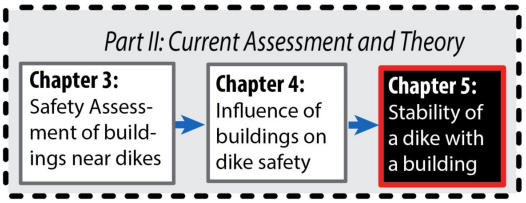

Chapter 5

Stability of a dike with a building

In this chapter the focus is shifted towards the failure mechanism macro stability, which is based on conclusions from the previous chapter. For this mechanism, the most interesting configuration has to be selected. Therefore in this chapter research question three is answered; *What configurations are most interesting to focus on, and why?*. First some theories relevant for macro stability are introduced combined with some basic stability calculations for a dike without a building. In the next section stability calculations for a dike with a building are performed for all different configurations. In the final section the conclusion is reported.

The basic calculations are based, at first, on a standard dike profile with a geometry that is shown in figure 5.1 and with properties from table 5.1. A typical simplified subsoil for the riverine area is used for this calculations. The dike is made of clay on a clay layer, above a normally packed sand layer, and above a densely packed sand layer. The dike is assumed to be fully made of clay. The slopes are assumed to have a relation : $3H : 1V$ and the crest is assumed to have a width of 10 m. The crest of the dike is assumed to be 6 meters higher than the land in front and behind the dike. A water level of +5 meters, above ground level, is assumed in these calculations.

TABLE 5.1: Soil properties used for principle calculations

	$c[kPa]$	$\phi[^\circ]$	$\gamma_{sat}[kN/m^3]$	$\gamma_{unsat}[kN/m^3]$	$k[m/s]$ [1]
Clay	9	22	17	17	$1 \cdot 10^{-7}$
Sand	0	30	18	20	$5 \cdot 10^{-5}$
Dense Sand	0	32	19	21	$5 \cdot 10^{-5}$

[1]For simplicity the permeability values for sand and dense sand are taken the same.

in which:

c	=	cohesion $[kPa]$
ϕ	=	angle of internal friction $[°]$
γ_{sat}	=	specific weight$[kN/m^3]$
γ_{unsat}	=	saturated specific weight$[kN/m^3]$
k	=	permeability$[m/s]$

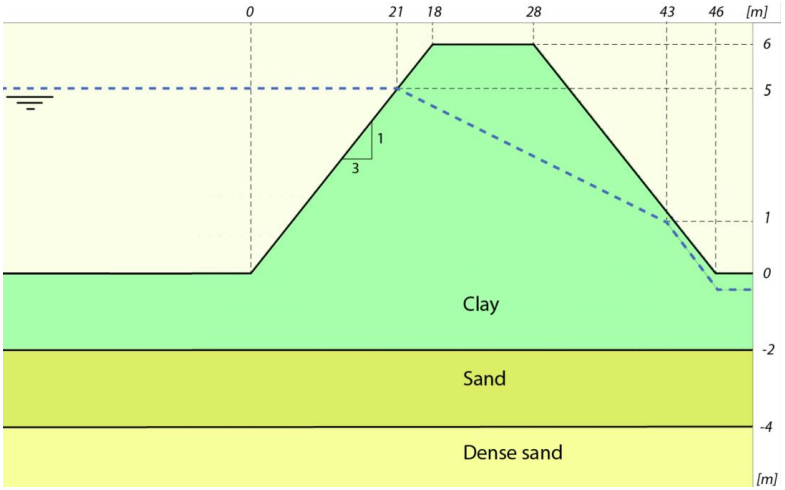

FIGURE 5.1: Geometry of dike used in basic calculations (vertical scale ≠ horizontal scale)

5.1 Stability of a dike

This chapter is started with an overview of common instability problems for dikes. This is done to get an overview of all important forces that are present and influence the stability of a dike.

Within instability a distinction can be made between horizontal stability, vertical stability, and moment stability. Horizontal instability of a dike is often called shearing, while vertical instability for dikes is referred to as uplift. Sliding of the slope of a soil body occurs when no moment stability is guaranteed[2]. These three instabilities for dikes are explained while some basic calculations are made. This is done to get an impression of all forces and moments that are relevant for dikes, so that later this can be extended for the configurations with a building.

5.1.1 Uplift

Uplift is a vertical instability issue for dikes that have a low permeable blanket layer (aquitard) on top of a more permeable layer (aquifer). When the river level rises the piezometric head in the aquifer also increases, and this can result in a upward pressure

[2]Moment instability could also refer to the failure mechanism 'tumbling over', but this is normally not normative for a dike, so it is not further elaborated here.

on the blanket layer. If this pressure is higher than the self-weight of the blanket layer uplift takes place (see figure 5.2). This causes the cover layer to rupture and can result in seepage through the layer, but the layer does not (necessarily) have to break so it is not a direct failure mechanism. The uplift mechanism is one of the underlying mechanisms of piping. The development of the piezometric head in the aquifer is of main importance to this vertical stability, therefore this is further elaborated and a calculation method is presented in appendix B.1 on page 157. This calculation method is used for a basic calculation of uplift, which is performed in appendix B.2 on page 159. The result from these calculations is that for the assumed properties of this basic case uplift of the blanket layer will occur.

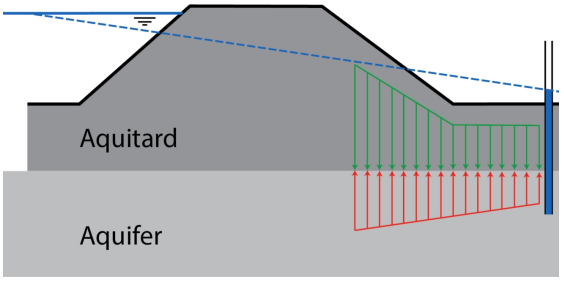

FIGURE 5.2: Force scheme uplift instability. (The dashed line represents the piezometric head in the aquifer. The line in the figure is simplified to a linear relation.)

5.1.2 Lateral shearing

Horizontal instability of a dike is commonly called lateral shearing. This mechanism occurs when the resultant horizontal force from the water pressure exceeds the shear capacity of the dike along it's base (see figure 5.3). The shear capacity depends on the soil properties and on the local effective stresses in the soil. The effective stresses in the soil body depend on the local height of the freatic level, and therefore the freatic level influences the shear capacity of the soil. This is extensively elaborated and exemplified in appendix A.2 on page 144.

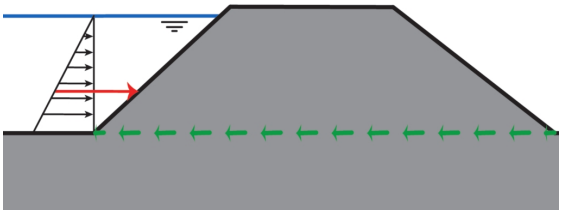

FIGURE 5.3: Force scheme shearing instability

The shear capacity of the soil also depends on whether the soil behaves drained or undrained. Relatively permeable materials will behave drained, also when they are saturated. But when a soil is relatively impermeable and is saturated, pore water pressures can develop during loading and this can influence the shear strength. When this occurs the soil behavior is referred as undrained. This is explained in more detail in appendix A.3 on page 145. In this appendix also the approach concerning undrained soil behavior within the new assessment tools (WBI2017) is summarized.

In appendix B.3 on page 159 a calculation for this failure mechanism is performed for the basic case. This is done by a comparison of the hydrostatic loading of the water and the shear capacity of the soil along the dike base. This capacity is calculated for a drained situation but also for an undrained situation. The undrained shear capacity is calculated with two methods being: 1. Undrained modification of Mohr Coulomb theory. 2. SHANSEP [3] method which is the method prescribed within WBI2017. Since shear capacity of the soil is also relevant for slope stability and soil pressures against a building, the results of shear capacity are shown in figure 5.4[4]. The here calculated properties of the shear capacity of the soil are also used in subsequent calculations.

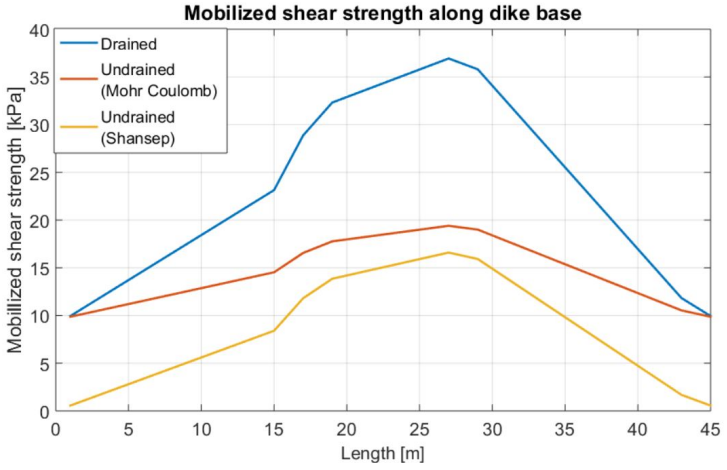

FIGURE 5.4: Mobilized shear strength at the dike base according to three different methods. (corresponding numerical values are given in table B.1 on page 162)

5.1.3 Slope stability

The best known instability issue for a dike is the sliding of a slope. For the inner slope this is most likely to occur when the freatic line in the soil body is high, due to a flood event or a heavy rainfall event. The driving moment is activated by the soil in the active

[3] SHANSEP = Stress Histroy And Normalized Soil Engineering Properties

[4] The differences between the drained results and the SHANSEP method are rather large. This is partly due to the relative high value of the cohesion that is assumed in this basic case.

zone, while the resisting moments come from the soil in the passive zone and the shear along the sliding plane (see figure 5.5). These sliding planes can have all kind of shapes and the way of the least resistance determines the normative plane. The shear along the sliding plane highly depends on the effective stresses and thus also the freatic line in the dike.

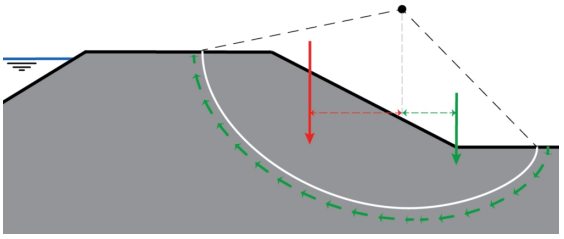

FIGURE 5.5: Force scheme for inner slope stability

The slope stability of the presented simplified dike profile is calculated. These kind of calculations are usually performed by dividing the slip plane in a number of slices and then different methods are available to calculate the stability. These kind of methods analytically calculate the moment equilibrium for a sliding plane and are called Limit Equilibrium Model (LEM). Here the calculation will be done according to the method of Fellenius (Verruijt, 2010) since it is convenient for hand calculations. In this method the factor of safety is determined as the ratio between driving moments and the ultimate resisting moment, which includes the maximum available shear strength of the soil. Another simplification of this method is that the forces between the slices are neglected.

The calculation here will be further simplified to divide the slip plane in two slices, one on the resisting side and one on the driving side, see figure 5.6. Normally numerous different

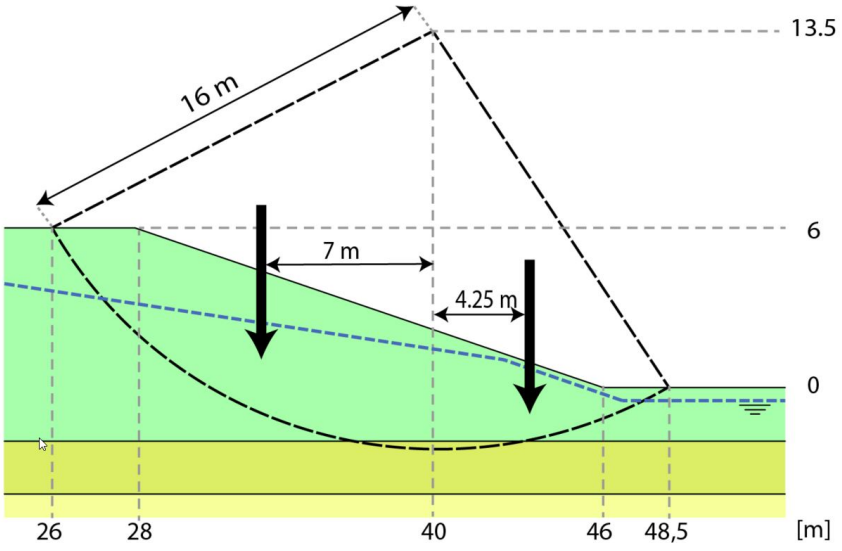

FIGURE 5.6: Geometry of calculated slip plane

sliding planes have to be checked, but now only one sliding plane is checked. Later on in this thesis, similar slip plane calculations are performed with help of a computer. The slip plane, that later on appear to be normative in the computer calculations, is the same plane as is checked here in the hand calculations. This plane is a quarter circle with a radius, r, of 16 meters. The mean shear strength along this plane is based on drained Mohr-Coulomb values from table B.1 (appendix B.3) and is given below. The length of the slip plane, l_{slip} becomes:

$$l_{slip} = \frac{2 \cdot \pi \cdot r}{4} = 25\ m \tag{5.1}$$

$$\tau_{mean} = 23.4\ kN/m^2 \tag{5.2}$$

in which:
l_{slip} = length of the slip plane $[m]$
τ_{mean} = mean shear strength along slip plane $[kPa]$
r = radius of circle $[m]$

The unity check will be performed by adding all moments that have the same direction and to divide it with the moments with an opposite direction. The moments generated by soil slices are calculated with their weights and moment arms. The moment generated by the shear along the plane is a multiplication of the shear strength, the length of the plane and its moment arm.

$$M_{a,\gamma} = b_{slice} \cdot h_{mean} \cdot \gamma_{sat} \cdot r = 14 \cdot 4.4 \cdot 17 \cdot 7 = 7330\ kNm/m \tag{5.3}$$

$$M_{p,\gamma} = b_{slice} \cdot h_{mean} \cdot \gamma_{sat} \cdot r = 8.5 \cdot 3 \cdot 17 \cdot 4.25 = 1840\ kNm/m \tag{5.4}$$

$$M_{p,\tau} = \tau_{mean} \cdot l_{slip} \cdot r = 23.4 \cdot 25 \cdot 16 = 9430\ kNm/m \tag{5.5}$$

$$FoS = \frac{M_{p,\gamma} + M_{p,\tau}}{M_{a,\gamma}} = \frac{9430 + 1840}{7330} = 1.54 \tag{5.6}$$

in which:
$M_{a,\gamma}$ = active moment generated by weight of the soil $[kNm/m]$
$M_{p,\gamma}$ = passive moment generated by weight of the soil $[kNm/m]$
$M_{p,\tau}$ = passive moment generated by shear along slip plane $[kNm/m]$
h_{mean} = average height of soil slice $[m]$
r_{arm} = moment arm $[m]$
b_{slice} = width of soil slice $[m]$
FoS = factor of safety [-]

So in this calculation example, the safety for slope stability is guaranteed since the resisting moment is 54 % larger than the driving moment. This result is obtained assuming drained soil behavior, when undrained behavior would occur the FoS comes out lower.

5.2 Analysis of building effects on the stability

To investigate which configuration is most interesting, in this section stability calculations for the different configurations are performed. The influence of the effects mentioned in the subsections 4.1.4 & 4.2.1 are calculated.

5.2.1 Introduction

The different building configurations from figure 1.3 on page 8 for the inner slope stability are investigated in this section. This is done for two different assumptions, the first being; the building does not collapse, the second being; the building does collapse due to conditions caused by high water.

The building is assumed to have dimensions of $10 \cdot 10\ m$. The location is varied from ahigh location on the outer slope towards the hinterland. In total the calculations are performed for six different locations see figure 5.7.

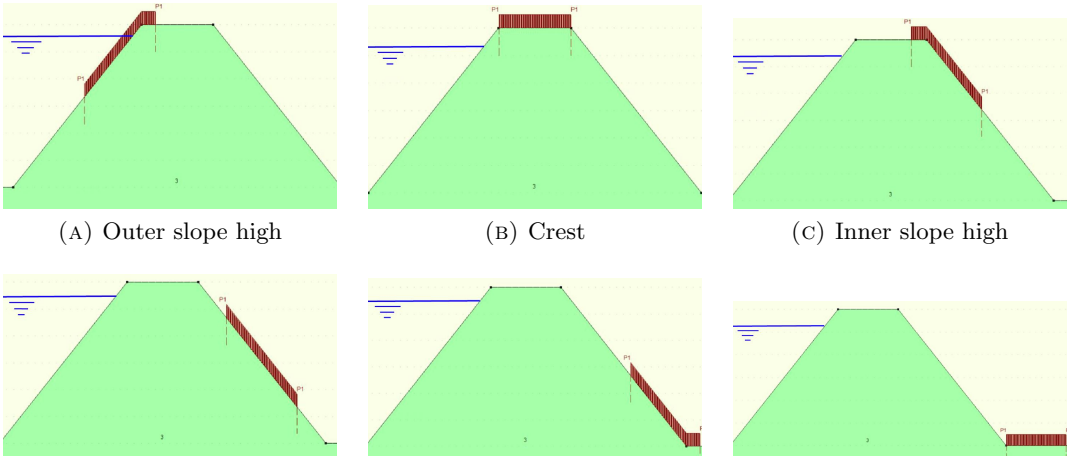

(A) Outer slope high (B) Crest (C) Inner slope high

(D) Inner slope mid (E) Inner slope low (F) Hinterland

FIGURE 5.7: The different locations in the stability analysis

Instead of the Fellenius method the Bishop method is used. The difference between the Bishop and Fellenius method is that the resisting moment caused by the shear is reduced for the influence of the factor of safety itself. This results in a iterative solving procedure, which is not desired for hand calculations but is not problematic for computer calculations. Therefore the FoS is not based on a comparison with the maximum available shear strength, but with the actually occurring shear strength and therefore also the vertical force equilibrium is met. This is done by a comparison of resisting moment, M_r and driving moment M_s, this ratio is expressed as a factor of safety.

$$FoS = \frac{M_r}{M_s} \tag{5.7}$$

Normally the driving moment depends on the weight of the soil on the active zone and the resisting moment depends on the weight of the soil on the passive zone and the shear capacity along the sliding surface. The shear capacity of the soil is based upon the assumption of drained soil behavior and the Mohr-Coulomb criterion (Verruijt, 2010). Furthermore, for this calculation a drained situation is assumed. This factors of safety are calculated with the Deltares software package D-Geo Stability. This software package can calculate the stability for multiple slip planes. A grid of possible centers of slip circles and matching tangent lines has to be inserted, afterward the program calculates the stability for all possible circular slip planes. (Deltares, 2014)

The possible effects from a building on the Macro-stability from sections 4.1.4 & 4.2.5 are modeled here for different configurations. A recap of these effects is given below.

1. The introduction of selfweight of a building. This effect can influence the stability positively but also negatively, dependent on the location. (4.1.4 page: 44)
2. The resistance against instability caused by foundation piles that cross slip circles. This is a positive effect. (4.1.4 page: 45)
3. The leakage of water under a foundation of a building in the outer slope that causes an increase of the freatic line in the dike. This results in a reduction of the strength parameters of the soil and is therefore a negative effect. (4.1.4 page: 45)
4. The additional strength provided by a structural element in the dike, this is a positive effect. (4.1.4 page: 46)
5. The occurrence of soil failure due to a collapsed building, this is a negative effect. (4.2.5 page: 51)
6. The reduction of selfweight of the building after collapse due to high water flow conditions, this effect can be positive or negative.

In table 5.2 the possible effects that are included in the model for the different configurations and also influence the stability are shown.

5.2.2 Model assumptions

In this subsection the used modelling methods for calculating the stability of the different configurations is explained. These assumptions are described compact in this subsection

TABLE 5.2: Overview of the different effects that can be seen in the sensitivity analysis for the inner slope stability (positive effects in green, negative effects in red)

	NO COLLAPSE				BUILDING COLLAPSE			
	On Profile		In Profile		On Profile		In Profile	
Location:	**Shallow**	**Piles**	**Shallow**	**Piles**	**Shallow**	**Piles**	**Shallow**	**Piles**
Outer slope high			③	③	⑥	⑥	⑥ & ③	⑥ & ③
Crest	①	②	① & ④	② & ④	①	②	① & ⑤	② & ⑤
Inner slope high	①	②	① & ④	② & ④	①	②	① & ⑤	② & ⑤
Inner slope mid	①	②	① & ④	② & ④	①	②	① & ⑤	② & ⑤
Inner slope low	①	②	① & ④	② & ④	①	②	① & ⑤	② & ⑤
Hinterland	①	②	① & ④	② & ④	①	②	① & ⑤	② & ⑤

and this is done per effect according the enumeration of effect of the previous subsection. These assumptions are described in more detail in appendix B.4 on page 162 where also calculations are performed which are necessary for the input of the software package.

Since the scope of this study is on relatively old buildings the assumptions are based on such a building. Furthermore the buildings in the soil profile, are assumed to be two meters deep in the profile.

1. For all buildings that have a shallow foundation, their selfweight is inserted as a surcharge load at the location of the building. This is illustrated in figure 5.8 *A*. The calculation of selfweight i.e. surcharge load is performed in appendix B.4 equation: (B.26).

2. The buildings that are founded on piles are modeled with help of the function of soil nails in D-Geo-Stability. This is illustrated in figure 5.8 *B*. For these nails, properties are inserted as that they are wooden foundation piles. The assumed properties of the wood are shown in appendix B.4 equation: (B.33), and these are used for the calculation of the nail properties: equation (B.37). Also background information on the soil nails feature of D-Geo-Stability is given in appendix B.4.

3. For buildings in the outer slope, it is assumed that leakage under the building causes a rise in freatic level in the dike. This increase in freatic line has been put in the model for this configuration. See figure 5.8 *E*.

4. For buildings that have not been collapsed the beneficial effect of structural elements is modeled with help of 'forbidden lines'. This option allows the user to define certain lines in the profile, for which the intersection with the sliding plane is prohibited. The forbidden lines are used to model wall and foundation/floor elements of the building. The foundation/floor elements are only modeled with a forbidden line when these are located in the passive zone. This is illustrated in figure 5.8 *C*. When the building is collapsed all structural elements are assumed to collapse and therefore no 'forbidden lines' are present in these models.

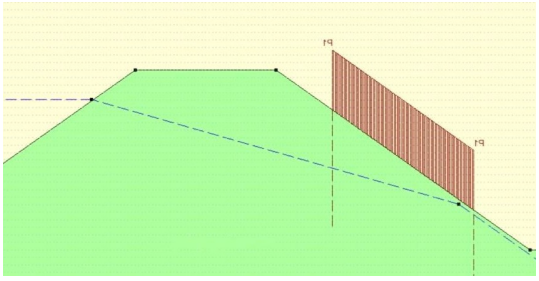

(A) Example of modelling of a building with a shallow foundation

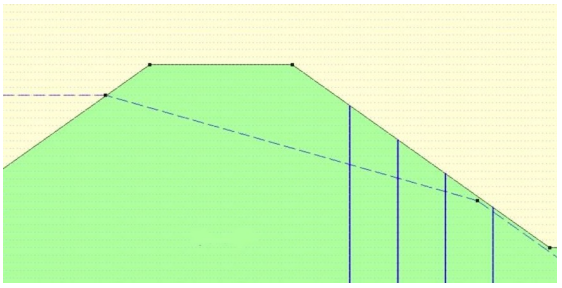

(B) Example of modelling of a building with a pile foundation

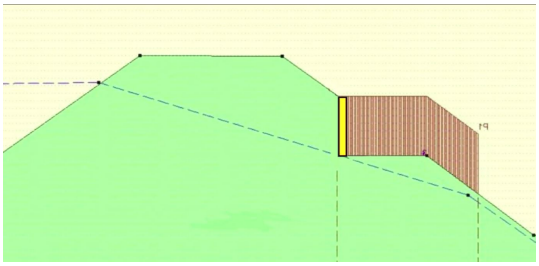

(C) Example of the use of forbidden line (yellow line) for a wall element in profile that is assumed to withstand

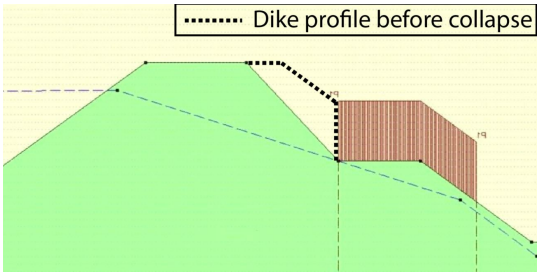

(D) Example of building in profile that is assumed to collapse, which modeled including soil failure

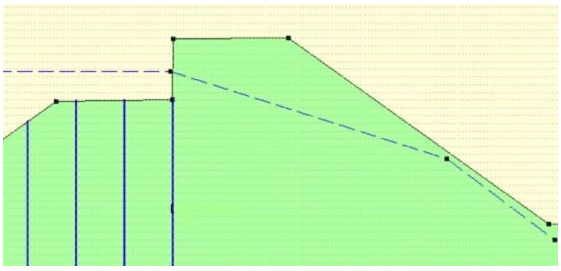

(E) Example of increased freatic line due to leakage under a building that is in the profile

FIGURE 5.8: Overview of modeling method and assumptions in D-Geo

5. If collapse of a building is assumed and the building is situated in the profile, it is assumed that the surrounding earth will fail. The slope of this earth disturbance is assumed to be $1V : 2H$ (Zwanenburg et al., 2013). The failed soil from the disturbance zone is assumed to disappear. This is illustrated in figure 5.8 *D*.

6. When collapse is assumed and the building is located on the outer slope the surcharge for the buildings with a shallow foundation is assumed to be halved because of displacements of the rubble by flow conditions of the river during a high water event.

5.2.3 Results

For the profile of the basic profile the inner slope stability is calculated without building with the D-Geo software package. The resulting factor of safety for the normative slip circle (see figure 5.9) is:

$$FoS = 1.62 \tag{5.8}$$

This stability slip plane calculation is also performed by hand with the equation (5.6) on page 62. But another method is used (Fellenius vs. Bishop) and different amount of slices are used. This explains the different outcomes.

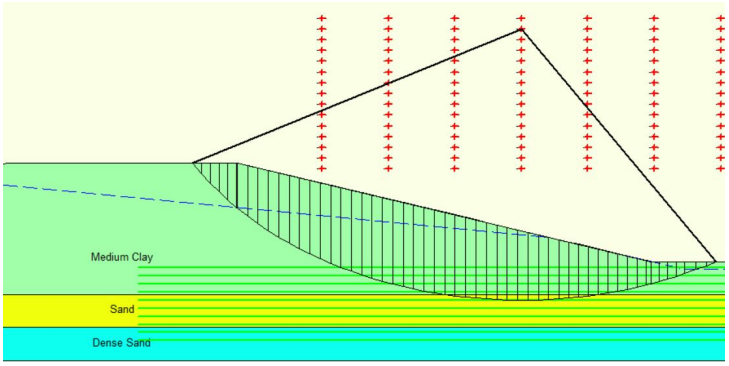

FIGURE 5.9: Normative slip circle of the inner slope for dike profile without building

Now the stability calculations are presented for the different configurations. In table 5.3 the results of the configurations '*on* profile' are shown, this are sufigures *A, B, E, F, I, J, M, N, Q, R* from figure 1.3 (page: 8). In table 5.4 the results of the configurations '*in* profile' are shown, this are sufigures *C, D, G, H, K, L, O, P, S, T* from figure 1.3.

in which: Δ_{nb} = relative change in FoS due to the building [%]
Δ_{col} = relative change in FoS due to collapse [%]

TABLE 5.3: Results of configurations '*On* Soil Profile' (positive effects in green, negative effects in red)

	No Building Collapse				**Building Collapse**					
	Shallow		**Piles**		**Shallow**			**Piles**		
Location:	FoS	Δ_{nb}	FoS	Δ_{nb}	FoS	Δ_{nb}	Δ_{col}	FoS	Δ_{nb}	Δ_{col}
Outer slope high	1.62	0 %	1.62	0 %	1.62	0 %	0 %	1.62	0 %	0 %
Crest	1.55	-4 %	1.69	4 %	1.55	-4 %	0 %	1.69	4 %	0 %
Inner slope high	1.45	-10 %	1.90	17 %	1.45	-10 %	0 %	1.90	17 %	0 %
Inner slope mid	1.61	-1 %	1.97	22 %	1.61	-1 %	0 %	1.97	22 %	0 %
Inner slope low	1.93	19 %	1.83	13 %	1.93	19 %	0 %	1.83	13 %	0 %
Hinterland	1.72	6 %	1.73	7 %	1.72	6 %	0 %	1.65	2 %	-5 %

The results are discussed in the following enumeration which is done in accordance with the list of effects of subsection 5.2.1.

TABLE 5.4: Results of configurations '*In* Soil Profile' (positive effects in green, negative effects in red)

	No Building Collapse				**Building Collapse**					
	Shallow		**Piles**		**Shallow**			**Piles**		
Location:	FoS	Δ_{nb}	FoS	Δ_{nb}	FoS	Δ_{nb}	Δ_{col}	FoS	Δ_{nb}	Δ_{col}
Outer slope high	1.52	-6 %	1.58	-2 %	1.53	-6 %	1 %	1.53	-6 %	-3 %
Crest	1.65	2 %	1.69	4 %	1.73	7 %	5 %	1.73	7 %	2 %
Inner slope high	1.64	1 %	2.00	23 %	1.67	3 %	2 %	2.04	26 %	2 %
Inner slope mid	1.77	9 %	1.95	20 %	1.88	16 %	6 %	2.13	31 %	9 %
Inner slope low	1.88	16 %	1.71	6 %	1.57	-3 %	-16 %	1.58	-2 %	-8 %
Hinterland	1.73	7 %	1.76	9 %	1.11	-31 %	36 %	1.31	-19 %	26 %

1. In the columns of table 5.3 for shallow foundations, the effects of selfweight of the building are observed. See figure 5.8 *A*. The largest negative effect is observed for the location high on the inner slope, while the largest positive influence is observed low on the inner slope.

2. The positive influence of pile foundations is observed in the corresponding columns of table 5.3. See figure 5.8 *B*. The effect is largest for a building located on the middle of the inner slope. That is because the piles for this location intersect with all possible slip planes.

3. In table 5.4 at the location, high on the outer slope, the negative effect of an increased freatic line due to leakage under the building is observed. See figure 5.8 *E*. When this rise of freatic line occurs due to leakage, this affects the stability significantly.

4. The positive effect of structural elements is largest for buildings that are located in the profile. See figure 5.8 *C*. As for instance can be seen by comparing the results of table 5.4 with table 5.3 for the scenario that the building remains intact.

5. The effect of soil failure due a collapsing building is observed in the right part of table 5.4. See figure 5.8 *D*. Especially for locations close to the hinterland this effect appears to be large. Because the soil from the disturbance zone is assumed to disappear some odd results are observed at the higher locations. This is caused due to the disturbance zone is located in the active side of the sliding plane, and therefore the driving moment seems to decrease after soil failure.

6. The effect of moved rubble from a building at the outer slope does not have an influence on the inner slope stability. That is because the surcharge on this location is not part of the normative sliding plane. This can be observed in table 5.3 for building collapse at the location high on the outer slope.

5.2.4 Discussion

Some remark concerning the results and the calculation method are given below:

- Probably some situations, for instance buildings on the crest, might get a lower FoS when other methods like Spencer are used, because these methods have more freedom in the shape of the slip plane, while the Bishop method is bounded to circular slip planes.
- The result for buildings that are located in the profile are also influenced because locally less soil in the profile is present. This interferes with the studied effects.
- The current approach for assuming the residual profile after collapse of a building in the profile is not very realistic. It is assumed that the soil from the disturbance zone disappears after failure. Depending whether the soil was in the passive or the active zone this has respectively a negative or a positive effect. A more realistic model would be to change the profile of the soil body after collapse, so that no soil is assumed to be disappeared, but soil slides towards the location of the former building. In section 6.3.1 such kind of approach is compared with the approach that was used in this section.

5.3 Conclusions

In this section conclusions from this chapter are drawn which will give a compact answer to the subquestion that has been researched throughout this chapter. The following subquestion was treated in this chapter: *"What configurations and failure mechanism are most interesting to focus this study on, and why?"* The failure mode which is focused on is the inner slope stability, and therefore to answer the remainder of the subquestion the amount of influence of the effects of a building on the stability has to be determined. The conclusions from this are also given in this section.

For building elements that in a way reinforce the slope, like a wall, a pile foundation or a shallow founded building on the passive side, the beneficial influence is the largest when they are located on or in the slope. This can be explained by the fact that all potential slip planes go through the slope. For instance, a pile foundation located in the hinterland or the crest has a marginal beneficial influence because there are also slip planes that do not intersect with the piles.

When a building affects the stability negatively the above mentioned does not apply. For instance a shallow founded building on the crest has a rather negative effect because the normative slip plane becomes a plane that fully contains the building as a surcharge.

The calculations with the different configurations show that the possible collapse of buildings can indeed severely impact the stability. The lowest calculated Factor of Safety is also found for a situation where the building is collapsed. The largest consequences of the collapse scenario are found for buildings located low in the inner slope or in the hinterland, that are located inside the soil profile. On the other hand when buildings, from these situations, remain intact, they have a beneficial effect on the stability of a dike.

FIGURE 5.10: Impression of building inside the inner slope

That is why these configurations are selected for further research in this thesis. In the following part a method is developed to investigate the influence of buildings for these configurations. Besides these configurations are occurring quite frequently near Dutch dikes, and often these buildings are relatively old which makes the reliability of these building quite unclear. In figure 5.11 the selected configuration is shown.

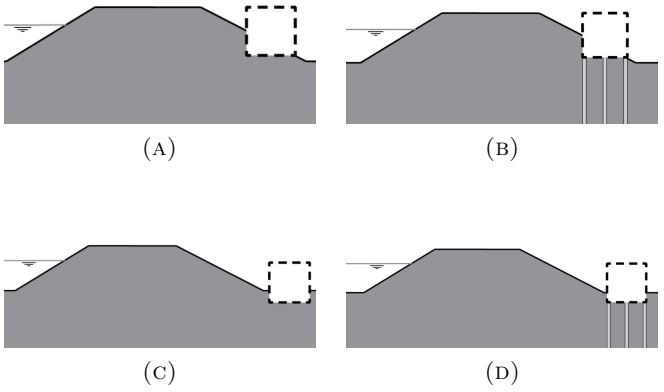

FIGURE 5.11: Macro stability of these configurations are the focus for the remaining of this thesis

Part III

Development and application of a method for a building inside the inner slope

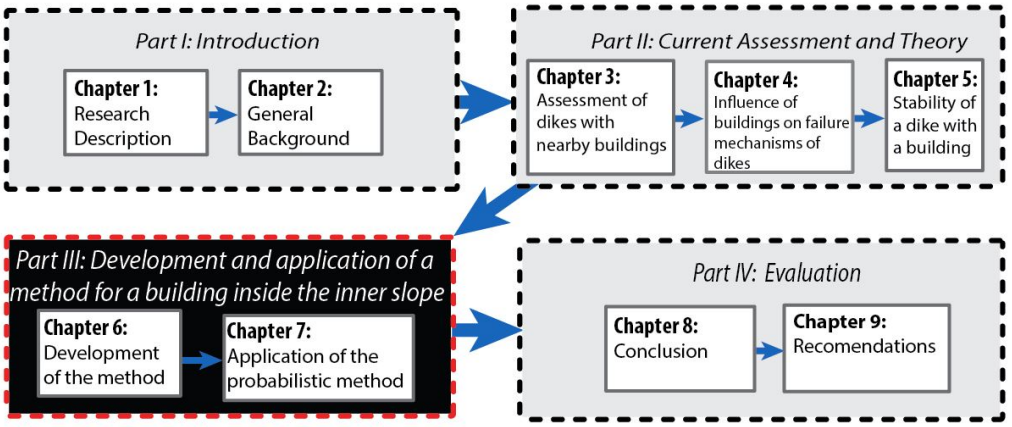

This page intentionally left blank.

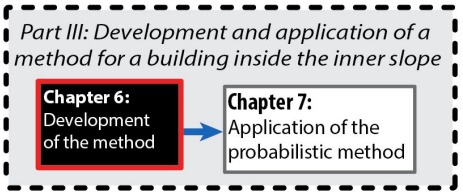

Chapter 6

Development of the method

In this part of the thesis a probabilistic method to determine the influence of a building is developed and applied to a case study. The method is developed for a building that is located inside the inner slope and therefore the possible collapse of the building is relevant. Chapter 6 focuses on the development of this probabilistic method while in chapter 7 the method is applied to a case study.

In this chapter the following research question is treated: *How can the influence of a building for the selected configuration be determined, and which information should be available to perform this method?* The result of the first part of the question is a probabilistic method that is developed and explained in section 6.1. In sections afterwards, theories and calculations are collected that are necessary to perform the method for the selected configuration. In section 6.2 the possible collapse of the building is treated and in section 6.3 the interaction between building collapse and dike stability is discussed. In section 6.4 conclusions from this chapter are drawn.

6.1 Probabilistic method

In this section the general approach of the probabilistic method is discussed. In the first subsection the method is explained and in the next subsection the sensitivty of the method is analyzed.

6.1.1 Development and explanation of method

This method is developed for buildings located in the soil profile of a dike. This means that possible collapse of the building will affect this soil profile. Therefore this possible

collapse of the building has to be included in the method. The method consists of three steps:

1. **Structural model**
   The goal of the structural model is to define the performance of the building during a highwater event. This is expressed in a probability of building collapse ($P_{collapse}$). See top left part of figure 6.4 on page 78.

2. **Geotechnical model**
   The goal of the geotechnical model is to define the performance concerning slope stability of the dike profile given a scenario of a collapsed building or an intact building. This is expressed in probabilities of instability of the slope given that the building collapses or that it remains intact ($P_{(instab|collapse)}$ & $P_{(instab|intact)}$). See top right part of figure 6.4.

3. **Integration of both models**
   The goal of the final step is to integrate the results from the first two steps in order to define the performance for the slope stability of the combined system of dike and building. This is expressed in a probability of inner slope instability (P_{instab}). See bottom part of figure 6.4.

The different steps of the probabilistic method are individually treated below. After this explanation the method is over viewed by means of a flow chart.

Structural model

In the structural model the performance of the building during a high water event has to be determined. Important parameters of this model are:

h_w	=	outer water level $[m]$
$f_{(h_w)}$	=	PDF of water level
$F_{(collapse\|h_w)}$	=	cdf of the event "building collapses" given a certain water level $[-]$
$P_{collapse}$	=	probability of the event "building collapses"
P_{intact}	=	probability of the event "building does not collapses" i.e. building remains intact

First the cdf of collapse given a certain water level ($F_{(collapse|h_w)}$) is to be determined. To illustrate the results of this, the concept of fragility curves is useful. Within hydraulic engineering a fragility curve shows the performance of a flood defence as a function of the water level or in this case the performance of the building (Van Gelder, 2014). A fragility curve of such a building might look like as is depicted in figure 6.1 *B*.

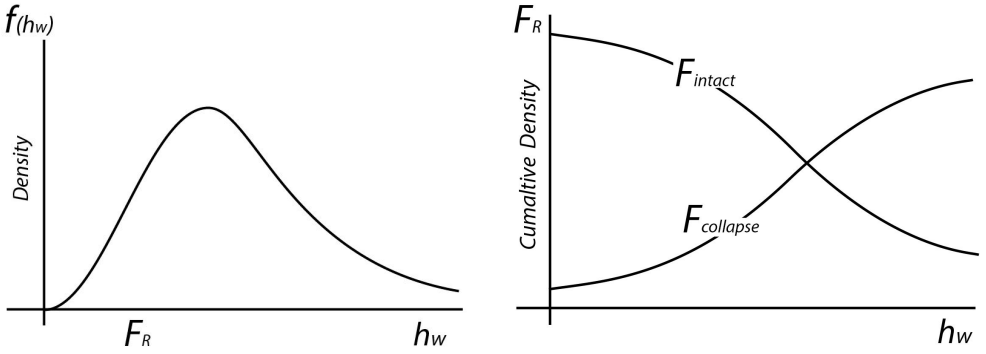

(A) Pdf of outer water level

(B) Fragility curve of the building and complementary cdf (building intact) describing the performance of the building during highwater conditions

FIGURE 6.1: Description of structural model

From this fragility curve it can be seen that the probability of collapse increases for increasing water levels. This is due to the increased loads during high water conditions. The integrated probability of collapse ($P_{collapse}$) is obtained when the convolution integral of the fragility curve (figure 6.1 *B*) and the PDF of the water level (figure 6.1 *A*) is calculated. The convolution integral is an integral from which the outcome is the failure probability and it can consist of an integral of a multiplication of the CDF of the resistance and the PDF of the loading (Jonkman et al., 2015). For more background on this integral, referred is to appendix A.6 on page 151. The convolution integral for the integrated probability of collapse, based on figures 6.1 *A* & B, becomes:

$$P_{collapse} = \int_{-\infty}^{+\infty} F_{(collapse|h_w)}(h_w) \cdot f(h_w)\, dh_w \tag{6.1}$$

This is the outcome result of the structural model.

Geotechnical model

In the geotechnical model the performance of the soil structure has to be determined. Depending on the event "building collapse", this soil profile has two appearances: A soil profile given that the building remains intact and a soil profile given that the building collapses, see figure 6.2. The important parameters that have to be determined in this model are listed below.

(A) Building remains intact, with probability: $P_{(instab|intact)}$

(B) With building collapse, with probability: $P_{(instab|collapse)}$

FIGURE 6.2: Two possible scenarios of a dike containing a building inside the soil profile

$F_{(instab\|intact,h_w)}$	=	cdf for inner slope instability given that the building remains intact and a certain water level occurs [−]
$F_{(instab\|collapse,h_w)}$	=	cdf for inner slope instability given that the building does collapse and a certain water level occurs [−]
$P_{(instab\|intact)}$	=	probability for inner slope instability given that the building remains intact
$P_{(instab\|collapse)}$	=	probability for inner slope instability given that the building does collapse

First the two conditional cdf for instability given a certain water level ($F_{(instab|collapse/intact,h_w)}$) are to be determined. When these results are obtained, two fragility curves could be drawn just like is done in 6.3 *A*. The fragility curve of the soil profile given building collapse is shifted more to the left, which means that at lower water levels the probability of instability already increases. This is expected since the collapse of the building will probably negatively influence the soil profile of the dike.

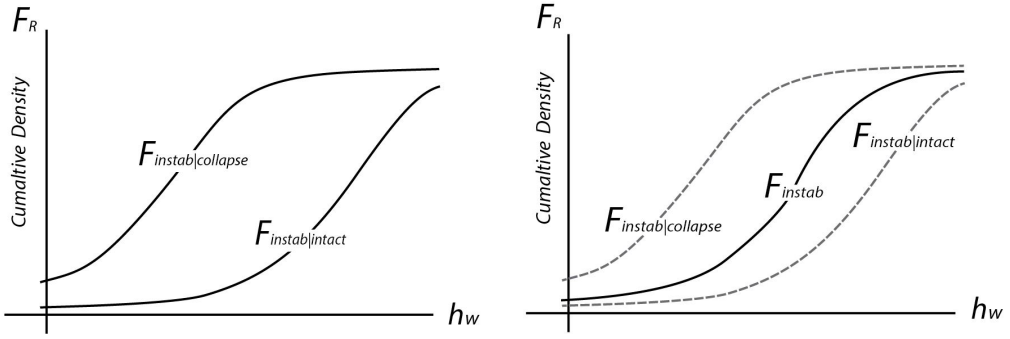

(A) Fragility curves for the dike given building collapse or building intact

(B) Weighted fragility curve after integration of both models

FIGURE 6.3: Description for geotechnical model

The integrated probabilities can be obtained from the convolution integrals from the fragility curves of figure 6.3 *A* and the PDF of the water level (figure 6.1 *A*). This results

in:

$$P_{(instab|intact)} = \int_{-\infty}^{+\infty} F_{(instab|intact,h_w)}(h_w) \cdot f(h_w)\, dh_w \tag{6.2}$$

$$P_{(instab|collapse)} = \int_{-\infty}^{+\infty} F_{(instab|collapse,h_w)}(h_w) \cdot f(h_w)\, dh_w \tag{6.3}$$

These two probabilities are the outcome of the geotechnical model.

Integration of both models

When the fragility curves for instability and for collapse are observed, it can be seen that when the water level increases both the probability of building collapse and the probability of instability increases. This can be illustrated by the 'weighted' fragility curve depicted in figure 6.3. This fragility curve represents the dike system containing a building while possible collapse is included. This is done to combine the fragility curves from figure 6.1 *B* and figure 6.3 *A*. The result is a fragility curve that shifts from the $P_{instab|intact}$ curve towards the curve of $P_{instab|collapse}$ as the water level increases. The desired outcome of the method could be obtained by the convolution integral of this fragility curve and the PDF of the water level. The final step of the integration of the two models is described below.

The probability of instability of the combined system of dike and building is calculated with help of the "law of total probability" (Jonkman et al., 2015). This law relates normal probabilities to conditional probabilities. It gives an expression for the total probability of an outcome that can be realized through a number of different events. The law of total probability is described by equation (6.4). When this is applied to the results of the structural and the geotechnical model equation (6.6) is obtained. And since the two events are mutually exclusive[1] and complementary[2] this can be further simplified to (6.7)

$$P_f = \sum_{i=1}^{2} P_{(instab|collapse/intact)} \cdot P_{collapse/intact} \tag{6.4}$$

$$P_{instab} = P_{(instab|intact)} \cdot P_{intact} + P_{(instab|collapse)} \cdot P_{collapse} \tag{6.5}$$

$$P_{intact} + P_{collapse} = 1 \tag{6.6}$$

$$P_{instab} = P_{(instab|intact)} \cdot (1 - P_{collapse}) + P_{(instab|collapse)} \cdot P_{collapse} \tag{6.7}$$

[1] $P_{intact} \cap P_{collapse} = \oslash$: The two events can not occur simultaneously i.e. there is no intersection of the two events

[2] $P_{intact} \cup P_{collapse} = \Omega$: The union of the two events represent the whole probability space.

in which: P_{instab} = probability of inner slope stability of the combined system

This is the outcome of the final step of the probabilistic method to determine the influence of buildings located in the soil profile of a dike.

Overview

The here presented probabilistic method to determine the influence of a building, is further on in this thesis referred to as the method.

With this method it is now possible to assess the instability of a combined system of building and dike. The possible positive influence of a building is accounted in the $P_{(instab|intact)}$ while eventual negative influence due to building collapse is accounted in $P_{(instab|collapse)}$. A flow chart of the method is depicted in figure 6.4. The content of the first step, the structural model, is further researched and described in section 6.2. Background on the geotechnical model has already been described in chapter 5. The interaction between building collapse and dike instability is further described in section 6.3.

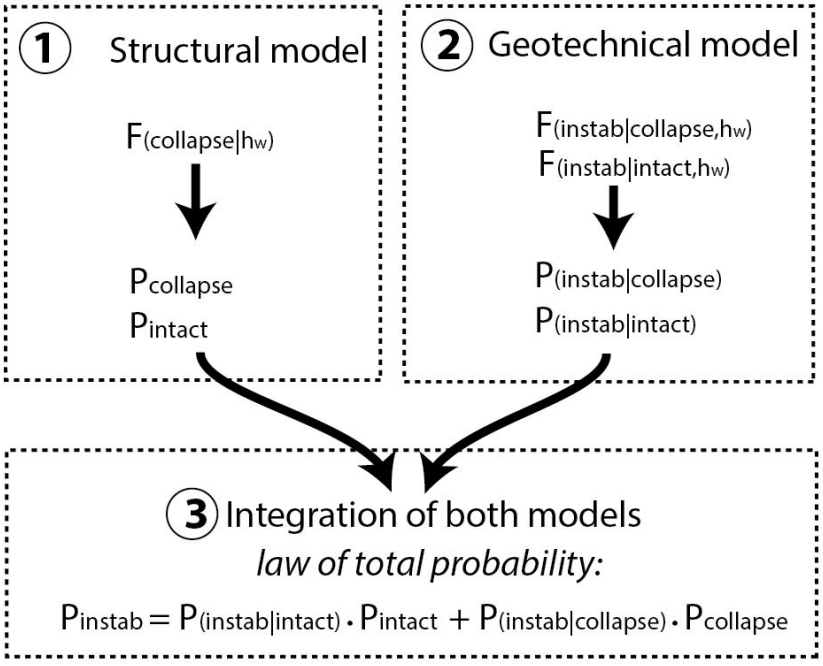

FIGURE 6.4: Overview chart of the probabilistic method

6.1.2 Sensitivity analysis

In the previous subsection a probabilistic method has been presented to determine the influence of a building, including possible collapse, on the dike stability. In this subsection the possible effects of a combined system of dike and building are analyzed according to this method by means of a calculation example. This calculation example is based on the approach of the earlier presented new statutory assessment tools (WBI2017: section 2.3.1 on page 19).

When the new proposal probability values for Dutch water defenses are observed (figure 2.10 page 24) it is observed that large parts of the river dikes have been standardized with mid-probabilities of: (signal value, not a rejection limit, see figure 2.9 on page 23 for exemplification of the different probabilities within WBI2017)

$$P_{mp} = \frac{1}{30.000} = 3.33 \cdot 10^{-5} \tag{6.8}$$

The mid probability and the maximum allowable probability (rejection limit) are related to each other by a factor three:

$$P_{map} = 3.33 \cdot 10^{-5} \cdot 3 = 10^{-4} \tag{6.9}$$

in which: P_{mp} = mid probability $[yr^{-1}]$
P_{map} = maximum allowable probability $[yr^{-1}]$

For this calculation example a dike is assumed that should suffice to the norm values of equations (6.8) & (6.9). Furthermore it is assumed that the dike at this particular moment has a failure probability in between the mid probability and the maximum allowable probability, and therefore the actual failure probability of this dike is:

$$P_{ibt} = 3.33 \cdot 10^{-5} \cdot 1.5 = 2.22 \cdot 10^{-5} \tag{6.10}$$

With the failure space reserved for inner slope stability (table 2.2 on page 25) the corresponding probability of instability is:[3]

$$P_{instab,ibt} = \omega \cdot P_{ibt} = 0.04 \cdot 2.22 \cdot 10^{-5} = 8.89 \cdot 10^{-7} \tag{6.11}$$

And the corresponding probability for inner slope stability of the rejection limit is:

$$P_{instab,map} = \omega \cdot P_{ibt} = 0.04 \cdot 10^{-4} = 6.67 \cdot 10^{-6} \tag{6.12}$$

[3]The modification to imply the length effect is disregarded here since this analysis is only performed on a cross section level.

in which: P_{ibt} = probability in between P_{map} and P_{mp} $[yr^{-1}]$
$P_{instab,ibt}$ = corresponding probability of instability of inner slope of P_{ibt} $[yr^{-1}]$
$P_{instab,map}$ = corresponding probability of instability of inner slope of P_{map} $[yr^{-1}]$

Now the probabilistic method is tested in this example dike for different assumed values to analyze the effects of the system. The equation belonging to the probabilistic method is depicted below:

$$P_{instab} = P_{(instab|intact)} \cdot (1 - P_{collapse}) + P_{(instab|collapse)} \cdot P_{collapse} \tag{6.13}$$

First the conditional probabilities of instability given that the building remains intact, are exemplified. It is considered that for the most possible negative scenario the building does not provide any additional stability to the soil body. Therefore for the negative scenario the conditional probability is the same as for the dike without building (equation: (6.11)). In a positive scenario the building does improve the stability and therefore reduce the conditional probability of instability. A reduction by a factor 100 is assumed for this scenario. (red values belong to a negative scenario, green values to a positive and orange to a neutral scenario)

$$P_{(instab|intact)} = 8.89 \cdot 10^{-9} \tag{6.14}$$

$$P_{(instab|intact)} = 8.89 \cdot 10^{-7} \tag{6.15}$$

Now the conditional probabilities of instability given that the building collapses, is exemplified. It is considered in this example that when a building collapses the stability of the dike is always affected. Therefore for the positive scenario a reduction of conditional probability by a factor 100 is assumed, and for the negative scenario a reduction by a factor 10.000 is assumed.

$$P_{(instab|collapse)} = 8.89 \cdot 10^{-5} \tag{6.16}$$

$$P_{(instab|collapse)} = 8.89 \cdot 10^{-3} \tag{6.17}$$

Finally the probability of building collapse, is exemplified. The neutral scenario here is based on a re-assessment standard for buildings (NEN8700, 2011). The value that belongs to a building belonging to consequence class two[4] (CC2) is adopted in the neutral scenario. Regular residential and office buildings are part of this consequence class (EC-0, 2011). In (Vrouwenvelder et al., 2011) it is stated that the maximum allowable failure

[4]It might be better to classify these buildings in CC-3 since they are part of the water defenses.

probability for a building from CC-2 concerning human safety is $P = 3 \cdot 10^{-4}$. For the positive scenario a probability 100 times smaller is adopted, which then represents a over-dimensioned building, according to this standard. For the negative scenario a probability 100 times larger is adopted, which then represents a building that does not meet the standards.

$$P_{collapse} = 3 \cdot 10^{-6} \tag{6.18}$$

$$P_{collapse} = 3 \cdot 10^{-4} \tag{6.19}$$

$$P_{collapse} = 3 \cdot 10^{-2} \tag{6.20}$$

For all different combinations of the above mentioned scenarios the probabilistic method is analyzed. The outcome results are presented in the second last column of table 6.1. In the penultimate column the calculated stability is compared to the same dike without building, equation (6.11). In the final column the calculated stability is compared to the rejection limit for inner slope stability of this dike, equation (6.12).

TABLE 6.1: Outcome results for calculation example with different values (green values belong to a positive scenario, red to a negative and orange to a neutral scenario)

	$P_{(instab\|intact)}$	$P_{(instab\|collapse)}$	$P_{collapse}$	P_{instab}	$P_{instab} >$ $P_{instab,ibt}$	$P_{instab} >$ $P_{instab,map}$
1.	$8.89 \cdot 10^{-9}$	$8.89 \cdot 10^{-5}$	$3 \cdot 10^{-6}$	$9.16 \cdot 10^{-9}$	No	No
2.	$8.89 \cdot 10^{-9}$	$8.89 \cdot 10^{-3}$	$3 \cdot 10^{-6}$	$3.56 \cdot 10^{-8}$	No	No
3.	$8.89 \cdot 10^{-9}$	$8.89 \cdot 10^{-5}$	$3 \cdot 10^{-4}$	$3.56 \cdot 10^{-8}$	No	No
4.	$8.89 \cdot 10^{-9}$	$8.89 \cdot 10^{-3}$	$3 \cdot 10^{-4}$	$2.68 \cdot 10^{-6}$	Yes	No
5.	$8.89 \cdot 10^{-9}$	$8.89 \cdot 10^{-5}$	$3 \cdot 10^{-2}$	$2.68 \cdot 10^{-6}$	Yes	No
6.	$8.89 \cdot 10^{-9}$	$8.89 \cdot 10^{-3}$	$3 \cdot 10^{-2}$	$2.67 \cdot 10^{-4}$	Yes	Yes
7.	$8.89 \cdot 10^{-7}$	$8.89 \cdot 10^{-5}$	$3 \cdot 10^{-6}$	$8.89 \cdot 10^{-7}$	Yes	No
8.	$8.89 \cdot 10^{-7}$	$8.89 \cdot 10^{-3}$	$3 \cdot 10^{-6}$	$9.16 \cdot 10^{-7}$	Yes	No
9.	$8.89 \cdot 10^{-7}$	$8.89 \cdot 10^{-5}$	$3 \cdot 10^{-4}$	$9.16 \cdot 10^{-7}$	Yes	No
10.	$8.89 \cdot 10^{-7}$	$8.89 \cdot 10^{-3}$	$3 \cdot 10^{-4}$	$3.56 \cdot 10^{-6}$	Yes	No
11.	$8.89 \cdot 10^{-7}$	$8.89 \cdot 10^{-5}$	$3 \cdot 10^{-2}$	$3.53 \cdot 10^{-6}$	Yes	No
12.	$8.89 \cdot 10^{-7}$	$8.89 \cdot 10^{-3}$	$3 \cdot 10^{-2}$	$2.68 \cdot 10^{-4}$	Yes	Yes

From the first three combinations of scenarios (row one till three) it is concluded that a building can improve the stability, also when possible collapse is included. Furthermore it can be seen that when a dike is overdimensioned, and a building influences the stability negatively, the resulting probability of instability may still be above the rejection limit. Only for the combinations in row 6 and 12 a probability of instability is retrieved that is below the rejection limit.

6.2 Building collapse

In this section the possible collapse of a building inside the dike is investigated. This is done for the basic case from the previous chapter (figure 5.1 and properties from table 5.1) in which a building is added to the soil profile. See figure 6.5. First the loads on such a building are identified.

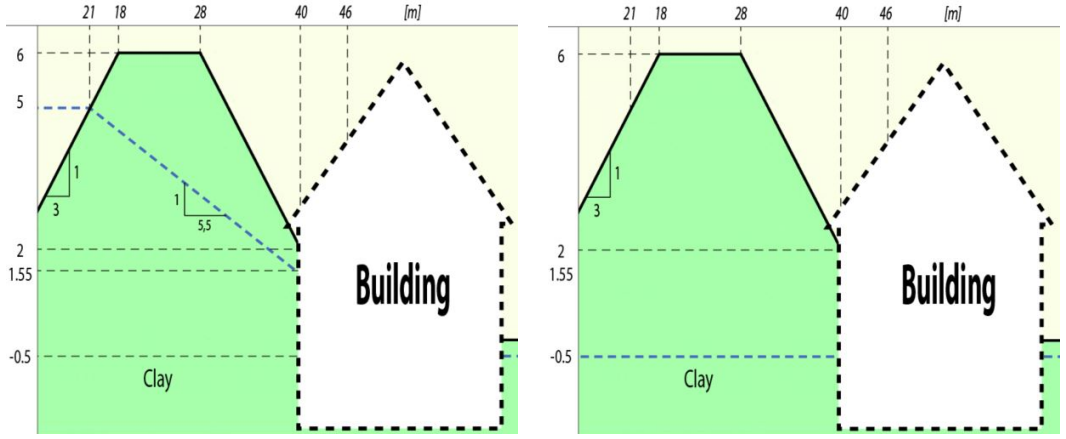

(A) Freatic line for high water conditions

(B) Freatic line for normal conditions

FIGURE 6.5: The two situations for which loads are identified

6.2.1 Loads

The development of horizontal soil pressures caused by vertical effective stresses is proportional to the lateral earth pressure coefficients. For a wall that somewhat displaces due this soil pressures, the active lateral earth pressure coefficient has to be used. For rigid structures, that do not displace, the developing pressures are higher and therefore the neutral lateral ground pressure has to be used. On the other side of the building, where the building is pushed against the soil the developed soil pressures are even higher and the passive pressure coefficient has to be used. These different pressures depend on the angle of internal friction of the soil, according to (Verruijt, 2010). For the soil properties assumed in the basic case this results in[5]:

$$K_0 = 1 - \sin(\phi) = 1 - \sin(22) = 0.63 \tag{6.21}$$

$$K_a = \frac{1 - \sin(\phi)}{1 + \sin(\phi)} = \frac{1 - \sin(22)}{1 + \sin(22)} = 0.45 \tag{6.22}$$

$$K_p = \frac{1 + \sin(\phi}{1 - \sin(\phi)} = \frac{1 + \sin(22)}{1 - \sin(22)} = 2.20 \tag{6.23}$$

[5]The effect of cohesion on the soil pressures coefficients is neglected.

in which: K_0 = neutral lateral earth pressure coefficient [−]
K_a = active lateral earth pressure coefficient [−]
K_p = passive lateral earth pressure coefficient [−]

When the soil pressures would be calculated with these values, the resultant force would be underestimated because the ground surface in front of the wall is not horizontal. So further away of the wall the soil body becomes higher, and this soil also adds additional horizontal pressures. This results in new pressure coefficients. For K_0, (EC-7, 2012) gives a formula which results in the following:

$$\beta_{sl} = \tan^{-1}(\frac{1}{3}) = 18.4^\circ \tag{6.24}$$

$$Radians(18.4^\circ) = 0.32 \tag{6.25}$$

$$K_{0,\beta} = K_0 \cdot (1 + \sin(\beta)) = 0.63 \cdot (1 + \sin(0.32)) = 0.83 \tag{6.26}$$

$$K_{0,\beta,h} = \frac{0.83 \cdot 3}{\sqrt{10}} = 0.79 \tag{6.27}$$

in which: $K_{0,\beta,}$ = neutral earth pressure coefficient for an inclined ground surface, perpendicular to the ground surface [−]

$K_{0,\beta,h}$ = neutral earth pressure coefficient for an inclined ground surface, horizontally decomposed [−]
β_{sl} = inclination of ground surface in front of the building [°]

The active ground pressure coefficient for an inclined ground surface is also determined but for this coefficient a graph is used (EC-7, 2012). See appendix B.5 on page 165 for the extended values and graph that is used to obtain the following value:

$$K_{a,\beta,h} = 0.65 \tag{6.28}$$

in which: $K_{a,\beta,h}$ = active earth pressure coefficient for an inclined ground surface, horizontally decomposed [−]

When this active and neutral coefficients are used and the resulting horizontal soil pressures on the wall of the building for the two freatic levels of figure 6.5 can be calculated. The results can be seen in figure 6.6. When the subfigures E & F are compared with the subfigures B & C from figure 6.6 it can be seen that the risen freatic level indeed causes an increase in horizontal stresses. Since it appears that the development of the freatic line is responsible for increased loads on the soil retaining wall, the possible collapse of such a building is dependent to a high water event.

The development of freatic levels inside a dike during a high water is described in more detail in appendix A.4 on page 147. In this appendix some background on this topic is

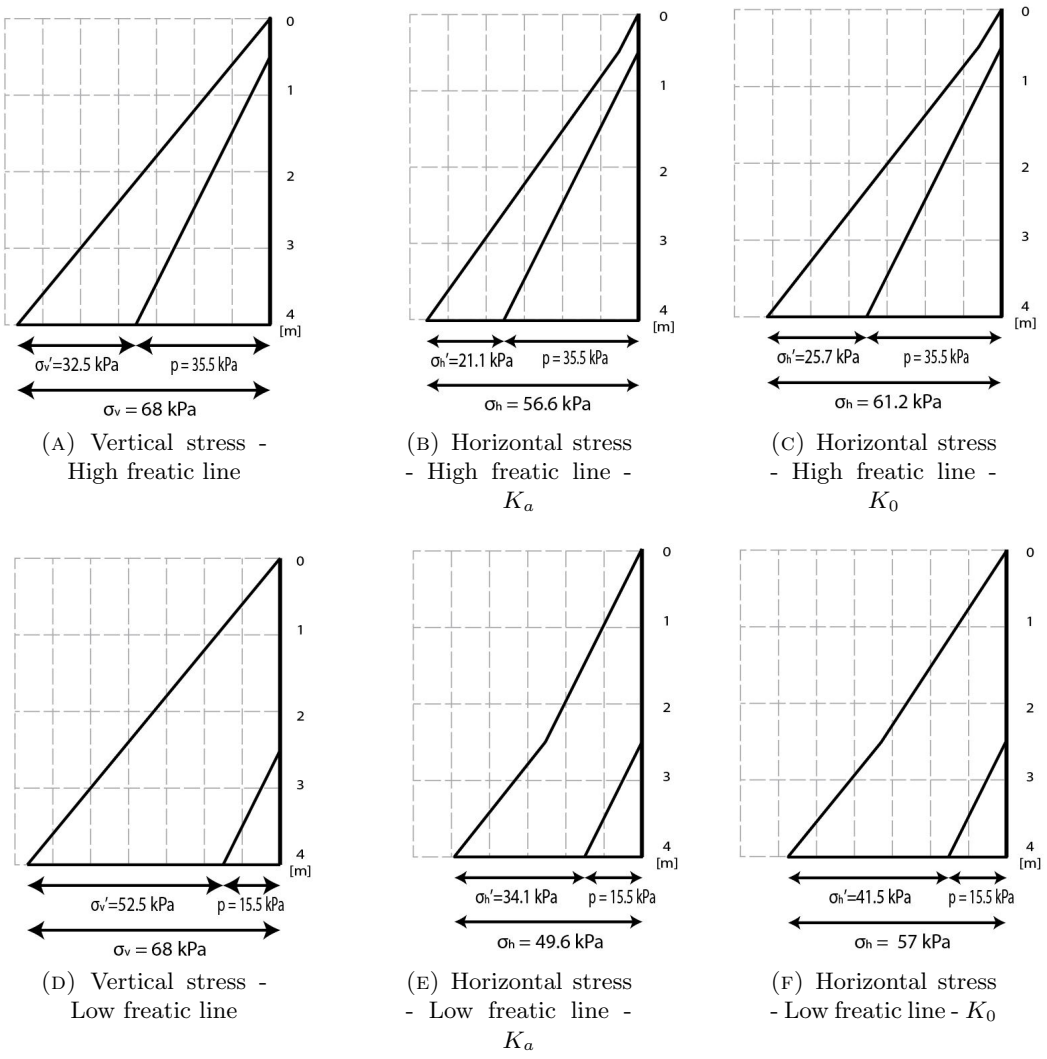

(A) Vertical stress - High freatic line

(B) Horizontal stress - High freatic line - K_a

(C) Horizontal stress - High freatic line - K_0

(D) Vertical stress - Low freatic line

(E) Horizontal stress - Low freatic line - K_a

(F) Horizontal stress - Low freatic line - K_0

FIGURE 6.6: Vertical and horizontal soil pressures for the two different freatic lines

presented as well as a schematisation method for freatic lines in dikes is presented. This schematisation method is also applied to the situation of figure 6.5.

The derivation of active and neutral lateral earth pressure coefficients is based on drained soil properties. This means that when the soil behaves undrained these coefficients could become higher which results in higher soil pressures on the wall. In appendix B.6 on page 166 the possible increase of soil pressures due to undrained soil behavior is exemplified. Another cause of increased soil pressures on the building could be induced by a traffic load present on the dike. This is further explained in appendix A.5 on page 150.

Displacements of the soil body

In the explanation of the different lateral earth pressure coefficients it already became clear that the magnitude of displacements of the wall has an influence on the resulting

lateral soil pressures. On the active side of the soil, the less the displacements of the wall are, the higher the resulting soil pressures against it are. But during high water conditions, when the dike is retaining water on one side, the dike itself is also loaded and can also displace and compact (see figure 6.7). When the displacements of the soil body are larger than the displacements of the building this will lead to additional soil pressures and compaction of the soil might also increase the soil pressures. Besides that these displacements depend on their loading, they also depend on their stiffness's. The loading will be transferred according to the stiffness relation between the building and the dike. The stiffness of the soil body depends on the soil properties while the stiffness of the whole building depends on the foundation properties. So the development of additional soil stresses due to deformations of the soil body could vary due to different foundation methods, because these can influence the stiffness of the building as a whole.

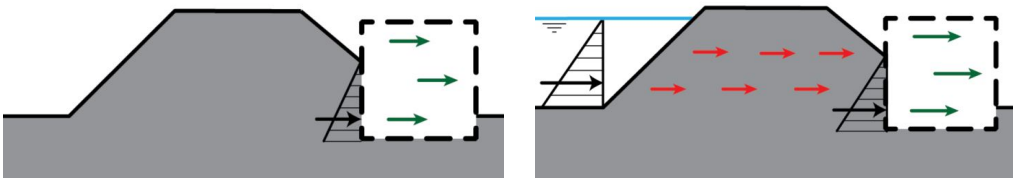

(A) Forces and displacements during normal conditions

(B) Forces and displacements during high water conditions

FIGURE 6.7: Influence of high water on the soil pressures

In fact it is a combined system, of soil and structure and where they both influence each other. For instance when the wall displaces, the soil will displace resulting in lower soil pressures on the wall. To describe the loading better concerning these effects, the soil structure interaction for such a system should be studied.

Arching

That the stiffness of the building has an influence on the development of horizontal soil pressures is clear. But also stiffness differences across the soil retaining wall influences the soil pressures. Since the sides of the wall are supported by perpendicular walls these parts are stiffer than the middle of the soil retaining wall (stiffness differences in length direction of the wall). And also the presence of a floor behind a soil retaining wall can lead to stifness differences along the wall (stiffness differences in height direction of the wall). Due to this stiffness differences along the wall, soil pressures are redistributed to the stiffer parts of the wall. This effect is called arching. See figure 6.8 [6].

The local stiffness of the wall can also be related to the lateral pressure coefficients.

[6] These figures assume only stifness differences in the length direction of the wall.

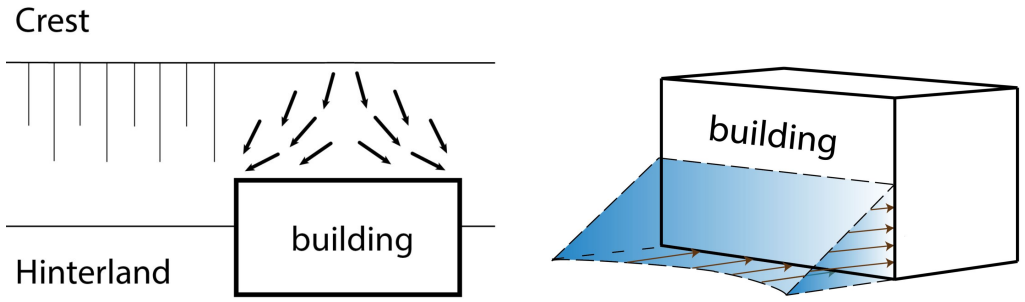

(A) Top view of arching effect

(B) 3 D visualisation of soil pressures due to arching

FIGURE 6.8: Soil pressures influenced by arching

A starting point for the introduction of the arching effect could be to assume that the active pressure coefficient is valid at mid span of the retaining wall, because the deflection here will be the largest. And if the sides of the wall are assumed to be rigid the neutral

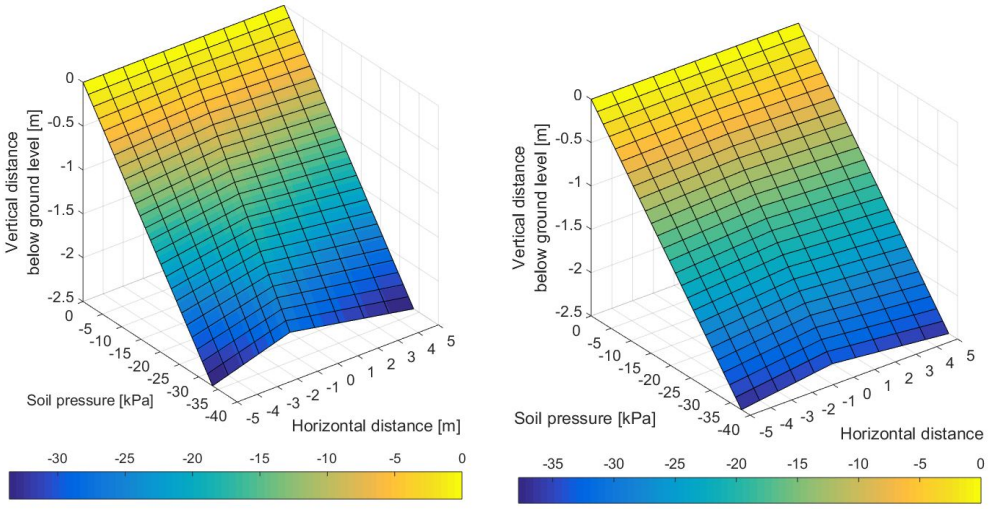

(A) Result for freatic line belonging to low water

(B) Result for freatic line belonging to high water

FIGURE 6.9: Soil pressures along retaining wall when different ground pressure coefficients are assumed

pressure coefficients should be valid here. If this method is applied to the earlier assumed triangular loads in table 6.2, 3 dimensional soil pressures could be plotted for the basic case. (see figure 6.9[7])

It can be seen that the rise of freatic line causes an larger increase in horizontal pressures at mid span than at end span, because the water pressures do not arch. In low water conditions the soil pressures at mid span are lowered due arching, but when the freatic line rises the pore water rises and the effective soil pressures drop and therefore also the

[7]These figures assume only stiffness differences in the length direction of the wall.

beneficial effect of arching reduces. This may have a negative effect also since this mid span of the wall is a normative section since the highest bending moments occur at this location.

6.2.2 Strength

The loading on the soil retaining wall has been investigated. To complete the research on building collapse also the strength properties are discussed in this subsection. First the mechanical schematisation of the retaining wall is discussed and this is continued by discussing possible collapse mechanisms and the elaboration of an important mechanism.

Mechanical schematisation

When a building is located inside the soil profile of a dike, the front wall parallel to the dike crest is a soil retaining wall. As has been discussed previously this wall is loaded with soil pressures and possibly also with hydrostatic water pressures. These soil retaining walls are often made of concrete or masonry. (Schipper, 2004) These walls mechanically behave like plates, with four boundaries with possible different support conditions. Depending on the loading and support conditions, bending moments and shear forces in two directions occur in the wall. The top support boundary will often be influenced by a floor in the building. Dependent on the dimensions and material properties of this floor this support acts like a simply support or a spring support in the direction of the floor. These floors can for instance be made of wood or concrete. For a concrete floor a simply support seems plausible while for a wooden floor a spring support might be more plausible. The conditions of the side supports are influenced by the connection with the perpendicular walls of the building. Dependent on this connection this support can be schematized as a simply support, a rotational spring or a fixed end. The conditions of the bottom support are caused by (the connection with) the foundation plate, and depending on this, can also be schematized as a simply support, a rotational spring or a fixed end. For instance when the wall lies deeper in the soil than the foundation plate and is well fixed with this foundation plate (see figure 6.10 A for a detail of a cross-section of a building inside a dike (Schipper, 2004)), a fixed end support seems plausible. See also figure 6.10 B for an overview of possible supports per boundary.

The occurring moments also depend on the ratio between the length dimensions (l_x & h_{base}) of the wall.

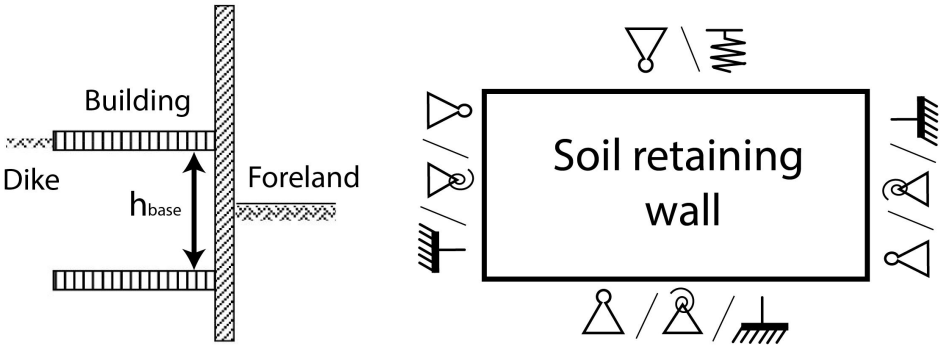

(A) Detail of soil retaining wall of a dike building (Schipper, 2004)

(B) Possible supports per boundary

FIGURE 6.10: Figure discussing supports of soil retaining wall

in which: h_{base} = height of soil retaining wall $[m]$
l_x = length of soil retaining wall $[m]$

The height of the soil retaining wall will lie in the range of 1 m & 2.5 m and the length of the wall in between the 4 m & 10 m. The height will often be based on the height of the basement/crawl space/first floor while the length is based upon the distance between the perpendicular walls that support the soil retaining wall. When the length dimension is much larger than the height dimension ($h_{base} > 2 \cdot l_x$) the normative span for bending is only influenced by the supports at the top and the bottom. In figure 6.11 this can be seen, where the bearing envelop is drawn for a uniform load where all boundaries have the same support conditions (see also figure 6.15 on page 92). This will often be the case for soil retaining walls of a building inside a dike. In that case this normative cross-section can be modeled as a beam with the properties of 1 m of the wall. See the blue dotted area in figure 6.11.

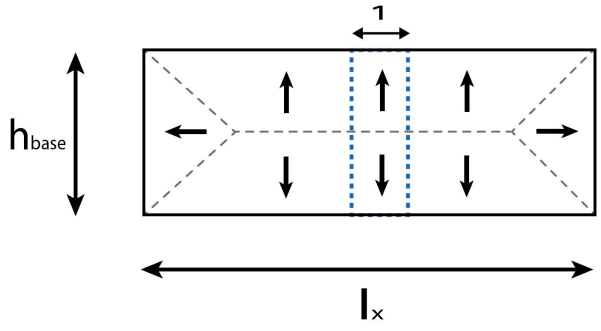

FIGURE 6.11: Bearing envelope for wall under uniform loading and same boundary supports

To get an idea what kind of internal forces occur due to the soil pressures some schematizations of the soil retaining wall from figure 6.5 on page 82 are checked. This wall has a soil retaining part of four meters, since it is not very realistic that no supporting floors

are present behind these four meters of wall, it is assumed that the soil retaining wall is 2.5 m high. So that the bottom is located at -0.5 m relative to ground level of the hinterland (see figure 6.12). The soil pressures (for 2.5 m depth) from figure 6.6 (page 84) are used and simplified to triangular distributed loads. The load will be exerted on two different beams, one simply supported and one with a fixed end.

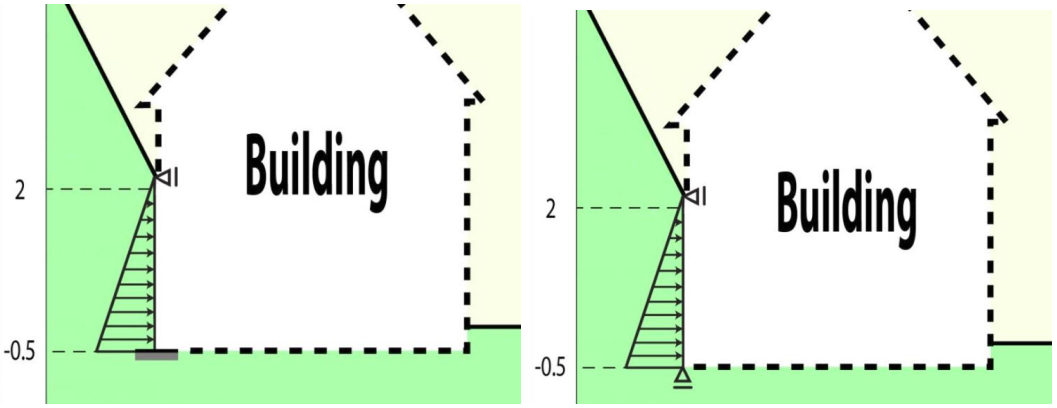

(A) Schematization as simply supported beam

(B) Schematization as fixed end beam

FIGURE 6.12: Schematizations of soil retaining wall of the building (vertical and horizontal scale are not the same)

For the simply supported beam (figure 6.13 A) the maximum bending moment and shear force under a triangular load can be calculated with the following formulas (Vrijling et al., 2011). The resulting moment and shear force diagrams are shown in figure 6.13. The maximum bending moment occurs at the zero shear location:

$$h_{M_{max}} = \frac{h_{base}}{\sqrt{3}} = h_{base} \cdot 0.58 \tag{6.29}$$

$$\Delta_{M_{max}} = \frac{h_{M_{max}}}{h_{base}} = 0.58 \tag{6.30}$$

$$V_{max} = \frac{q \cdot h_{base}}{3} \tag{6.31}$$

$$M_{max} = \frac{q \cdot h_{base}^2}{9 \cdot \sqrt{3}} \tag{6.32}$$

in which:

$h_{M_{max}}$	=	distance from top support to location of M_{max} on the soil retaining wall $[m]$
$\Delta_{M_{max}}$	=	location of M_{max} at soil retaining wall expressed as fraction of h_{base}
V_{max}	=	maximum shear force in retaining wall $[kN]$
M_{max}	=	maximum bending moment in retaining wall $[kNm]$

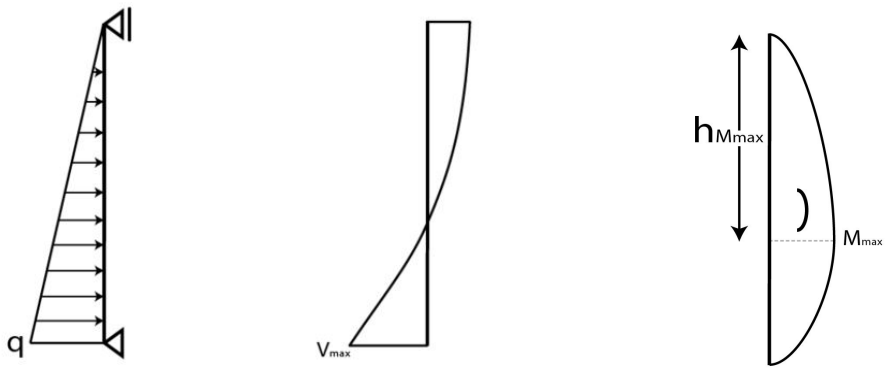

(A) Simply supported beam (B) Shear force diagram (C) Bending moment diagram

FIGURE 6.13: Moment and shear force diagram for simply supported beam

For the beam with a fixed end (figure 6.14 A) the maximum bending moment and shear force under a triangular load can be calculated with the following formulas (Vrijling et al., 2011). The resulting moment and shear force diagrams are shown in figure 6.14.

$$V_{max} = \frac{4}{10} \cdot q \cdot h_{base} \tag{6.33}$$

$$M_{max} = \frac{1}{15} \cdot q \cdot h_{base}^2 \tag{6.34}$$

The resulting values for these maximum internal shear forces and bending moments

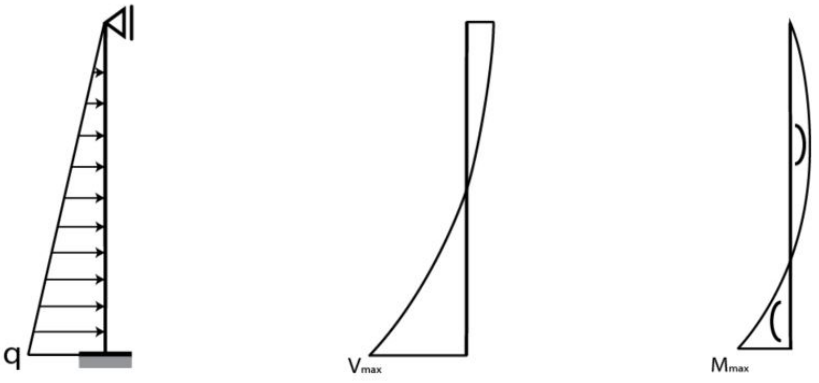

(A) One sided fixed beam (B) Shear force diagram (C) Bending moment diagram

FIGURE 6.14: Moment and shear force diagram for one sided fixed beam

for the different loading manners and the two different schematizations of the wall are shown in table 6.2. When the occurring moments are compared, it can be seen that the chosen schematisation does not have a very large influence on the maximum moment. For the simply supported beam $q \cdot l^2$ is divided by $9 \cdot \sqrt{3} \approx 15.6$, while for the fixed end beam $q \cdot l^2$ is divided by 15. But the maximum moments do occur on a different location; for the simply supported beam this is nearly in the middle, while for the fixed

Table 6.2: Overview of resulting bending moments for two different beam schematizations

				Simply supported beam		**One sided fixed beam**	
Freatic line	K	$q[kN/m]$	$h_w[m]$	$V_{max}[kN]$	$M_{max}[kNm]$	$V_{max}[kN]$	$M_{max}[kNm]$
High water	K_a	34.6	2.5	28.83	13.87	34.60	14.42
	K_0	37.8	2.5	31.50	15.16	37.80	15.75
Low water	K_a	27.6	2.5	23.00	11.07	27.60	11.50
	K_0	33.6	2.5	28.00	13.47	33.60	14.00

end beam this is at the bottom. When the beam is made of a material with relative weak tensile strength properties (for instance masonry or concrete) and is also loaded with a normal (compression) force, the location of the maximum moment for the fixed end beam is more favorable because the normal force due to own weight will be higher at this location. This higher compression force adds up to the bending capacity of a horizontally loaded wall (see for further explanation of this principle including formulas section 6.2.3 on page 97).

Concluding, the bottom support of the schematized beam is fixed or simply supported or something in between (rotational spring). For the maximum occurring bending moments, the simply supported beam is favorable. However the capacity of the fixed beam is more favorable, because the maximum bending moment is lower and therefore the favorable compression stress is higher. Therefore it is concluded that this choice of schematisation is not really important, and future calculations are performed with a simply supported beam.

When this loading is executed on a 2D wall with a FEM program the moments with the same direction for two different support schematisations can be seen in figure 6.14 [8]. In the mid span the same bending moment diagram can be recognized as in the figures before.

Building collapse mechanisms

The possible collapse of a building is a series system where the components represent different failure mechanisms of a building. When it is assumed that these different mechanisms are mutually exclusive the total probability of collapse, in accordance with reliability of systems (Jonkman et al., 2015), can be described as below:

$$P_{collapse} = \sum_{i=1}^{n} P_{f,mech,i} \tag{6.35}$$

[8] The direction of the bending moments of these figures corresponds to bending parallel to the joints regarding masonry walls

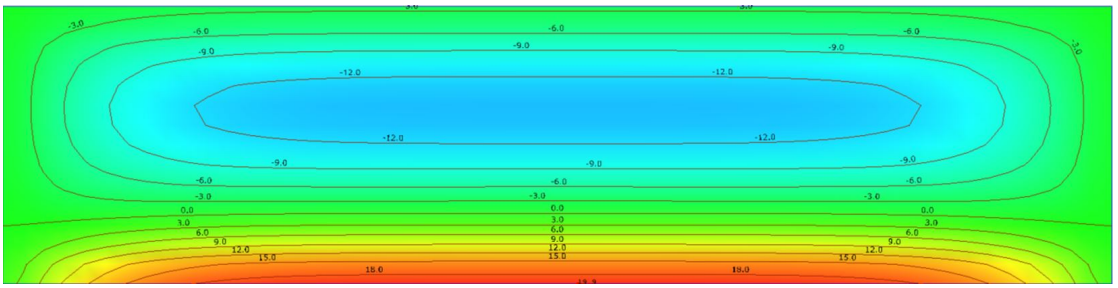

(A) My for wall with fixed end at bottom

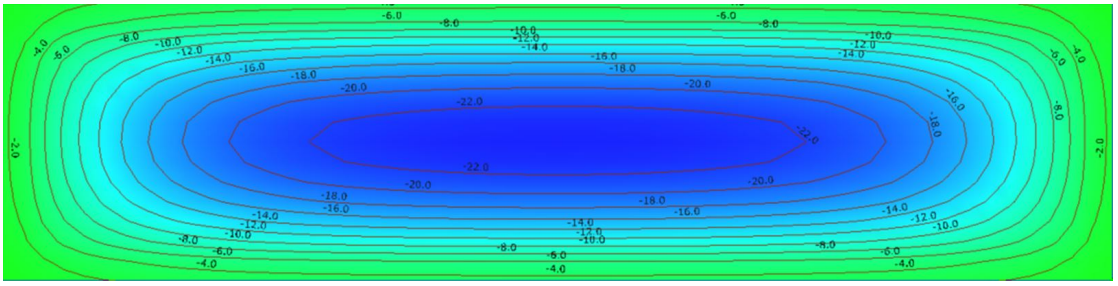

(B) My for wall with only simple supports

FIGURE 6.15: Moments and shear forces in wall when bottom is fixed and top and sides are simply supported (dimensions of these soil retaining wall are: $h_{base} = 2.5\ m$ & $l_x = 10\ m$, direction of M_y corresponds with bending failure parallel to bed joints for a masonry wall)

in which: $P_{collapse}$ = the probability of building collapse
$P_{f,mech,n}$ = failure probability according failure mechanism n

This is a upper bound value, assuming no dependencies between the different mechanisms. It might be possible that certain mechanisms are somewhat dependent to each other.

Some possible failure mechanisms are: [9]

1. Bending failure of soil retaining wall - normative in the mid span.
2. Shear failure soil retaining wall - normative at end span.
3. Instability of walls that stand perpendicular to soil retaining wall.
4. Failure at supports and or connections.
5. Failure or instability of floor that supports the soil retaining wall.
6. Failure of foundation - building shifts away.
7. Failure of foundation - rotation of building results in loss of support.
8. Uplift due to high pore water pressures in aquifer resulting in building collapse.

[9] This list contains only mechanisms that are dependent to a highwater event

Since every building has different dimensions, also the influence of the different mechanisms on the failure probability of the building will differ. The most interesting failure mechanisms, for this research, are those that could lead to soil failure when they occur. This could still occur due to multiple mechanisms of building collapse.

In order to get an idea of collapse of such a building, a mechanism is chosen, that is further investigated. By doing this the strength properties for this mechanism can be identified. There is chosen for the first mechanism of the above enumeration: "out of plane bending of the soil retaining wall". This mechanism is further on investigated under the assumption that this wall is made out of masonry. Considering the typical dimensions of such a building it is conceivable that this mechanism has a substantial contribution to the total failure probability. In addition the occurrence of this mechanism will most certainly result in local soil failure in front of the former wall, resulting in a less stable soil profile after collapse.

Out of plane bending failure

In this subsection the resistance of a masonry wall for the failure mode 'out of plane bending' is discussed.

The possibility of bending failure can occur in two directions (see figure 6.16). The bending tensile strength of masonry differs in the different directions. When dimensions

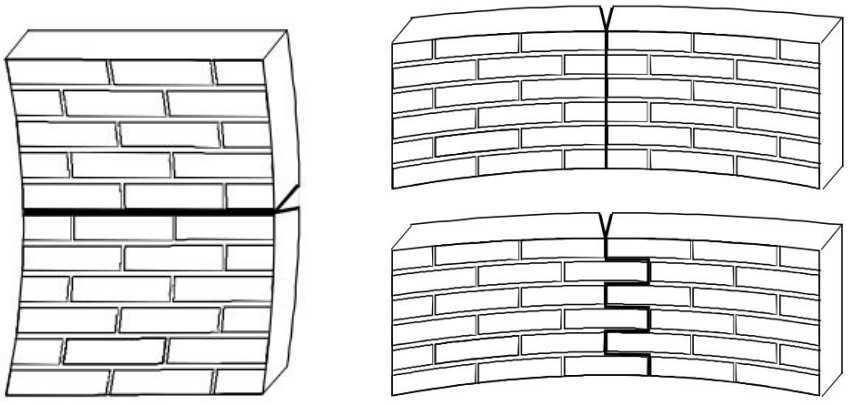

(A) Bending failure parallel to joints - $f_{x,k1}$

(B) Bending failure perpendicular to joints - $f_{x,k2}$

FIGURE 6.16: Two different bending modes for masonry (EC-6.1, 2013)

of a wall are chosen with a width of 10 m and a height of 2.5 m the weak direction corresponds to the $f_{x,k1}$ and the assessment can be accomplished by only assessing this direction.

The moment capacity can be calculated with the following formulas:

$$M_{Rd} = f_{x,k1} \cdot W \tag{6.36}$$

$$f_{xd,1/2,app} = f_{x,1/2} + \sigma_d \tag{6.37}$$

$$\sigma_d = \frac{N_{ed}}{b \cdot t} \tag{6.38}$$

$$W = \frac{1}{6} \cdot b' \cdot t^2 \text{ for weak direction} \tag{6.39}$$

Formula (6.37) takes the positive effect of a compression force into account.

in which:

M_{Rd}	=	calculation value of the bending moment capacity $[kNm]$
$f_{x,k1}$	=	characteristic value of bending tensile strength for failure in plane parallel to joint $[\frac{N}{mm^2}]$
W	=	section modulus $[mm^2]$
$f_{xd,1,app}$	=	apparent calculation value for bending tensile strength adjusted for compression stress $[\frac{N}{mm^3}]$
σ_d	=	calculation value of the compression stress $[\frac{N}{mm^2}]$
N_{ed}	=	calculation value of the normal force in the masonry $[N]$
b'	=	width of a running meter wall that is simplified as beam $[m]$
t	=	thickness of masonry wall $[m]$

This formulas are based on linear elastic failure, for a horizontally loaded wall which is simultaneously under a compression force. The horizontal loading causes bending

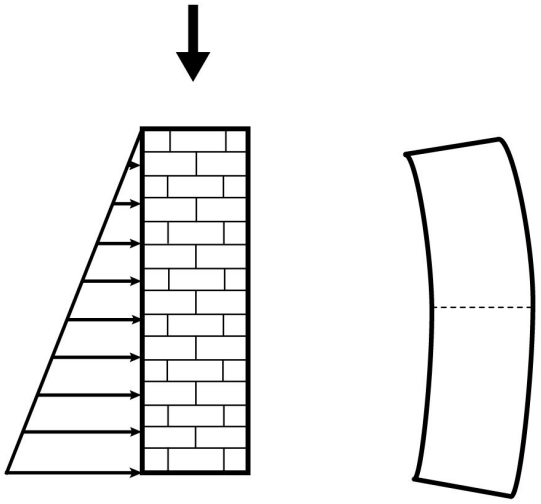

(A) Horizontally loaded wall with normal force

(B) Out of plane bending

FIGURE 6.17: Masonry wall under triangular horizontal load and normal force

moments in the masonry wall. These moments create a linear stress course from the front to the back of the masonry. When the normal force in the wall is divided by

the surface, the compression stresses are obtained and these are added to the stresses caused by the bending moment. Now the occurring tensile stress at the tensile side can be determined. When this value exceeds the bending tensile strength failure is assumed. See figures 6.17 & 6.18.

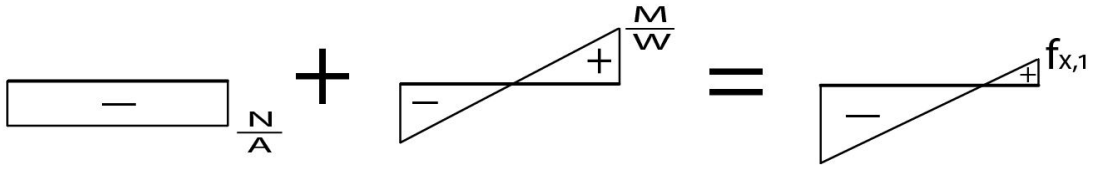

FIGURE 6.18: Stresses according to linear elasticity

Often there is some reserve capacity, after failure according to linear elasticity, available. But for masonry it could be imagined that there is no reserve capacity. For instance when the bending tensile strength is exceeded and cracking occurs, this results in a reduced section modulus and therefore the cracking might proceed until failure occurs.

For brick stones (EC-6.1, 2013) gives a characteristic value that is valid for the whole Euro Code (EC) region of:

$$f_{x,k1} = 0.10 \ \frac{N}{mm^2} \tag{6.40}$$

For The Netherlands the characteristic value that can be found in the dutch guideline for brick stones is: (NPR-9096, 2012)

$$f_{x,k1} = 0.20 \ \frac{N}{mm^2} \tag{6.41}$$

In (EC-6.1, 2013) it is mentioned that these values of $f_{x,k1/2}$ may not be used for the calculation of masonry walls that are loaded by horizontal soil pressures. This applies to all basement walls of masonry and thus also for masonry walls that are located inside a dike profile. When this flexural strength may not be included in a calculation, no tensile stresses are allowed at the tension side of the wall. This means that the remaining bending capacity of the wall only relies on the present normal force in the wall. The reason of this statement in the Euro Code has to do with the permanent character of the soil pressures and because cracks within a soil retaining wall of masonry are difficult to detect. These cracks are the reason for the possible diminishing of the flexural tensile strength of the masonry. Cracks in masonry can be caused by different phenomena for instance: shrinkage due to temperature stresses, settlements, or growth of roots.

Concerning the variation of the flexural bending strength of masonry parallel to the bed joints, Graubner and Brehm mentions a Coefficient of Variation (CoV) of 30%.

CoV is defined as the ratio of the standard deviation (σ) to the mean ($mean$) of a stochastic parameter. Besides it is mentioned that these values are best represented by a log-normal distribution. With this information the mean value of the flexural tensile strength, where the characteristic value is based on, can be determined.

With some iterative calculations a lognormal-distribution is found that has a 5 % probability of exceedance under a value of 0.2 and has a $CoV = 30\%$. With the following formulas this calculation has been performed: (Jonkman et al., 2015)

$$\sigma_{log-normal} = \sqrt{ln(1 + \frac{\sigma^2_{normal}}{\mu^2_{normal}})} \tag{6.42}$$

$$\mu_{log-normal} = ln(\mu_{normal}) - 0.5 \cdot \sigma^2_{log-normal} \tag{6.43}$$

$$\sigma_{normal} = CoV \cdot \mu_{normal} \tag{6.44}$$

With these equations and the earlier mentioned demands the following properties are retrieved:

$$\mu_{normal} = 0.367 \tag{6.45}$$

$$\sigma_{normal} = 0.11 \tag{6.46}$$

$$\mu_{log-normal} = -1.127 \tag{6.47}$$

$$\sigma_{log-normal} = 0.29 \tag{6.48}$$

A plot of this distribution can be seen in figure 6.19. So for this distribution the following applies:

$$F_{F_{x1}}(f_{x1}) = P(f_{x1} < 0.2) = 0.05 \tag{6.49}$$

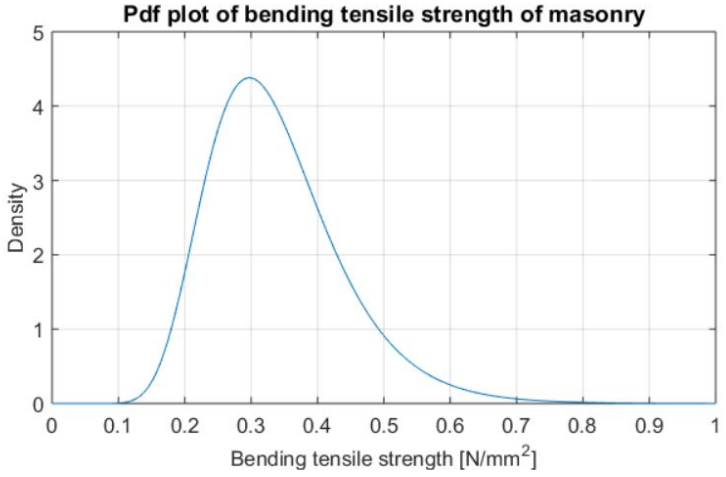

FIGURE 6.19: Pdf plot bending tensile strength

In (van der Pluijm, 1999) laboratory tests have been performed for bending tensile strength parallel to the bed joints for similar clay bricks. The test was based on 8 samples and delivered a mean value of 0.45 $\frac{N}{mm^2}$. This mean value is still a bit higher than is found in the lognormal distribution but this could be explained by the fact that these test were performed in a laboratory on newly made samples.

6.2.3 Limit state

In design guidelines masonry walls for bending failure are assessed with a unity check in which the applied moments are compared with the moment capacity. Unity check (UC) for out of plane bending of masonry walls under a horizontal loading is according to (EC-6.1, 2013):

$$M_{Ed} \leq M_{Rd} \tag{6.50}$$

in which: M_{Ed} = design value of the applied bending moment $[kNm]$
M_{Rd} = design value of the bending moment capacity $[kNm]$

These values are calculation values which represent unfavorable values for the outcome of the UC. For the loading part, M_{Ed}, this means that this calculation value is a relatively high value and is based on a small probability of exceedance of this calculation value (on the right side of the S curve of figure 6.20). For the resistance part, M_{Rd}, the calculation value is a low value that is based on a small cumulative probability that lower values occur (on the left side of the R curve of figure 6.20). So these values are based on the expected distributions of the loading and the resistance, in such a way that the expected failure probability is acceptable low. This failure probability is represented by the area for which the loading is larger than the resistance (see figure 6.20).

In subsection 6.2.1 the increased loads on a building in a dike due to highwater conditions are indicated. From this it could be deducted that the expected distribution of the loads increases. Besides the variation of the distribution of the loads may increase due to more uncertainties on which the loads depend. Graphically this could be illustrated like is done in the bottom figure of 6.20. This increase of the loading results in higher failure probabilities for such a building during a highwater, when it is compared to the same building. This increased failure probability is further investigated in a case study in the next chapter, since it could have negative impacts on the dike stability.

Schipper states about these kind of buildings: “soil retaining walls of buildings in a dike are additionally loaded by a higher freatic level. Concrete walls are often designed to withstand these loads, but older masonry walls are often designed with help of rules of

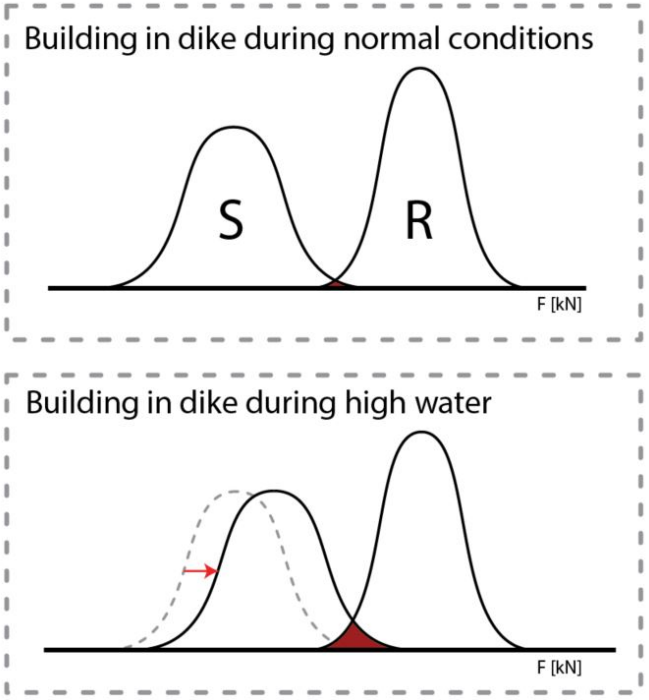

FIGURE 6.20: Shifted distribution of loads on a building within a dike during a high water, resulting in an increase probability of building collapse

thumb and do often not satisfy these extra loads. However in daily practice these walls appear to withstand during a higher freatic level and (excess) traffic loads." This confirms the selection of developing a probabilistic method for a dike containing a building with masonry walls inside the slope.

To become familiar with the needed dimensions and calculation methods of a masonry wall that is checked for bending, deterministic calculations are performed. These are reported in appendix B.7 on page 168.

In the first part of this appendix, calculations are performed with the characteristic flexural strength adopted from (EC-6.1, 2013) ($f_{x,1} = 0.1\ \frac{N}{mm}$). The most important conclusion from these calculations is that, the thickness of the wall that is needed to meet the requirements of this UC, becomes very large. For instance for a soil retaining wall of 2 meters high the wall has to have a thickness of at least 575 mm. The statement that no flexural strength is allowed for the calculations of soil retaining walls, is still ignored in this calculation. When this would be implemented in the calculations this would result in unrealistic large wall thicknesses. Therefore it is concluded that, when this statement from (EC-6.1, 2013) is adopted, buildings in dikes with soil retaining walls will not satisfy the current guidelines.

In the second part of appendix B.7 also a calculation is performed for a building from which the wall thickness is known. Now not a characteristic value ($f_{x,1}$) from the EC is

used but an expectation value based on figure 6.19 is used. For this case the bending moment capacity is larger than the applied moments and thus the UC suffices.

This statement from the (EC-6.1, 2013) is not adopted in the probabilistic calculations of the next chapter. On the one hand this is done because probabilistic calculations should be performed with probability distributions and not with negative scenario values. Besides it is unknown how often this loose of flexural strength occurs and therefore it can not be implemented in the probability distribution. In addition, the deterministic calculations from appendix B.7 show that this loose of flexural strength does not occur for a large amount of buildings, since these are still intact.

6.3 Interaction building collapse and dike stability

In the previous section the occurrence of building collapse has been investigated. In this section the interaction of building collapse and dike stability is discussed. First the residual profile, which is defined as the dike profile after collapse, is treated. And secondly the three dimensional interaction between dike and building is qualitatively discussed for the scenario's: 'building collapse' and 'building does not collapse'.

6.3.1 Residual profile

When a building with a soil retaining wall in a dike collapses the profile of the dike is affected. Namely the soil in front of the wall will slide towards the location of the former building. Because this soil sliding affects it's stability it is important to know how much and under which slope the soil will slide. In (VTV, 2006) no clear approach is suggested for the formation of a residual profile after building collapse.

For the assessment of residual profiles after a sliding of the inner slope, inclinations are determined for different soils which can be used to estimate the residual profile after instability on the hinterland side. For clay these are: $H : V = 2 : 1$ and for sand $H : V = 4 : 1$ (Zwanenburg et al., 2013). In chapter 5 section 5.2 calculations have been performed with these suggested inclinations but under the assumptions that the soil of the disturbance zone disappeared after collapse. But this approach does not represent correctly what happens with the soil after collapse, since this soil does not disappears but slides towards the former building. Below a new approach is suggested and is compared with the approach from chapter 5.

Suggested approach residual profile

A more realistic residual profile after building collapse can be constructed with soil sliding in the hole of the remaining building. This method is compared with the approach used in chapter 5. An example of this new approach is shown in figure 6.21 *D*. The slope of the residual profile is still based on (Zwanenburg et al., 2013) but now the amount of soil before and after collapse is kept the same. This means that it is assumed that the soil before and after collapse has the same compaction. It is recommended to check this assumption in further research, as well as the interaction between the failing/sliding soil and collapsing building that is occurring simultaneously.

A comparison is made for the profile depicted in figure 6.21. The results of these calculations are shown in table 6.3. It is concluded that the new approach is a better estimation of the residual profile after building collapse and is therefore also applied in the remainder of this research.

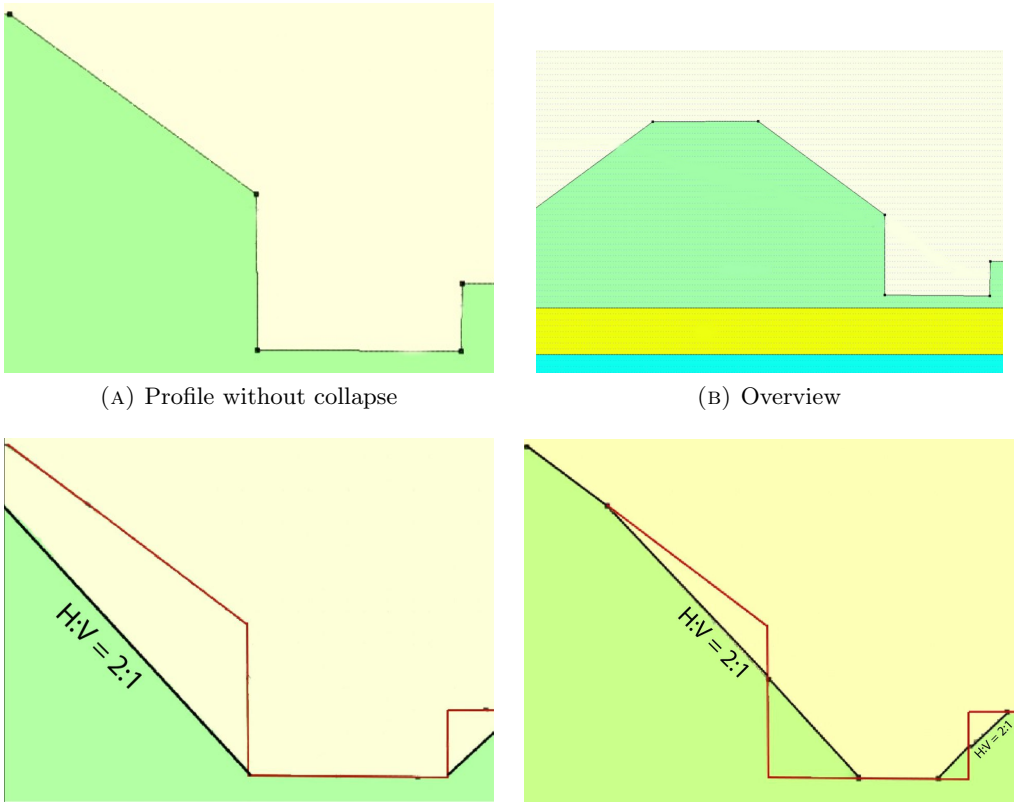

(A) Profile without collapse

(B) Overview

(C) Approach chapter 5

(D) Suggested approach

FIGURE 6.21: Different schematisations for residual profiles that arise after collapse of a building that is located in the profile'. (Red lines show the profile before collapse)

TABLE 6.3: Comparison result for different residual profiles for soil profile after building collapse

Soil profile:	FoS
Building intact	1.85
Collapse: Approach chapter 5	1.30
Collapse: Suggested approach	1.48

6.3.2 3D effect

The width of a sliding plane is often wider than a building. This means that 2D calculations and schematisations do not fully represent reality. The width of a sliding plane is typical around $30 - 50\ m$ (CUR 219, 2007). When this is applied to the selected configuration the top views are shown in two drawings in figure 6.22 . When the building withstands, the location of the building is locally stronger than it's adjacent parts. But when 3D effects are included this strengthening is smaller than expected. When the building does collapse this location on the dike becomes a local weak spot. But because this weak spot is surrounded by the regular soil profile this weakening effect is smaller than expected in advance.

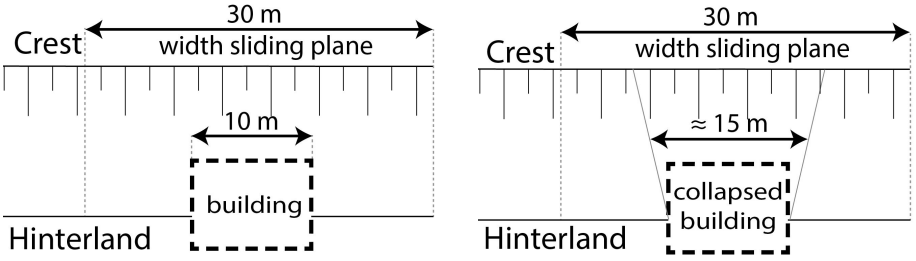

(A) Top view when a building does not collapse

(B) Top view when a building does collapse

FIGURE 6.22: 3D effects for buildings in the dike when it does not collapse and when it does

6.4 Conclusion

In this section conclusions from this chapter are drawn and this will give a compact answer to the subquestion belonging to this chapter: "*How can the influence of a building for the selected configuration be determined, and which information should be available to perform this method?*"

In the beginning of this chapter a probabilistic method has been developed that is suited to determine the influence of buildings inside the dike profile, for which possible collapse of the building is relevant. This method consists of three steps: a structural

model, a geotechnical model, and integration of both models. Afterwards the method is analyzed by means of a numerical example from which it appears that a positive influence or a negative influence of such a building can potentially be determined. In the sequence of this chapter information is made available concerning the first two steps of the probabilistic method, which is used for the case study in the next chapter. The most important conclusions from this are described below.

The loads that are exerted on a building during a highwater can indeed increase due to a higher freatic level. Therefore it is proven that possible collapse of a building can be dependent on a high water event. Other effects that also may have an influence on this loading are undrained soil behavior, effects induced by the combined system of dike and building and arching effects within the soil and the dike.

The effects of an increasing freatic line could be implemented in a schematisation in which the masonry soil retaining wall of the building is checked for out of plane bending failure. This derivation is used to acquire insight in the probability of building collapse. This schematisation is also used in the case-study of the next chapter. Furthermore it is striking that when the Euro Code is strictly enforced, the masonry soil retaining walls of buildings in dikes do not satisfy the guidelines. Therefore it is recommended to further investigate the reason for this rejection, which is caused due to possibility of loose of flexural strength due to cracking of the masonry.

When a building collapses the profile of the dike changes in a so called residual profile. In this chapter an approach is suggested on how this residual profile can be assumed. This approach is also adopted into the case-study of the next chapter.

When three dimensional effects are included the negative influence of building collapse are smaller than expected from a 2D analysis. On the other hand the positive influence of a building that does not collapse is, when the analysis is performed three dimensional, smaller than expected from a 2D analysis.

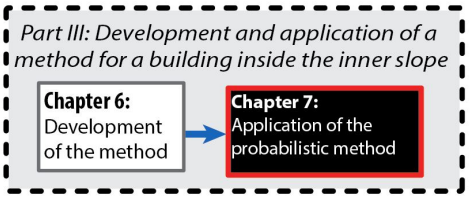

Chapter 7

Application of the probabilistic method

In this chapter the probabilistic method is applied to a case study. This case study is selected because it corresponds with the selected failure mechanism (inner slope stability, selected in chapter 4) and the selected configuration (building inside the inner slope with a shallow foundation, selected in chapter 5) where the scenario of building collapse (described in chapter 6) might have an important influence. This is all done to answer the following research question: "*Can this probabilistic method be applied to a case study to determine the influence of a building?* The probabilistic method contained three steps (1. structural model 2. geotechnical model 3. Integration of both models) below the approach of these steps for the case study is briefly introduced.

Within the structural model the performance of the building during a high water event is described. The probability of building collapse, $P_{collapse}$, is calculated with the probabilistic software package Prob2B (Courage and Steenbergen, 2007). This calculation is performed and described in subsection 7.3. The calculation method is based on the calculation scheme that has been derived in section 6.2. This probability is calculated for only one failure mode of building collapse, being out of plane bending failure of the soil retaining wall. At the end of this chapter the total probability of building collapse, including the other failure modes, is discussed qualitatively.

For the geotechnical model the performance of the two appearances of the soil profiles are described. The soil profile that arises after building collapse, the so called residual profile, is modeled after the theory of subsection 6.3.1. The conditional probabilities of instability, $P(_{instab|collapse/intact})$, are calculated with the reliability module of the slope stability software package D-Geo Stability (Deltares, 2014). This calculation is

performed and described in subsection 7.4. This calculation is based on theory and previous slope calculations of chapter 5.

The final step of the probabilistic method, the integration of the two models, is performed in section 7.5.

Before the probabilistic calculations are performed the general case and method is introduced. Afterwards the probabilistic calculations are performed, followed by conclusions.

7.1 Case description

The selected case consists of a river dike (primary water defense) in The Netherlands where a building is present in the inner slope of the dike. A lot of properties of the case were available, the general properties are introduced in this section. Some other properties had to be assumed, these general assumptions are also described in this section.

7.1.1 The building

A sketch of the building is given in figure 7.1. As can be seen the front of the building consists of three floors, of which the bottom floor is below ground level. The wall of the bottom floor, at the dike side of the building, is assumed to be made of masonry. Furthermore it is assumed that the soil retaining wall is supported by one perpendicular wall. This results in a horizontal span of five meters (see figure 7.2). The height of the soil retaining wall is 2.03 m and the first floor is connected to the the soil retaining wall on ground level (see figure 7.3). The surcharge loading of the building is based on earlier performed calculations (B.26) & (B.32) in appendix B.4 (page: 163):

$$S_{3fl} = 13 \ \frac{kN}{m^2} \tag{7.1}$$

$$S_{2fl} = 10 \ \frac{kN}{m^2} \tag{7.2}$$

7.1.2 The dike profile

The profile of the case location can be seen in figure 7.3. The green line that overlaps the first floor of the building shows the dike profile next to the building

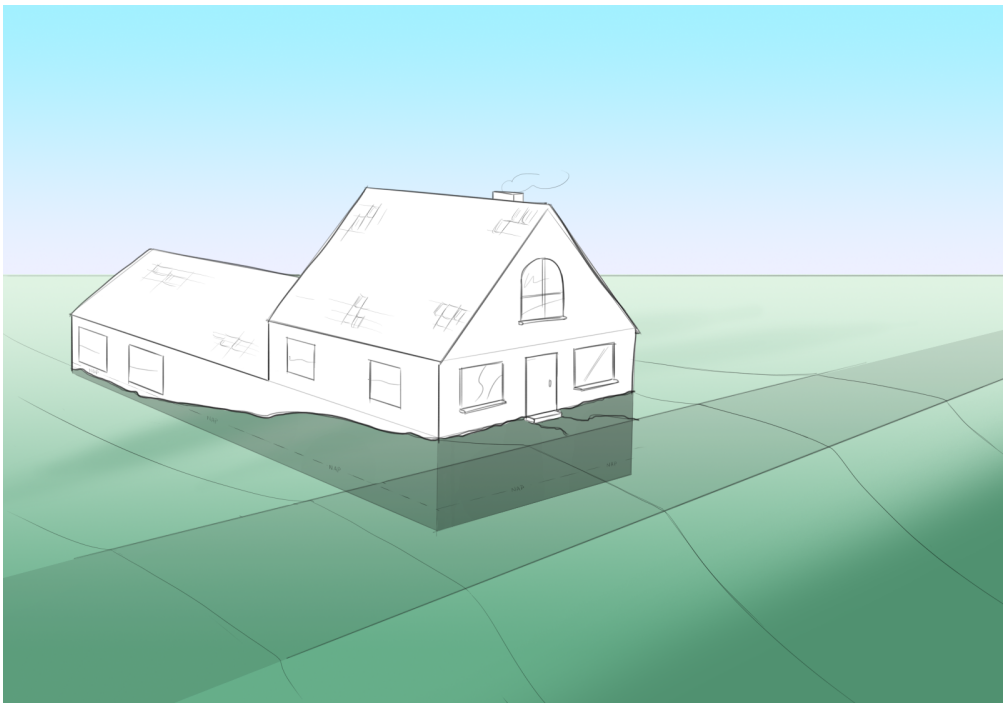

FIGURE 7.1: Sketch impression of the building belonging to the case-study

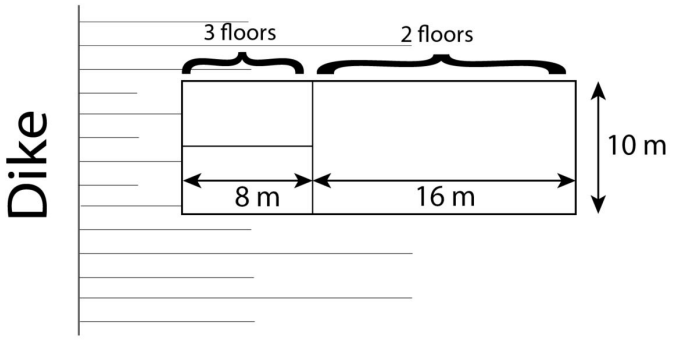

FIGURE 7.2: Assumed top profile of the building

7.1.3 The subsoil

The model of the subsoil is illustrated in figure 7.4. The numbers correspond with the layer names in table 7.1. The different properties of these layers are given in tables 7.1 (volumetric weight), 7.2 (cohesion) and 7.3 (angle of internal friction). In the following the background of these properties are explained.

Often for calculations characteristic values are used, which are often further modified to design values by means of partial coefficients (level I). These characteristic values correspond to a low percentile for strength distribution and a high percentile for loading distributions. This is done to include some safety into the calculation results. When calculations are performed with a reliability method of a higher order (level II or III)

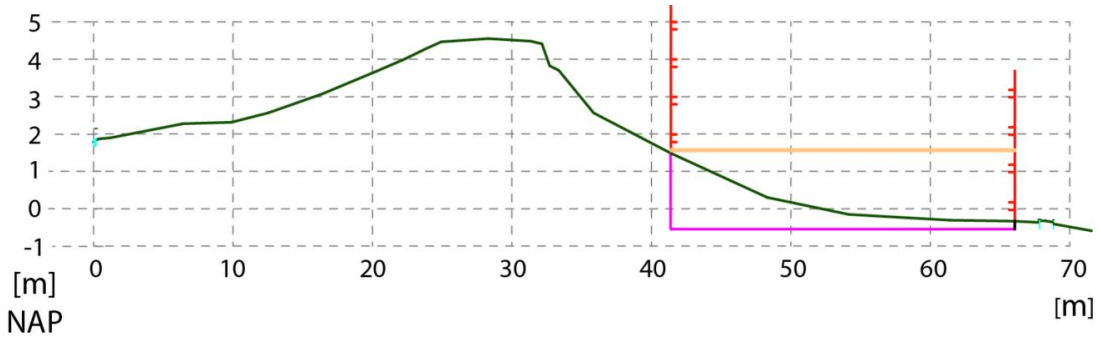

FIGURE 7.3: The soil profile of the case location (horizontal and vertical scale differs)

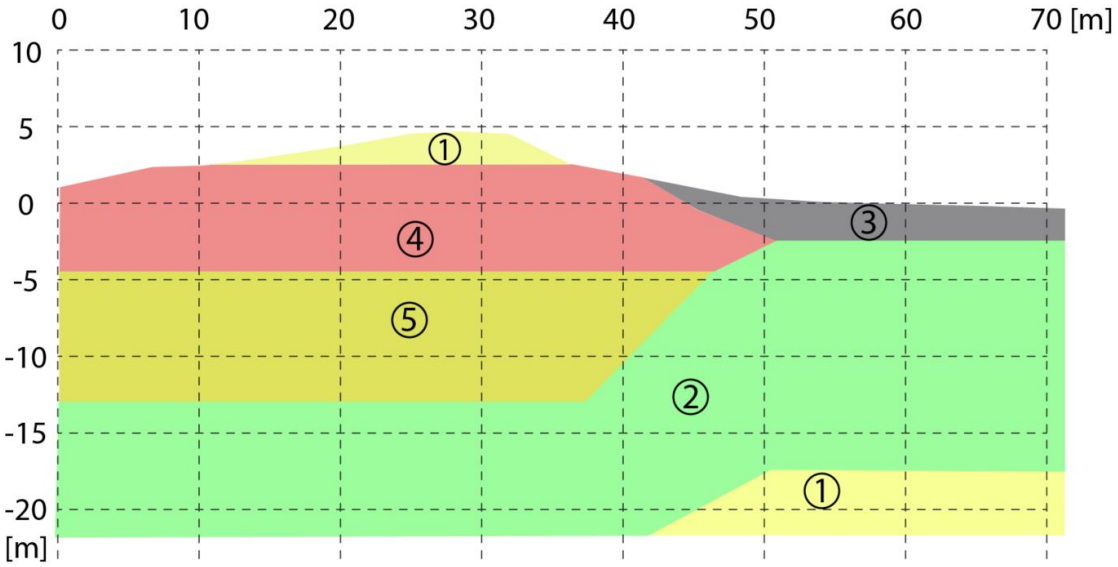

FIGURE 7.4: Geometric subsoil profile of case location (Numbers match layer names given in table 7.1)

these design values are not used. Instead expectation values and an indication of the variation of the parameters are needed.

For the volumetric weights of the different soils that are present in the subsoil of the case location mean values are available. Both for the soils in saturated as in unsaturated state (see table 7.1). For level I calculations mean values of volumetric weight are used. This is, among others, because the location of the specific soil determines whether the weight has a positive or a negative influence.

TABLE 7.1: Volumetric weight of soil types

Layer number	*Layer name*	γ_{sat} $[kN/m^3]$	γ_{unsat} $[kN/m^3]$
1	Sand, moderately packed	20.0	18.0
2	Clay, sandy	16.0	16.0
3	Clay, covering layer	16.5	16.5
4	Dike material	18.0	18.0
5	Sand with clay lenses	20.0	18.0

For the geotechnical parameters c & ϕ calculation values and material factors are available. According to (EC-7, 2012) these can be regressed to characteristic values with the following formula:

$$c_c = c_d \cdot \gamma_m \tag{7.3}$$

in which:
c_d = design value of cohesion $[kPa]$
c_c = characteristic value of cohesion $[kPa]$
c_μ = mean value of cohesion $[kPa]$
σ_c = standard deviation of stochastic cohesion $[kPa]$
$\gamma_{m,c}$ = partial material factor for cohesion parameter $[-]$
CoV_c = Coefficient of Variation of stochastic cohesion $[-]$

Subsequently (EC-7, 2012) mentions that this characteristic value has to be determined in such a way that the cumulative probability of a lower value is 5 %. So to regress these characteristic values to mean values, an appropriate distribution fit and variation are needed of the stochastic parameter. (Baker and Calle, 2006) suggests a normal distribution for the parameters c & ϕ. Also the CoV is adopted from low mentioned values in (Baker and Calle, 2006), with this information the mean values and standard deviation of the stochastic parameters are determined, the results are given in tables 7.2 & 7.3. For layer 3 a detailed example, how this transformation from calculation value to stochastic parameter is performed, is given in appendix C.1 on page 173. In appendix C.2 on page 174 the PDF (Probability Density Function) plots of the geotechnical stochastic parameters are collected.

TABLE 7.2: Cohesion values for soil layers

Layer	c_d $[kPa]$	$\gamma_{m,c}$ $[-]$	c_c $[kPa]$	CoV_c $[-]$	c_μ $[kPa]$	σ_c $[kPa]$
1	0	1.5	0	0.1	0	0
2	0	1.5	0	0.1	0	0
3	4.0	1.25	5.0	0.1	6	0.6
4	2.2	1.25	2.8	0.1	3.3	0.33
5	0	1.5	0	0.1	0	0

TABLE 7.3: Angle of internal friction values for soil layers

Layer	ϕ_d [°]	$\gamma_{m,\tan(\phi)}$ [°]	ϕ_c [°]	$CoV_{\tan(\phi)}$ $[-]$	ϕ_μ [°]	σ_ϕ [°]	CoV_ϕ $[-]$
1	28.0	1.2	32.5	0.1	34.7	1.3	0.038
2	23.9	1.2	28.0	0.1	30.1	1.3	0.042
3	14.7	1.2	17.5	0.1	19.3	1.1	0.056
4	25.2	1.2	29.5	0.1	31.6	1.3	0.041
5	27.0	1.2	31.4	0.1	33.6	1.3	0.039

7.1.4 Residual profile

The residual profile is the soil profile that occurs after collapse of the building. This is needed to calculate the conditional failure probability for macro stability given that the building collapses. The determination of the residual profile is based on theory that is given in subsection 6.3.1. This results in a residual profile that is depicted in figure 7.5. The extensive description how this residual profile is determined can be found in appendix C.3 on page 177. Within the definition of the = residual profile also the

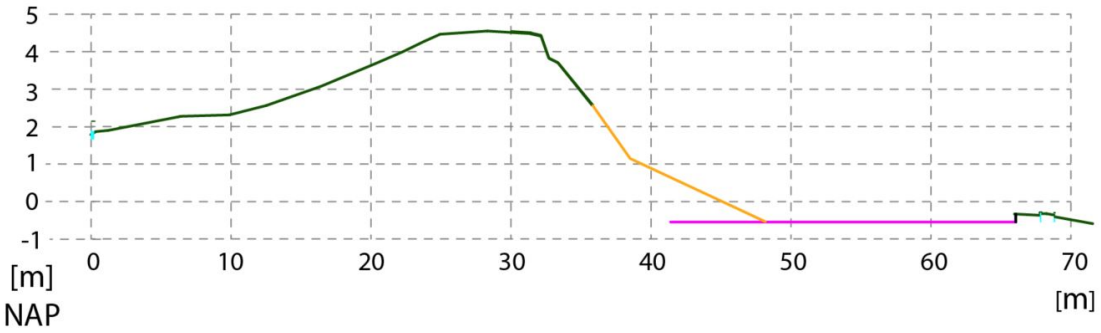

FIGURE 7.5: Assumed soil profile after building collapse

structural elements that are still present after collapse are included. It is assumed that the collapse is induced by the collapse of the soil retaining wall. And that therefore a part of the soil, that was retained by the wall, slides towards the bottom floor of the building. At the same time the building collapses which results in falling of rubble towards the bottom floor. The surcharge loading of the former building therefore does not change after collapse. It is also assumed that the bottom floor/foundation plate of the building stays intact.

7.1.5 Outer water level

An important stochastic variable that plays a part in the calculations is the outer water level. This water level infiltrates in the dike body, which causes a reduction of the strength of the dike, and also causes an increase of hydrostatic loading on the soil retaining wall. To impose a reference period of a year for the calculation results, a distribution is made for yearly maximum water levels.

From (Rijkswaterstaat, 2016) yearly maximum water levels are retrieved for a measurement station very close to the case location. This is done to make a distribution of extreme water levels with a reference period of one year. Different distributions are fitted to these date (see for details appendix C.4 on page 177). Especially the right tail of the chosen distribution is important since these values have a large influence on

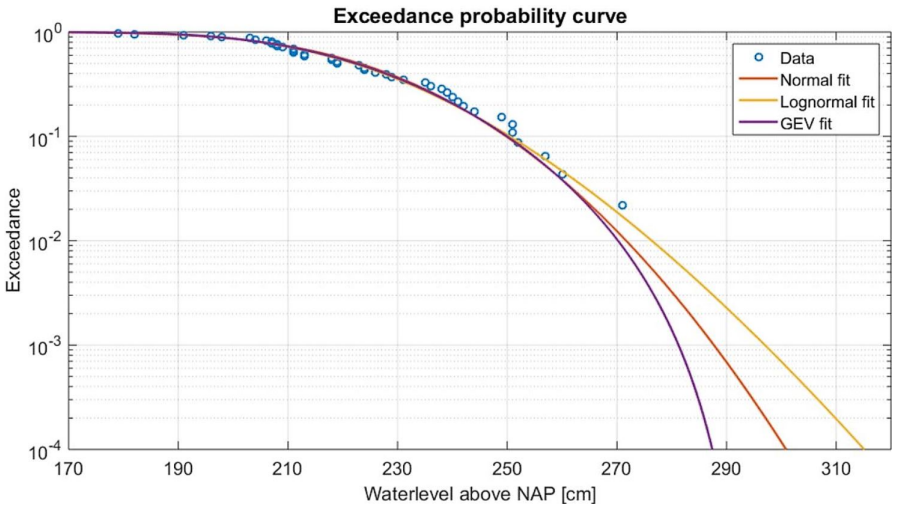

FIGURE 7.6: Exceedance probability curve of fitted distributions

the failure probability. When the right tails of the fits are compared (see figure 7.6), it can be seen that the lognormal distribution fits the tail data best. This lognormal distribution (see figure 7.7) has the following parameters:

$$\mu_{log-normal} = 5.40 \tag{7.4}$$

$$\sigma_{log-normal} = 0.094 \tag{7.5}$$

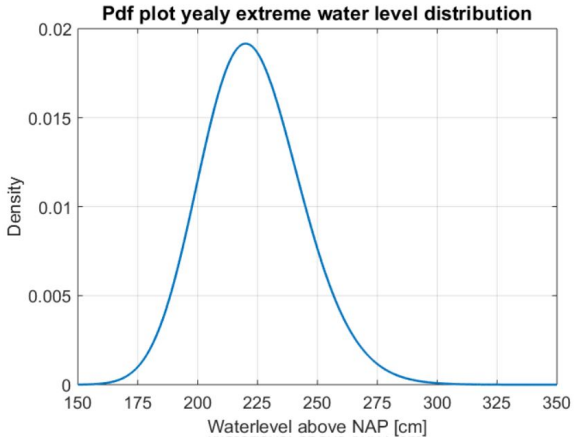

FIGURE 7.7: Pdf plot of extreme water level distribution

7.1.6 Freatic line in dike body

The outer water level influences the freatic line in the dike body. This freatic line influences the total failure probability of the dike-building system in two ways: 1. A rise of the freatic line reduces the strength of the soil body for the macro-stability failure

mode of the dike. 2. A rise of freatic line increases the hydrostatic loading on the soil retaining wall and on the building as a whole. In reality the actual occurring freatic line for a given water level is often not exactly known, and depends besides the water level also on the precipitation. To investigate the influence of a building on the stability, in this case-study the freatic lines for different water levels are assumed. Within these assumed freatic lines only a small amount of uncertainty is included (The amount of uncertainty is further explained in section 7.3).

The assumed freatic lines for different waterlevels are given in figure 7.8. These freatic lines are proposed under the assumption that the duration of a normative high water is long (In the Netherlands this applies to the so called "Bovenrivierengebied"). Since the dike is made up of a clay and a sand part, for waterlevels at the transition of these materials, large differences in freatic line are observed. Therefore three water levels are modeled close to this transition. The detailed explanation for the assumed freatic lines is given in appendix C.5 on page 179.

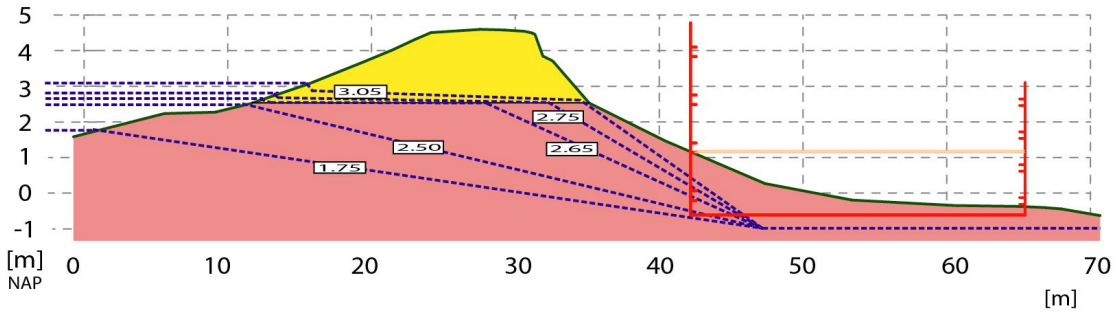

FIGURE 7.8: Assumed freatic lines for different outer water levels (yellow area is made of sand, and pink area is made of clay)

7.2 Method description

Within the probabilistic module of D-Stab some parameters can be inserted stochastically while other parameters can only be inserted deterministic. For consistency these deterministic parameters are also used in the probabilistic calculation of the soil retaining wall. The following parameters are therefore assumed to be deterministic:

- The uncertainty of the freatic line in the dike body due to precipitation is not taken into account.
- The uncertainty of the volumetric weight of the soil is not taken into account.
- The uncertainty in the soil profile and the uncertainty in the boundaries of the different soil layers are not taken into account.
- The uncertainty in the occurring residual profile after building collapse is not taken into account.

- The uncertainty in the structural elements of the building that might be still present after collapse, are not taken into account.
- The uncertainty that are imposed by certain models/schematisations (Bishop, occurring plate moments, mechanical schematisation) are neglected and not taken into account. This means that the assumption is made that the specific model is an exact reproduction of reality, which is normally not the case. This choice is made there is still more information needed to include all these model uncertainties, especially within the structural model. Since the amount of model/schematisation uncertainties of the structural model are not yet clear, these kind of uncertainties are also neglected within the geotechnical model.
- The probability of the event building collapse is calculated for only one mechanism. Afterwards the failure probability of this mechanism is converted to a total probability for collapse by making an assumption of the failure space for the calculated mechanism.
- The influence of undrained soil behavior and arching effects are not included in the the description of the loading in this model.
- The effects that are induced by the fact that this system is actually a composite system of building and dike are not taken into account. So the structural and geotechnical model are treated individually and do not interact with each other.

7.3 Structural model

In this section the probability of collapse that are input of equation (6.7) (page 77) are calculated.

Assumptions and principles

- When the water pressure is present, the pressure distribution is bi-linear. In the probabilistic calculation this is simplified to one triangular loading. See figure 7.9

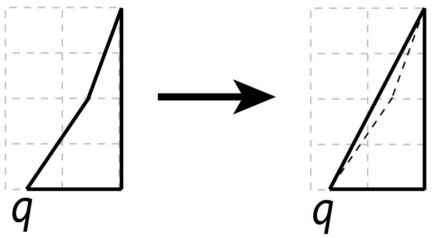

FIGURE 7.9: Simplification to a triangular load for a water level at half of the height of the wall.

- In this case-study the floor, that functions as a support of the soil retaining wall, is at the same level of the ground level in front of the building. This causes that two different variables within this calculation have by definition the same value. These are the 'height of the soil retaining wall' and 'height of the soil column in front of the building'. Since both have the same size they are described by the same symbol h_{base}.

Calculation description

The probabilistic calculation for out of plane bending for the soil retaining wall made out of masonry is based on the descriptions in chapter 6. Some adjustments have been made for the probabilistic calculation and these are explained below:

Δ_p is added to include the uncertainty in the amount of hydraulic pressure in the soil, due to variations of the freatic line for instance. This parameter has a mean value of zero but a standard deviation that should account for the uncertainty.

$$p = (h_{frea} \cdot \gamma_{water}) + \Delta_p \tag{7.6}$$

The calculation of the active soil pressure coefficient, K_a, is performed with the Muller-/Breslau equations[1] from Vrijling et al. (2011). This is done to include the effect of slope of the ground level. $K_{add,\theta}$ is a stochastic variable used to include uncertainty of the sloping ground.

$$K_a = \frac{\cos^2(\phi)}{(1 + \sqrt{\frac{\sin(2\cdot\phi)\cdot\sin(\phi-\beta)}{\cos(-\phi)\cdot\cos(\beta)}}^2)} + K_{add,\beta} \tag{7.7}$$

The compression stress occurring in the masonry is split into the top loading from upper floors and the self weight of the soil retaining masonry wall:

$$\sigma_d = \overbrace{\frac{N}{l_{wall} \cdot t}}^{loading\ from\ upper\ floors} + \overbrace{\rho_{mas} \cdot g \cdot \Delta_{M_{max}} \cdot h_{base}}^{self\ weight\ masonry} \tag{7.8}$$

The top loading is based on a calculation of surcharge load of a building with two floors for which the weight of the foundation is subtracted. This load (based on walls/roof/floors/live load) is in this calculation totally smeared out over the first floor. Subsequently this smeared load is assumed to be transferred equally over the outer walls that support this floor. This loading from the upper floors is subsequently divided

[1] This formula is valid for the assumption that the structure has no obliqueness and the angle between the resultant force and the normal of the wall is equal to the angle of internal friction. This is influenced by the roughness of the wall.

into a live load and a variable loading to include variation differences between these two. A background calculation to clarify the normal force that is used in this calculation is presented in appendix B.8 on page 170.

$$N = A \cdot (\overbrace{N_{ow}}^{self\ weight} + \overbrace{N_{vl}}^{variable\ loading}) \tag{7.9}$$

Furthermore a relation between the outer water level and the height of the freatic line at the soil retaining wall has to be determined. This is done in appendix C.6 on page 181. This is done by fitting a formula to the data points that are obtained from the assumed freatic lines. The result is the empirical formula (7.10) [2].

The formulas below give a stepwise overview of the input equations of the probabilistic calculation for the soil retaining wall. The loading part is mainly based on section 6.2.1, the resistance on section 6.2.2 and the limit state function has been treated in section 6.2.3.

Loading:

$$\begin{aligned}
h_{frea} =& a1 \cdot \exp(-((h_w - a2)/a3)^2) + \\
& a4 \cdot \exp(-((h_w - a5)/a6)^2) && (7.10)\\
p =& (h_{frea} \cdot \gamma_{water}) + \Delta_p && (7.11)\\
\sigma' =& (\gamma_{sat} \cdot h_{base}) - p && (7.12)\\
K_a =& \frac{\cos^2(\phi)}{(1 + \sqrt{\frac{\sin(2\cdot\phi)\cdot\sin(\phi-\beta)}{\cos(-\phi)\cdot\cos(\beta)}}^2)} + K_{add,\beta} && (7.13)\\
\sigma_h =& \sigma' \cdot K_a && (7.14)\\
q =& (\sigma_h + p) \cdot b && (7.15)\\
M_e =& \frac{q \cdot h_{base}^2}{9 \cdot \sqrt{3}} && (7.16)
\end{aligned}$$

Resistance:

$$\begin{aligned}
W =& \frac{1}{6} \cdot b \cdot t^2 && (7.17)\\
N =& A \cdot (N_{ow} + N_{vl}) && (7.18)\\
\sigma_d =& \frac{N}{l_{wall} \cdot t} + \rho_{mas} \cdot g \cdot \Delta_{M_{max}} \cdot h_{base} && (7.19)\\
f_{1,app} =& f_{x1} + \sigma_d && (7.20)\\
M_r =& f_{1,app} \cdot W && (7.21)
\end{aligned}$$

[2] This formula returns correct values for outer water levels: $h_w < 4.0\ m$. See figure C.14 on page 183.

Limit state function:

$$Z = M_r - M_e \tag{7.22}$$

in which:

a_n	=	empirical fitting constant $[mm]$
q	=	value for the triangular load$[kN/m]$
h_w	=	height of the outer water $[m]$
h_{frea}	=	height of the freatic water in front of the soil retaining wall $[m]$
Δ_p	=	parameter to include uncertainty for freatic level $[m]$
h_{base}	=	height of the soil retaining wall $[m]$
t	=	thickness of the soil retaining wall $[mm]$
$\Delta_{M_{max}}$	=	location of M_{max} at soil retaining wall expressed as fraction of h_{base} $[-]$
l_{wall}	=	perimeter of walls that transfer loading from upper floors down $[m]$
γ_{water}	=	specific weight of water$[kN/m^3]$
$K_{add,\beta}$	=	additional amount of active coefficient due slope of the ground level $[-]$
ρ_{mas}	=	density masonry$[kg/m^3]$
N	=	loading upper floors, total $[kN/m^2]$
N_{ow}	=	loading upper floors, self weight $[kN/m^2]$
N_{vl}	=	loading upper floors, variable loading $[kN/m^2]$

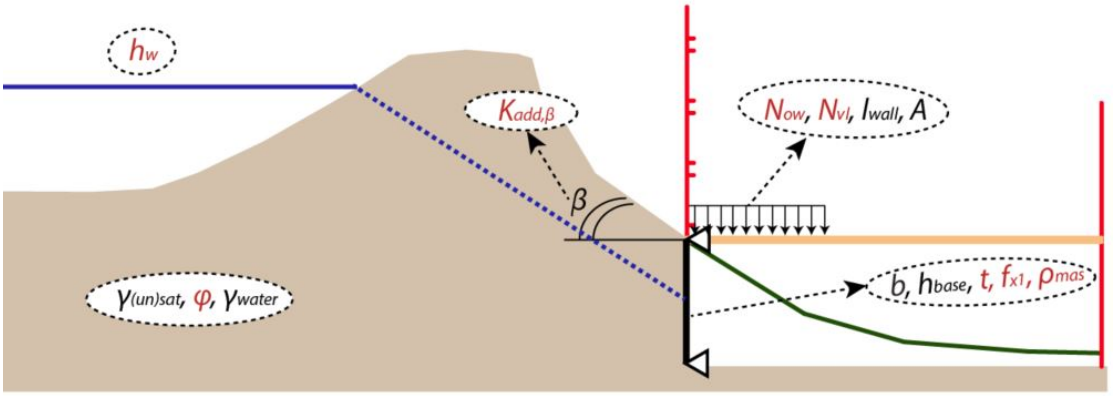

FIGURE 7.10: Illustration of (stochastic) variables for input in probabilistic calculation (red variables are modeled stochastically and for the black variables the input is deterministic)

For plots of the stochastic variables see appendix C.7 on page 183. The explanation of the selection of the stochastic parameters from table 7.4 is treated below.

Explanation of values of stochastic variables

- ϕ **-** The soil retaining wall of the building is located in the soil layer four of table 7.3 on page 107. The stochastic parameters that belong to this soil type are derived in section 7.1.3. The figure of the PDF-plot is shown in appendix C.7 figure C.16.

TABLE 7.4: Description of parameters used in probabilistic calculation (the triangular distribution is expressed in shape parameters a,b & c)

Var:	**Unit:**	**Distribution:**	μ	σ		μ	σ	**Unit:**
$\gamma_{(un)sat}$	N/mm^3	Deterministic	$1.8 \cdot 10^{-5}$			18		kN/m^3
h_{base}	mm	Deterministic	2030			2.03		m
$\Delta_{M_{max}}$	-	Deterministic	0.58					
ϕ	rad	Normal	0.552	0.0223		31.6	1.3	$^\circ$
$K_{add,\beta}$	-	Triangular	-0.01	0.00	0.01			
β_{sl}	$^\circ$	Deterministic	8					
b	mm	Deterministic	1000					
t	mm	Normal	440	10				
A	mm^2	Deterministic	$8 \cdot 10^7$			80		m^2
N_{ow}	N/mm^2	Normal	$4 \cdot 10^{-3}$	$4 \cdot 10^{-4}$		4	0.4	kN/m^2
N_{vl}	N/mm^2	Normal	$1.5 \cdot 10^{-3}$	$3.75 \cdot 10^{-4}$		1.5	0.375	kN/m^2
l_{wall}	mm	Deterministic	36000			36		m
f_{x1}	N/mm^2	Lognormal	-1.1273	0.2936				
ρ_{mas}	kg/mm^3	Normal	$2.1 \cdot 10^{-6}$	$1.05 \cdot 10^{-7}$		2100	105	Kg/m^3
h_w	mm	Lognormal	7.7052	0.094		5.40	0.094	cm
γ_{water}	N/mm^3	Deterministic	$1 \cdot 10^{-5}$			10		kN/m^3
Δ_p	N/mm^2	Normal	0	0.0005		0	0.5	kN/m^2

- $\boldsymbol{K_{add,\beta}}$ - This parameter is included to account for the uncertainty of the slope of the ground level in front of the building. When this uncertainty is assumed to be 20% and are inserted in (7.13), this results in a enlargement or reduction of the K_a value with 0.01. Therefore these values are chosen as boundaries for a triangular distribution. Chosen is for a triangular distribution to exclude the possibility of very high or low values that do not represent realistic values. The figure of the PDF-plot is shown in appendix C.7 figure C.17.
- **t** - The thickness of the masonry wall is unknown for the building of the case. In (Schipper, 2004) five buildings located in the outer slope of a similar dike were assessed. Three of these buildings had soil retaining walls of masonry with similar heights. From which two had a thickness of 440 mm and one had a thickness of 550 mm. This difference of 110 mm is typically the width of a brick. For this building a thickness of 440 mm is assumed. But also different wall thicknesses are researched. A standard deviation of 10 mm is assumed which could be caused by brick and or execution inaccuracies or joint erosion. The figure of the PDF-plot is shown in appendix C.7 figure C.15.
- **N** - The top loading from the upper floors is based on calculations (equations (B.26) & (B.32)) performed in appendix B.4 on page 162. This is split into permanent loading and variable loading. The used variations of these are based on (Vrouwenvelder e.a., 2001). The figure of the PDF-plot is shown in appendix C.7 figure C.18.
- $\boldsymbol{f_{x1}}$ - The derivation of the stochastic flexural bending strength is performed in

subsection 6.2.2 on page 96 and is based on (Graubner and Brehm, 2011), (EC-6.1, 2013) and (NPR-6791, 2009). The PDF plot is shown in figure 6.19 on page 96.

- $\boldsymbol{\rho_{mas}}$ - The mean value of the density of the masonry is adopted from (NPR-6791, 2009). The suggested distribution and variation are adopted from(Vrouwenvelder e.a., 2001). The figure of the PDF-plot is shown in appendix C.7 figure C.19.
- $\boldsymbol{\Delta_p}$ - This parameter represents the uncertainty of the present hydraulic pressure in the soil and thus the height of the freatic line in the dike body. The mean value of the freatic line is already assumed (subsection 7.1.6) and therefore the mean value of this parameter is zero[3]. For the standard deviation a value of 0.5 $\frac{Kn}{m^2}$ is chosen. This corresponds with the default value that is suggested by (Deltares, 2014). Converted to a variation in height of the freatic line this equals a standard deviation of 5 cm. It should be realized that in terms of freatic line this is a small variation that in practice could only be obtained after extensive soil investigation. In part this is done because higher variations could lead to unrealistic heights of the freatic line. The figure of the PDF-plot is shown in appendix C.7 figure C.20.
- $\boldsymbol{h_w}$ - The derivation of the stochastic outer water level is performed in subsection 7.1.5 (page:108) and in appendix C.4 (page:177) and is based on data of (Rijkswaterstaat, 2016). The PDF plot is shown in figure 7.7 on page 109.

Results

The probabilistic calculations are incrementally performed. 1. First a calculation without an external water level is performed. 2. Secondly calculations are performed for given (deterministic) water levels. 3. Finally a calculation is performed where the water level is a probability distribution. The reliability methods that are used are First Order Reliability Method (FORM) and Monte Carlo simulation (MC), for background information on these methods referred is to appendix A.6 on page 151.

Without hydraulic pressure The probabilistic calculations are started without the influence of hydraulic pressure on the soil retaining wall. This is done to see how the system without the influence of ground water works. To research the effect of different wall thicknesses in this first calculation the mean value of the thickness is varied from 330 to 660 mm in steps of 110 mm, which is typical width of a brick. This is done with a FORM. The calculation results can be seen in table 7.5. As was expected has the thickness of the wall a large influence on the reliability of the soil retaining wall. For

[3]The mean value of the hydraulic pressure corresponds with the assumed freatic line

TABLE 7.5: FORM results of runs with different wall thicknesses ($h_w = 0$)

t $[mm]$	β	P_f
330	4.21	$1.27 \cdot 10^{-5}$
440	6.97	$1.65 \cdot 10^{-12}$
550	9.48	$1.30 \cdot 10^{-21}$
660	11.85	$5.29 \cdot 10^{-32}$

the case, a wall is expected and assumed with a thickness of 440 mm. Therefore the extensive FORM results of this case are shown in table 7.6.

in which: α = influence coefficient $[-]$
X_d = value of design point

The influence coefficient is a measure how large the influence of this parameter is on the outcome of the probabilistic calculation. The design point is defined as the combination of input values for which $Z \leq 0$ and has the greatest joint probability density.

TABLE 7.6: Influence coefficients and values of design point for stochastic parameters (results from a FORM run with $t = 440$ mm and $h_w = 0$)

Stochast:	f_{x1}	ϕ	t	Δ_p	N_{ow}	N_{vl}	$K_{add,\beta}$	ρ_{mas}
α:	0.885	0.318	0.231	-0.167	0.114	0.107	-0.077	0.060
X_d:	0.053	28.8	424	0.00058	0.0037	0.0012	0.0023	0.000002

The value of the design point of the most important parameter, f_{x1}, is very small in comparison with it's mean value. This can be explained by the small failure probability, namely in the order of 10^{-12}. Therefore only very low strength values result in failure.

An important conclusion from this is that the probabilistic calculation is dominated by the value of the bending tensile strength of the masonry, f_{x1}. Graphically this is also observed in the graph in figure 7.11 in which sample values from a MC calculation are collected and f_{x1} values are plotted against the outcome of LSF. A strong lineair correlation between f_{x1} and the outcome of LSF is observed. This linear relation is retrieved because the bending moment capacity depends linearly on the bending tensile strength (equation (7.20)).

For a given waterlevel When the outer water level is adjusted to a normative water level the freatic line in the dike rises which results in hydraulic pressures against the soil retaining wall. A probabilistic calculation is performed with a water level that has a probability of exceedance of $\frac{1}{2000}$ yr^{-1} being: $h_w = 3050$ mm. This is done for the building with a soil retaining wall of 440 mm. As expected this has a large influence

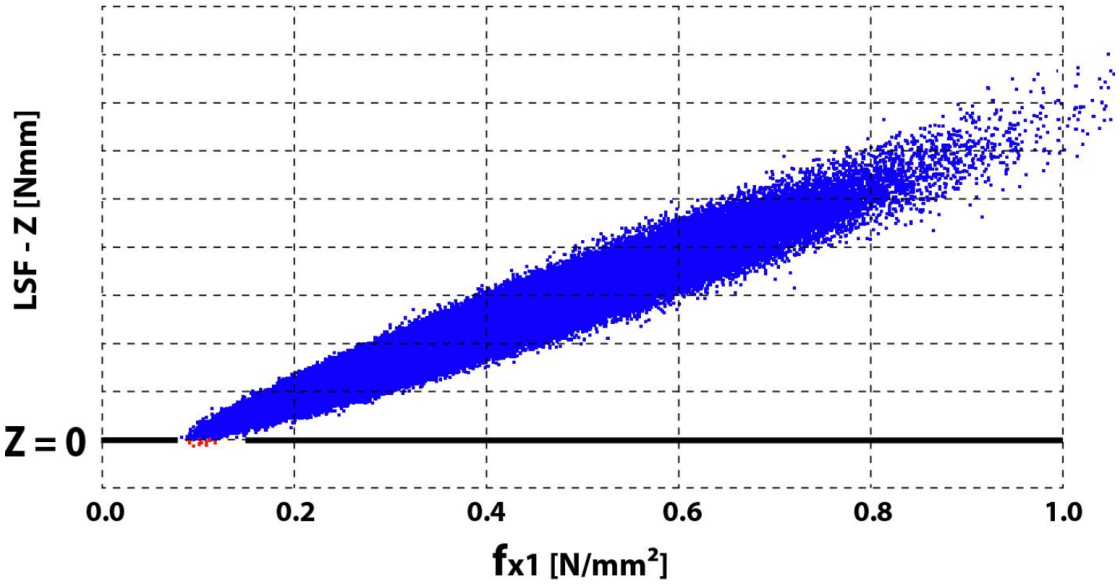

FIGURE 7.11: Samples from a MC calculation plotted against f_{x1} and the outcome of LSF (MC with: $t = 330$ and $h_w = 0$ with $n = 10^6$)(red dots represent a failure sample, blue dots represent a non failure sample)

on the reliability. The reliability index is halved and the failure probability is enlarged with a factor 10^8.

$$\beta = 3.306 \tag{7.23}$$

$$P_f = 4.73 \cdot 10^{-4} \tag{7.24}$$

FORM ($t = 440\ mm$ & $h_w = 3050\ mm$)

In table 7.7 the extensive calculation results are shown. The influence of f_{x1} has become even larger. Furthermore the value of the design point for f_{x1} increased, which is an indication that also more probable strength values could lead to failure. To verify the

TABLE 7.7: Influence coefficients and values of design point for stochastic parameters (results from a FORM run with $t = 440\ mm$ and $h_w = 3050\ mm$)

Stochast:	f_{x1}	ϕ	t	Δ_p	N_{ow}	N_{vl}	$K_{add,\beta}$	ρ_{mas}
α:	0.973	0.074	0.191	-0.077	0.051	0.048	-0.019	0.030
X_d:	0.126	31.3	434	0.00013	0.0039	0.0014	0.00026	0.000002

results of the FORM, a MC simulation is performed with $n = 10^7$ samples. The results are shown below and give practically the same result as the FORM.

$$\beta = 3.305 \tag{7.25}$$

$$P_f = 4.74 \cdot 10^{-3} \tag{7.26}$$

MC ($t = 440\ mm$ & $h_w = 3050\ mm$)

The reliability of MC calculations depend on the ratio between failure probability and the amount of samples. For the relative error of a MC result (Jonkman et al., 2015) mentions the following formula. Since this error is very small the MC results and also the FORM results are considered as accurate.

$$V_{p_f} = \frac{1}{\sqrt{n \cdot P_f}} \tag{7.27}$$

$$V_{p_f} = \frac{1}{\sqrt{10^7 \cdot (4.74 \cdot 10^{-3})}} = 0.015 \tag{7.28}$$

in which: n = number of Monte Carlo computations [−]
V_{p_f} = relative error of Monte Carlo result [−]

When a new FORM calculation is performed for which the outer water level is parametric inserted and gradually increased, the relation between the reliability and the outer water level can be explored. The results of these calculations can be illustrated in a fragility curve as is done in figure 7.12.

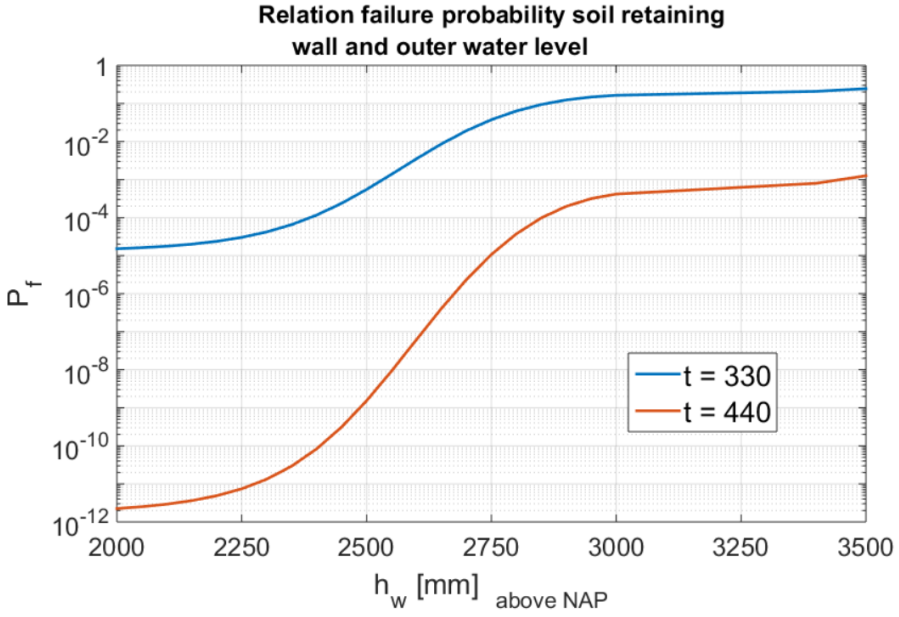

FIGURE 7.12: Fragility curve of the building of the case-study

Observing this some comments and conclusions can be made. The relation between the outer water level, h_w, and the height of the freatic line at the wall, h_{frea}, (equation (7.10) and figure C.14 on page 183) is clearly observed in this result. Furthermore the conclusion can be drawn that by enlarging the thickness of the wall by one brick (110 mm), for a wall that is loaded by hydraulic pressures, the reliability is of the same magnitude of a wall without loading by hydraulic pressures.

For a stochastic waterlevel Until now the outer water level has only been inserted deterministically in the probabilistic calculations. Therefore the resulting failure probabilities are a bit meaningless in practice, since the outer water level shows typically stochastic behavior. The stochastic parameters of h_w are mentioned in table 7.4 and derived in appendix C.4 on page 177 (lognormal distribution). The results are given below.

$$\beta = 4.55 \tag{7.29}$$

$$P_f = 2.63 \cdot 10^{-6}\ yr^{-1} \tag{7.30}$$

FORM ($t = 440\ mm$ & $h_w = stochastic$)

In table 7.8 the extended results are shown. The influence coefficient of f_{x1} is still the largest but the influence coefficient of the outer water level is almost as large.

TABLE 7.8: Influence coefficients and values of design point for stochastic parameters (results from a FORM run with $t = 440\ mm$ and $h_w = stochastic$)

Stochast:	f_{x1}	h_w	ϕ	t	Δ_p	N_{ow}	N_{vl}	$K_{add,\beta}$	ρ_{mas}
α:	0.775	-0.601	0.071	0.155	-0.067	0.050	0.042	-0.018	0.027
X_d:	0.115	2872	31.2	433	0.00015	0.0039	0.0014	0.00034	0.000002

So together f_{x1} & h_w dominate the outcome of the LSF. Graphically this can be observed in figure 7.13. In which the sample results of a MC run (for $t = 330\ mm$) are plotted in a graph with f_{x1} on the horizontal axis and h_w on the vertical axis. A line for which the outcome of the LSF equals zero can been drawn. This line divides the domain of building collapse from the domain of building remains intact.

Evaluation

In the subsection above, calculations have been performed for a failure probability of building collapse. This has only been done for one specific mechanism that could lead to building collapse namely out of plane bending failure of the soil retaining wall. In subsection 6.2.2 on page 91 other failure mechanisms of the building are mentioned. For the case-study only the mechanisms that could result in a residual profile of the dike as has been described in section 7.1.4 are relevant. When it is assumed, based on an enumeration of subsection 6.2.2 (page: 91), that for instance five collapse mechanisms could result in a residual profile. And when these other mechanisms are assumed to be independent and of the same order of magnitude, an estimation of the total failure probability of building collapse could be made. This is a very rough assumption. This can be done to assume the failure space of bending collapse of the total failure probability

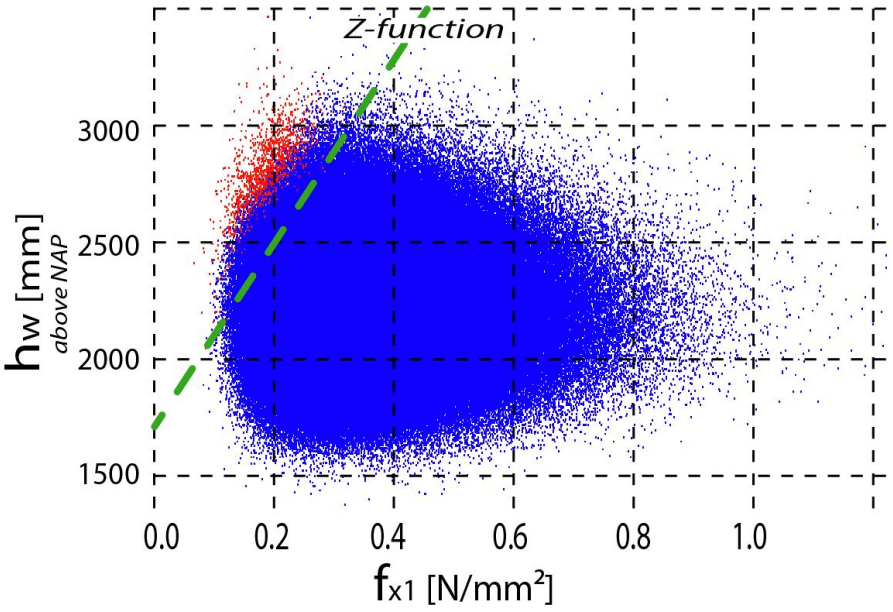

FIGURE 7.13: Graphic representation of MC ($t = 330\ mm$ and h_w =stochastic) results where f_{x1} is plotted against h_w (red dots represent a failure sample, blue dots represent a non failure sample)

of building collapse.[4] This results in:

$$\omega = \frac{1}{5} = 0.2 \tag{7.31}$$

$$P_{collapse,t} = \frac{4.73 \cdot 10^{-4}}{0.2} = 2.37 \cdot 10^{-3} \tag{7.32}$$
$$h_w = 3050\ mm$$

$$P_{collapse,t} = \frac{2.63 \cdot 10^{-6}}{0.2} = 1.32 \cdot 10^{-5} \tag{7.33}$$
$$h_w = stochastic$$

in which: ω = failure space
$P_{collapse,t}$ = assumed failure probability of building collapse concerning all mechanism $[yr^{-1}]$

7.4 Geotechnical model

In this section the conditional probabilities of instability that are input of equation (6.7) (page 77) are calculated.

[4]This is a very rough assumption, but a necessary one. Further research is needed to avoid this rough assumption

Assumptions and principles

The (soil) properties that are derived and assumed in section 7.1 are inserted in the D-Geo Stability software package. Furthermore the same assumptions and calculation principles have been used as for the D-Geo Stability calculations in chapter 5. Some modifications of the calculations that are performed here:

- The residual profile is assumed on basis of the proposed theory in section 6.3.1.
- A minimum slip plane length of 10 m is imposed to prevent that extremely small slip planes are normative.
- The calculations are now performed in a probabilistic way. This is done with help of the probabilistic module of D-Geo-Stability. The probabilistic method of this module is explained in appendix A.6 on page 151
- On this dike a road is present. Therefore traffic loads that could negatively impact the stability could be present. These loads are not included in the probabilistic calculation, in part because the software package does not have the option to include this loading in a probabilistic way.

Results

First some deterministic calculations are performed with the mean values. The resulting FoS are given below: The normative slip planes that belong to these values are presented in figures 7.14, 7.15, 7.16.

$$FoS = 2.13 \tag{7.34}$$

Without Building

$$FoS = 2.14 \tag{7.35}$$

Intact Building

$$FoS = 1.38 \tag{7.36}$$

Collapsed Building

From these deterministic results of the different profiles an important conclusion is observed. This is that the building, when it remains intact, does not have a (significant) beneficial effect on the macro stability of the slope. The reason for this is that the normative slip plane, for the normative water level, does not intersect with the building. Therefore the FoS of the profile without a building (figure 7.14 and equation (7.34)) is practically the same as the FoS of the profile with an intact building (figure 7.15 and equation (7.35)).

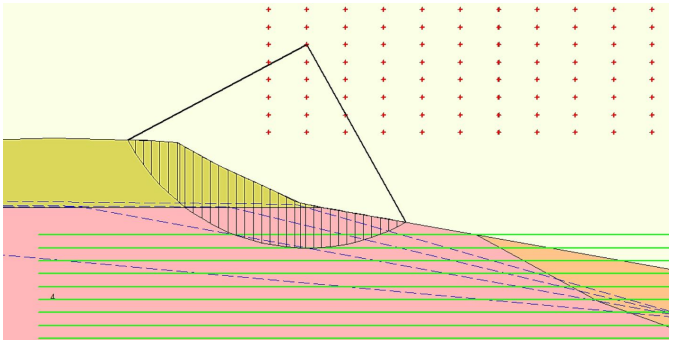

FIGURE 7.14: Normative slip plane for profile without building for calculation with design values

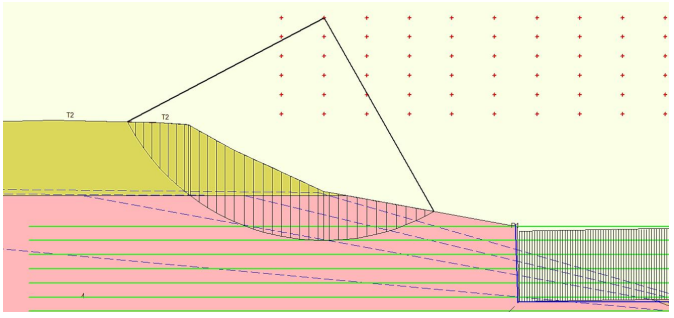

FIGURE 7.15: Normative slip plane for profile with intact building for calculation with design values

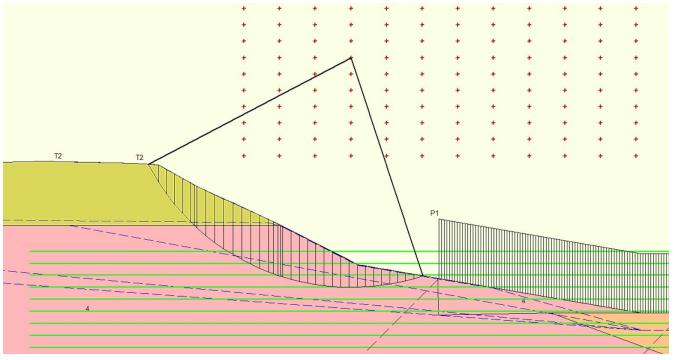

FIGURE 7.16: Normative slip plane for profile with a collapsed building for calculation with design values

In table 7.9 the probabilistic results of the different profiles are presented. To clarify these results the probabilistic method of D-Geo-Stability is introduced shortly. Extended background on this method is given in appendix A.6 on page 151. Extended calculation results (slip planes and calculation results for other outer water levels) are collected in appendix C.8 on page 184.

1. First a slip plane analysis is performed for multiple water levels, where the mean values from the distributions are used as input parameters. This results in the FoS that is presented in column two in table 7.9.

2. For this normative slip plane a FORM analysis is performed which results in a conditional failure probability given a certain water level. These are reported in column three and four of table 7.9 for the design water level. For the conditional failure probabilities that belong to other water levels, see appendix C.8.

3. In the last step the conditional failure probabilities for different water levels are combined with the probability density of the occurring water levels into integrated failure probabilities. These are presented in column five and six of table 7.9.

TABLE 7.9: Probabilistic soil stability results

Profile:	FoS	$\beta_{\|h_w=3050}$	$P_{instab\|h_w=3050}$	β	P_{instab}
Without Building	2.13	13.67	$8.04 \cdot 10^{-43}$	14.03	$5.40 \cdot 10^{-45}$
Intact Building	2.14	13.88	$4.11 \cdot 10^{-44}$	14.26	$1.94 \cdot 10^{-46}$
Collapsed Building	1.38	5.51	$1.84 \cdot 10^{-8}$	5.55	$1.41 \cdot 10^{-8}$

7.5 Integration of two models

With the calculations that have been performed in this chapter the influence of the building, including the effect of possible collapse correlated to a highwater event, on the stability of the dike can be determined. This is done by filling in equation (6.7) from page 77. First this is done for the design water level and subsequently when the variation of the water level is included.

Design water level

Below the integrated probability of instability for the profile with a building ($P_{instab,2}$) is determined for the design water level of $h_w = 3050\ mm + NAP$. This is compared with the probability of instability of the profile without a building $P_{instab,1}$.

$$P_{instab,2} = P_{(instab|intact)} \cdot (1 - P_{collapse}) + P_{(instab|collapse)} \cdot P_{collapse} \tag{7.37}$$

$$P_{instab,2} = (4.11 \cdot 10^{-44}) \cdot (1 - (2.37 \cdot 10^{-3})) + (1.84 \cdot 10^{-8}) \cdot (2.37 \cdot 10^{-3})$$

$$P_{instab,2} = 4.35 \cdot 10^{-11} \tag{7.38}$$

$$P_{instab,1} = 8.00 \cdot 10^{-43} \tag{7.39}$$

Variation water level

Below the integrated failure probability for macro stability for the profile with a building ($P_{instab,2}$) is determined for a stochastic water level, that has been introduced in section

7.1.5. This is compared with the failure probability for macro stability of the profile without a building $P_{instab,1}$.

$$P_{instab,2} = P_{(instab|intact)} \cdot (1 - P_{collapse}) + P_{(instab|collapse)} \cdot P_{collapse} \tag{7.40}$$

$$P_{instab,2} = (1.94 \cdot 10^{-46}) \cdot (1 - (1.32 \cdot 10^{-5})) + (1.41 \cdot 10^{-8}) \cdot (1.32 \cdot 10^{-5})$$

$$P_{instab,2} = 1.85 \cdot 10^{-13} \tag{7.41}$$

$$P_{instab,1} = 5.40 \cdot 10^{-45} \tag{7.42}$$

This calculation including the result is also graphically presented in figure .

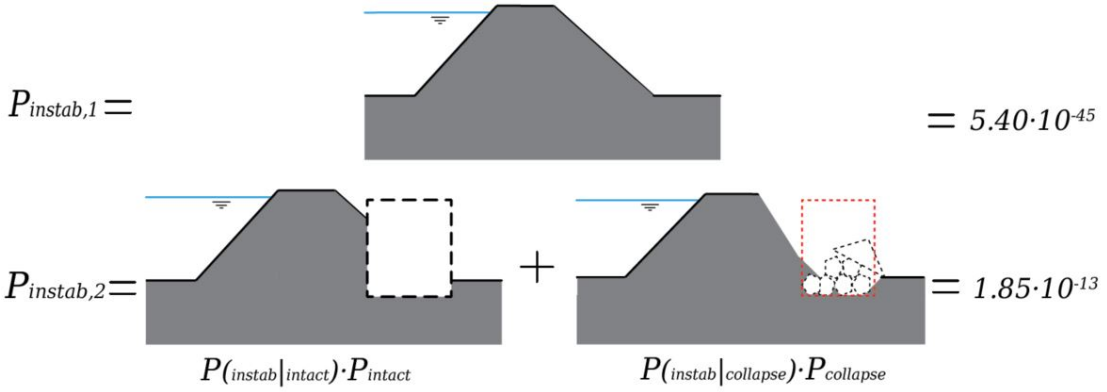

FIGURE 7.17: Graphical illustration of results of the case-study

In subsection 6.3.2 the effects of three dimensional effects are identified qualitatively. When this is applied to the case study this would result in a reduction of the negative effect of building collapse. Because, the residual profile that arises after collapse, would be less wide than the width of a sliding plane.

7.6 Conclusion

In this section first the results and limitations of the case-study are discussed. Afterwards a link is established to the answer of the research question belonging to this chapter, which was: "*Can this method be applied to a case study to determine the influence of a building?*"

The failure probability for macro-stability of a combined system, that consists of a dike profile containing a building, depends on the conditional probabilities for the two soil profiles and the probability of building collapse. For the case-study these probabilities have been calculated in order to determine the failure probability of the combined system. This has been done according to the developed method that has been presented at the beginning of the previous chapter.

First the probability of building collapse has been determined in subsection 7.3. This has been done for one possible mechanism of collapse for a masonry soil retaining wall. One of the purposes of this was to analyze how and to determine whether this probability was influenced during a high water event. From the results it appears, under the conditions and assumptions of this case-study, that this probability is indeed influenced by a high water. When the wall thickness is known, the bending tensile strength of the masonry and the water level are the properties with the largest influence on the probability of collapse. The wall thickness itself also appears to have a very large influence on the reliability of the soil retaining wall. It is suspected that the reliability of concrete soil retaining walls, generally speaking, is less problematic, since the variation of the material (resistance) properties of concrete are less.

Subsequently the conditional probabilities of soil (macro)instability, given that the building does collapse or the building does not collapse, are determined in subsection 7.4. For this case study it appeared that the building did not had a beneficial effect on the stability since it was not part of the normative slip plane. The possible collapse of the building, under the made assumptions, did have a negative influence on the stability of this residual soil profile.

In section 7.5 the determined probabilities from the two above mentioned paragraphs are combined with the method presented at the start of this chapter. From this it can be concluded that the building from the case-study, when possible collapse is included, has a negative influence on the dike stability. Important assumptions and properties that have lead to this conclusion for the case-study are:

- A long duration of a highwater, that results in fully developed freatic levels, resulting in hydraulic pressures on the soil retaining wall.
- A building with a soil retaining wall of masonry, of which it is known that the material properties are characterized by a large variation.
- A building that when it remains intact does not have a beneficial influence on the stability since it is located outside of the normative slip plane.
- A heterogeneous dike consisting of a base of clay and a top of sand. This results in large differences of the freatic level inside the dike, for outer water levels around the border of sand and clay at the outer slope.

For situations with different properties on the above mentioned bulletpoints, the negative influence might be less or there might not even be a negative influence. But this does prove that assessing also the absence of a NWO may indeed be necessary, as is prescribed by (VTV, 2006).

Some of the calculated failure probabilities, especially some of the probabilities of the soil profiles are extremely small. For the geotechnical model two reasons for this are:

- The uncertainty of the freatic lines are assumed rather small, since for all points on the freatic line the same uncertainty has to be selected, which could be seen as a limitation of the software package. When larger variations are inserted this could easily result in unrealistic values of the freatic level, for instance because some freatic lines might be bounded at some locations.
- The possibility of traffic loads has been left out of the model since the software package offers no ability to do this in a probabilistic way.

However the largest reason for the outcome of relatively small probabilities from both the structural as the geotechnical model, is that model uncertainties have not been included.

Because these model uncertainties are not included, the outcome of the geotechnical and structural model, can not be used for a comparison with acceptable probabilities. This is why the current models still can not be used to include the effects of a building in the safety assessment. When these model uncertainties and other effects that still require further research, would be included in the models, the used method, would result in probabilities that could be used for a comparison with acceptable probabilities or for including them in the safety assessment of flood defences.

For instance when such an improved method would be used and would show that buildings in a dike would enlarge the failure probability regarding macro stability with a factor two. This increased failure probability could, within WBI2017, be accommodated with failure space (ω) from the remaining mechanisms (30 % available) of table 2.2 on page 25. When this dike for macro stability does meet the failure space requirements (4 %) for this mechanism, another 4 % of the remaining mechanisms would be needed to include the influence of the buildings.

This page intentionally left blank.

Part IV

Evaluation

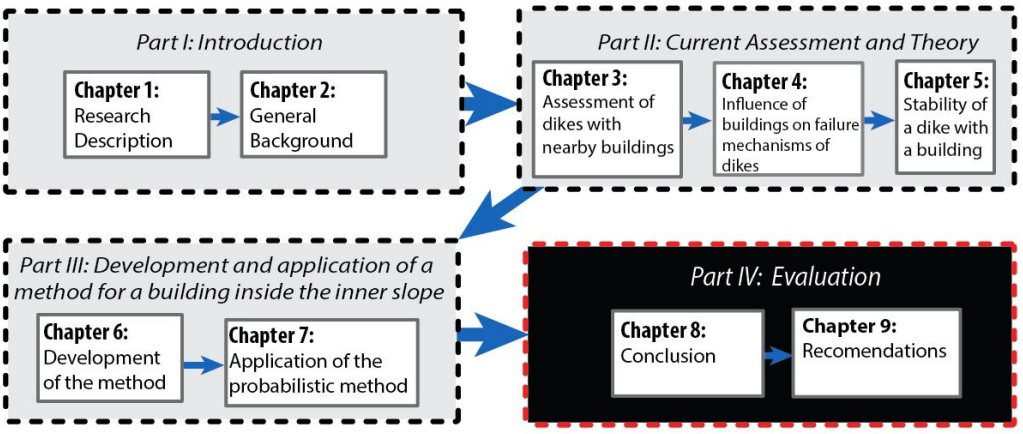

This page intentionally left blank.

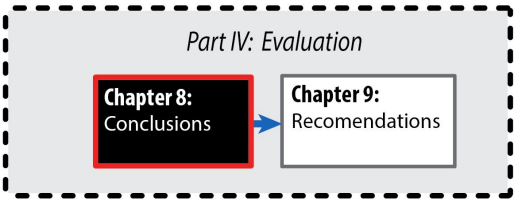

Chapter 8

Conclusion

In this chapter the main conclusions of this research are presented. First the subquestions are treated compactly and subsequently the main research question is answered.

The most important conclusions following from this research are described below. Later on compact answers to the research questions are presented.

- **No advanced assessment**
  In the current guidelines for the assessment of water defenses (VTV, 2006), an advanced assessment for NWO's is mentioned. It appears that such an assessment step has never been fully performed for buildings. This is one of the reasons that the assessment for many buildings have not been completed. In order to help with the use of an advanced assessment, it would be good to create a starting point for this advanced assessment. To decrease the amount of buildings for which the assessment has not been completed, it is also recommended to provide more simple assessment steps to come to an assessment.

- **Dependent collapse**
  The dependent collapse of a building to a high water has a much larger influence on the reliability of a dike, compared with an independent cause of building collapse. A cause of building collapse dependent to a high water can be the development of the freatic line in the dike. For buildings inside the soil profile of a dike the collapse can significantly reduce the stability.

- **Buildings do not satisfy**
  It is remarkable that, masonry buildings that are located inside the soil profile of a dike, do not satisfy the current guidelines for buildings (EC-6.1, 2013). This is due to the statement that the flexural tensile strength should not be taken

into account for masonry soil retaining walls, because of possible cracking of the masonry. It must be noted that the safety philosophy where the guidelines for buildings and water defenses are based on may differ, and therefore it is unclear what this building rejection means for the reliability of a water defense.

- **Developed method**
  In this research a probabilistic method is developed that can be seen as a starting point for an advanced assessment for building for inner slope stability. In particular for buildings that are located inside the soil profile and where possible collapse may affect the soil profile of the dike.

- **Application in practice**
  When model- and schematisation uncertainties would be implemented into the models belonging to the method, it could be used as an advanced assessment for building inside the soil profile. That would make it possible to accommodate the effects, imposed by the presence of a building, at the failure space that is reserved for the 'remaining mechanisms' within the new assessment tools (WBI2017). In that case a building does have a negative influence, but this can be accommodated by failure space, and therefore the dike itself does still meet the requirements of the total probability of flooding.

Research questions

The first subquestion has been treated in chapter 3, this continued incrementally till the last subquestion, which was treated in chapter 7.

Subquestion 1: *How is the assessment of water defenses, with buildings nearby, at the moment performed?*

Buildings around water defenses are classified as NWO's. The assessment of NWO's starts with a check whether they intersect with the assessment profile. When this is not the case the NWO is approved otherwise the assessment has to be continued with more complicated assessment steps. Since the elaboration of these steps is not very clear and lasts long, this results in a large amount of NWO's for which the assessment has not been finished. This is also because of the large amount of NWO's around Dutch water defenses.

Subquestion 2: *How can building characteristics have influence on the failure mechanisms of a dike?*

Buildings can influence the known failure mechanisms of dikes by multiple effects. These effects are classified by failure mechanisms in table 4.1 for the building characteristics: horizontal position, foundation method and vertical position relative to the soil profile. Also for the scenario of building collapse such a table has been made, see table 4.2. For some of these effects it is not clear whether they in practice really affect the safety of the water defense. Especially for the failure mechanism of the inner slope stability multiple effects, both positive and negative may be expected. These effects are further researched in this study, so the following subquestions focus on this mechanism. Furthermore it is concluded that the scenario of building collapse is most relevant when the collapse could be dependent to a high water event.

Subquestion 3: *What configurations and failure mechanism are most interesting to focus this study on, and why?*

From stability calculations it appears that a possible collapse of a building, when it is located in the soil profile, can indeed negatively influence the slope stability of a dike. Especially on locations at the inner slope or at the hinterland tangent to the inner slope. On the other hand when these kind of buildings remain intact they may beneficially influence the stability. Buildings with these properties often occur along Dutch dikes, often with soil retaining walls of masonry, from which the reliability might be uncertain. Therefore this study lies focus on these configurations.

Subquestion 4: *How can the influence of a building for the selected configuration be determined, and which information should be available to perform this method?*

In chapter 6 a probabilistic method is developed, consisting of a structural model of the building and a geotechnical model for the soil profiles, that could be used to determine the influence of buildings inside the dike profile, for which possible collapse of the building is relevant. This is used to research the combined system of a dike with a building.

For the selected configuration loads on the building can increase during a highwater, as a consequence of an increasing freatic line. Therefore it is proven that possible collapse of a building can be dependent on a high water event. This is further studied with a case study. When collapse of the building occurs the soil retaining wall will collapse. This leads to soil failure and a changed soil profile which is referred to as the residual profile. In chapter 6 a method is proposed to schematize the residual profile after building collapse.

Subquestion 5: *Can this probabilistic method be applied to a case study to determine the influence of a building?* The developed method is applied to a case study. For this case it is concluded that the building, when possible collapse is included, has a negative influence on the dike stability. At this moment the method could not yet be used to include the effects of a building into the assessment. This is because, model uncertainties and other effect that might require further research, have not been included yet into the structural and geotechnical model. When this would be added to these models, the results could be used to include the effects of a building from the selected configuration into the assessment according to WTI2017.

Main research question:

What is the influence of a non-water retaining building on the reliability of a dike, and how can this be determined and included into the assessment of water defenses?

In this study effects of buildings on different failure mechanism are described qualitatively. These effects have also been sorted for relevant building properties. The influence of a building on the dike reliability, and how this can be determined can be studied more extensively. In this thesis this has been done for macro stability in combination with a building inside the innerslope. For this configuration a method, containing a structural and a geotechnical model, is proposed and used to determine the influence of such a building, taking also the possible collapse of the building into account. This method is at the moment not yet ready to include the effects of buildings into the assessment, but it should be possible to extend the models, so that the method could be used to do this.

The goal of this research was to further investigate the possibilities of buildings near dikes. For one selected configuration and failure mechanism this has been done. This could also be done for more configurations, other categories of NWO's (pipelines, trees etc.) and different failure modes. This could result in methods to include the effects of NWO's, belonging to these different configurations, into the assessment. But above all it gives insight in the functioning of the combined system of dike and NWO. These insights could be used to develop clear filters (assessment steps) that should simplify and accelerate the assessment of NWO's.

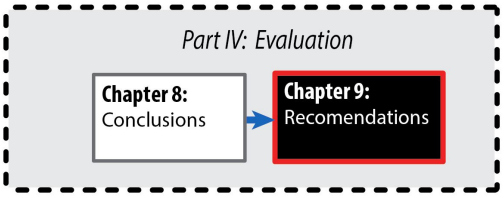

Chapter 9

Recommendations

In this chapter recommendations resulting from this study are collected. These are explained in the following paragraphs.

General assessment concerning NWO's

In the last assessment round of the Dutch water defenses, many NWO's have not been fully assessed. In many cases only the intersection of the NWO with the assessment profile was performed. To reduce the amount of undjudged NWO's it is recommended to develop more specific filters that could lead to the approval of NWO's. This should also result in a reduction of the amount of work needed for the assessment. Furthermore it is recommended to check for which kind of NWO's the possibility of absence of the object could be let out of the assessment. It is recommended to check whether this is possible in accordance with the dependency of possible collapse of the object to a high water, since when this collapse is independent to a high water the effect might be negligible.

Loads on a building during highwater conditions

It is recommended to further investigate the soil behavior during a highwater event. Effects like: undrained soil behavior, arching within the soil and or the building should be investigated. Furthermore the loads are now determined separately for the two subsystems (dike and building), while in reality this is a combined system. These effects may have an influence on the magnitude and the distribution of the loads on the building. A finite element model like Plaxis, preferably 3D, might give insight in these effects. Besides the influence of the 3D effects that are predicted (section 6.3.2) because a building

is often less wide than the width of a sliding plane needs further research to include this in the models.

Probability of building collapse

The probability of the event building does collapse due to highwater conditions could be further researched. Now this has only be done for one mechanism of collapse, and therefore it is recommended to investigate how other mechanisms are influenced during conditions of a high water. Also the influence of the safety of these buildings concerning age effects would be interesting to implement. The development of a simple guideline, that describes for which building specifications, minimal collapse probabilities for the building under highwater conditions could be assured, would be interesting. This guideline could simplify the developed method for including building effects into the assessment.

Other failure mechanisms of dikes

In this research the effects of buildings on the macro stability are extensively investigated. But as is described in chapter 4 buildings also influence other failure mechanisms of dikes. Therefore it is recommended to also perform more research on the influence of buildings on other failure mechanisms like piping, overflow/overtopping and erosion of the outer slope.

Residual profile

In this study an approach is suggested how to schematize a residual profile after building collapse. This is done in a graphical way based on reference on the slope corresponding to the material. More research could be performed on how such a residual profile might develop, and how the sliding soil and simultaneously collapsing building interact. Possibly this could be done with physical models.

Extend method with model uncertainties

The current method that has been used for the case-study consists of a structural model and a geotechnical model. Because model uncertainties have not been included into these models yet, the outcome can in practice not be compared with certain limit values. The model uncertainty for the geotechnical model could easily be added, since a lot of

research on the reliability of this soil model (Bishop) has been performed. To add the uncertainty to the structural model is more complex. The uncertainties imposed by occurring moments and mechanical schematisations should then be included. When these uncertainties and other effects are included in the models, the method could be used for including building effects into the assessment.

Reinforcing buildings

This method could also create opportunities to reinforce buildings in order to enlarge the stability of the dike. For instance by reinforcing the soil retaining wall with concrete or fibers, the probability of building collapse could be decreased, which could result in approval of the NWO. Perhaps it is also possible to reinforce the soil retaining wall, in such a way that it can remain intact even when the building itself collapses. In that case the building collapse scenario would not lead to a less stable residual profile, and therefore the building collapse scenario could be dropped. Possible drainage at the bottom of a soil retaining wall might also be interesting because it might take away the hydraulic pressures on the wall during a high water event. Then the building collapse scenario would not be dependent on a high water anymore, which significantly reduces the probability of instability of the combined system.

This page intentionally left blank.

Part V

Appendices

This page intentionally left blank.

Appendix A

Background theory

In this appendix background theories are presented that have been investigated as part of this study but are not in detail described in the main report. The contents of this appendix are depicted below:

Contents

A.1 Dike reinforcements around buildings

In this appendix an overview is given of possible measures when dike reinforcements need to be executed close to present buildings.

In the past there have been numerous dikes which have been reinforced and also in the future these reinforcements will have to continue 2e Deltacommissie (2008a). These reinforcements often consist of heightening, widening or applying/enlarging a berm. Close to houses these reinforcements are always extra challenging, because preferably the house is kept in place without damage. Enlarging the berm or the dike can cause damage to the building due to differences of settlements because of consolidation and creep of soft soils in the subsoil (ENW, 2007). When an dike reinforcement needs to be

executed with buildings close to the dike there are a lot of options on how to approach this. An incomplete overview of these options is given below.

Demolishing house If the reinforcement intersects with a building a possible solution is to demolish the existing building. Apart from the public resistance that is hereby caused also the houses have to be bought out. (Jonkman and Schweckendiek, 2015)

Sheetpiles Sheetpiles can be used for dike reinforcements. When due to a building the dike can not be widened the sheetpiles can allow for a steeper slope. Sometimes sheetpiles are also placed in the dike to take over the function of the dike. This results in a much smaller profile of the water defense, where the building will lie outside this profile. For these constructions often anchorage might be necessary (Jonkman and Schweckendiek, 2015).

Dike reinforcement on the outside Another option is to shift the dike around the building. This can be done on the outside, so that the building stays inside the dike ring. The draw down of this is that area of the floodplain reduces. The dike can also be shifted to the inside but then the building is located on the floodplain side. See figure A.1. (Waterschap Rivierenland, 2013)

FIGURE A.1: Example of shift of dike to outside (Waterschap Rivierenland, 2013)

Buildings on jacks To avoid that a building 'disappears' in the dike after a reinforcement it is possible to jack up the building. This can be done with already present buildings but also new buildings near a dike can be equipped with a special foundation to easily jack them up when the dike needs to be reinforced See figure A.2. (van Leeuwen and van der Giessen, 2015)

Mixed in place Another reinforcement method is Mixed in Place(MIP). The goal of MIP is to increase the stability of the slope to increase the shear strength of the soil. This is done by mixing the soil with cement, the method is thus a soil improvement method. See figure A.3. (de Klant et al., 2011)

FIGURE A.2: Preparation of jacking up a building near the Lek dike (van Leeuwen and van der Giessen, 2015)

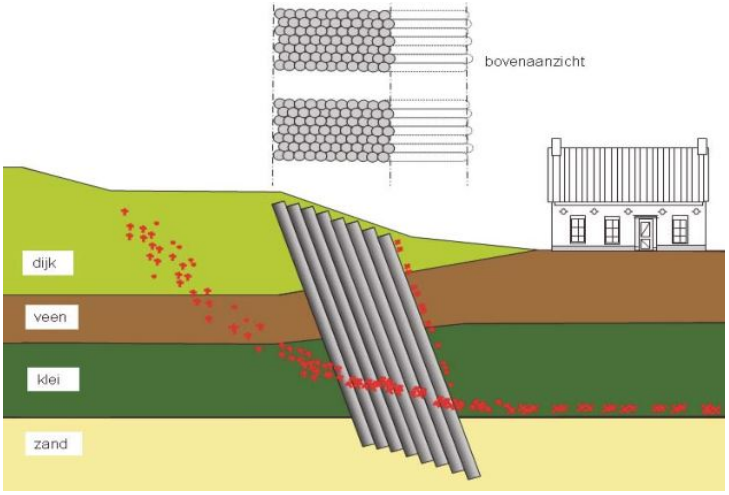

FIGURE A.3: Schematization of Mixed in Place in a dike (de Klant et al., 2011)

Reinforced vertical soil construction With this method it is possible to realize a vertical slope, through this it is not necessary to widen the dike when it is heightened. The construction consists of vertical concrete plates which are anchored with horizontal strips in the soil behind the plate. The force is transferred by the friction between the soil and the strips. See figure A.4. (TAW, 1994)

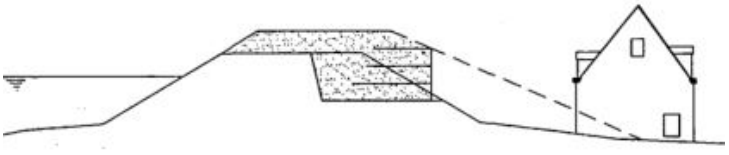

FIGURE A.4: Example of reinforced vertical concrete structure as alternative for widening of the dike

Slurry wall A dike reinforcement with a slurry wall consists of the same idea as the sheetpile wall. Either it is used for stability to cope with a steeper slope or it will be used to take over the water retaining function of the dike. The slurry wall is an on site constructed reinforced concrete wall. (TAW, 1994)

Ground nailing Also the method ground nailing can be used to reinforce the ground to allow for locally steeper slopes. The technique is based upon the placement of steel or plastic nails enveloped with grout that should guarantee a good attachment of the nails and the soil. The idea is that this nails intersect with the normative slip circle and that the soil around a nail acts as a soil body with the length of a nail. This large soil body should increase the safety against sliding of a slope. See figure A.5. Waterschap Rivierenland (2015)

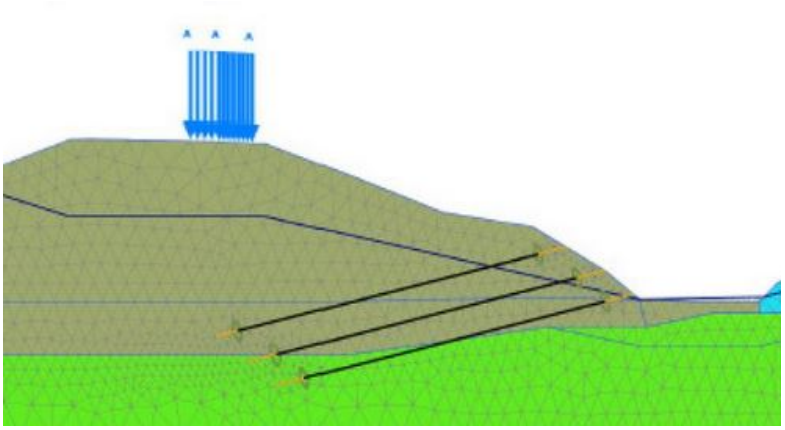

FIGURE A.5: Schematization of ground nailing reinforcement (Waterschap Rivierenland, 2015)

A.2 Shear strength and freatic level

In this appendix the relation between shear capacity and the height of the freatic line is elaborated and exemplified.

The freatic line in a dike body is important because pore pressures influence the stresses between the grains (effective stresses) and therefore the strength properties of the soil. The freatic level can rise due to high river levels and/or due to rainfall. The level of the freatic line depends on the permeability of the soil and the time that it is exposed to the high water levels and or rainfall. The effect of the freatic line on the effective stresses is illustrated below in figure A.6. First a freatic line with some bulge is modeled (A), then a linear freatic line (B), and as last a freatic line that could occur due to a more

impermeable outer slope of the dike (C) is modeled.[1] With help of the formulas below,

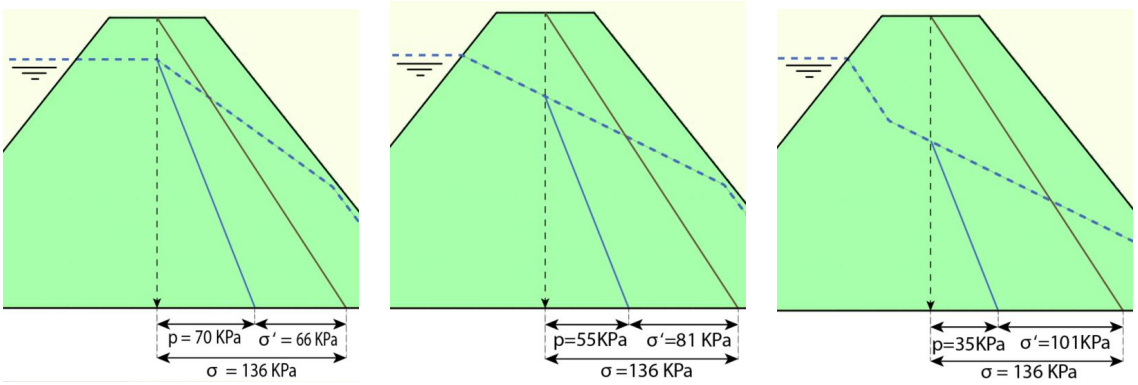

(A) (B) (C)

FIGURE A.6: Different freatic lines and their influence on the stresses in the soil. (blue solid line is pore pressures, brown solid line is total stresses.)

based on drained Mohr-Coulomb theory:

$$\sigma' = \sigma - p \tag{A.1}$$

$$\tau = \sigma' \cdot \tan(\phi') + c' \tag{A.2}$$

in which: p = pore water pressure $[kPa]$
τ = shear strength $[kPa]$
σ = normal vertical total stress $[kPa]$
$\sigma\,'$ = normal vertical effective stress $[kPa]$

The mobilized drained shear strength under the middle of the dike becomes:

$$(A)\ : \tau = 66 \cdot \tan(22) + 9 = 35.66\ kPa \tag{A.3}$$

$$(B)\ : \tau = 81 \cdot \tan(22) + 9 = 41.72\ kPa \tag{A.4}$$

$$(C)\ : \tau = 101 \cdot \tan(22) + 9 = 49.8\ kPa \tag{A.5}$$

A.3 Undrained soil behavior

In this appendix additional background on undrained soil behavior is presented.

In the determination of the shear strength an important consideration is whether the soil acts drained or undrained. For relatively permeable soils no excess pore water pressures develop and therefore in the calculation of the shear strength only effective stress parameters are used. When the soil is rather impermeable excess pore water pressures

[1] No change of slope of the total stress path is drawn because the wet and dry specific weight of clay are assumed to be equal. These equal weights are realistic because of the capillary function

can develop during loading and this can influence the available shear strength. This generation of excess pore pressures influences the shear strength of the soil (Hardeman and van Duinen, 2015) (see figure A.7).

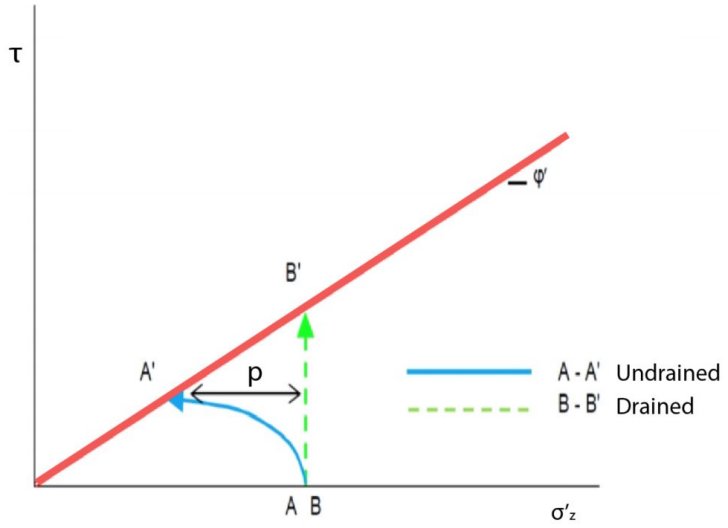

FIGURE A.7: Development of pore pressure influences the shear strength (Hardeman and van Duinen, 2015)

When the undrained behavior is applied to dikes, it has to be represented as follows: When the shear strength of the soil is mobilized and strains occur excess pore water pressures are generated. These pore pressures reduce the shear strength of the soil.[2] Whether the soil acts drained or undrained thus depends mainly on the permeability, the drainage length and the speed of deformation. In general it can be said that undrained behavior occurs if soil deformations occur quicker than the dissipation of pore pressures. This is determined by the drainage length, the permeability, the compressibility and the time of deformation.

For the new assessment tools (WTI 2017) it is suggested to use the drained shear strength for sand, and for peat and clay the normative soil behavior.

- For low effective stresses a drained analysis is normative and therefore suggested.
- For higher effective stresses an undrained analysis is normative and suggested.
- For heavily over-consolidated clays and peats a drained analysis is normative and thus suggested[3]

Furthermore the use of the Critical State Soil Model (CSSM) for the combination of the undrained behavior is imposed in the new assessment tools. (van Duinen, 2015)(van Duinen, 2014)

[2]This only applies to normally consolidated soils and slightly over-consolidated soils ($OCR < 2$). Soils that are even more over-consolidated show an increase in shear strength. ($OCR > 3$)

[3]During deformation of these soils the pore water pressures drop and therefore the shear strength increases.

A.4 Development of freatic line

In this appendix the development of the freatic line in a dike is explained in more detail. Besides a schematisation method to assume freatic levels for clay dikes is presented. This method is also applied to a general case to experience the results of this method.

When the freatic line is not influenced by precipitation or overtopping water the freatic level mainly depends on the duration of the high water event and the hydraulic conductivity of the dike material. Here a situation for a dike of clay (low permeability) and a duration that typically belongs to an event that is caused by high river discharges (2 weeks) is elaborated.

The effect of the duration of the high water wave is illustrated in figure A.8. As can be seen a 2 dimensional freatic surface in the soil body is formed. This means that also the seepage follows a two dimensional flow path through the soil. This flow, and therefore the freatic surface, is governed by the hydraulic conductivity of the soil, which is generally anisotropic. The horizontal conductivity is generally speaking larger than the vertical conductivity. Therefore this relation between horizontal and vertical conductivity also influences the shape of the freatic surface. In addition to that the freatic line

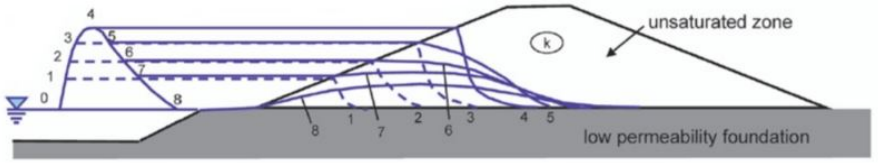

(A) Development for a transient high water wave

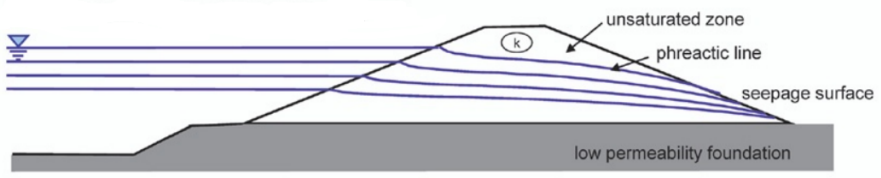

(B) Development for a permanent increase of water level

FIGURE A.8: Examples of development of freatic lines (CIRIA C731, 2013)

is affected by the (duration of) the water level and the permeability, overtopping water and precipitation can also raise the freatic surface, which is called bulge. To model the freatic line in a dike, groundwater flow models are available, but these can be rather complex.

In (TAW, 2004) a method is handed to schematize the freatic line in a dike under the influence of a high water and bulge. This schematisation is used to show the effect of

the permeability of the dike material on the development of the freatic surface. This is done for the earlier assumed basic dike profile (5.1). The approach is based on the

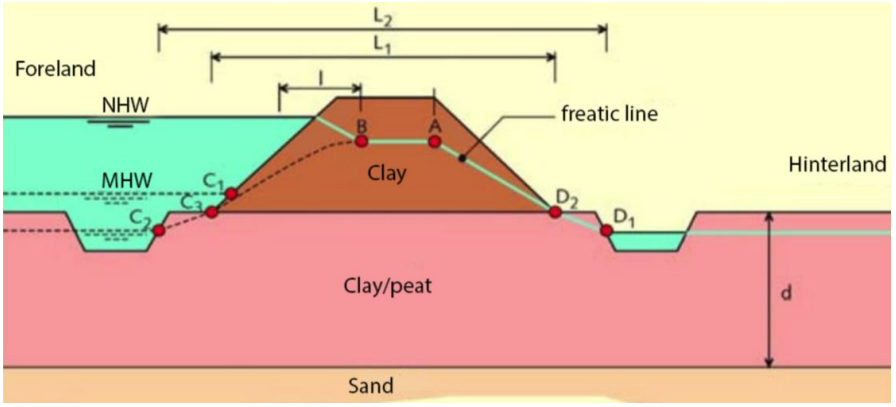

FIGURE A.9: Schematisation method freatic line according to (TAW, 2004)

determination of certain points that together form the schematized freatic surface. In this approach the freatic line is schematized for an assumed Normative High Water level (NHW).

B Point B is located at the height of the entry point and is horizontally located *a intrusion length* from the outer slope. The entry point is defined at the outer slope in between NHW and MHW (Mean High Water). The location of this point has to do with the infiltration of the water at the outer slope. The intrusion length can be calculated with the following formula.

$$I_l = \sqrt{\frac{2 \cdot K_z \cdot MHW \cdot t_{HW}}{n_z}} \tag{A.6}$$

in which:
I_l = intrusion length $[m]$
K_z = hydraulic conductivity of the dike material $[\frac{m}{s}]$
t_{hw} = duration of high water wave at MHW $[s]$
n_z = porosity of the dike material $[-]$

A Point A is located under the intersection of the crest and the inner slope and is vertically determined by the bulge effect. For this given situation, (TAW, 2004) gives that, the height of this point becomes $\frac{1}{10}$ of the length of the dike, so: 4.6 m

D Point D is located at the inner toe of the dike.

To calculate the intrusion length some assumptions have to be made. The entry point is assumed to be located four meters above the toe of the dike. The duration of the high water at MHW is taken 5 days. And for the porosity, n_z, a value of 0.4 is assumed. According to (TAW, 1996) the hydraulic conductivity for in-situ clay material is typically in between $k = 10^{-4}$ $\frac{m}{s}$ & $k = 10^{-5}$ $\frac{m}{s}$. These values are lower than expected, but this is

caused by cracking and drying out. When three different values of hydraulic conductivity of this range are inserted in equation (A.6) this results in three different intrusion lengths, which are given in table A.1. The resulting schematisations, with and without the bulge effect, are elaborated in figures.

TABLE A.1: Intrusion length for different values of the hydraulic conductivity

$\mathbf{k}$ $[\frac{m}{s}]$	$1 \cdot 10^{-4}$	$5 \cdot 10^{-5}$	$1 \cdot 10^{-5}$
$\mathbf{l}$ $[m]$	10.4	7.3	3.3

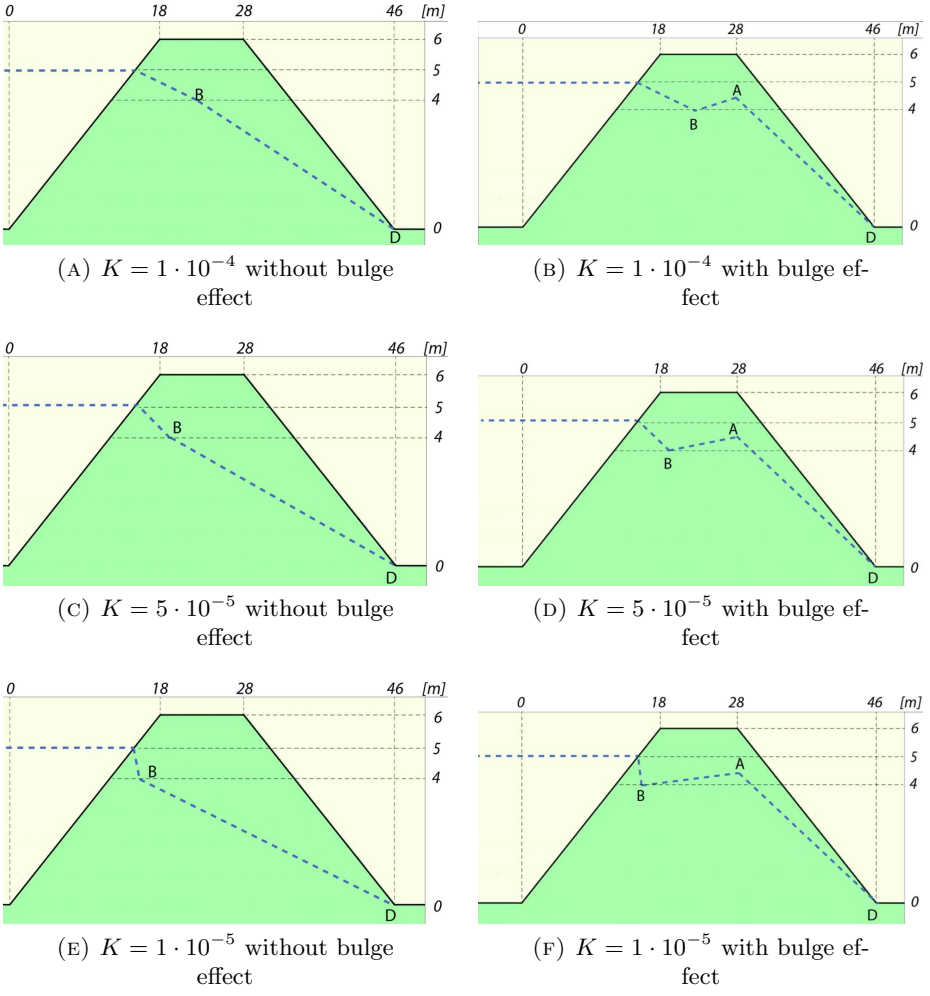

(A) $K = 1 \cdot 10^{-4}$ without bulge effect

(B) $K = 1 \cdot 10^{-4}$ with bulge effect

(C) $K = 5 \cdot 10^{-5}$ without bulge effect

(D) $K = 5 \cdot 10^{-5}$ with bulge effect

(E) $K = 1 \cdot 10^{-5}$ without bulge effect

(F) $K = 1 \cdot 10^{-5}$ with bulge effect

FIGURE A.10: Freatic line schematizations for different hydraulic conductivities, with and without bulge effect

When these figures are observed it can be seen that the bulge effect can have a very large effect on the hydrostatic pressures that are exerted on a soil retaining wall that is located in the inner slope.

In this schematisation the resulting bulge height (point C) is for the three different hydraulic conductivities the same, but in reality the amount of bulge also depends on

the freatic line for the situation without bulge. Therefore the situation in figure A.10 *F*, where the rise of freatic line due to the bulge effect is really large, it could be wise to adjust this freatic line accounting for a smaller bulge effect.

A.5 Traffic load on dike

In this appendix the possible increase of soil pressures against a building inside the dike, induced by a traffic load on the dike is elaborated.

On many dikes traffic roads are located. When vehicles are driving over the dike this enlarges the driving moment of the slip plane of the slope. But also an increase in vertical effective pressures in the soil is expected. An increase of effective pressures is normally associated with an increase in the shear strength properties of the soil. But when low permeable soils are loaded with a surcharge, consolidation effects may occur. This can result in an increase in the pore water pressure, if the water can not flow out quickly. When this consolidation effect is 100 % the whole surcharge loading is absorbed by excess pore water pressures. Because the total stress increases with the same amount as the pore pressures, the effective soil stresses remain the same. And therefore also the shear strength of the soil remains the same. (TAW, 1994) specifies the normative traffic load to be 13 $\frac{kN}{m^2}$. This is based on a calamity situation, for when a truck with sandbags has to be transported over the dike. This implies that a combination of a traffic load and a high water loading on the dike can also coincide.

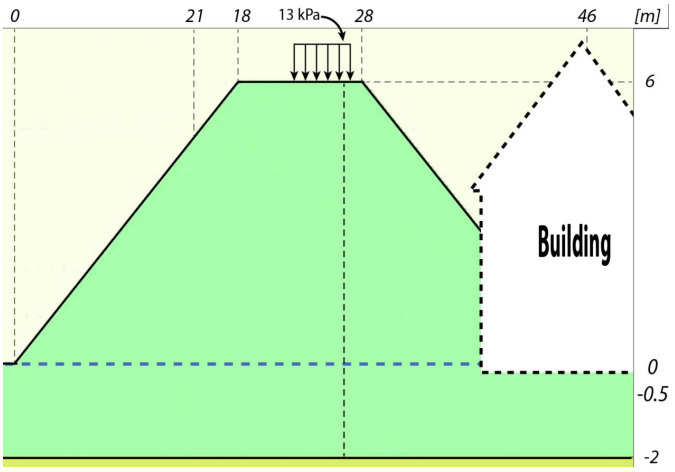

FIGURE A.11: Increased soil pressures on soil retaining wall induced by a traffic load

The traffic load on the soil body may also induce an increase in the loading on the soil retaining wall of a building. To investigate this, a situation as in figure A.11 is analyzed. To do this the vertical stresses in the soil, under the surcharge load and on the dotted line, are illustrated in figure A.12 . This is done for a drained situation and

for an undrained situation. In reality for clay dikes something in between will occur depending on the specific soil properties. In the drained situation the vertical effective stresses increase with the amount of the surcharge and therefore the horizontal pressure increases with more or less 50 % of the surcharge (depending on the K_a value, see equation (6.23)). For the undrained situation the pore water pressure increases with the amount of the surcharge, since pore pressures are isotropic, the potential increase in pressure on the wall is as large as the surcharge. Besides this (un)drained effect also the horizontal distance between a truck and the building is of importance. When the building is very close the increases will be as described above, but when there is some distance the horizontal pressures may spread out and decline. Especially excess pore water pressures dissipate quickly horizontal.

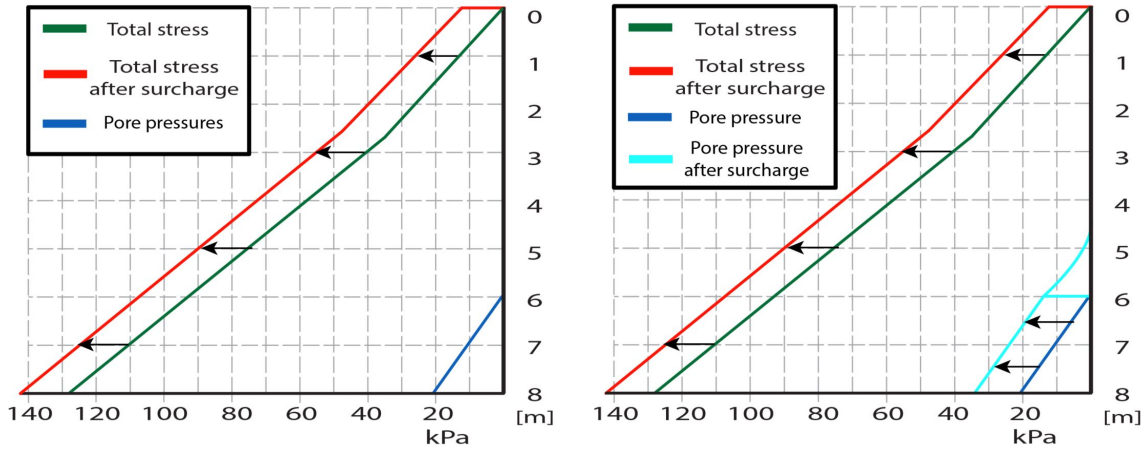

(A) Drained vertical soil pressures with and without traffic load

(B) Undrained vertical soil pressures with and without traffic load

FIGURE A.12: Effects of a traffic load for (totally) undrained and drained situation

A.6 Reliability methods

In this appendix background information is provided on the reliability methods that have been used for the case-study of chapter 7.

Probabilistic calculation of soil retaining wall

For the calculation of the reliability of the soil retaining wall of the building, two different reliability methods are used. Most of these calculations have been performed with a First Order Reliability Method (FORM). This is done because one of the big advantages of FORM is that it is a quick method. Besides also Monte Carlo simulations (MC) are

performed for verification of the FORM results and to provide some graphical calculation results.

First Order Reliability Method

This method is based on a linearization of the LSF in the so called design point. This point is defined as the point in the domain $LSF : \ Z = 0$ with the highest joint probability density. The FORM procedure is performed with help of a set of standard normally distributed variables. These are related to the stochastic variables that have been inserted in the FORM calculation. In the FORM calculation the reliability index is calculated by dividing the mean value of the LSF with the standard deviation of the LSF. This reliability index can be converted to a failure probability:

$$\beta = \frac{\mu_z}{\sigma_z} \tag{A.7}$$

$$P_f = \Phi(-\beta) \tag{A.8}$$

in which: μ_z = mean value of the LSF
σ_z = standard deviation of the LSF
Φ = standard normal distribution

The determination of the design point is done with an iterative procedure that converges to the design point. In this point the LSF: $Z(X_1, ..., X_i)$ is linearized and could be written as:

$$Z_L = C + D_1 \cdot u_1 + ... + D_i \cdot u_i \tag{A.9}$$

in which: C, D_i = values obtained after linearization
u_i = standard normally distributed variable i

The stochastic variables of the LSF can now be obtained due to the statistical properties of the normalized distributions:

$$\mu_z = C \tag{A.10}$$

$$\sigma_z = \sqrt{\sum D_j^2} \tag{A.11}$$

This summation goes from $j = 1$ to $j = n$ with n the amount of stochastic variables.

When the linearized LSF is divided by $\sqrt{\sum D_i^2}$ the reliability index and so called influence coefficients are identified in the LSF:

$$Z_L = \beta +_1 \cdot u_i + ... + \alpha_i \cdot u_i \tag{A.12}$$

$$\alpha_i = \frac{D_i}{\sqrt{\sum D_j^2}} \tag{A.13}$$

in which: α_i = influence coefficient of parameter i [−]

These influence coefficient indicate the relative influence of parameter i on the outcome of the LSF. (Courage and Steenbergen, 2007)

Monte Carlo simulation

The MC procedure works as follows: For every stochastic variable n realizations are simulated according to their probability distribution. Each set of variables is inserted in the LSF for which the outcome is calculated. If $Z \leq 0$ a counter n_f is increased by one. The failure probability is then calculated with the following formula:

$$P_f = \frac{n_f}{n} \tag{A.14}$$

in which: n_f = amount of realization in the failure domain
n = amount of MC realizations

The reliability of this method depends on the ratio between the number of simulations, n, and the failure probability, P_f. To determine the reliability of the outcome of a MC formula (7.27) on page 119 can be used. (Jonkman et al., 2015)

Probabilistic calculation of soil profiles

For the probabilistic calculations that are performed for the soil profiles the reliability module of the Deltares software package D-Geo-Stability is used. In this module the probability calculation is built up in two steps. First a reliability index and failure probability is calculated for a given water level and freatic level. And afterward, when this is done for different water levels, and properties that describe the occurrence probabilities of the water levels, these probabilities are combined into the integrated probability of failure. The method is described for these two steps in the following subsections based on (Deltares, 2014).

Fixed water level

First the program determines the normative slip plane with the mean values from the given distributions. For the slip plane with the lowest FoS a probabilistic method deployed. This probabilistic method makes use of a FORM approach, as has been described above. In order to provide this method, the software package can apply a standard normalized probability distribution for the stochastic parameters. With help of iterative procedure to determine the design point and by a linearization of the LSF.

$$Z = FoS - FoS_{required} \tag{A.15}$$

For this LSF with help of FORM techniques the reliability index can be calculated:

$$\beta = \frac{\mu_{FoS} - FoS_{required}}{\sigma_{FoS}} \tag{A.16}$$

in which: μ_{FoS} = expected mean value of the safety factor
σ_{FoS} = standard deviation of the safety factor

Two limitations imposed by the software package and relevant to notice concerning this research are:

- Uncertainty in geometry, unit weight and loadings can not be included in the probabilistic calculation in this module.
- The FORM procedure is only applied to the slip plane surface that has been derived from a mean value analysis.

Randomness of water level

Before this step the program has calculated a couple of conditional failure probabilities for different water and freatic levels. With these conditional probabilities a cumulative resistance distribution can be made as function of the loading parameter: $F_R(h_w)$. See figure A.13 A. In order to calculate the integrated probability of failure, the probability density of the occurring water levels has to be known. To do this some stochastic properties of the water level have to be inserted in the software package. Namely a design water level has to be identified with a corresponding exceeding frequency. Also a decimate height has to be inserted, which is defined as the rise of water level that is needed to reduce the probability of exceedance of this level by a factor 10. From these properties the probability distribution is estimated, assuming a Gumbel distribution

with parameters: B, u_{gumbel}.

$$P(h_w > h_{design}) = 1 - \exp(-\exp(-\frac{2.3}{B_{dh}}(h_{design} - u_{gumbel}))) \tag{A.17}$$

in which:	$P(h_w > h_{design})$	=	exceeding probability of the design water level
	B_{dh}	=	gumbel parameter, decimate height
	h_{design}	=	design water level
	u_{gumbel}	=	gumbel parameter

So now a loading probability density distribution of the water level is assumed: $f_s(h_w)$. See figure A.13 B.

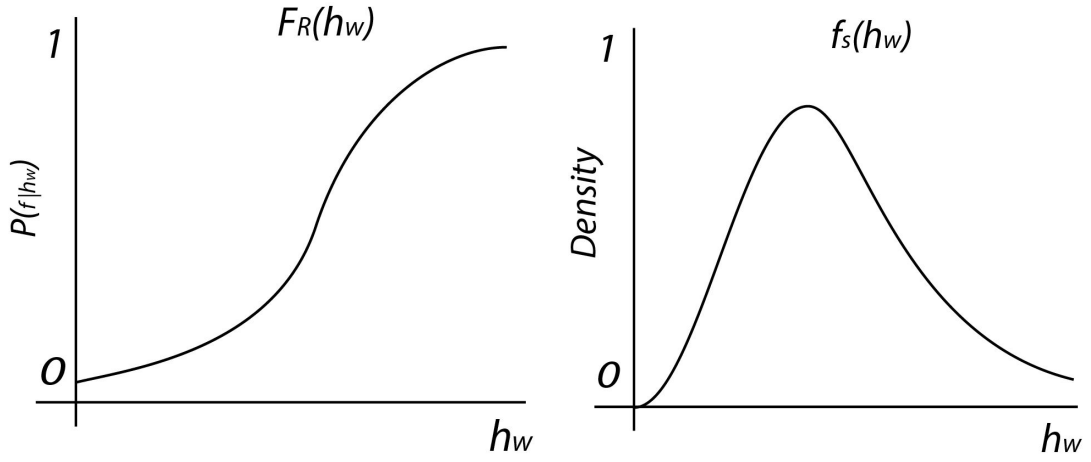

(A) Cumulative density resistance distribution of water level

(B) Probability density loading distribution of water level

FIGURE A.13: Two components of the convolution integral

The integrated failure probability now can be calculated with the so called "convolution integral". Below this integral is derived (Jonkman et al., 2015):

$$P_f = \iint\limits_{r<s} f_R(r) \cdot f_S(s)\, dr\, ds \tag{A.18}$$

$$P_f = \int\limits_{-\infty}^{+\infty} \left[\int\limits_{-\infty}^{R=s} f_R(r)\, dr \right] f_s(s)\, ds \tag{A.19}$$

$$P_f = \int\limits_{-\infty}^{+\infty} F_R(s) \cdot f_S(s)\, ds \tag{A.20}$$

For this situation the convulation integral becomes:

$$P_f = \int\limits_{-\infty}^{+\infty} F_R(h_w) \cdot f_S(h_w)\, dh_w \tag{A.21}$$

in which:	$F_R(h_w)$	=	cumulative density resistance distribution of water level
	$f_S(h_w)$	=	probability density loading distribution of water level
	R	=	parameter or subscript referring to resistance
	S	=	parameter or subscript referring to loading

The software package approximates this convolution integral by a FOSM (First Order Second Moment) method. From this the final integrated failure probability is returned.

Appendix B

Background calculations

In this appendix background on calculations are presented that are performed as part of this study but are not in detail described in the main report. The contents of this appendix are depicted below:

Contents

B.1 Piezometric head in aquifer

In this appendix the topic of a piezometric head in a aquifer under a dike is further elaborated. This has been done for the description of vertical instability in subsection 5.1.1 on page 58. A calculation method is presented to determine the piezometric head in an aquifer which is used in the calculations of the next appendix B.2.

The piezometric head in an aquifer is an key property for vertical equilibrium. But when the piezometric head in the aquifer is higher than in the aquitard, the head in the bottom part of the aquitard also rises , which results in a decrease of the shear strength

of this part of the aquitard.[1]. The piezometric head in a relatively permeable layer under a dike is influenced by the piezometric head at the river and the piezometric head in the hinterland (This is the piezometric head that is not influenced by the river, in Dutch: "polder-peil"). The relation between these heads is determined by the damping of the system, which itself is influenced by the permeability of the aquifer and blanket and corresponding thicknesses. For a simple cross section, as is reviewed for the principle calculations here, the heads can be estimated on an analytical groundwater flow model based on Dupuit (TAW, 2004) (horizontal aquifer flow with vertical leakage). Such a model can be schematized by figure B.1 and the equations below.

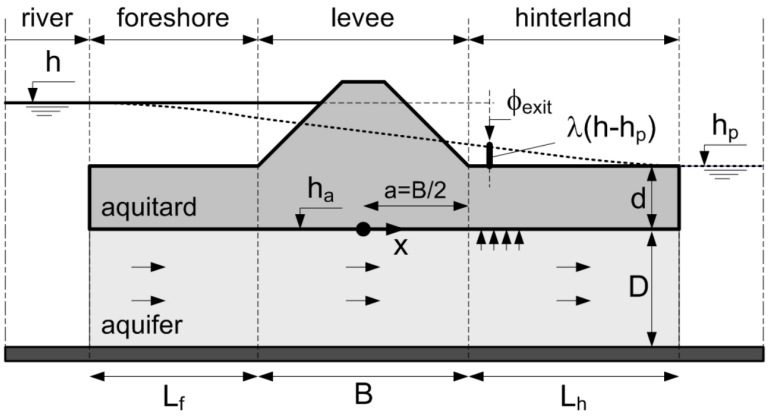

FIGURE B.1: Groundwaterflow model for an aquifer under an dike with a cover layer (TAW, 2004)

$$\lambda_h = \sqrt{k_{af} \cdot D \cdot d / k_{at}} \tag{B.1}$$

$$\lambda = \frac{\lambda_h}{L_f + B + \lambda_h} \cdot \exp^{((\frac{B}{2} - x_{exit})/\lambda_h)} \tag{B.2}$$

$$\phi_{exit} = h_p + \lambda(h - h_p) \tag{B.3}$$

in which:

h_w	=	water level at river-side of the dike	$[m]$
h_p	=	polder level at hinterland	$[m]$
B	=	width of dike base	$[m]$
L_f	=	length foreshore	$[m]$
ϕ_{exit}	=	potential at exit point	$[m]$
x_{exit}	=	distance from exit point to center of dike base	$[m]$
λ	=	damping	$[-]$
λ_h	=	leakage factor	$[m]$
k_{af}	=	hydraulic conductivity aquifer	$[m/s]$
k_{at}	=	hydraulic conductivity aquitard	$[m/s]$
D	=	aquifer thickness	$[m]$
d	=	blanket thickness	$[m]$

[1]This effect is neglected in the basic calculations.

B.2 Uplift

In this appendix basic hand calculations are performed for the uplift failure mechanism of the basic case of figure 5.1 (page: 58). This calculation belongs to section 5.1.1 page: 58.

When the occurrence of uplift is checked first the piezometric head in the aquifer at the toe of the dike has to be determined. One possibility to do this is to calculate it analytically with the equations presented in the previous appendix. When the length of the foreshore is assumed to be 20 meters and the properties from table 5.1 and figure 5.1 are used- the piezometric head becomes:

$$\lambda_h = \sqrt{\frac{5 \cdot 10^{-5} \cdot 4 \cdot 2}{1 \cdot 10^{-7}}} = 63.25 \ m \tag{B.4}$$

$$\lambda = \frac{63.25}{20 + 46 + 63.25} \cdot \exp^{((\frac{46}{2} - 23)/63.25)} = 0.49 \tag{B.5}$$

$$\phi_{exit} = 5 + 0.49(5 - -0.5) = 2.19 \ m \tag{B.6}$$

If an uplift assessment with this head is performed, this can be done with a comparison of the pore pressures in the aquifer and the weight of the blanket, according to (TAW, 1999).

$$\delta\phi_{c,u} = d \cdot \frac{\gamma_{sat} - \gamma_w}{\gamma_w} = 2 \cdot \frac{17 - 10}{10} = 1.4 \ m \tag{B.7}$$

$$\delta\phi = \phi_{exit} - h_p = 2.19 - -0.5 = 2.69 \ m \tag{B.8}$$

$$FoS = \frac{\delta\phi_{c,u}}{\delta\phi} = \frac{1.4}{2.69} = 0.52 \tag{B.9}$$

in which:
- $\delta\phi_{c,u}$ = potential of the weight of the blanket layer $[m]$
- $\delta\phi$ = potential of the pore pressure in the aquifer $[m]$
- FoS = outcome of the unity check $[-]$

So uplift of the blanket layer would occur in this situation, which is not surprisingly concerning the relatively low thickness of the blanket layer.

B.3 Lateral shearing

In this appendix basic calculations are performed belonging to the failure mechanism shearing (section 5.1.2 page 59). The calculated properties of the shear capacity of the soil are also used in subsequent calculations.

When the horizontal stability of the presented dike (from figure 5.1) is calculated, first the horizontal force on the dike body has to be determined:

$$\frac{1}{2} \cdot \rho_{wat} \cdot g \cdot h_w^2 = 0.5 \cdot 1000 \cdot 9.81 \cdot 5^2 = 245.25\ kPa \tag{B.10}$$

in which: h_w = outer water level $[m]$
g = gravitational acceleration $[m/s^2]$
ρ_{wat} = density water$[kg/m^3]$

The mobilized drained shear strength along the dike base can be calculated with formula (A.2). This is done by dividing the dike cross section in 23 parts and calculating the shear strength at the bottom of this parts, the total mobilized shear strength is reached by adding all the parts.

$$\tau = \sigma' \cdot \tan(\phi') + c' \tag{B.11}$$

$$\tau_{total} = 1069.56\ kPa \tag{B.12}$$

$$FoS = \frac{1069.56}{245.25} = 4.36 \tag{B.13}$$

The safety against shearing for this calculation approach is, as can be seen,abundantly guaranteed.

See table B.1 on page 161 for the detailed results of the different parts of the dike cross section, also for the undrained calculations that follow below.

In (Verruijt, 2010) an approach for the determination of the undrained shear strength is given when only drained parameters are available. This approach is based on Mohr-Coulomb and given below:

$$\sigma'_0 = \frac{(\sigma' + 2 \cdot \sigma'_{xx})}{3} \tag{B.14}$$

$$\tau_u = c \cdot \frac{\cos\phi}{1 - \frac{1}{3}\cos\phi} + \sigma'_0 \frac{\sin\phi}{1 - \frac{1}{3}\sin\phi} \tag{B.15}$$

in which: σ' = effective stress in vertical direction [kPa]
σ'_{xx} = lateral effective stress [kPa]
σ'_0 = mean effective stress [kPa]
τ_u = undrained shear strength based on drained parameters[kPa]

For the basic calculation this results in the following:

$$\tau_{u,total} = 670.16\ kPa \tag{B.16}$$

$$FoS = \frac{670.16}{245.25} = 2.73 \tag{B.17}$$

For the WTI2017 the determination of undrained shear strength is suggested to be obtained with the SHANSEP[2] method and the following formula: (van Duinen, 2014)

$$S_u = \sigma'_{zz} \cdot S \cdot OCR^m \tag{B.18}$$

in which:
S = normally consolidated undrained shear strength ratio [-]
OCR = over-consolidation ratio [-]
m = power function for strength increase [-]
S_u = undrained shear strength [kPa]

If it is assumed that the dike from figure 5.1 consists of normally consolidated clay (OCR=1) and the S-ratio is 0.24 according to (van Duinen, 2014) this results in the following:

$$S_{u,total} = 389.44\ kPa \tag{B.19}$$

$$FoS = \frac{389.44}{245.25} = 1.59 \tag{B.20}$$

The results of the three different calculation approaches for the shear strength under the dike are given in figure 5.4 on page 60[3] As can be seen the drained or undrained behavior plays an important part in the available shear strength of the soil. Since it is not always entirely clear whether the soil acts drained or undrained an conservative conclusion can be to use the undrained (SHANSEP) shear strength as a lower limit and the drained shear strength as an upper limit.

[2]SHANSEP = Stress History And Normalized Soil Engineering Properties

[3]The differences between the drained results and the SHANSEP method are rather large. This is partly due to the relative high value of the cohesion that is assumed for the clay.

Table B.1: Extended values for calculated shear strength along dike base from section 5.1.2 and figure 5.4 on page 160

x	x [m]	y [m]	σ [kPa]	p [kPa]	σ' [kPa]	$\sigma'_{,0}$ [kPa]	Drained (Mohr-Coulomb) τ [kPa]	Undrained (Mohr-Coulomb) S_u [kPa]	Undrained (SHAN SEP) S_u [kPa]
0-2	1	0.3	52.33	50.00	2.33	0.78	9.94	9.87	0.56
2-4	3	1.0	57.00	50.00	7.00	2.33	11.83	10.53	1.68
4-6	5	1.7	61.67	50.00	11.67	3.89	13.71	11.20	2.80
6-8	7	2.3	66.33	50.00	16.33	5.44	15.60	11.87	3.92
8-10	9	3.0	71.00	50.00	21.00	7.00	17.48	12.53	5.04
10-12	11	3.7	75.67	50.00	25.67	8.56	19.37	13.20	6.16
12-14	13	4.3	80.33	50.00	30.33	10.11	21.26	13.86	7.28
14-16	15	5.0	85.00	50.00	35.00	11.67	23.14	14.53	8.40
16-18	17	5.7	96.33	47.14	49.19	16.40	28.87	16.55	11.81
18-20	19	6.0	102.00	44.29	57.71	19.24	32.32	17.77	13.85
20-22	21	6.0	102.00	41.43	60.57	20.19	33.47	18.18	14.54
22-24	23	6.0	102.00	38.57	63.43	21.14	34.63	18.59	15.22
24-26	25	6.0	102.00	35.71	66.29	22.10	35.78	18.99	15.91
26-28	27	6.0	102.00	32.86	69.14	23.05	36.94	19.40	16.59
28-30	29	5.7	96.33	30.00	66.33	22.11	35.80	19.00	15.92
30-32	31	5.0	85.00	27.14	57.86	19.29	32.38	17.79	13.89
32-34	33	4.3	73.67	24.29	49.38	16.46	28.95	16.58	11.85
34-36	35	3.7	62.33	21.43	40.90	13.63	25.53	15.37	9.82
36-38	37	3.0	51.00	18.57	32.43	10.81	22.10	14.16	7.78
38-40	39	2.3	39.67	15.71	23.95	7.98	18.68	12.95	5.75
40-42	41	1.7	28.33	12.86	15.48	5.16	15.25	11.74	3.71
42-44	43	1.0	17.00	10.00	7.00	2.33	11.83	10.53	1.68
44-46	45	0.3	5.67	3.33	2.33	0.78	9.94	9.87	0.56
					τ_t (over 23 m)		534.80	335.08	194.72
					τ_t **(over 46 m)**		**1069.60**	**670.16**	**389.44**

B.4 Configuration analysis

In this appendix background information and calculations regarding the configuration analysis from section 5.2 on page 63 are collected.

Building

Weight and size will be of a large living house with 3 floors. In case the building is in the dike profile a basement of 2 meters deep will be used. The building is assumed to have a surface of 10 m *by* 10 m. The weight calculation of the house with 3 floors is

based on load characteristics from (Leijendeckers, 2003) and performed below:

$$Walls = 3 \cdot 0.5 = 1.5 \frac{kN}{m^2} \tag{B.21}$$

$$Tiled\ roof = 0.75 \frac{kN}{m^2} \tag{B.22}$$

$$Wooden\ floors = 3 \cdot 0.4 = 1.2 \frac{kN}{m^2} \tag{B.23}$$

$$Foundation\ plate = \frac{0.2 \cdot 2400 \cdot 9.81}{1000} = 4.8 \frac{kN}{m^2} \tag{B.24}$$

$$Variable\ loads = 1.5 \cdot 3 = 4.5 \frac{kN}{m^2} \tag{B.25}$$

$$Total = 12.75 \frac{kN}{m^2} \approx 13 \frac{kN}{m^2} \tag{B.26}$$

When a building consists of 2 levels this calculation becomes:

$$Walls = 2 \cdot 0.5 = 1.0 \frac{kN}{m^2} \tag{B.27}$$

$$Tiled\ roof = 0.75 \frac{kN}{m^2} \tag{B.28}$$

$$Wooden\ floors = 2 \cdot 0.4 = 0.8 \frac{kN}{m^2} \tag{B.29}$$

$$Foundation\ plate = \frac{0.2 \cdot 2400 \cdot 9.81}{1000} = 4.8 \frac{kN}{m^2} \tag{B.30}$$

$$Variable\ loads = 1.5 \cdot 2 = 3.0 \frac{kN}{m^2} \tag{B.31}$$

$$Total = 10.35 \frac{kN}{m^2} \approx 10 \frac{kN}{m^2} \tag{B.32}$$

Pile foundation

In case of pile foundation wooden piles are assumed since these are most common for this kind of buildings. A foundation with a total of 16 circular piles is assumed (4 x 4). The horizontal spacing between the piles that has to be inserted in the software package is 3.33 m. The following properties of the wood are assumed: (de Vries and van de Kuilen, 2010)

$$E_{0,mean} = 10000 \frac{N}{mm^2} \tag{B.33}$$

$$r_{pile} = 100\ mm \tag{B.34}$$

$$f_{m,0,rep} = 30 \frac{N}{mm^2} \tag{B.35}$$

$$f_{t,0,rep} = 18 \frac{N}{mm^2} \tag{B.36}$$

in which:
$E_{0,mean}$ = yield modulus of wood in SLS $[\frac{N}{mm^2}]$
r_{pile} = pile diameter $[mm]$
$f_{m,0,rep}$ = representative bending strength $[\frac{N}{mm^2}]$
$f_{t,0,rep}$ = representative tension strength (parallel)$[\frac{N}{mm^2}]$

The reinforcement option nails in D Geo needs some characteristics of the reinforcement. These are calculated below with the assumed wood properties (de Vries and van de Kuilen, 2010).

$$W = \frac{\pi \cdot 2r^3}{32} = 785000\ mm^3 \tag{B.37}$$

$$M_{pl} = M_{el} = f_{m,0,rep} \cdot W = 23.55\ kNm \tag{B.38}$$

$$I = 0.25 \cdot \pi \cdot r^4 = 78500000\ mm^4 \tag{B.39}$$

$$EI = 785\ kNm^2 \tag{B.40}$$

$$F_y = f_{t,0,rep} \cdot A = 565\ kN \tag{B.41}$$

in which:
W = section modulus $[mm^3]$
M_{pl} = plastic moment capacity $[kNm]$
M_{el} = elastic moment capacity $[kNm]$
I = moment of inertia $[mm^4]$
F_y = tension yield force nail $[kN]$

The nail option in D-Geo is meant for the technique soil nailing, which is a soil reinforcement method. The nails are calculated in D-Geo for four failure mechanisms:

- The exceeding of the maximum shear stress of the nail.
- The exceeding of pull-out capacity of the nail.
- The failure due to soil failure below the nail.
- The failure due to nail breaking because of exceeding plastic moment capacity.

Surcharge after collapse

For buildings that have a shallow foundation, are located on the crest, inner slope or hinterland and collapse, it is assumed that their weight stays in place after collapse. For buildings on the outer slope and foreland it is assumed that half of the weight will 'disappear' due to highwater conditions, since the collapsed building now practically lies in a flowing river.

Buildings on the slope

For buildings that are on the dike profile but are situated on top of the inner or outer slope normally some extra soil outside the profile will be present under the building.

See figures E,F,M & N on page 8. The extra weight of this soil is neglected in these calculations.

B.5 Active ground pressure coefficient

In this appendix the graph from (EC-7, 2012) which is used for the determination of the active ground pressure coefficient, equation (6.28), on page 83 is given below in figure B.2. The masonry wall is assumed to be rough and thus the angle of friction between

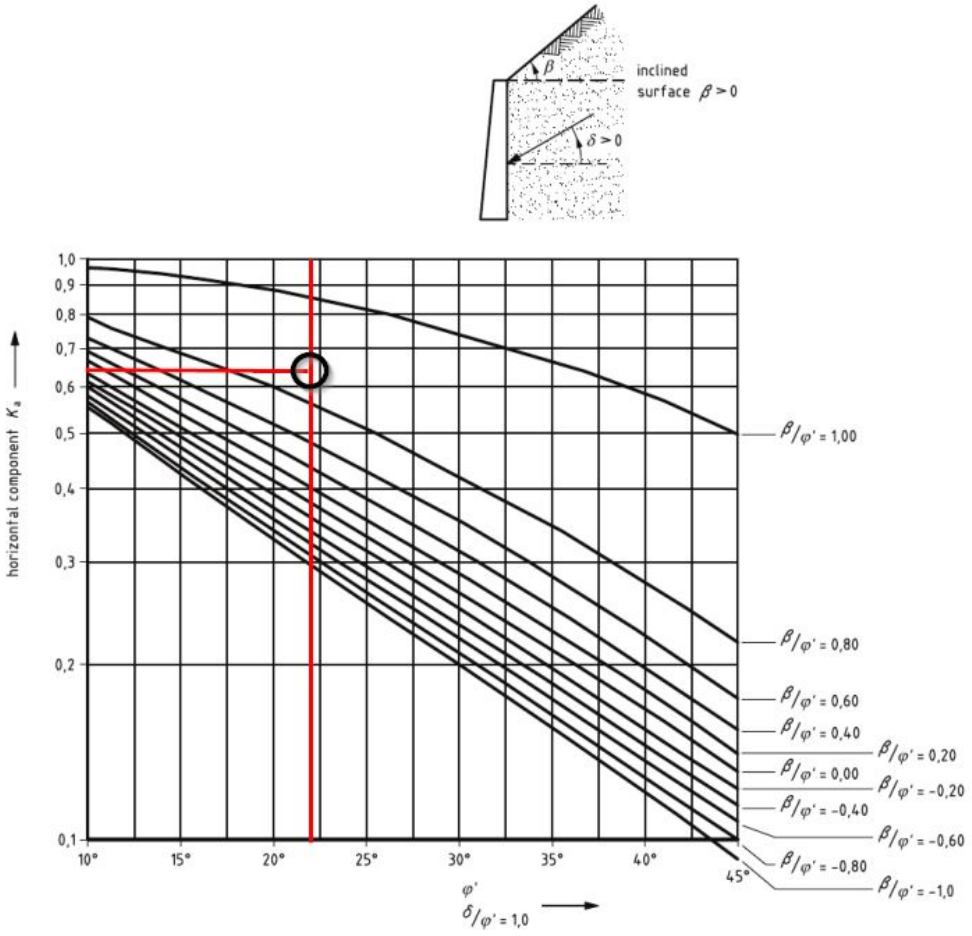

FIGURE B.2: Graph for determination of active ground pressure coefficient from (EC-7, 2012)

wall and soil (δ) is assumed to be as large as ϕ.

$$\frac{\delta}{\phi} = 1.0 \tag{B.42}$$

$$\frac{\beta_{sl}}{\phi} = \frac{18.4^\circ}{22^\circ} = 0.84 \tag{B.43}$$

B.6 Undrained soil pressure

In this appendix a calculation is performed that should illustrate that, undrained soil behavior could lead to higher soil pressures on a building that is located inside the soil profile of a dike.

When a situation as in figure B.3 is considered, the moment equilibrium has to be satisfied and consists of a driving moment generated by the soil and a resisting moment generated by the shear along the sliding plane and a force from the building. By calculating this resisting moment generated by the building, conclusions about the forces on the wall of the building can be drawn.

$$\Sigma_M = 0 \tag{B.44}$$

$$M_{a,\gamma} = M_{p,\tau} + M_{p,building} \tag{B.45}$$

in which: Σ_M = sum of moments $[kNm]$
$M_{p,building}$ = moment generated by pressure of the building $[kNm]$

If the slip plane is now divided into four slices (like in figure B.3), and the slice parameters from table B.2 are used, the active moment generated by the soil becomes:

$$M_{a,\gamma} = b \cdot h_{gem} \cdot \gamma_{sat} \cdot r = 4851 \ kNm \tag{B.46}$$

TABLE B.2: Calculation parameters for four slices of slip plane belonging to figure B.3

Slice :	h_{gem} $[m]$	b $[m]$	r $[m]$	$M_{a,\gamma}$ $[kNm]$
1	2	3.25	11.375	1257
2	4.1	3.25	8.125	1841
3	4.9	3.25	4.875	1320
4	4.6	3.25	1.625	413
Total				4830

The resisting moment generated by the shear will be calculated in two ways, with a lower limit (undrained, SHANSEP) and a upper limit (drained). So first the mean available shear strengths along the slip plane are estimated. This is based on the effective stresses in the slip plane and the corresponding values for shear strength from appendix B.3 table B.1 on page 161 and results in:

$$\tau_{mean,upp} = 25.8 \ kN/m^2 \tag{B.47}$$

$$S_{u,mean,low} = 10.1 \ kN/m^2 \tag{B.48}$$

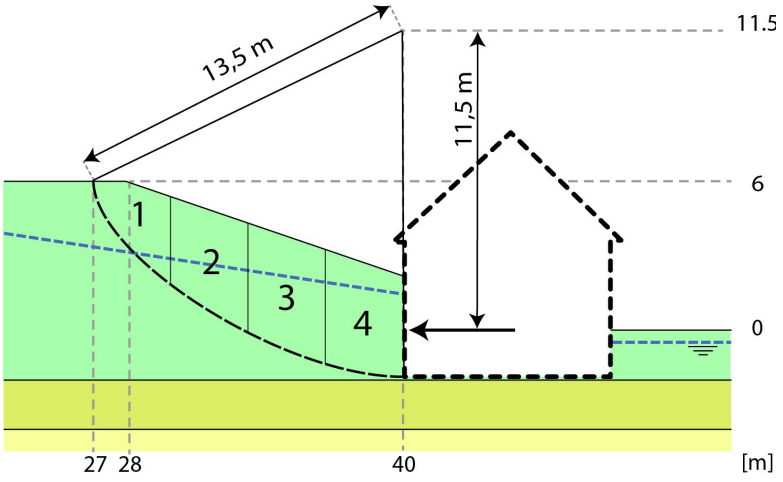

FIGURE B.3: Slip plane with building on the passive side

in which: τ_{mean} = mean drained shear strength, upper limit $[kPa]$
$S_{u,mean}$ = mean undrained shear strength, lower limit $[kPa]$

The slip plane that is drawn in figure B.3 is $\frac{1}{6}$ of a circle with a radius of 13.5 m. This results in the following maximum passive moments generated by shear along the slip plane, calculated with the drained and undrained shear values from equation (B.48). [4]

$$l_{slip} = \frac{2 \cdot \pi \cdot r}{6} = 14.13 \ m \tag{B.49}$$

$$M_{p,\tau} = \tau_{mean,upp} \cdot l_{slip} \cdot r = 25.8 \cdot 14.13 \cdot 13.5 = 4926 \ kNm \tag{B.50}$$

$$M_{p,Su} = S_{u,mean,low} \cdot l_{slip} \cdot r = 10.1 \cdot 14.13 \cdot 13.5 = 1930 \ kNm \tag{B.51}$$

Because $M_{p,\tau,upp} > M_{a,\gamma}$, this means that no force of the building is required to guarantee moment equilibrium, when the soil acts drained. This does not mean that no force is present because the shear along the slip plane does not necessarily adopt this maximum value. But when the soil acts undrained a force from the building has to guarantee moment equilibrium, because $M_{p,Su,low} < M_{a,\gamma}$. This force has to be equal to the pressure of the soil against the wall. Since the moment arm of the force of the building can be calculated the force that is needed for moment equilibrium can also be calculated:

$$r_{build} = 13.5 - 2 = 11.5 \ m \tag{B.52}$$

$$F_{build,Su} = \frac{M_{p,Su,low} - M_{a,\gamma}}{r_{build}} = \frac{4830 - 1930}{11.5} = 252 \ kN/m \ width \tag{B.53}$$

in which: r_{build} = moment arm of force supplied by building $[m]$
$F_{build,Su}$ = force supplied by building when soil acts undrained $[kN]$

[4] These moments are *not* bending moments occurring in the masonry wall but moments relative to an arbitrary chosen middle point of a sliding circle.

When the resulting vertical force on the wall was calculated with the soil pressures from 6.6 for a soil retaining wall of 4 meters, this would result into:

$$\sigma_h = 61.2kPa \tag{B.54}$$

$$F_{build} = 61.2 \cdot 4 \cdot 0.5 = 122.4kN/m\ width \tag{B.55}$$

So besides that arching and displacements of the soil body can result in different soil pressures than would be expected at first, also undrained behavior might have a significant role in the loading of the soil retaining wall.

B.7 Deterministic calculations of soil retaining wall

To become familiar with the needed dimensions of a masonry wall under certain loads, deterministic calculations will be made for the the soil retaining wall for bending in this appendix.

When the most likely to occur bending moment is used for the calculation of the thickness of the masonry wall when it is dimensioned on bending failure, the following applied bending moment is used: (belonging to high water conditions active soil pressure and a simply supported beam, see table 6.2 on page 91)

$$M_{Ed} = 13.87\ kNm \tag{B.56}$$

When the normal force in the masonry wall is taken to be 19 kN, as is done in (Hageman, 2013) for a building with a similar height the moment capacity becomes:

$$M_{Rd} = f_{x,d1,app} \cdot Z = 0.1 \cdot \frac{1}{6} \cdot 1000 \cdot t^2 \tag{B.57}$$

$$f_{xd,1,app} = f_{x,1} + \sigma_d = 0.1 + \sigma_d \tag{B.58}$$

$$\sigma_d = \frac{N_{ed}}{b \cdot t} = \frac{19000}{1000 \cdot t} \tag{B.59}$$

The smallest value of the thickness, t, that results in a larger bending moment capacity than the assumed occurring moment is:

$$t \geq 825\ mm \tag{B.60}$$

When the same schematisation is applied for retaining walls with a different height this results in different moments in the wall. These minimal thicknesses for different heights are shown in table B.3

TABLE B.3: Resulting minimal wall thicknesses for different heights of the wall concerning bending failure

l $[m]$	1	1.5	2	2.5	3
t $[mm]$	160	345	575	825	1125

When soil retaining walls have to satisfy (EC-6.1, 2013) the needed thickness seems very large. Therefore a real situation is checked, of which it is known that the wall has never collapsed

In (Schipper, 2004) some buildings that are located in the outer slope of the dike are checked. So the specifications of one of these buildings is borrowed and used to check the calculations performed in this thesis. The specifications of this building are:

- Soil retaining wall of masonry.
- Thickness is 440 mm.
- Height of the soil retaining wall is 2.20 m.

From figure 6.6 the triangular horizontal load on the wall is picked. This is now done for a low freatic level in the soil and still the active soil coefficient is used (figure 6.6 E on page 84).

$$q = 24.3\ kPa \tag{B.61}$$

When this load is inserted in equation (6.32) the occurring moment, for a simply supported beam, becomes:

$$M_{Ed} = \frac{24.3 \cdot 2.2^2}{9 \cdot \sqrt{3}} = 7.54\ kNm \tag{B.62}$$

Since a realistic situation is checked, from which it is known that the wall has not collapsed, for the flexural tensile strength not the characteristic value is used but the mean value. This mean value was determined in equation (6.48) to be $f_{x,1} = 0.37\ \frac{N}{mm^2}$. Furthermore the same normal force assumptions are made for this wall as was done in equation (B.59) the moment capacity becomes:

$$\sigma_d = \frac{19000}{1000 \cdot 440} = 0.04\ \frac{N}{mm^2} \tag{B.63}$$

$$f_{xd,1,app} = 0.37 + 0.04 = 0.41\ \frac{N}{mm^2} \tag{B.64}$$

$$M_{Rd} = 0.41 \cdot \frac{1}{6} \cdot 1000 \cdot 440^2 = 13.23\ kNm \tag{B.65}$$

The unity check now becomes:

$$UC = \frac{M_{Rd}}{M_{Ed}} = \frac{13.23}{7.54} = 1.75 \tag{B.66}$$

So when this calculation method and mean values are used, it can be seen why these buildings are still standing unless that they might not satisfy the current guidelines.

B.8 Normal force in the probabilistic soil retaining wall calculation

In this appendix a calculation example is presented to clarify the strategy that is used to determine the normal force in the probabilistic calculation in section 7.3.

For the case study the compression stress, caused by a normal force in the masonry, is determined by the following formula: (see section 7.3 for explanation of the symbols)

$$\sigma_d = \frac{\overbrace{N}^{loading\ from\ upper\ floors}}{l_{wall} \cdot t} + \overbrace{\rho_{mas} \cdot g \cdot \Delta_{M_{max}} \cdot h_{base}}^{self\ weight\ masonry} \tag{B.67}$$

The loading from the upper floors is smeared out over the first floor and then divided by all outer walls that that equally transfer the load to the ground surface. This smeared out load is based on values from (Leijendeckers, 2003) and presented below:

$$Walls = 2 \cdot 0.5 = 1.0 \ \frac{kN}{m^2} \tag{B.68}$$

$$Roof\ and\ girders = 1.0 \ \frac{kN}{m^2} \tag{B.69}$$

$$Floors\ and\ girders = 2 \cdot 1.0 = 2.0 \ \frac{kN}{m^2} \tag{B.70}$$

$$Live\ loads = 0.75 \cdot 2 = 1.5 \ \frac{kN}{m^2} \tag{B.71}$$

$$Total = 5.5 \ \frac{kN}{m^2} \tag{B.72}$$

When these values are inserted, the normal force at the top of the soil retaining can be calculated:

$$N = A \cdot (\overbrace{N_{ow}}^{self\ weight} + \overbrace{N_{vl}}^{variable\ loading}) \tag{B.73}$$

$$N = A \cdot (N_{ow} + N_{vl}) = 80 \cdot (4 + 1.5) = 440 \ kN \tag{B.74}$$

$$N_{vert} = \frac{N}{l_{wall}} = \frac{440}{36} = 12.22 \ \frac{kN}{m} \tag{B.75}$$

in which: N_{vert} = normal force at the top of the soil retaining wall per running meter $[\frac{kN}{m}]$

The assumption that this load can be smeared out is a very rough one. When performing a more detailed calculation the normal force has to be determined on specific building properties like the transfer directions of the floor and roof. Besides walls transfer their loads vertically down to other walls. But since these building properties are unknown for this case this very rough assumption is made.

This page intentionally left blank.

Appendix C

Background on case-study

In this appendix background calculations and assumptions regarding the case-study are presented which are not presented in detail in the main report. The contents of this appendix are depicted below:

Contents

C.1 Derivation of stochastic geotechnical parameters

In this appendix a calculation example is presented how to transform the given geotechnical calculation values from the case-study to the stochastic parameters presented in tables 7.2 & 7.3 on page 107. This is done for layer three (clay covering layer) for the cohesion (c) and for the angle of internal friction (ϕ).

The calculation value of the cohesion, $c_c = 4.0\ kPa$, of soil layer 3 is given together with the material factor (γ_m=1.25). With both, the corresponding characteristic value can be derived.

$$c_c = \gamma_m \cdot c_d = 4.0 \cdot 1.25 = 5.0\ kPa \tag{C.1}$$

The corresponding mean value and standard deviation now is determined with a iterative procedure. The mean value is assumed, from which follows a standard deviation and subsequently the cumulative probability of the characteristic value is compared with the 5 % demand.

$$CoV = 0.1 \tag{C.2}$$

$$\sigma_c = CoV \cdot c_\mu = 0.1 \cdot 6.0 = 0.6\ kPa \tag{C.3}$$

$$F_C(c) = P(c \leq 5.0) = 0.05 \tag{C.4}$$

When the requirement of equation (C.4) is met, the assumed parameters of the stochastic parameter are chosen correctly.

For the angle of internal friction values of the soil, the same procedure is followed. But because the CoV is only given for $\tan(\phi)$ the transformation is more laborious:

$$\phi_c = \gamma_{m,\tan(\phi)} \cdot \phi_d \tag{C.5}$$

$$\phi_c = \arctan(\tan(14.7) \cdot 1.2) = 17.5^\circ \tag{C.6}$$

To retrieve the stochastic parameters from the characteristic value:

$$CoV_{\tan(\phi)} = 0.1 \tag{C.7}$$

$$\sigma_{\tan(\phi)} = 0.1 \cdot \tan(\mu_\phi) = 0.1 \cdot \tan(19.3) = 2^\circ \tag{C.8}$$

$$\sigma_\phi = \arctan(\sigma_{\tan(\phi)}) = \arctan(2^\circ) = 1.1^\circ \tag{C.9}$$

$$F_\Phi(\phi) = P(\phi \leq 17.5) = 0.05 \tag{C.10}$$

$$CoV_\phi = \frac{\sigma_\phi}{\mu_\phi} = \frac{1.1}{19.3} = 0.056 \tag{C.11}$$

The derivation of the stochastic parameters of the other soil layers has been performed in the same way.

C.2 PDF plots of geotechnical parameters

In this appendix the Pdf plots of the geotechnical stochastic parameters from the case-study that are presented in tables 7.2 & 7.3 on page 107 are collected.

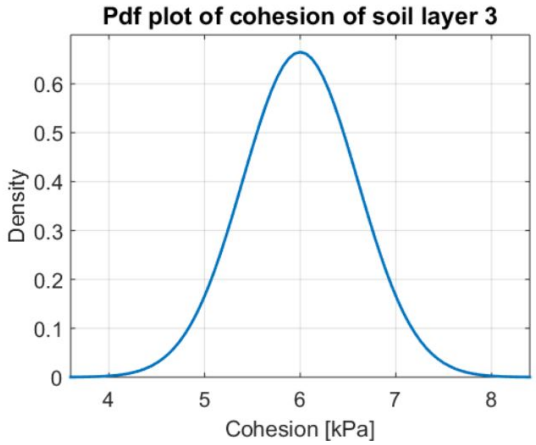

FIGURE C.1: Pdf plot of c of layer 3

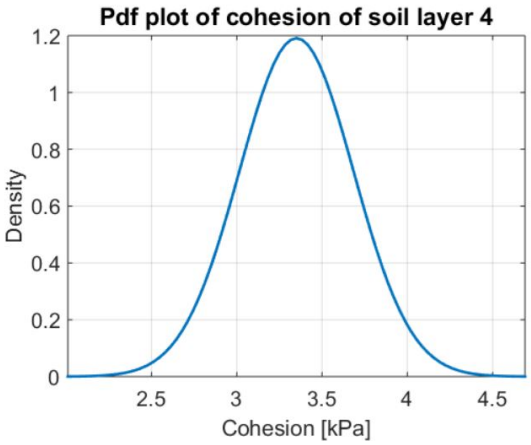

FIGURE C.2: Pdf plot of c of layer 4

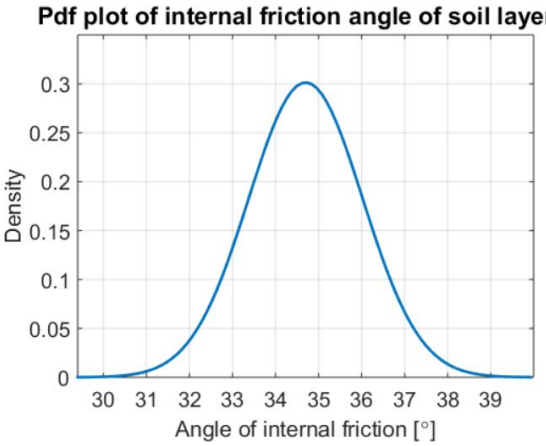

FIGURE C.3: Pdf plot of ϕ of layer 1

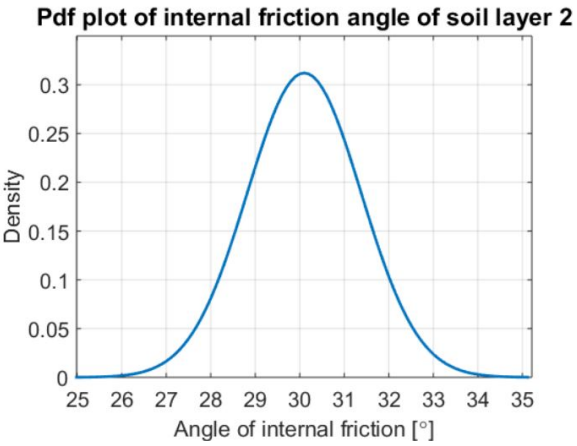

FIGURE C.4: Pdf plot of ϕ of layer 2

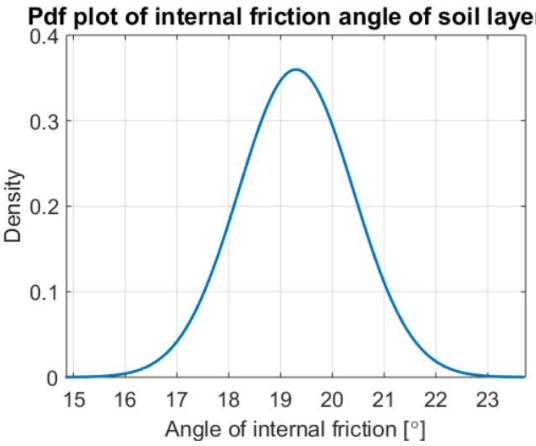

FIGURE C.5: Pdf plot of ϕ of layer 3

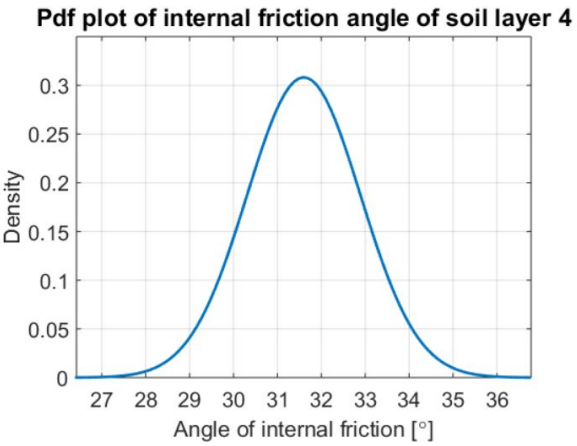

FIGURE C.6: Pdf plot of ϕ of layer 4

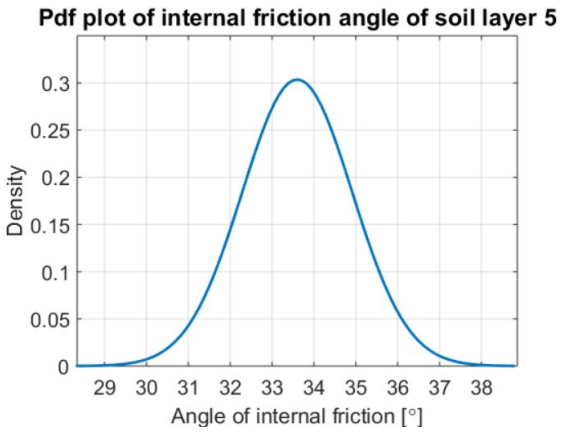

FIGURE C.7: Pdf plot of ϕ of layer 5

C.3 Determination residual profile

In this appendix the residual profile that arises after building collapse for the soil profile of the case location is distracted. This is based on theory of subsection on page

When the soil retaining wall collapses it is assumed that the clay in-between: the wall, the former soil profile and the assumed slope of the residual profile of clay ($H : V$ - $2 : 1$) (Zwanenburg et al., 2013) slides towards the bottom floor. This area is hatched in the top figure of C.8. The residual profile is depicted in the bottom figure of C.8 and is based on a equal area of sliding soil before and after collapse. This also means that there is assumed that the soil after sliding preserves the same volume and volumetric weight. Since soil is a granular material it could be possible that soil after sliding has a different volume due to a change of packing.

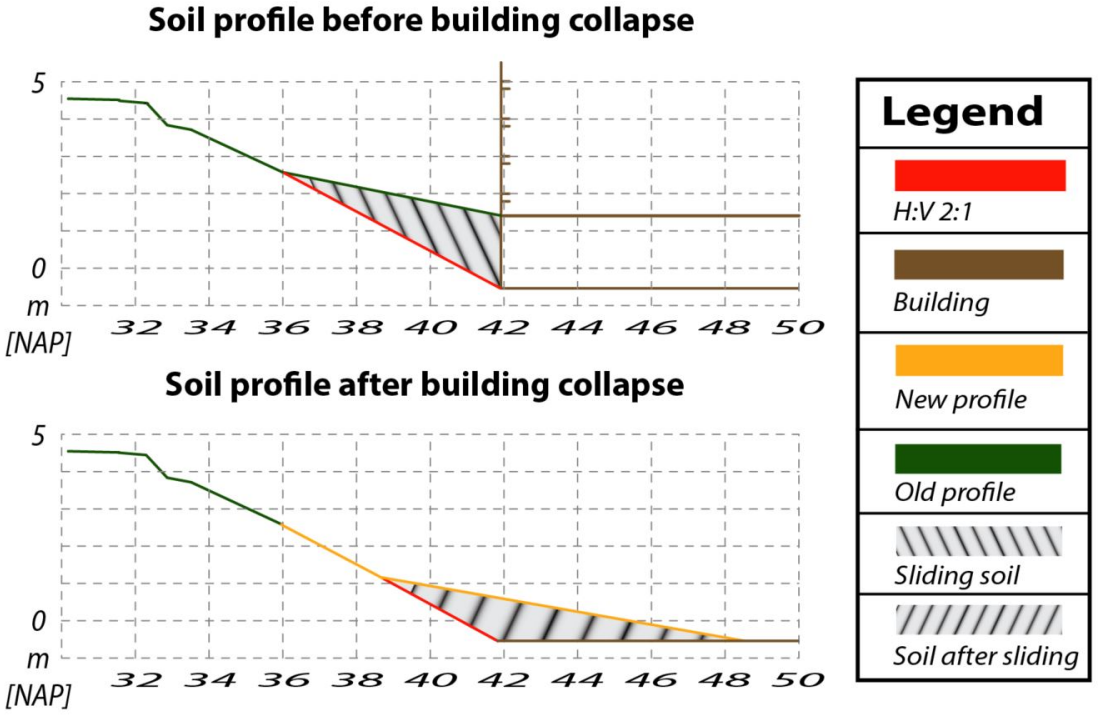

FIGURE C.8: Derivation residual profile

C.4 Distribution of water level

In this appendix background information is given for the derivation of the probability distribution of the outer water level for the case study. In the main report this is discussed in subsection 7.1.5 on page 108.

The yearly maximum water levels are shown in table C.1. The parameters of the distributions that are fitted to the data is shown in table C.2. In figures C.9 & C.10 the data and the fits are depicted in pdf and cdf format. Chosen is for a normal, lognormal and GEV(Generalized Extreme Value) fit.

Table C.1: Yearly maximum waterlevels at measuring station near case location (Rijkswaterstaat, 2016)

Year	**Level [cm]**	**Year**	**Level [cm]**	**Year**	**Level [cm]**
1971	211	1986	231	2001	191
1972	211	1987	207	2002	224
1973	251	1988	219	2003	223
1974	240	1989	211	2004	236
1975	198	1990	251	2005	213
1976	257	1991	213	2006	211
1977	244	1992	204	2007	209
1978	208	1993	239	2008	235
1979	241	1994	271	2009	179
1980	218	1995	249	2010	196
1981	226	1996	208	2011	207
1982	219	1997	182	2012	242
1983	252	1998	228	2013	260
1984	229	1999	224	2014	238
1985	203	2000	206	2015	218

Table C.2: Fitted distributions to yearly maximum waterlevels

	μ	σ	k
GEV	215.4	20.15	0.25
Lognormal	5.40	0.094	-
Normal	223.0	20.95	-

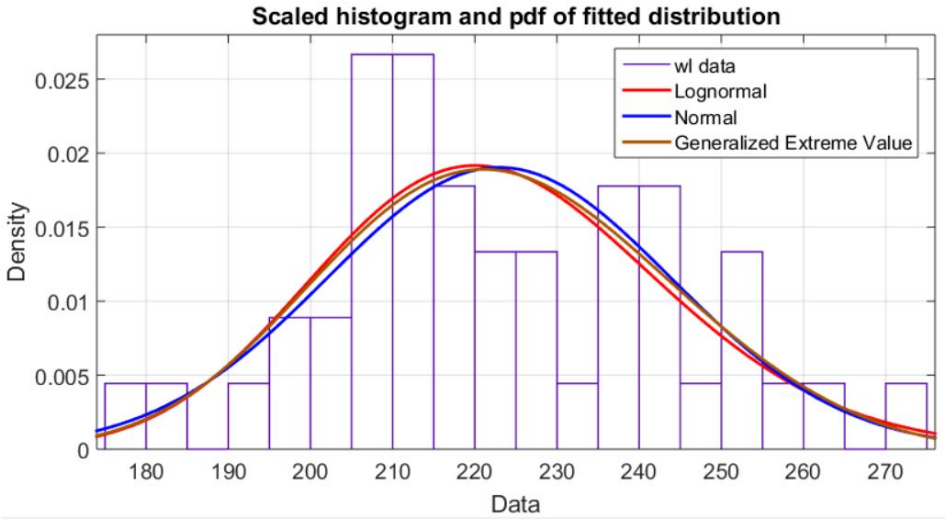

FIGURE C.9: Pdf of data and the three distribution fits

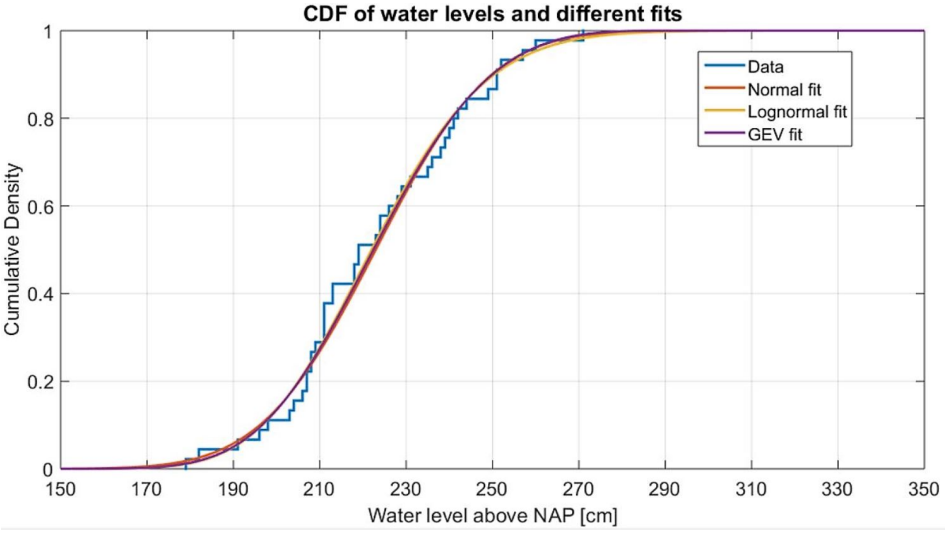

FIGURE C.10: Cdf of data and the three distribution fits

C.5 Freatic line in dike body

In this appendix the assumed freatic lines for different water levels are clarified of the case-study. This is done according to a schematisation proposed by (TAW, 2004). In the main report the results of this appendix are shown in subsection 7.1.6 on page 109.

The dike consists of a base of clay with a sand part on top of it. For a highwater level (NAP +3.05 m) with a return period of $\frac{1}{2000}$ $[yr^{-1}]$ (see figure 7.6 on page 109) the freatic line is schematized according to figure C.11, which is suitable for dikes with a sand core on a compressible subsoil. Thereafter the other freatic lines are made with help of some assumptions. Three of the five freatic lines are based on water levels close

to the sand/clay transition. This is done because these freatic lines are very sensitive. The background of the different lines is listed below.

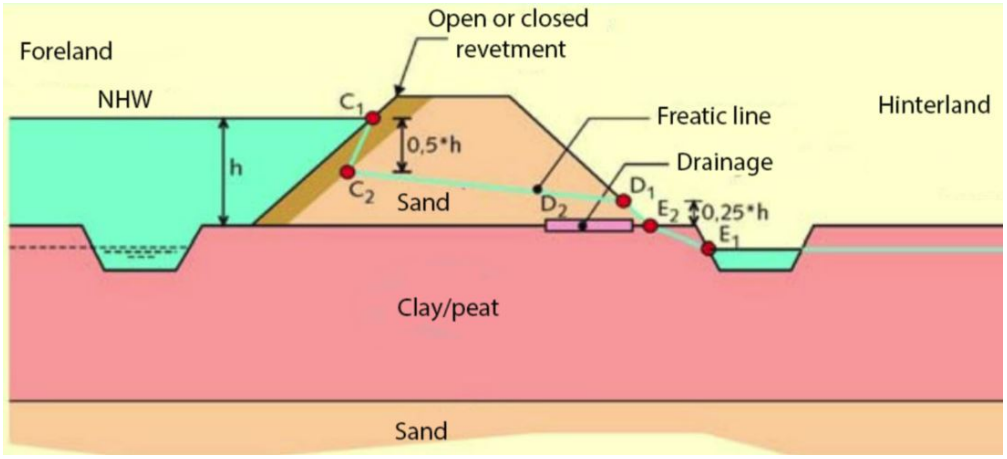

FIGURE C.11: Schematisation used to determine freatic lines

- **NAP + 3.05**
  The top of the sand layer is assumed to have some kind revetment that lowers the freatic line. So according to C.11 this is the first part of the freatic line. So in the revetment the height above the clay layer is halved, from there it further decrease to $\frac{1}{4}$ at the inner slope, from where it goes to toe of the sand part of the dike. From there it is assumed that the freatic line is linearly decreasing to a fixed point at the toe of the dike at [X-Y] = [49-−1]
- **NAP + 2.75**
  This freatic line is schematized on the same principles as the line of NAP +3.05 m. But since this water level is lower it is assumed that the freatic line does not fully develop till the outer slope of the sand part of the dike.
- **NAP + 2.65**
  This freatic line is schematized on the same principles as the line of NAP +3.05 m. But since this water level is lower it is assumed that the freatic line does not fully develop till the outer slope of the sand part of the dike.
- **NAP + 2.50**
  This water level does not intersect with the sand part of the dike. Where the water level intersects the clay outer slope of the dike it is assumed that the freatic line linearly decreases to the fixed point.
- **NAP + 1.75**
  This is the lowest water level for which a freatic line is made. Where the water level intersects the clay outer slope of the dike it is assumed that the freatic line linearly decreases to the fixed point.

The result of the used schematisation and assumptions is shown in figure 7.8.

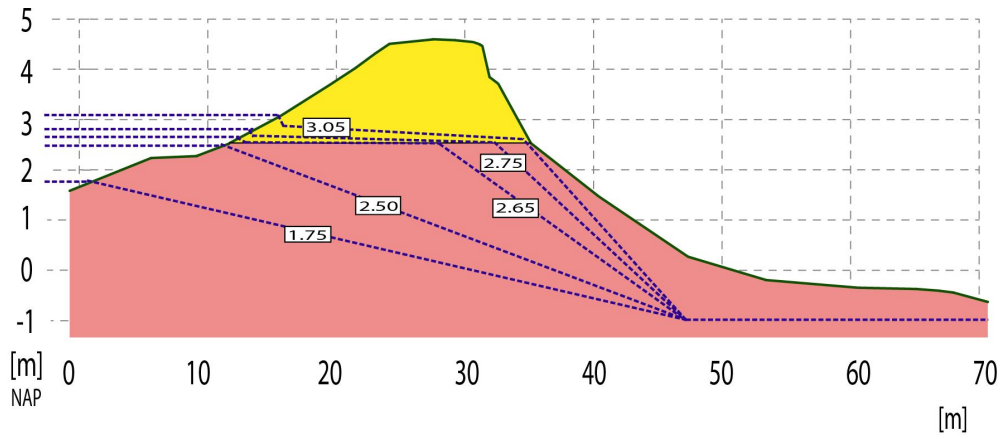

FIGURE C.12: Assumed freatic lines for diffeent outer water levels

C.6 Relation outer water level and freatic level at wall

In this appendix an empirical relation between the outer water level and the freatic level at the soil retaining wall is determined for the case-study.

In the probabilistic calculation of the soil retaining wall the outer water level is an input parameter. But this is not equal to the height of the hydrostatic water pressure against the soil retaining wall, this namely depends on the height of the freatic line at the front of the building.

From the assumed freatic lines for different water levels the corresponding freatic levels at the building can be determined (see figure C.13). These data points are collected in table C.3. When this data is supplemented with inter- and extra-polation data points and the negative values of h_{frea} are replaced by zeros. This is done because when the freatic level is lower than the bottom of the wall no hydrostatic pressure on the wall is present and therefore this value has to be zero. These modified data points are collected in table C.4.

TABLE C.3: Data points of outer water level and locally freatic line at the soil retaining wall

h_w [m]	1.75	2.50	2.65	2.75	3.05
h_{frea} [m]	-0.1	0.14	0.74	1.15	1.46

When an equation fitting tool, for a double Gaussian equation (see formula (C.12)), is applied to these data points the formula of (C.13) is retrieved.

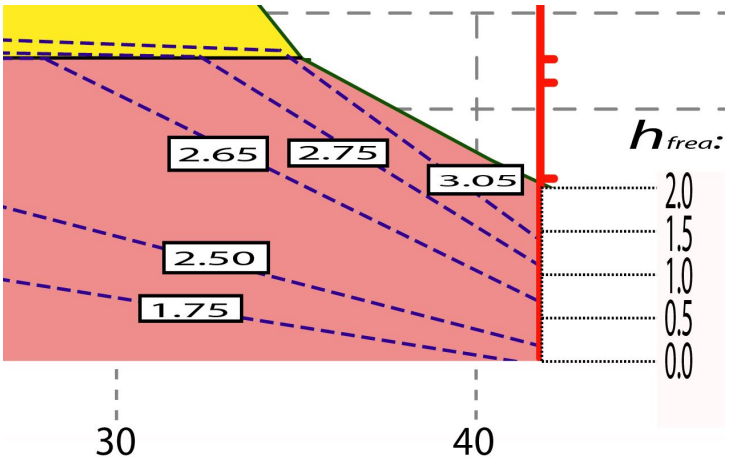

FIGURE C.13: Intersection of freatic lines and soil retaining wall

TABLE C.4: Data points of outer water level and locally freatic line at the soil retaining wall (including inter/extra-polation)

h_w [m]	h_{frea} [m]	h_w [m]	h_{frea} [m]	h_w [m]	h_{frea} [m]
1.00	0.00	2.60	0.54	3.25	1.59
1.25	0.00	2.65	0.74	3.35	1.65
1.50	0.00	2.70	0.94	3.45	1.70
1.75	0.00	2.75	1.15	3.55	1.73
2.00	0.00	2.85	1.26	3.65	1.75
2.25	0.06	2.95	1.36	3.75	1.77
2.50	0.14	3.05	1.46	3.85	1.78
2.55	0.34	3.15	1.54	3.95	1.79

The double Gaussian equation with emirical fitting constants is shown below:

$$\begin{aligned} h_{frea} = \quad & a1 \cdot \exp(-((h_w - a2)/a3)^2) \\ + \quad & a4 \cdot \exp(-((h_w - a5)/a6)^2) \end{aligned} \tag{C.12}$$

The results of the best fit to the data points results in the following values for the empirical constants:

$$\begin{aligned} a1 &= 1830\ [mm] \\ a2 &= 3738\ [mm] \\ a3 &= 777.5\ [mm] \\ a4 &= 808.3\ [mm] \\ a5 &= 2913\ [mm] \\ a6 &= 337.8\ [mm] \end{aligned}$$

When this is inserted in formula (C.12), this results in:

$$\begin{aligned} h_{frea} = & 1830 \cdot \exp(-((h_w - 3738)/777.5)^2) \\ & + 808.3 \cdot \exp(-((h_w - 2913)/337.8)^2) \end{aligned} \tag{C.13}$$

In figure C.14 the data points and the fitted equation are depicted. For the domain of $0 > h_w < 4.0$ the fit is a good representation of the data points. An even better fit could be made with a combination of different equations, but for this *if* statements would be needed, to tell the program which equation is valid for which water level. Unfortunately these statements are not available in the software package Prob2B therefore there is chosen for this empirical formula. When values of $h_w > 4.0$ are present this could lead to a significant error for this specific value. This has to be kept in mind.

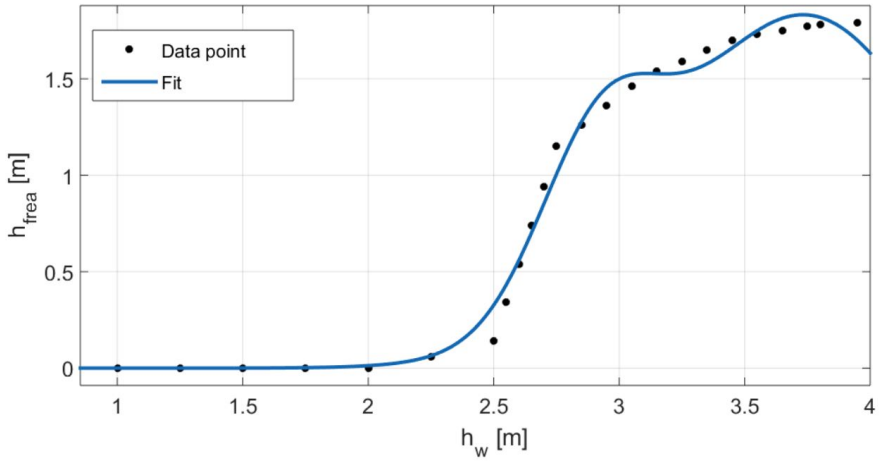

FIGURE C.14: Formula fit relation h_w and h_{frea}

C.7 PDF plots of stochastic parameters

In the following appendix the pdf plots of the stochastic parameters from the case-study that have been used for the probabilistic calculation of the soil retaining wall in section 7.3 on page 111 are collected.

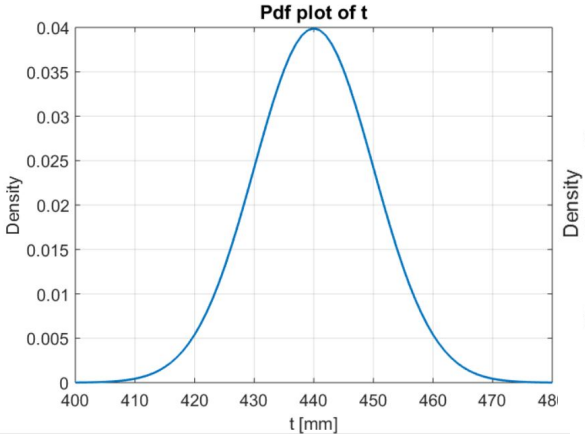

FIGURE C.15: Pdf plot of stochastic variable: t

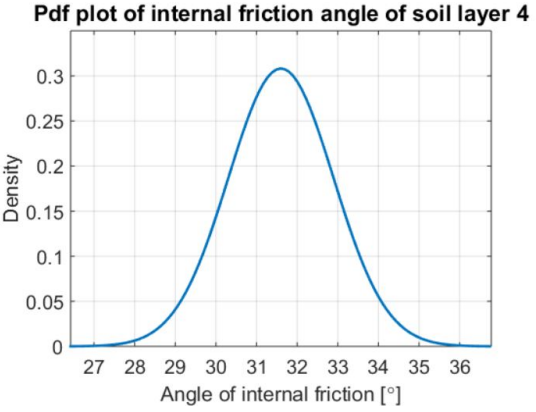

FIGURE C.16: Pdf plot of stochastic variable: ϕ

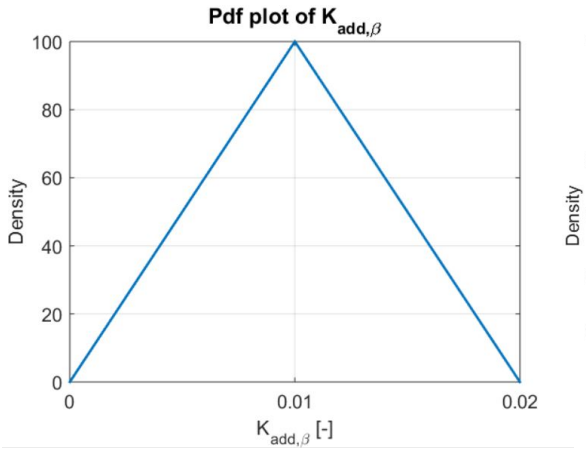

FIGURE C.17: Pdf plot of stochastic variable: $K_{add,\beta}$

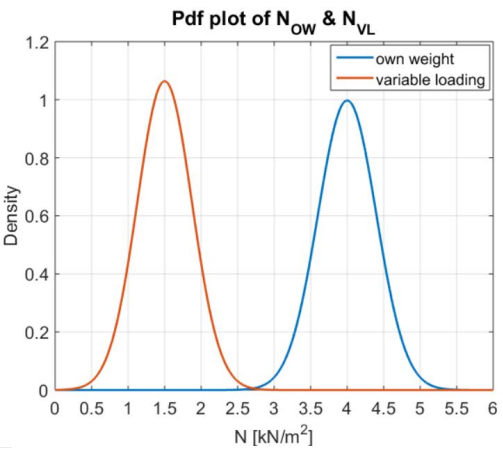

FIGURE C.18: Pdf plot of stochastic variable: N_{ow} & N_{vl}

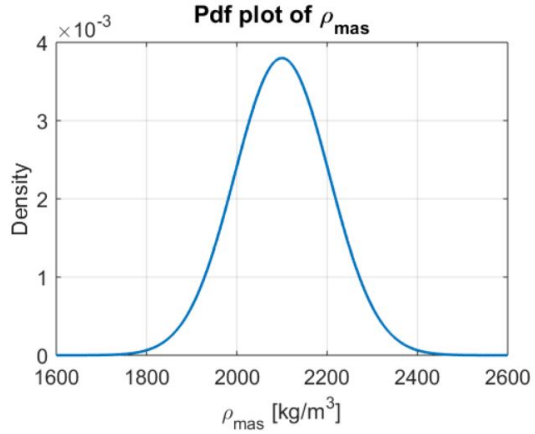

FIGURE C.19: Pdf plot of stochastic variable: ρ_{mas}

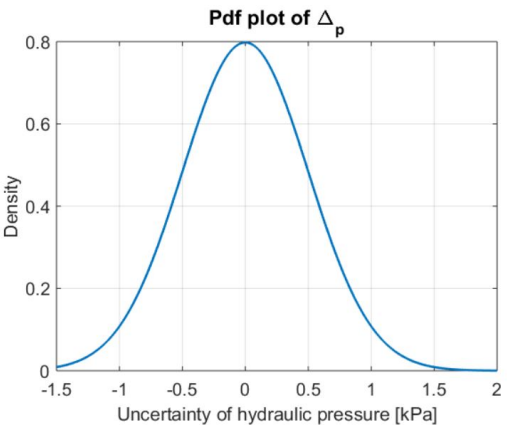

FIGURE C.20: Pdf plot of stochastic variable: Δ_p

The pdf plot of the bending tensile strength of masonry is given in figure 6.19 on page 96. The pdf plot of the distribution of the maximum occurring water level is given in figure 7.7 on page 109.

C.8 Extended results of probabilistic soil stability calculations

In this appendix extended calculation results of subsection 7.4 of page 121 are presented. This is done respectively for the soil profiles wtihout a building, with an intact building and finally with a collapsed building. In detail the conditional failure probabilities for the different water levels are presented, which are input for the calculated integrated failure probability of subsection 7.4. Besides their normative slip planes are also presented.

TABLE C.5: Calculation results for different water levels for profile without building

h_w	FoS	β	$P_{f\|h_w}$
3.05	2.13	13.67	$8.04 \cdot 10^{-43}$
2.75	2.16	13.90	$3.08 \cdot 10^{-44}$
2.65	2.28	15.93	$1.87 \cdot 10^{-57}$
2.50	2.40	16.20	$2.37 \cdot 10^{-59}$

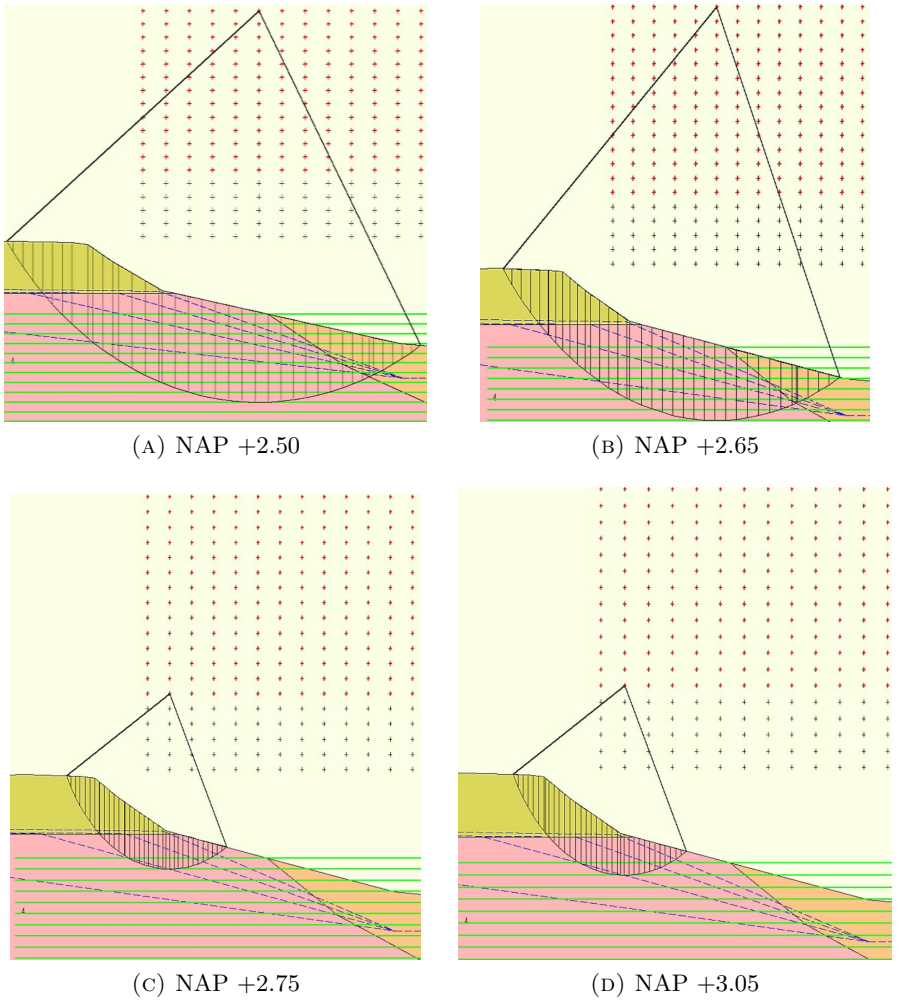

(A) NAP +2.50 (B) NAP +2.65

(C) NAP +2.75 (D) NAP +3.05

FIGURE C.21: Normative slip planes for the profile without building

TABLE C.6: Calculation results for different water levels for profile with building

h_w	FoS	β	$P_{(f\|h_w)}$
3.05	2.14	13.88	$4.11 \cdot 10^{-44}$
2.75	2.17	14.10	$1.86 \cdot 10^{-45}$
2.65	2.31	14.64	$7.88 \cdot 10^{-49}$
2.50	2.62	17.53	$4.17 \cdot 10^{-69}$

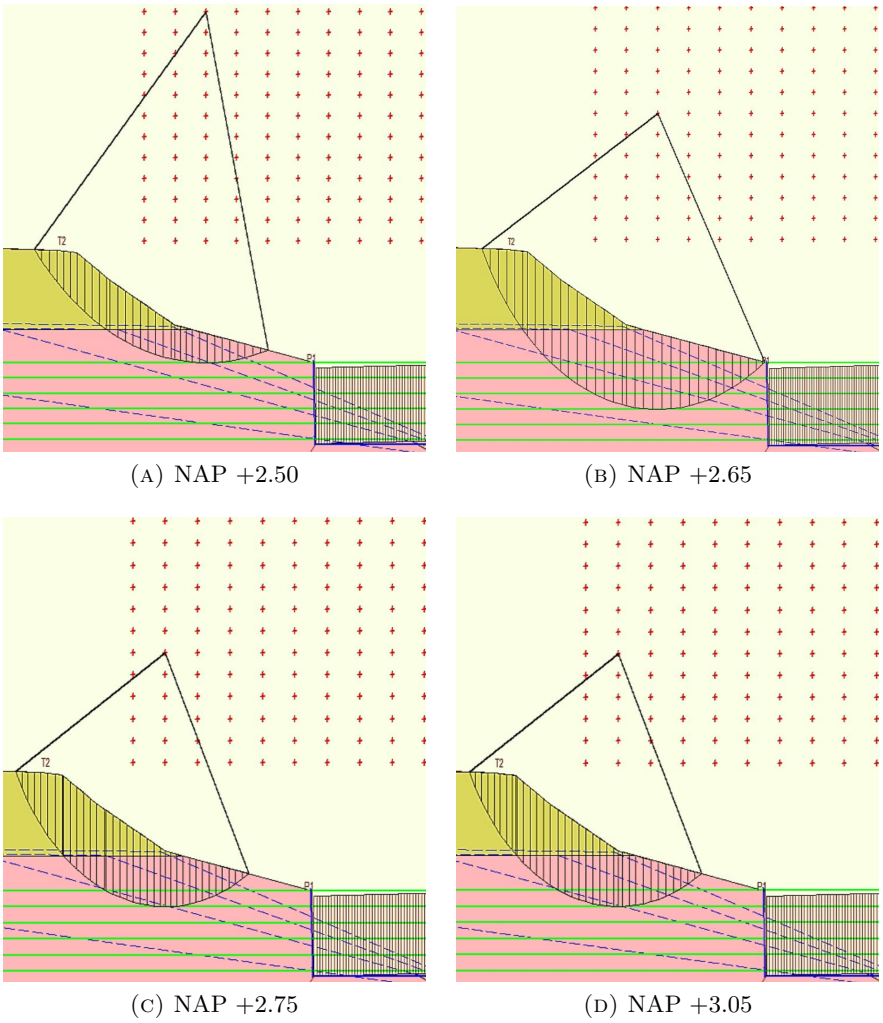

(A) NAP +2.50 (B) NAP +2.65

(C) NAP +2.75 (D) NAP +3.05

FIGURE C.22: Normative slip planes for the profile with building

TABLE C.7: Calculation results for different water levels for profile with collapsed building

h_w	FoS	β	$P_{(f\|h_w)}$
3.05	1.38	5.51	$1.84 \cdot 10^{-8}$
2.65	1.47	7.24	$2.13 \cdot 10^{-13}$
2.50	1.82	1.82	$1.09 \cdot 10^{-28}$
2.35	1.94	1.94	$3.33 \cdot 10^{-32}$

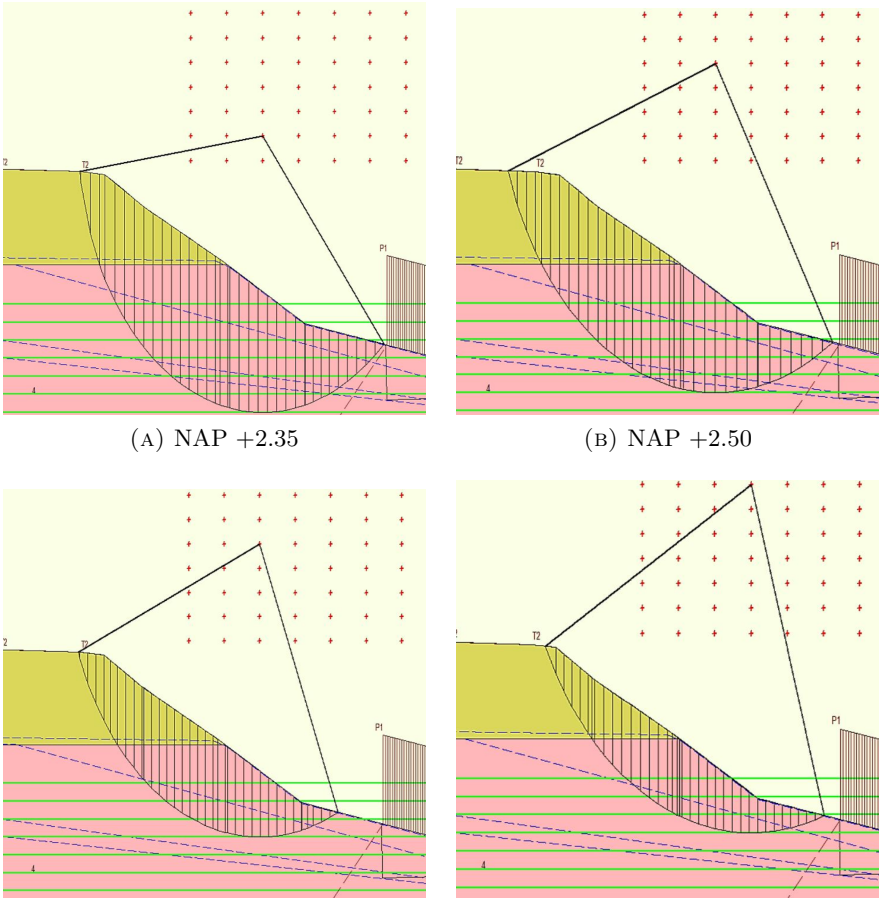

(A) NAP +2.35 (B) NAP +2.50

(C) NAP +2.65 (D) NAP +3.05

FIGURE C.23: Normative slip planes for the profile after building collapse

This page intentionally left blank.

Appendix D

List of interviews

To get to know how the assessment of NWO's is performed in practice some interviews have been taken with professionals from the field. Among them colleagues from Royal Haskoning DHV and professionals from water boards and knowledge centers.

Steven Sjenitzer	Royal Haskoning DHV	08-07-2015
Jaap van Koppen & Bas Molenkamp	Waternet	03-08-2015
Harry Schelfhout	Deltares	04-08-2015
Monique Sanders	Royal Haskoning DHV	04-08-2015
Peter van der Scheer	Royal Haskoning DHV	13-08-2015
Leo van Nieuwenhuijzen	Royal Haskoning DHV	20-08-2015
Etienne Faassen	Hoogheemraadschap Rijnland	27-08-2015
Sander Kapinga	Waterschap Rivierenland	28-08-2015
Dirk-Jan van Dijk	Royal Haskoning DHV	30-08-2015
Pim Schipper	Ingenieursbureau Concretio	20-11-2015

This page intentionally left blank.

Bibliography

J Baker and E.O.F Calle. JCSS probabilistic model code, section 3.7: Soil properties. Technical report, JCSS, 2006.

J.A. Beijersbergen and G.R. Spaargaren. Vuistregels, voor het beheerdersoordeel bij de toetsing van niet-waterkerende objecten. Technical report, Provincie Zuid Holland, 2009.

M. Boers and H. Steetzel. Voorverkenning nwo's in duinen. Technical report, Arcadis and Deltares, 2012.

CIRIA C731. *International Levee HandBook*. CIRIA, 2013. ISBN 978-0-86017-734-0.

W.M.G. Courage and H.M.G.M. Steenbergen. Prob2b: variables, expressions and excel, installation and getting started. Technical report, TNO, 2007. 2007-D-R0887/A.

CUR 166. *CUR-publicatie 166 (vijfde druk) 'Damwandconstructies'*. Stichting CUR-NET, Gouda, november, 2008.

CUR 219. *INSIDE Innovatieve dijkversterking*. Stichting CURNET, Gouda, november, 2007.

2e Deltacommissie. Samen werken met water. Technical report, Ministerie van Verkeer en Waterstaat, 2008a.

2e Deltacommissie. Een veilige toekomst voor de nederlandse delta, 2008b. URL `http://www.deltacommissie.com/index`.

Deltares. *D-Geo Stability, Slope stability software for soft soil engineering, User Manual*, 14.1.00 edition, 2014.

T.A. van Duinen. Handreiking voor het bepalen van schuifsterkte parameters, wti2017 toetsregels stabiliteit. Technical Report 1209434-003, Deltares, 2014.

T.A. van Duinen. Wanneer een su analyse uitvoeren?, cursus s-u rekenen. Presentation, 24-04, 2015. Deltares, Waternet.

EC-0. *Eurocode: Grondslagen van het constructief ontwerp*, stichting nederlands normalisatie-instituut (nen), nen-en 1990+a1+a1/c2(nl) edition, 2011.

EC-6.1. *Eurocode 6 - Ontwerp en berekening van constructies van metselwerk - Deel 1-1:Algemene regels voor constructies van gewapend en ongewapend metselwerk*, stichting nederlands normalisatie-instituut (nen), nen-en 1996-1-1+a1(nl) edition, 2013.

EC-7. *Eurocode 7: Geotechnisch ontwerp - Deel 1: Algemene regels*, stichting nederlands normalisatie-instituut (nen), nen-en 1997-1+c1 (nl) edition, 2012.

ENW. Addendum bij het technisch rapport waterkerende grondconstructies. Technical report, Expertise Netwerk Waterveiligheid, 2007.

EurECO. Derde toetsronde primaire waterkeringen 2006-2011, 2014. URL `http://www.zodenaandedijk.com/dijkentoetsing.html`.

C.A. Graubner and E. Brehm. JCSS probabilistic model code part 3: Resistance models 3.2 masonry properties. Technical report, JCSS, 2011.

J.G. Hageman. Construeren in ytong cellenbeton. Technical Report Rapport 7547-1-0, Adviesbureau ir. J.G. Hageman B.V., Xella Nederland B.V., 2013.

B. Hardeman and A. van Duinen. Macrostabiliteit, veranderingen in het wti2017. Presentation, 2015. Ministerie van Infrastructuur en Milieu.

Helpdesk Water. Helpdeskwater, 2015. URL `www.helpdeskwater.nl/onderwerpen/waterveiligheid`.

G. Hoffmans and H. Knoeff. Achtergrondrapport vtv technisch deel. Technical report, Deltares, 2012.

I-L&T. Verlengde derde toets primaire waterkeringen. Technical report, Inspectie Leefomgeving en Transport, Ministerie van Infrastructuur en Milieu, 2013.

I-V&W. Derde toets primaire waterkeringen. Technical report, Inspectie verkeer en waterstaat, Ministerie van Infrastructuur en Milieu, 2011.

R. Jongejan. Vaststellen uitgangspunten definitieve kalibratie. Technical Report 1207803-003, Deltares, 2013.

S.N. Jonkman and T. Schweckendiek. *Flood Defences, Lecture notes CIE5314*. Delft University of Technology, 2015.

S.N. Jonkman, R.D.J.M Steenbergen, O. Morales-Napoles, A.C.W.M. Vrouwenvelder, and J.K. Vrijling. *Probabilistic Design: Risk and Reliability Analysis in Civil Engineering, Lecture Notes CIE4130*. Delft University of Technology, 2015.

M. de Klant, R.M. Bos, and A. Terluin. Mixed-in-place dijkversterking proefproject nieuw-lekkerland. *Geotechniek*, April:32 – 37, 2011.

KPR. De betekenis van de norm. Memo, 19-03, 2015. Kennis Platform Risicoanalyse, R. Jongejan.

H. Larsen. Geavanceerde toetsing bebouwing in paralleldijk krimpenerwaard. Technical report, GeoDelft, 2004. review by J. Dekker.

M. van Leeuwen and H.J van der Giessen. Vijzelen woningen voor dijkverbeteringen kinderdijk-schoonhovenseveer. *Civiele Techniek*, 4:32 – 34, 2015.

P.P.H Leijendeckers. *Polytechnisch zakboek*. Reed Business Information, 2003.

B van Leusen and J.W. Velden. *Rivieren en Stuwen*. Noordhoff Uitgevers B.V., 1998. ISBN 9011045882.

J. van Mechelen. Multifunctional flood defences, reliability analysis of a structure inside the dike. Master's thesis, Delft University of Technology, 2013.

NEN8700. *Beoordeling van de constructieve veiligheid van een bestaand bouwwerk bij verbouw en afkeuren - Grondslagen*, stichting nederlands normalisatie-instituut (nen), nen 8700 (nl) edition, 2011.

NPR-6791. *Steenconstructies - Eenvoudige ontwerpregels, gebaseerd op NEN 6790:2005*, stichting nederlands normalisatie-instituut (nen) edition, 2009.

NPR-9096. *Steenconstructies - Eenvoudige ontwerpregels, gebaseerd op NEN-EN 1996-1-1+C1*, stichting nederlands normalisatie-instituut (nen), npr 9096-1-1 (nl) edition, 2012.

R Pijpers. Vulnerability of structural transitions in flood defences. Master's thesis, Technical Unversity of Delft, 2013.

E.J. Pleijster and C van der Veeken. *Dijken van Nederland*. LOLA Landscape Architects, nai010, 2015. ISBN 978-94-6208-150-5.

R. van der Pluijm. *Out of Plane Bending of Masonry, Behaviour and Strength*. PhD thesis, Technische Universiteit Eindhoven, 1999.

Rijkswaterstaat. Hoogwaterbeschermingsprogramma, een introductie, 2014. URL `http://www.hoogwaterbeschermingsprogramma.nl/Programma/Een+introductie/default.aspx`.

Rijkswaterstaat. Waterdata, 2016. URL `http://live.waterbase.nl/waterbase_wns.cfm?taal=nl`.

Rijkswaterstaat, Deltares, and Projectbureau VNK2. Handreiking ontwerpen met overstromingskansen. Technical Report OI2014v2, Rijkswaterstaat, 2014.

Rijkswaterstaat, Deltares, and Projectbureau VNK2. Handreiking ontwerpen met overstromingskansen. Technical Report OI2014v3, Rijkswaterstaat, 2015.

M.P.M. Sanders and A.G. Wiggers. Semi-probabilistic safety assessment of pipelines near levees. Technical report, Royal Haskoning DHV, 2015.

P. Schipper. Werk: toetsing panden in waterkeringen krimpen a/d lek bijlage van geavanceerde toetsing bebouwing in paralleldijk krimpenerwaard. Technical report, Ingenieursbureau Concretio, 2004. review by A. van der Kraan.

P. Schipper. Start document handleiding toetsen bebouwing in waterkeringen. Technical report, Ingenieursbureau Concretio, 2012.

Staf deltacommissaris. Synthese document deelprogramma veiligheid, achtergrondrapport bij deltaprogramma 2015. Technical report, Ministerie van Infrastructuur en Milieu and Ministerie van Economische Zaken, 2014.

STOWA. *Leidraad toetsen op veiligheid regionale waterkeringen.* Stichting Toegepast Onderzoek Waterbeheer, 2015.

TAW. *Handreiking Constructief ontwerpen, Onderzoek en berekening naar het constructief ontwerp van de dijkversterking.* Technische Adviescommissie Waterkeringen, 1994.

TAW. *Technisch Rapport Klei voor dijken.* Technische Adviescommissie voor de Waterkeringen, 1996.

TAW. *Grondslagen voor waterkeren.* Technische Adviescommissie voor Waterkeren, 1998.

TAW. *Technisch Rapport Zandmeevoerende Wellen.* Technische Adviescommissie voor de Waterkeringen, 1999.

TAW. *Technisch Rapport Waterkerende Grondconstructies.* Technische Adviescommissie Waterkeringen, 2001.

TAW. *Leidraad Kunstwerken.* Technische Adviescommissie voor de Waterkeringen, 2003.

TAW. *Technisch Rapport Waterspanningen bij Dijken.* Technische Adviescommissie voor de Waterkeringen, 2004.

K.C. Terwel. *Structural Safety, Study into critical factors in the design and construction process.* PhD thesis, Delft University of Technology, 2014.

P.H.A.J.M. Van Gelder. What is the concept of fragility curve?, 2014. URL `https://www.researchgate.net/post/What_is_the_concept_of_fragility_curve`.

A. Verruijt. *Soil Mechanics*. Delft University of Technology, 2010.

Projectbureau VNK2. Overschrijdingskansen en overstromingskansen. Technical Report HB 1679810, Rijkswaterstaat, 2011a.

Projectbureau VNK2. De methode van vnk 2 nader verklaard. Technical Report HB 1267988, Rijkswaterstaat, 2011b.

Projectbureau VNK2. De veiligheid van nederland in kaart. Technical Report HB2540621, Rijkswaterstaat, 2014.

P.A. de Vries and J.W.G. van de Kuilen. *Houtconstructies, Dictaat CT2052*. TU Delft, 2010.

J.K. Vrijling, H.K.T. Kuijper, S. van Baars, K.G. Bezuyen, C. Molenaar, W.F. van der Hoog, B. Hofschreuder, and M.Z. Voorendt. *Manual Hydraulic Structures, CT3330*. TU Delft, 2011.

A.C.W.M Vrouwenvelder, N.P.M. Scholten, and R.D.J.M. Steenbergen. Veiligheidsbeoordeling bestaande bouw achtergrondrapport bij nen 8700. Technical report, TNO, 2011. TNO-060-DTM-2011-03086.

A.C.W.M. Vrouwenvelder e.a. JCSS probabilistic model code part 2: Load models. Technical report, JCSS, 2001.

VTV. Voorschrift toetsen op veiligheid, primaire waterkeringen. Technical report, Ministerie van Infrastructuur en Milieu, 2006.

Waterschap Rivierenland. Overzicht toetsresultaten per dijkringgebied en verbindende waterkeringen. internal document.

Waterschap Rivierenland, 2013. URL `http://www.dijkverbetering.waterschaprivierenland.nl/`.

Waterschap Rivierenland. (bijna) beproefd en bewezen: dijkvernageling, 2015. URL `http://www.waterschaprivierenland.nl/common-nlm/waternieuws/nummer-2-jaargang-2015/bijna-beproefd-en-bewezen-dijkvernageling.html`.

C. Zwanenburg, T.A. van Duinen, and A.P.C. Rozing. Technisch rapport macrostabiliteit. Technical Report 1204203-007, Deltares, 2013.

This page intentionally left blank.

List of Figures

This page intentionally left blank.

List of Tables

Abbreviations

CC	**C**onsequence **C**lass
CSSM	**C**ritical **S**tate **S**oil **M**echanics
CoV	**C**oefficient **o**f **V**ariation
CDF	**C**umulative **D**ensity **F**unction
EC-#	**E**uro **C**ode number #
FORM	**F**irst **O**rder **R**eliability **M**ethod
FOSM	**F**irst **O**rder **S**econd **M**oment
GEV	**G**eneralized **E**xtreme **V**alue distribution
HT	toets-spoor falen door gebrek aan **H**oog**T**e
	Assessment track failure due to lack of height
HWBP	**H**oog **W**ater **B**eschermings **P**rogramma
	Dutch Flood Protection Program
LEM	**L**imit **E**quilibrium **M**odel
LIR	**L**ocal **I**ndividual **R**isk
LSF	**L**imit **S**tate **F**unction
MC	**M**onte **C**arlo simulation
MIP	**M**ixed **I**n **P**lace technique
MHW	**M**ean **H**igh **W**ater
	Gemiddeld Hoog Water (GHW)
NHW	**N**ormative **H**igh **W**ater
	Maatgevend Hoog Water (MHW)
NWO	**N**on **W**ater-retaining **O**bject
PDF	**P**robability **D**ensity **F**unction
VNK-2	**V**eiligheid **N**ederland in **K**aart **2** Project
	Flood Risk in the Netherlands 2 project
SBW	Onderzoeksprogramma **S**terkte **B**elastingen **W**aterkeringen
	Researchprogram Strength and Loads on Waterdefenses
SHANSEP	**S**tress **H**istory **A**nd **N**ormalized **S**oil **E**ngineering **P**roperties

SLS	**S**erviceability **L**imit **S**tate
STBI	toets-spoor macro-**St**abiliteit **Bi**nnenwaarts Assessment track macro-stability inside
STBU	toets-spoor macro-**St**abiliteit **Bu**itenwaarts Assessment track macro-stability outside
STMI	toets-spoor **Mi**cro-**St**abiliteit Assessment track micro-stability
STPH	toets-spoor **St**abiliteit door **P**iping & **H**eave Assessment track Piping & Heave
STBK	toets-spoor **St**abiliteit door falen **B**e**K**leding Assessment track failure of revetment
STOWA	**S**tichting **T**oegepast **O**nderzoek **Wa**terbeheer Dutch foundation for Applied Water Research
UC	**U**nity **C**heck
VTV-2006	**V**oorschrift **T**oetsen **V**eiligheid **2006** Regulation Safety Assessment 2006
WBI-2017	**W**ettelijk **B**eoordelings **I**nstrumentarium **2017** Statutory Assessment Tools 2017

Symbols

a	factor related to the sensitivity of the length to the failure mechanism	$[-]$
a_n	empirical fitting constants	$[mm]$
b	factor related to length of independent equivalent sections	$[m]$
B	width of the dike base	$[m]$
b'	width of a running meter wall that is simplified as beam	$[m]$
B_{dh}	gumbel parameter, decimate height	$[m]$
b_{slice}	width of soil slice	$[m]$
c	cohesion	$[kPa]$
C	value obtained after linearization for FORM procedure	$[kPa]$
c_μ	mean value of cohesion	$[kPa]$
c_c	characteristic value of cohesion	$[kPa]$
c_d	design (calculation) value of cohesion	$[kPa]$
CoV	coefficient of variaton	$[-]$
CoV_ϕ	coefficient of variation of stochastic phi	$[-]$
CoV_c	coefficient of variation of stochastic cohesion	$[-]$
$CoV_{tan(\phi)}$	coefficient of variation of stochastic tan(phi)	$[-]$
D	aquifer thickness	$[m]$
d	blanket thickness	$[m]$
D_i	value obtained after linearization for FORM procedure	$[-]$
$E_{0,mean}$	yield modulus of wood in SLS	$[N/mm^2]$
$F_{build,Su}$	force supplied by building when soil acts undrained	$[kN]$
$f_{m,0,rep}$	representative bending strength	$[N/mm^2]$
$f_R(h_w)$	cumulative density resistance distribution of water level	
$f_s(h_w)$	probability density loading distribution of water level	
$f_{t,0,rep}$	representative tension strength	$[N/mm^2]$
$f_{x,k1}$	characteristic value of bending tensile strength for failure in plane parallel to joint	$[N/mm^2]$
$f_{x,k2}$	characteristic value of bending tensile strength for failure in plane perpendicular to joint	$[N/mm^2]$
$f_{xd,1,app}$	apparent calculation value for bending tensile strength adjusted for compression stress	$[N/mm^2]$
F_y	tension yield force nail	$[kN]$
FoS	Factor of Safety; loading divided by resistance	$[-]$
$F_{(instab\|intact,h_w)}$	cdf for inner slope instability given that the building remains intact and a certain water level occurs	$[-]$
$F_{(instab\|collapse,h_w)}$	cdf for inner slope instability given that the building does collapse and a certain water level occurs	$[-]$
$F_{(collapse\|h_w)}$	cdf of the event "building collapses" given a certain water level	$[-]$
g	gravitational acceleration	$[m/s^2]$

h_{base}	height of soil retaining wall	$[m]$
h_{design}	design water level	$[m]$
h_{Mmax}	distance from top support to location of M_{max} on the soil retaining wall	$[m]$
h_{mean}	average height of soil slice	$[m]$
h_p	polder level at the hinterland	$[m]$
h_w	water level at river side of the dike	$[m]$
I	moment of inertia	$[mm^4]$
I_l	intrusion length	$[m]$
k	permeability	$[m/s]$
K_0	neutral lateral earth pressure coefficient	$[-]$
$K_{0,\beta}$	neutral earth pressure coefficient for an inclined ground surface, parallel to ground surface	$[-]$
$K_{0,\beta,h}$	neutral earth pressure coefficient for an inclined ground surface, horizontally decomposed	$[-]$
K_a	active lateral earth pressure coefficient	$[-]$
$K_{a,\beta,h}$	active earth pressure coefficient for an inclined ground surface, horizontally decomposed	$[-]$
$K_{add,\beta}$	additional amount of active coefficient due slope of the ground	$[-]$
k_{af}	hydraulic conductivity aquifer	$[m/s]$
k_{at}	hydraulic conductivity aquitard	$[m/s]$
K_p	passive lateral earth pressure coefficient	$[-]$
K_z	hydraulic conductivity of the dike material	$[m/s]$
L_f	length of the foreshore	$[m]$
$L_{section}$	length of a dike section	$[m]$
L_{seep}	seepage length	$[m]$
l_{slip}	length of the slip plane	[]
l_{wall}	perimeter of walls that transder loading from upper floors down	$[m]$
l_x	length of soil retaining wall	$[m]$
m	power function for strength increase SHANSEP method	$[-]$
$M_{a,\gamma}$	active moment generated by weight of the soil	$[kNm/m]$
M_{ed}	calculation value of the applied bending moment	$[kNm]$
M_{el}	elastic moment capacity	$[kNm]$
M_{max}	maximum bending moment in retaining wall	$[kNm]$
$M_{p,building}$	moment generated by pressure of the building	$[kNm]$
$M_{p,gamma}$	passive moment generated by weight of the soil	$[kNm/m]$
$M_{p,\tau}$	passive moment generated by shear along slip plane	$[kNm/m]$
M_{pl}	plastic moment capacity	$[kNm]$
M_r	resisting moment	$[kNm/m]$
M_{rd}	calculation value of the bending moment capacity	$[kNm]$
M_s	driving moment	$[kNm/m]$
M_y	plate bending moment direction corresponding to bending parallel to joints of masonry wall	$[kNm]$
N	length effect factor	$[-]$
n	number of Monte Carlo computations	$[-]$
N_{ed}	calculation value of the normal force in the masonry	$[kN]$
n_f	amount of realizations in failure domain	$[-]$
N_{ow}	loading upper floors, own weight	$[kN/m^2]$
N_{vl}	loading upper floors, variable loading	$[kN/m^2]$
n_z	porosity of the dike material	$[-]$
$\oslash$	probability space equal to zero	$[-]$
OCR	over consolidation ratio	$[-]$
p	pore water pressure	$[kPa]$

P_{instab}	probability of inner slope stability of the combined system	
P_{mp}	mid probability	$[yr^{-1}]$
P_{map}	maximum allowable probability $[yr^{-1}]$	
P_{ibt}	probability in between P_{map} and P_{mp}	$[yr^{-1}]$
P_{intact}	probability of the event "building does not collapses" i.e. building remains intact	
$P_{(instab\|intact)}$	probability for inner slope instability given that the building remains intact	
$P_{(instab\|collapse)}$	probability for inner slope instability given that the building does collapse	
$P(h_w > h_{design})$	exceeding probability of the design water level	$[yr^{-1}]$
P_{all-pf}	allowable probability of failure	$[yr^{-1}]$
$P_{collapse}$	the probability of building collapse	$[yr^{-1}]$
$P_{f\|rupture,HW}$	the conditional probability of failure of the dike given two simultaneous events: rupture and highwater event	$[yr^{-1}]$
$P_{f\|collapse,HW}$	the conditional probability of failure of the dike given two simultaneous events: collapse and a highwater event	
$P_{collapse,t}$	assumed failure probability of building collapse concerning all mechanisms	$[yr^{-1}]$
$P_{dem,fm}$	the demanded failure probability for a mechanism in a profile	$[yr^{-1}]$
P_f	failure probability	
$P_f(_{HW \bigcap collapse})$	the failure probability of the dike due to a collapsed building	$[yr^{-1}]$
$P_f(_{HW \bigcap rupture})$	failure probability that dike fails due to pipeline rupture	$[yr^{-1}]$
$P_{f,mech,n}$	failure probability according failure mechanism n	
P_{flood}	probability of flood of the hinterland	$[yr^{-1}]$
$P_{HW>res-prof}$	the probability of exceedance that the water level exceeds the dike after pipeline rupture/building collapse	$[yr^{-1}]$
$P_{overlap}$	probability that the period of high water level overlaps with the period that the dike is affected by building collapse.	$[yr^{-1}]$
P_{repair}	the probability that the period of high flood level overlaps with the period that is needed for repair of the dike after a rupture	$[-]$
$P_{rupture}$	the probability of rupture of a pipeline	$[yr^{-1}]$
q	distributed triangular load	$[kN/m]$
r	radius of circle	$[m]$
r_{arm}	moment arm	$[m]$
r_{build}	moment arm of force supplied by building	$[m]$
r_{pile}	pile diameter	$[mm]$
S	normally consolidated undrained shear strength ratio	$[-]$
S_{2fl}	surcharge load induced by building with 2 floors	$[kN/m^2]$
S_{3fl}	surcharge load induced by building with 3 floors	$[kN/m^2]$
S_u	undrained shear strength	$[kPa]$
$S_{u,mean}$	mean undrained shear strength	$[kPa]$
t	thickness of masonry wall	$[mm]$
t_{HW}	duration of high water wave at MHW	$[s]$
u_{gumbel}	gumbel parameter	$[-]$
u_i	standard normally distributed variable i	

V_{pf}	relative error of Monte Carlo result	$[-]$
V_{max}	maximum shear force in retaining wall	$[kN]$
W	section modulus	$[mm^3]$
X_d	value of design point	
x_{exit}	distance from exit point to center of dike base	$[m]$
Z	outcome of the LSF	
$\cap$	union of events	
$\cup$	intersection of events	
α	influence coefficient	$[-]$
α_i	influence coefficient of parameter i	$[-]$
β	reliability index	$[-]$
β_{sl}	inclination of ground surface	$[^\circ]$
$\gamma_{m,c}$	partial material factor for cohesion parameter	$[-]$
$\gamma_{m,tan(\phi)}$	partial material factor for angle of internal friction parameter	$[-]$
γ_{sat}	saturated specfic weight	$[kN/m^3]$
γ_{unsat}	specific weight unsaturated soil	$[kN/m^3]$
γ_{water}	specific weight of water	$[kN/m^3]$
δ	angle of friction between wall and soil	$[^\circ]$
δ_ϕ	potential of pore pressures in the aquifer	$[m]$
$\delta_{\phi,c,u}$	potential of weight of the blanket layer	$[m]$
Δ_{col}	relative change in FoS due to collapse	$[\%]$
Δ_H	hydraulic gradient	$[-]$
$\Delta_{M\,max}$	location of $Mmax$ at soil retaining wall expressed as fraction of h_{base}	$[-]$
Δ_{nb}	relative change in FoS due to a building	$[\%]$
Δ_p	parameter to include uncertainty for freatic level	$[m]$
μ	mean value of a stochastic parameter	
μ_{FoS}	expected mean value of FoS	$[-]$
μ_z	mean value of the LSF	
ρ_{mas}	density masonry	$[kg/m^3]$
ρ_{wat}	density water	$[kg/m^3]$
σ	standard deviation of a stochastic parameter	
σ'	effective stress in vertical direction	$[kPa]$
σ_c	standard deviation of stochastic cohesion	$[kPa]$
σ_d	calculation value of the compression stress in the masonry	$[N/mm^2]$
σ_ϕ	standard deviation of stochastic angle of internal friction	$[^\circ]$
σ'_{xx}	lateral effective stress	$[kPa]$
σ_z	normal vertical total stress	$[kPa]$
σ_Z	standard deviation of the LSF	
σ'_0	mean effective stress	$[kPa]$
Σ_M	sum of moments	$[kNm]$
τ	shear strength	$[kPa]$
τ_{mean}	mean drained shear strength	$[kPa]$
τ_u	undrained shear strength based on drained parameters	$[kPa]$
ϕ	angle of internal friction	$[^\circ]$
ϕ_c	characteristic value of angle of internal friction	$[^\circ]$
ϕ_d	design (calculation) value of angle of internal friction	$[^\circ]$
ϕ_{exit}	water pressure potential at exit point	$[m]$
ϕ_μ	mean value of angle of internal friction	$[^\circ]$
Φ	standard normal distribution	$[-]$
ω	failure space factor	$[-]$
Ω	the total probability space	